JAMES COOK UNIVERSITY
AUSTRALIA

Modelling transmission of Hendra virus from flying foxes to horses

Thesis submitted by

Gerardo Antonio Martín Muñoz de Cote [1]

B. V. Sc. (ULSAB), M. Sc. Cons. Biol. (INECOL)

Townsville, 17 May 2017

For the degree of Doctor of Philosophy

College of Public Health, Medical and Veterinary Sciences

James Cook University

[1] mailto:gerardommc@gmail.com

Acknowledgements

First of all I would like to thank my advisory team, Lee, Raina, Carla and David, for being immensely helpful and supportive, and for their kind and patient mentorship. My wife Rosaura, who has been an essential part of this journey, and who I hope did not suffer too much because of my wild idea of studying a PhD abroad. All the One Health Research Group members, current and past; Lee Berger, Laura Grogan, Laura Brannelly, Rebecca Webb, Rick Speare, Diana Mendez, Jon Kolby, Alex Roberts, Tiffany Kosch, Marcia Bianchi, Ben Scheele, Tory Llewelyn, Amy Shima, Carol Esson, Jenny Laycock, Sherryl Robertson, Sieara Claytor, Alicia Maclaine. Friends; Simon, Maria, Nasir and Shany, Salvador, Govinda, Townsville Gutiar Orchestra.

Special thanks to the funding bodies, the National Hendra virus Research Program for providing the funding to undertake this research project and part of my stipend (RIRDC PRJ-008213). The People of Mexico, my home country, for supporting me with the scholarship 239726 through the Consejo Nacional de Ciencia y Tecnología (CONACYT).

The field work planning I had to undertake would have been a lot more difficult if it hadn't been for Bruce Pott and Rob Hedleffs with whom I feel grateful. Janice Lloyd and Sally Watts, who helped me design the horse collars to attach the GPS trackers. Among everyone who helped me in this stage, Laurie Reilly's advice, horse handling mentorship and beers in the late arvo with the view of Mount Elliot, greatly compensated for the mozzy and green tree ant bites, not to mention his tolerance with my constant annoyance during the flying fox counts late in the night. For the same reasons I feel thankful with Wayne Krogh, who on top of that had to find the trackers that his *wild*-naughty horses kept loosing right where the grass was tallest. In doing so, Marcia and Bec, spent several hours with me walking up and down the paddocks looking for the lost GPS trackers, under the rain and steamy hot summer of Townsville, thanks so much for the help and company.

In the bat counting nights, Marcia an Bec helped, so regardless of the *peers* (not beers, but pears in portugese accent) thanks so much again. And to Bec, many thanks for all the help and advice during the field work, I hope Mav didn't break any of your toes.

I'd like to thank th Lee(o) and Lee(a) for their generous reception when we arrived in Townsville. Linda and Clive were also marvellously generous for letting us house sit and start getting used to our Australian life, and thanks for being so relaxed that we didn't get in trouble when we handed the house back with a green and turbid pool full of bat poo.

As for collaborators, special thanks to Deborah Middleton and Paul Selleck for granting access to the Hendra survival data. From the Queensland Centre of Emerging Infectious Diseases, Craig Smith and Hume Field for advice in the design of the GPS trackers, lending the infra-red cameras, and granting access to the Hendra virus spillover dataset and the Queensland horse population census; and David Jordan and Barbara Moloney, who helped me get access to the New South Wales horse population census.

During the study design stage, Hazel parry, David Westcott and Peter Durr, provided very useful feedback that eventually resulted in part of what is contained in the thesis. Many thanks to Peggy Eby too, who, in addition to granting access to the New South Wales vegetation data, helped me design a bat behaviour study. Collaborators Jaewoon Jeong and John Giles, for their ideas for the project on modelling the spillover system; and Carlos Yánñez-Arenas for his advise and ideas for all the niche modelling chapters.

The Bat Health focus group, part of Wildlife Health Australia, Keren Cox-Witton, Rupert Woods and Rick Speare, were immensely supportive in helping me negotiate with QCEID to have access to the existing data regarding Hendra spillover.

Finally, many thanks and apologies to anyone I have missed in this account of help, advice and collaboration.

The College of Public Health,Medical and Veterinary Sciences, James Cook University was contracted by the Rural Industries Research and Development Corporation to undertake this research project. This research was funded by the Commonwealth of Australia, the State of New South Wales and the State of Queensland under the National Hendra Virus Research Program.

Statement of the contribution of others

Intellectual support

Proposal writing: Lee F. Skerratt[2] and Raina Plowright[3]

Data analysis and statistics: Chapters 3 and 4: Carla Ewels[4] and David Kault[5]. Chapters 5, 6 and 7: Carlos Yánẽz-Arenas[6]. Chapter 8: Carla Ewels.

Editorial assistance: Lee Skerratt, Raina Plowright and Carla Ewels

Logistic support

Field research: Rebecca Webb[7]

Contact with horse owners: BVSc. Bruce Pott

Financial support

Field research: Lee Skerratt

Stipend: Lee Skerratt

Write-up grant: Lee Skerratt

Other collaborations

Access to unpublished data: Deborah Middleton and Paul Selleck[8], Craig Smith[9], Peggy Eby[10], David Jordan, Barbara Moloney[11], and Rosemary McFarlane.

Advice for study design: John R Giles, Jaewoon Jeong[12], David Westcott, Hazel Parry[13], Peggy Eby, Peter Durr[14].

Grants and scholarships

Research grant and scholarship: National Hendra virus Research Program, administered by the Rural Industries Research and Development Corporation (RIRDC), grant number PRJ-008213 (Models that predict risk for Hendra virus transmission from flying fox to horses).

Scholarship: Consejo Nacional de Ciencia y Tecnología (CONACYT).

[2]PhD. James Cook University, College of Public Health, Medical and Veterinary Sciences
[3]PhD. Montana State University, Department of Microbiology and Immunology
[4]PhD. Australian Institute of Marice Sciences
[5]PhD. James Cook University, School of Engineering and Physical Sciences
[6]PhD. Universidad Nacional Autónoma de México, Laboratorio de Conservación de la Biodiversidad
[7]BSc. James Cook University, College of Public Health, Medical and Veterinary Sciences
[8]CSIRO, Australian Animal Health Laboratory
[9]Queensland Biosecurity
[10]Private Consultant
[11]Department of Primary Industries, New South Wales
[12]Griffith University, School of Environment
[13]CSIRO, Ecosystem sciences
[14]CSIRO, Australian Animal Health Laboratory

Disclosure

Chapter 2 is a paper (Ecological dynamics of emerging bat virus spillover, Plowright et al., 2015) published by 22 authors of which I am the 10th author. My contribution towards the paper was to provide ideas regarding the potential mechanisms at play in the spillover system, help in figure preparation and providing ideas for the figures in the final paper, to help write and edit the paper, to calculate the spatial extent and number of spillover events that are cited in the paper, and providing details about environmental survival of HeV.

Abstract

Diseases that originate in wildlife and spillover to humans and domestic animals are of increasing public health concern. Of the wildlife groups in which emergent diseases originate, bats (Mammalia:Chyroptera) are a common source of some of the most virulent organisms: Ebola and Marburgh viruses, SARS *Coronavirus* and Nipah and Hendra viruses. Of these, Hendra virus (HeV, Paramyxoviridae:*Henipavirus*) is the only one that has not caused an epidemic outbreak after it spills over to horses and thence to humans. However, its geographic location in Australia represents an unparalleled opportunity to study spillover dynamics of emerging viruses, given the research capacity and human resources immediately available. The importance of understanding spillover dynamics lies in the potential ability of reducing the risk of epidemics by decreasing the frequency of spillover. Since emergence HeV has spilled over to horses on 55 occasions along a 1500 km coastal stripe in eastern Australia, from northern Queensland to central New South Wales, with mortality rates in infected horses and humans close to 50-75%.

In this study I used a series of modelling techniques to address basic questions of HeV epidemiology and ecology: What are the essential components of the spillover system? How is HeV transmitted from bats to horses? Which reservoir host species are more likely involved in spillover? What are the potential avenues to predict spillover occurrence? How does the spillover host affect spillover risk? How can we mitigate risk of HeV spillover?

To identify the components of the HeV spillover system I participated in a workshop with the National HeV Research Program investigators. We discussed the available evidence and theory regarding spillover and published a conceptual model that is included here as Chapter 2. The conceptual model consists of an explicit representation of the factors that have to be present for spillover to occur.

Then, to find out how HeV is transmitted, I used unpublished experimental data on HeV survival at different temperatures in the laboratory (Australian Animal Health Laboratory, Paul Selleck), to generate a HeV survival model in the form of an ordinary differential equation. I used the model to test if survival could predict spillover in space (Chapter 3). The poor predictive capacity of the HeV survival model suggested that transmission to horses could be direct. However, given that I could not completely rule out indirect transmission I quantified HeV decay in the microclimates it experiences once excreted in paddocks. With the simulations and analyses I found that HeV survival is lower on the ground than at ambient air temperatures, and that ground vegetation and tree shade increase survival. In addition, given that desiccation occurs in most circumstances and

further decreases survival, HeV can seldom be indirectly transmitted (Chapter 4).

At the time this project began in late 2012 it was not clear which of the four flying fox species were more important for spillover. To identify the most likely reservoir hosts I used the concept of ecological niche to see if spillover occurred where prevailing climatic conditions are preferred by a specific flying fox species. Using these methods I identified *P. alecto* and *P. conspicillatus* as the most important reservoir hosts explaining spillover, and therefore most likely to transmit HeV to horses (Chapter 5). Using similar methods I identified climatic correlates of the spatio-temporal pattern of spillover, and produced spillover risk maps in response to climate change. In Chapter 6 I modelled the spatio-temporal risk pattern and found that the most likely climatic factors involved are the seasonal amplitudes of minimum temperature and rainfall. Finally, I modelled HeV risk in response to the climatic suitability for *P. alecto* and *P. conspicillatus* (Chapter 7). With these models I found that the horse population at risk will increase by up to 165,000 by 2050, given the number of horses in 2007. In addition I predicted a reservoir host replacement in the northern limits of the HeV spillover distribution.

In my last results Chapter (8) I studied how horses affect spillover risk by modelling the effects of paddock structure on horse behaviour. To do this I deployed GPS trackers in horses and found that when horses are kept in small areas such as paddocks their movements tend to be random. This indicates that beyond the tree coverage of the paddock the effect of its structure on risk of contact with HeV is minimal.

The last Chapter of this thesis is a general discussion and conclusions, in which I present a series of mitigation strategies and recommendations and guidelines for future research. Among research recommendations and guidelines I included a simulation framework that can be extended to improve HeV risk prediction (Chapter 9).

Contents

Glossary

AUC Area under curve. 33, 87–89, 98, 99

BFF Black flying fox. 66

BOM Bureau of meteorology. 90, 94

BSL4 Biosecurity lever four. 2, 3, 24, 44

DNC Distance to the niche centroid. 66, 68, 70–72, 74, 77–79, 94, 102

EMEM Earle's minimum essential medium. 28, 39, 58

ENM Ecological niche modelling. 66

FF Flying foxes. 66–68, 70, 71, 77–79

GLA Gap light analyser. 46

GPS Global positioning system. xxii, 129, 130, 132–134, 136–139, 146

HeV Hendra virus. vii, viii, xiii, xiv, 1–5, 21–24, 26–28, 30, 32–46, 48, 49, 56–59, 63, 64, 66–68, 70, 71, 74, 76–79, 81–87, 99–103, 105–109, 111, 114, 115, 117, 120–123, 129–132, 147–150, 153–168

HL Half life. 54

MCMC Markov chain Monte Carlo. 45, 47, 110, 111, 117, 135, 165

NDVI Normalised difference vegetation index. 94

NHVRP National Hendra virus research program. 3

NiV Nipah virus. 1, 2, 23, 37

NSW New South Wales. xiv, 2, 3, 31, 35, 38, 40, 114, 115, 121

QLD Queensland. xiv, 2, 3, 5, 35, 107, 114, 118, 121–123, 132

RCP Representative concentration pathways. xvi, xvii, 113, 115, 121, 124, 125

ROC Receiver operator characteristic. 27, 28, 31, 68, 69, 87, 89, 98, 114

SFF Spectacled flying fox. 66

$TCID_{50}$ Tissue culture infectious dose. 25, 28, 37, 39

UV Ultra violet. 57, 58

List of Figures

List of Tables

Chapter 1

General introduction

The term "spillover" is often used to describe the transmission of diseases from a wild animal reservoir to a human or domestic animal host (Daszak, 2000). Viruses that spill over from bats (Mammalia:Chyroptera) to humans or domestic animals have gathered considerable attention from the scientific community for their capacity to cause lethal diseases and occasionally large outbreaks in humans. For instance, Nipah virus (NiV, Chua, 2003), SARS *Coronavirus* (He et al., 2004), Marburg virus and Ebola virus (Leroy et al., 2005), cause fatal disease in humans and some domestic animal species (NiV in pigs) and have a common origin with bats as their reservoir hosts. On occasions that epidemics of these diseases pose a sudden burden to public health systems and can affect the services they provide for other more common diseases, generating a negative feedback effect with long lasting consequences (Chang et al., 2004; Plucisnki et al., 2015).

The ecological dynamics[1] of disease spillover have been poorly studied, and the emergence of Hendra virus (HeV, Paramyxoviridae:*Henipavirus*) in 1994 in Australia, presented unparalleled opportunities to study these bat borne emerging diseases in greater detail, given the infrastructure and resources immediately available. Unlike epidemics which are propagating, disease spillover tends to occur intermittently in disparate locations (Lo Iacono et al., 2016). The exact location of spillover can be the product of simple randomness within the disease transmission system or the signal of undetected epidemics in some of the reservoir host populations (Keeling and Rohani, 2007), leading to greater risk of spillover (Amman et al., 2012). This is but one of the many complexities of spillover systems which have to be considered in order to understand them.

Hendra virus was discovered in the Brisbane suburb of Hendra, Queensland, Australia, in an outbreak of respiratory disease involving the death of 20 horses and one human (Murray et al., 1995b). The novel virus was initially classified as a *Morbillivirus*, but it was sufficiently different

[1] The study of how populations of organisms of different species change with time as a result of their interactions.

to be considered a new genus of the Paramyxoviridae family. After the discovery of a similar virus in Nipah, Malaysia in 1998, the genus *Henipavirus* was formed. After the outbreak two serological serological surveys of 1600 (Murray et al., 1995a) approximately and 2024 horses (Ward et al., 1996) took place and were unable to detect evidence of previous and widespread exposure. This suggested that the source of the novel pathogen was not horses, which led to a process of sampling 5000 specimens of 12 domestic and 34 wildlife species in search of reservoir hosts (Young et al., 1996). The search culminated in flying foxes, bats of the genus *Pteropus* being the first species found with antibodies against the same virus found in the outbreaks (Halpin and Field, 1996). After this finding, bat carers requested a survey that was unable to detect exposure to the virus in 128 samples (Selvey et al., 1996). Then, despite the serological finding in bats, it took several years to confirm, beyond any doubt, that flying foxes are the natural reservoir hosts of HeV and NiV (Halpin et al., 2000, 2011).

Due to the observed high case fatality rate in the first known outbreak (Murray et al., 1995b), potential to transmit among novel hosts, its probable use as a biological weapon and the lack of vaccination and therapeutic regimes, HeV was classified as a biosecurity level four (BSL4) pathogen (Eaton et al., 2006). The bio-containment conditions required to work with this type of organisms pose special circumstances that greatly limit diagnostic capacity and the number, scope and reach of experimental and observational studies (Wang and Daniels, 2012; Eaton et al., 2006).

Between HeV's emergence in 1994 and 17 May 2017, spillover to horses has been reported 55 times. From here on, the term "spillover" is used to describe an event of HeV transmission from flying foxes to horses. Transmission to humans has only been observed after close contact with contaminated fluids of HeV diseased horses, it has never been observed or attributed to occur directly from flying foxes (Halpin and Field, 1996; Halpin et al., 2000; Field et al., 2010), nor have studies of exposure been able to demonstrate it (Selvey et al., 1996). Spillover to horses occurs along 2500 km of the eastern Australian coast from central New South Wales (NSW) to far north Queensland (QLD). In some of the spillover events there are short chains of transmission between horses, as occurred during the index case in 1994 (20 cases, Murray et al., 1995b), and in 2008 in a private veterinary clinic (8 cases, Field et al., 2010). These two outbreaks likely began after HeV transmission from bats to a single horse, and all subsequent infections were probably acquired from other diseased horses (Murray et al., 1995b; Field et al., 2010). Although it is difficult to be certain about the origin of all the mentioned HeV cases, these self limiting transmission events

suggest there is potential for evolution of continued transmission among the novel hosts (Lo Iacono et al., 2016).

Between 1994 and 2010 HeV spillover detection and report was relatively rare, with close to one spillover event per year (Field et al., 2010). However, in 2011 a large cluster of 21 events occurred along a coastal strip of 160 km from southern QLD to northern NSW. In response to the increased spillover risk, potential for epidemics and the seemingly high virulence in both horses and humans (50-75%), the National HeV Research Program (NHVRP) was launched in 2012. The One Health Research Group[2], led by Lee Skerratt, applied to fund a project to model the transmission of HeV from flying foxes to horses. The funding obtained from NHVRP made possible the development of my PhD project and this thesis. The main reason for which I decided to undertake a modelling project, was that HeV's classification as a BSL4 pathogen makes experimental studies extremely expensive and often not feasible or unethical. For instance, measurement of HeV's survival in the environment would pose a great risk to the community, as it would involve placing virus cultures that most likely exceed natural environmental concentrations of the virus. Therefore, modelling can help to make sense out of disparate existing data relevant for understanding the HeV spillover system.

In November 2012, NHVRP principal investigators met in Byron Bay to identify gaps in knowledge and discuss possible research avenues for each research team. There, attendants agreed to collaborate and make research complementary, within each team's capacity, towards the common goal of improving understanding of the HeV spillover system and ultimately our predictive capacity. The main outcome of the workshop was a scientific paper (Plowright et al., 2015) that collated most of what was known about HeV's ecology and epidemiology at the time. This paper constitutes part I, Chapter 2 of this thesis, and is presented as a conceptual model of the HeV spillover system.

I structured the thesis in five thematic parts, and each part is divided into Chapters. In the following paragraphs I describe each of the thematic parts and their Chapters. Following on from Chapter 1 which introduces my PhD thesis, part I contains Chapter 2 which explains a conceptual model for HeV spillover.

Following the structured framework developed in Chapter 2 (Plowright et al., 2015), I identified three areas which I could elaborate given that data was available or collection was financially

[2] https://www.jcu.edu.au/college-of-public-health-medical-and-veterinary-sciences/public-health-and-tropical-medicine/one-health-research-group2

and logistically possible. The first of the HeV aspects I decided to investigate was the role of HeV environmental survival by using both published (Fogarty et al., 2008) and, at the time unpublished data, from experiments performed by Paul Selleck in 1996 in the Australian Animal Health Laboratory. In the end it was only possible to use Paul Selleck's experimental data which was published in Scanlan et al. (2014) during the course of my studies of HeV survival. However I generated a model that provided a better fit to the data and found ways of using the model to improve our understanding of HeV transmission to horses. This is Part II of this thesis and includes Chapters 3 and 4 which describe my studies of HeV survival. Using the laboratory HeV survival data in relation to temperature I found that even though HeV is capable of surviving for weeks in laboratory conditions, it is likely to be transmitted directly given real world environmental conditions (Chapter 3). These results led to Chapter 4 in which I estimate the potential survival of HeV once it is excreted in horse paddocks. These two studies have influenced official policy and it is now recommended to consider that HeV can be transmitted both directly and indirectly. More importantly, targeting direct transmission in mitigation may lead to greater reduction in risk.

Part III of the thesis, is a series of studies of the effects of climate on HeV's ecology and epidemiology. The three Chapters are based on the theory of ecological niche modelling, which attempts to estimate an organism's physiological and ecological requirements. When these requirements are represented in spatially reference data, they can be used to estimate the geographic distributions or find areas with the appropriate environmental conditions for the organism's presence (Owens et al., 2013). The most widely used tools to estimate the requirements are correlative statistical models, than can be broadly classified, in my own opinion, in multivariate similarity methods (environmental distance or range based rules, Farber and Kadmon, 2003; Busby, 1991), regression (Thuiller et al., 2003; Renner et al., 2015), machine learning (Phillips et al., 2006; Stockwell and Peters, 1999) and non-parametric classification algorithms (Elith et al., 2008). A common feature of these methods is that they have been adapted or developed to use presence only data, due to the complications that arise as result of sampling absence of an organism in continuous space (Elith et al., 2011). In this thesis I used several of these methods.

In Chapter 5 I describe how I used the climatic niches of the four Australian flying fox species, modelled with Maxent (Phillips et al., 2006), to identify which species were most likely involved in spillover. I found that spillover occurs in areas where *Pteropus alecto* and *P. conspicillatus* can have higher population densities, therefore increasing the evidence of these species acting as natural reservoirs. In Chapter 6 I studied the effects of climate on the spatio-temporal pattern of

spillover risk. For this Chapter I used presence-absence regression methods (parametric and non-parametric) that were combined in a consensus model. I found that the most likely explanation for HeV spatio-temporal pattern of spillover in southern latitudes and the relatively constant risk among seasons in the north, is influenced by bat species specific traits in response to the seasonal amplitude of minimum temperature and rainfall. In basic terms, dry and cold winters are associated with increased risk from black flying foxes. This species and the mentioned conditions are typically found in the southern portion of the area at risk of HeV spillover.

Chapter 7, constitutes the first attempt to predict HeV spillover, by modelling it as a spatial point process. The results are a series of maps that highlight where HeV spillover is more likely to occur based on how the two bat reservoir species involved in spillover will respond to climate change. While predictions are coarse both in space and time, they can be used to allocate resources for mitigation before the effects of climate change take place. In addition, the models predicted a probable replacement of reservoir hosts in northern QLD, because environmental suitability will decrease for *P. conspicillatus* and increase for *P. alecto*. These results have profound implications for, HeV ecology and epidemiology, flying fox and biodiversity conservation, ecosystem function and policy design. In addition, I found several novel avenues for future research, like investigating the possible consequences of the replacement of reservoir host species in northern QLD.

Part IV of this thesis consists of Chapter 8. Here I tracked the movement of paddocked horses to identify characteristics of the paddocks that increase the likelihood that horses interact with areas covered by trees. The rationale was that, because HeV is excreted by flying foxes while feeding in trees (Field et al., 2011), obtaining a measure of the frequency of such interactions would be informative of the contact frequency with HeV. I found that horse movements tend to be close to random, and for this reason the proportion of the paddock covered by trees is the main determinant of the time horses spend under trees, especially during the night. Based on these results I suggest that restricting access to trees during the night is likely to be a successful mitigation strategy.

Finally, in part V, Chapter 9, I consider the results of Chapters 3–8 in the context of Chapter 2 and each other. I compiled a section of future research directions, based on questions that arose as part of my research. I conclude the thesis by outlining an extensible mechanistic simulation framework that incorporates some of the key findings of this thesis, and which could be used in the future for spillover risk prediction.

In the end of the thesis, after the bibliography section, there is an appendix divided in nine

appendices, one for each of the Chapters. In the appendices all the necessary information to fully understand the analyses and results is given.

Part I

A Hendra virus spillover conceptual model

Chapter 2

Ecological dynamics of emerging bat virus spillover

This chapter was a collaborative effort among the researchers involved in the National Hendra Virus Research Program between November 2012 and December 2014 (Plowright et al., 2015). It consists of a review of bat-borne zoonotic viruses with Hendra virus (HeV) included as a case study and was led by Raina K. Plowright. We identified the separate components of a disease spillover system that are required for disease spillover. Therefore our study is a first attempt to explicitly represent all the processes that have to coincide in time and space for spillover of HeV to occur.

After the conceptual framework was designed we discussed the evidence and theory regarding each of the HeV spillover components that we identified. I used the resulting conceptual model to identify the components of the spillover system that required further study and designed my PhD project based on them.

The chapter finishes by listing a series of spillover risk mitigation strategies that can be applied at each level of the spillover system. During the course of my studies and in this thesis I have made refinements to some of these mitigation strategies based on my findings.

PROCEEDINGS B

rspb.royalsocietypublishing.org

Review

Cite this article: Plowright RK *et al*. 2015 Ecological dynamics of emerging bat virus spillover. *Proc. R. Soc. B* **282**: 20142124.
http://dx.doi.org/10.1098/rspb.2014.2124

Received: 11 September 2014
Accepted: 16 October 2014

Subject Areas:
ecology, health and disease and epidemiology, microbiology

Keywords:
emerging infectious diseases of bat origin, Hendra virus in flying-foxes, Nipah virus, severe acute respiratory syndrome coronavirus, Ebola virus, Marburg virus

Author for correspondence:
Raina K. Plowright
e-mail: raina.plowright@montana.edu

Electronic supplementary material is available at http://dx.doi.org/10.1098/rspb.2014.2124 or via http://rspb.royalsocietypublishing.org.

THE ROYAL SOCIETY PUBLISHING

Ecological dynamics of emerging bat virus spillover

Raina K. Plowright[1,2], Peggy Eby[3], Peter J. Hudson[2], Ina L. Smith[4], David Westcott[5], Wayne L. Bryden[6], Deborah Middleton[4], Peter A. Reid[7], Rosemary A. McFarlane[8], Gerardo Martin[9], Gary M. Tabor[10], Lee F. Skerratt[9], Dale L. Anderson[6], Gary Crameri[4], David Quammen[11], David Jordan[12], Paul Freeman[12], Lin-Fa Wang[4,13], Jonathan H. Epstein[14], Glenn A. Marsh[4], Nina Y. Kung[15] and Hamish McCallum[16]

[1]Department of Microbiology and Immunology, Montana State University, Bozeman, MT 59717, USA
[2]Center for Infectious Disease Dynamics, Pennsylvania State University, State College, PA, USA
[3]School of Biological, Earth and Environmental Sciences, University of New South Wales, Sydney, New South Wales 2052, Australia
[4]New and Emerging Zoonotic Diseases, CSIRO, Australian Animal Health Laboratory, East Geelong, Victoria 3220, Australia
[5]CSIRO Ecosystem Sciences and Tropical Environment and Sustainability Sciences, James Cook University, Atherton, Queensland 4883, Australia
[6]Equine Research Unit, School of Agriculture and Food Sciences, University of Queensland, Gatton, Queensland 4343, Australia
[7]Equine Veterinary Surgeon, Brisbane, Queensland 4034, Australia
[8]National Centre for Epidemiology and Population Health, Australian National University, Canberra 0200, Australia
[9]School of Public Health, Tropical Medicine and Rehabilitation Sciences, James Cook University, Townsville, Queensland 4811, Australia
[10]Center for Large Landscape Conservation, Bozeman, MT 59771, USA
[11]414 South Third Avenue, Bozeman, MT 59715, USA
[12]New South Wales Department of Primary Industries, 1423 Bruxner Highway, Wollongbar, New South Wales 2477, Australia
[13]Program in Emerging Infectious Diseases, Duke-NUS Graduate Medical School, Singapore 169857
[14]EcoHealth Alliance, New York, NY 10001 USA
[15]Animal Biosecurity and Welfare Program, Biosecurity Queensland, Department of Agriculture, Fisheries and Forestry, Brisbane, Queensland 4001, Australia
[16]Griffith School of Environment, Griffith University, Brisbane 4111, Australia

RKP, 0000-0002-3338-6590

Viruses that originate in bats may be the most notorious emerging zoonoses that spill over from wildlife into domestic animals and humans. Understanding how these infections filter through ecological systems to cause disease in humans is of profound importance to public health. Transmission of viruses from bats to humans requires a hierarchy of enabling conditions that connect the distribution of reservoir hosts, viral infection within these hosts, and exposure and susceptibility of recipient hosts. For many emerging bat viruses, spillover also requires viral shedding from bats, and survival of the virus in the environment. Focusing on Hendra virus, but also addressing Nipah virus, Ebola virus, Marburg virus and coronaviruses, we delineate this cross-species spillover dynamic from the within-host processes that drive virus excretion to land-use changes that increase interaction among species. We describe how land-use changes may affect co-occurrence and contact between bats and recipient hosts. Two hypotheses may explain temporal and spatial pulses of virus shedding in bat populations: episodic shedding from persistently infected bats or transient epidemics that occur as virus is transmitted among bat populations. Management of livestock also may affect the probability of exposure and disease. Interventions to decrease the probability of virus spillover can be implemented at multiple levels from targeting the reservoir host to managing recipient host exposure and susceptibility.

Content has been removed
due to copyright restrictions

Content has been removed
due to copyright restrictions

Content has been removed
due to copyright restrictions

Content has been removed
due to copyright restrictions

Content has been removed
due to copyright restrictions

Content has been removed
due to copyright restrictions

Content has been removed
due to copyright restrictions

Part II

Environmental survival of Hendra virus: inferring potential transmission routes and survival capacity

Chapter 3

Hendra virus survival does not explain spillover patterns and implicates relatively direct transmission routes from flying foxes to horses

Environmental survival of the virus was one of the key components of spillover systems that I identified in Chapter 2 (Plowright et al., 2015). The presence of this layer in the conceptual model assumes that HeV transmission is indirect; i.e. that the virus spends time in the environment such as on the ground before it is ingested by the horse to enter its body.

By studying HeV environmental survival I can find evidence of the importance of HeV survival for spillover risk. In the case that the spatiotemporal pattern of spillover is linked with the survival capacity of HeV in the environment, I can also estimate a potential time frame after excretion that transmission to horses is likely to occur. And perhaps more importantly, I can identify if some transmission routes from flying foxes to horses are more likely than others.

This chapter describes how I built a HeV survival model using unpublished data from experiments performed by Paul Selleck in the Australian Animal Health Laboratory. Then, I used the model to study the relationships between HeV environmental survival, as a distinct component of the spillover system, with spillover occurrence in space and time.

The methods that I used for the analyses were mainly maximum likelihood, geospatial modelling and frequentist statistics. The theoretical basis to build the temperature-survival model was derived from survival analysis with parametric methods, using the proportion of HeV surviving at each time as a response variable in a specified distribution (McCallum, 2000).

The main outcomes of the chapter are, better understanding of the potential pathways of HeV transmission, and improved estimates of HeV survival in the environment.

This chapter has already been published as (Martin et al., 2015):

- Gerardo Martin, Raina Plowright, Carla Chen, David Kault, Paul Selleck, and Lee Skerratt. Hendra virus survival does not explain spillover patterns and implicates relatively direct transmission routes from flying foxes to horses. *The Journal of General Virology*, pages vir.0.000073–, feb 2015. ISSN 1465-2099. doi: 10.1099/vir.0.000073. URL http://vir.sgmjournals.org/content/early/2015/02/09/vir.0.000073.abstract

ABSTRACT

*Hendra virus (HeV) is lethal to humans and horses, and little is known about its epidemiology. Biosecurity restrictions impede advances, particularly on understanding pathways of transmission. Quantifying the environmental survival of HeV can be used for making decisions and to infer transmission pathways. I estimated HeV survival with a Weibull distribution and calculated parameters from data generated in laboratory experiments. HeV survival rates 24 h after excretion based on air temperatures ranged from 2 to 10% in summer and from 12 to 33% in winter. Simulated survival across the distribution of the black flying fox (*Pteropus alecto*), a key reservoir host, did not predict spillover events. Based on the analyses I concluded that the most likely pathways of transmission did not require long periods of virus survival and were likely to involve relatively direct contact with flying fox excreta shortly after excretion.*

Introduction

Transmission of diseases depends on the successful transfer of live pathogens from an infectious to a susceptible host. Parasites have a great diversity of strategies to accomplish transference of live individuals to a susceptible host. But each of the transmission pathways used by a parasite depend on a series of characteristics of the host, the parasite, the host-parasite relationship and the environment (Ewald, 1987; Walther and Ewald, 2004). For instance the target organs in the host might determine the excretion and entrance routes most suitable to establish a new infection. And the entrance pathways that a parasite can use, depend partially on how pathogens leave the body of an infected host. Two strikingly different strategies are indirect environmental and vector transmission. For instance use of bodily fluids like urine to leave the body of an infected host might imply that transmission is possible through contaminated water, feed or any other substrate that will eventually be introduced in the body of a susceptible host. On the other hand pathogen transmission by vectors eliminates some of the restrictions imposed by the interactions

with the outer body environment. Vector transmission also implies the ability of surviving inside and leaving the body of a different species than the one used to reproduce. Both types of parasites are subject to evolutionary trade-offs that maximise the probability of establishing new infections. Those trade-offs might result in increased virulence, switch target organs or acquire the ability to infect a broader variety of host species (Day, 2001; Ewald, 1987). Therefore a pathogen's capacity to survive outside of a host's body is indicative of several biological processes.

Understanding of the mechanisms driving HeV emergence and transmission to spillover hosts has been slow to develop. Despite the recent availability of a commercial vaccine for horses, spillover events continue to occur. Many at-risk horses remain unvaccinated due to the cost of the vaccine, risk perceptions of horse owners and other factors (Middleton et al., 2014). Undertaking efficacious and more cost-effective alternative mitigation strategies is constrained by a lack of implementation of the management recommendations. Thus, improving the understanding of transmission routes of HeV from flying foxes to horses will result in reducing necessary costs and efforts to implement effective prevention. The most likely route is thought to be exposure of horses to infectious bat excretions (Field et al., 2011; Marsh et al., 2011).

According to the most plausible scenario, once HeV is excreted by bats, the time it remains infectious determines the transmission window within which horses must be exposed to become infected with HeV (Plowright et al., 2015). If virus survival is very short, rapid and direct exposure to bat excretions (faeces, urine, saliva or birth/foetal fluids) may be necessary. Longer survival provides more diverse opportunities for exposure. For example, infectious excreta may be able to accumulate in feed. Clearly, improving our understanding of virus survival in the environment will be critical for inferring likely transmission mechanisms and mitigating risk.

Studies of HeV survival in the environment have thus far been based on the effects of pH, desiccation, urine and fruit juice at two different temperatures. This study also examined Nipah virus (NiV) survival using the same conditions and substrates (Fogarty et al., 2008). HeV and NiV were resistant to a wide pH range (3–11) but sensitive to desiccation, surviving for <15 min without moisture at 37℃. Whilst these experiments indicated that the decay of infectious HeV occurs quickly, the effect of the magnitude of the environmental variables (and their change through time) on virus survival are still unknown. For this reason, we cannot estimate HeV survival in eastern Australia where spillover events occur (Figure 3.1). Moreover, we cannot use HeV survival to predict spillover events or infer the most likely transmission routes. To estimate and understand the contribution of virus survival in the environment to spillover risk I

developed a model from experimental data of HeV survival at three different temperatures. With the model I quantified the relationship between changes in temperature and survival of HeV. The model accounted for the effect of temperature on the decay rate of the virus and was based on the Weibull cumulative density function (CDF). The model was used to perform simulations under the temperature conditions in the current geographical distribution of HeV spillover events. The simulations estimated how much virus would survive 12 and 24 h after excretion at 3:00 a.m. across the distribution of the black flying fox (*Pteropus alecto*), which encompasses the current distribution of spillover events. In addition, I showed that previous calculations that estimated longer survival (Scanlan et al., 2014) are explained through recording errors, different model-fitting procedures and the nature of environmental data used in simulations (air versus soil temperatures). These differences had to be resolved before advances could be made in the understanding and managing of HeV transmission.

Methods

I developed two models based on the Weibull and exponential CDFs. I chose these distributions, firstly because I wanted to compare the distribution used by Scanlan et al. (2014) with another more flexible distribution. Secondly, I selected the Weibull because it is simple and allowed us to implement a simulation framework with simple modifications to the equation.The effect of temperature on survival was included when transforming parameters of each distribution into functions of temperature. To run simulations, I generated temperature profiles to represent temperature changes between day and night. The profiles accounted for the variability and extremes observed at meteorological stations over the previous 20 years in order to emulate real-world conditions. Simulations represented the survival of an excreted viral population over a period of at least 24 h. This method allowed us to assess the likelihood of virus accumulation in the environment on successive days. The model was constructed from experimental data at three constant temperatures.

Measurement of HeV survival

Survival experiments were performed by Paul Selleck [1] in the Australian Animal Health Laboratory (Commonwealth Scientific and Industrial Research Organisation, Geelong, Victoria, Australia) under BSL4 conditions with the isolated HeV strain in the index case. Survival of HeV was

[1] mailto:Paul.Selleck@csiro.gov.au

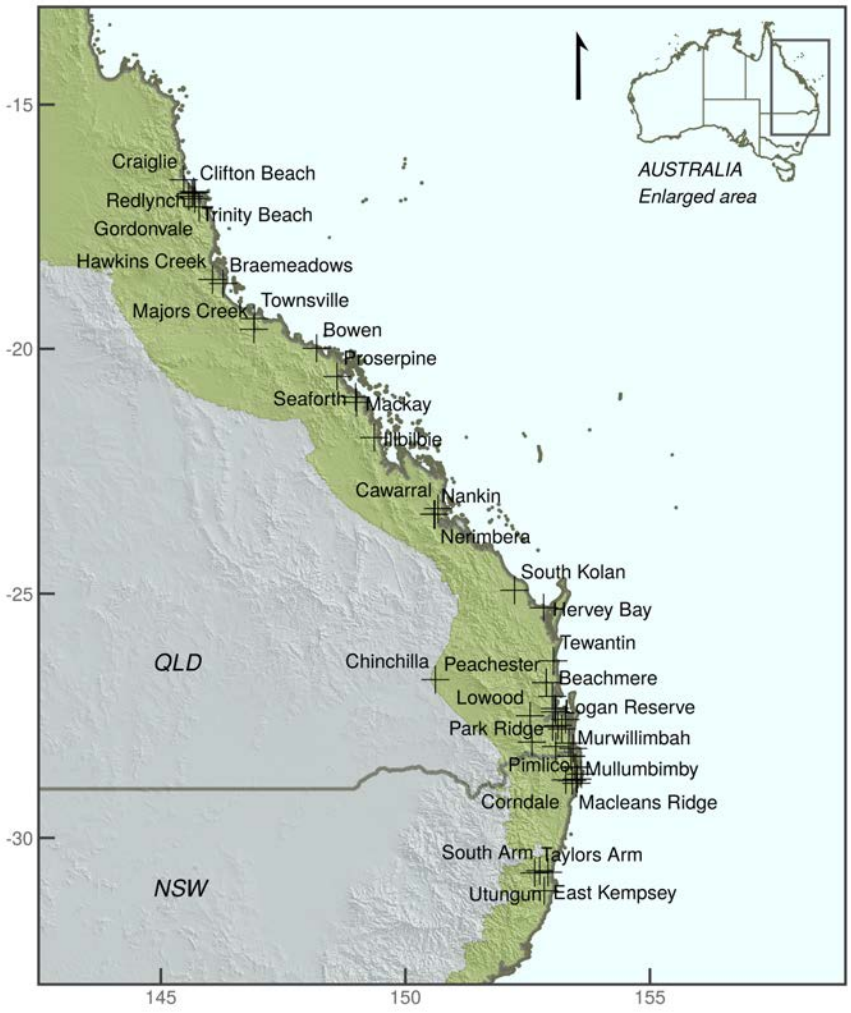

Figure 3.1: Map shows the names and geographical location of spillover sites.

measured at three constant temperatures: 4, 22 and 56 ℃. Virus cultures were titrated at intervals of 1 week for the experiments at 4 and 22℃, and 10 min at 56℃.Virus concentration was reported as $TCID_{50}$. The detailed experimental design and methods are described in Scanlan et al. (2014), however the interval between virus titrations of the experiment at 56℃ was reported to be 10 h instead of 10 min.

Model development, parameterisation and simulations

Optimisation was performed with the Gauss–Newton algorithm for non-linear regression implemented in the '`nls`' routine of the statistical computing language R 3.1.0 (R-Development-Team, 2014). The data used to fit the models is a series of two averaged virus titrations. Each titration

was divided by the initial titer and the remaining model fitting was performed over the natural logarithm of the surviving proportion. Originally data contained 15, 14 and 8 measurements at 4, 22 and 56 ℃ respectively. Due to heavy tailing with very few remaining particles in the final titrations I only used the first five measurements, which does not affect model survival estimates. This is because the model was never used to estimate survival at temperatures and times beyond those contained in the data used to fit the model. I began fitting separate curves to titres for each temperature. I estimated parameters for the Weibull and exponential CDFs (equations 4a). Then I modelled parameter values as variables dependent on temperature. The resulting parameter models were substituted in both the Weibull and exponential models. Finally, I ran an additional optimisation with a time-temperature coupled model. The initial values given to the optimisation routine were those estimated in the previous step. To select a model I used normality, autocorrelation of residuals and the Akaike information criterion (AIC) to compare models. AICs were compared with the Akaike weights test.

Simulations

Environmental data used in simulations was downloaded from the Bureau of Meteorology [2], and consisted of minimum and maximum daily air temperatures averaged from 1993 to 2012 from four locations where spillover events were recorded. Temperature was averaged to represent the most likely conditions to be observed in each locality. All simulations were run with the optimum parameter estimates and their standard errors with the R package `deSolve` (Soetaert et al., 2010).

The selected model was transformed to a differential equation (equation 7). Then I generated the temperature profiles with the average minimum and maximum temperatures for each month. These profiles assume that minimum temperature occurs at 3 am and maximum at 3 pm (equation 6). Simulations were run with the conditions of four locations comprising the latitudinal extremes of the spillover geographical distribution, Cairns in far north Queensland, Kempsey in central New South Wales (southernmost part of the distribution), and Rockhampton and Redlands for the center and the hotspot (highest density of spillover events, Plowright et al., 2015) of the distribution, respectively (Figure 3.1).

I also simulated the potential survival of HeV across the geographical distribution of *P. alecto* (black flying fox) using raster data sets of temperature —the black flying fox is the only bat species

[2] `http://www.bom.gov.au`

with a distribution covering all spillover sites and consistently found closer to spillover events (Field et al., 2011). These maps represented the proportion of HeV surviving 12 h (under soil temperature conditions) and 24 h (under air temperatures) after being excreted at 3:00 a.m. These simulations were used to test whether survival was a good predictor of the spatial location of spillover in each season. Data for these simulations were obtained from the microclim dataset (Kearney et al., 2014)[3] for soil temperatures and the Bureau of Meteorology for air temperatures. The resolution of the microclim data was 15km, and was interpolated to match the pixel size of the Bureau of Meteorology data at 2.7km. The spatial data for the simulations was handled with the `raster` 2.2-31 and `dismo` 0.9-3 R packages (Hijmans, 2013; Hijmans et al., 2013).

For spatial simulations in the soil I used a series of layers of ground temperature at zero cm depth and two shade levels, 0 and 50%, obtained from the microclim dataset (Kearney et al., 2014). For each shade cover I accounted for the effect of the soil types available in microclim. The areas with the soil types of Australia were obtained from a categorical layer generated by the Australian Bureau of Agricultural and Resource Economics and Sciences (ABARES), from which I only distinguished the three types; soil, sand and rock, which correspond to the data available in microclim. I extracted the areas with each soil type from their corresponding ground temperature layer and then merged them with its complementary layers. For simulations I assumed that shade cover did not affect minimum temperatures as these occur in the night.

Each 2.7 km pixel of the minimum and maximum temperature layers (from all datasets, soil and air temperatures) were used as the parameters of the oscillating temperature profiles. Then I ran a simulation for every pixel in the layer and the last value of each simulation was stored in another layer. From the resulting simulated maps I extracted the value of the pixels corresponding to the location of every event by season. Then the values of all the pixels in summer, autumn, winter and spring maps were cross tabulated to run the partial ROC test with the Partial ROC tool allowing a 20% omission rate.

Measuring the predictive ability of survival

Assuming that inter-annual variation in temperature would affect virus survival over the entire geographical region, I performed a Partial ROC (receiver operating characteristic) analysis to assess the performance of virus survival as predictor of spillover (Peterson et al., 2008). The

[3] http://figshare.com/articles/microclim:_Global_estimates_of_hourly_microclimate_based_on_long-term_monthly_climate_averages/878253

Partial ROC test measures the area under curve (AUC) formed by the predicted extent versus the proportion of predicted events and compares it to a random predictor (Peterson et al., 2008). The random predictor is determined by the proportion of area predicted within the survival threshold. For instance 50% of the area predicted is expected to predict 50% of the spillover events in the spatial simulation that is being tested. If the model predicts more than the 50% of the spillover events expected by randomness the survival model is a better predictor than random. Tests were run with the Partial ROC tool (Barve, 2008). This is because the model and resulting survival maps can represent the fundamental niche of spillover events (Hutchinson, 1957; Kearney and Porter, 2009), which is given by an organism's response to the set of environmental conditions it is usually exposed to. Detailed methods are provided in the Appendix 9.6.3.2. Under the same assumption, I extracted 100 random samples of survival rates from the entire area assumed to be available for spillover occurrence and from a 40 km buffer around spillover localities (no-event areas). The samples were compared with survival in the location of spillover to with a Kolmogorov–Smirnov test. Significance of the test was assessed by calculating the probability that the measured P values were 0.05 if they were drawn from a normal distribution of P values.

Results

Observed survival in laboratory and calculated half-lives

The experimental data consisted of measurements of the concentration of viral particles in $TCID_{50}$ (processed data in table 3.1). My estimates of virus rates of decay differed substantially from previously published analyses of the data (Scanlan et al., 2014, Figure 5 in Appendix 9.6.3.2). For instance, my estimations of virus half-life at 56 and 22℃ were 1900 and 17.3 times less, respectively, than reported by Scanlan et al. (2014). HeV survival was relatively short and highly dependent on temperature. A small proportion of HeV particles were capable of surviving for several hours in Earle's minimum essential medium (EMEM) at 22℃, whilst survival increased at 4℃ and decreased significantly at 56℃ (Figure 3.2). The half-life of virus decreased exponentially with increasing temperature; therefore, small increases in temperature resulted in large increases in decay rates. The relationship between $\ln S$ (where S is the proportion of virus surviving at time t) and time was increasingly non-log-linear at higher temperatures. Consequently, half-life decreased not only exponentially with temperature, but followed a power law dependent on temperature. This resulted in higher decay rates immediately after virus excretion, because the

shape parameter of the Weibull model was < 1 at all temperatures and decreased even more at higher temperatures (Figure 3.2, table 3.1).

Table 3.1: Data used to fit models. To obtain better fit to the initial points I only used the first five measurements of viral titres for experiments at 4 and 22 °C. Time has been standardised to weeks, although the scale of the measurements at 56°C was minutes. $\ln S$ is the logarithm of the surviving proportion at time T. Time units are weeks (w) and minutes (min).

Time	$\ln S$	Temperature (℃)
0 w	0	4
1 w	-0.7494845504	4
2 w	-0.6216511789	4
3 w	-1.6433024264	4
4 w	-1.4426317309	4
0 w	0	22
1 w	-4.8761644932	22
2 w	-6.4307941692	22
3 w	-7.5096038305	22
4 w	-10.2782786535	22
0 min	0	56
10 min	-7.4160777725	56
20 min	-10.2475069948	56
30 min	-12.5202391246	56
40 min	-13.8493750719	56

As a result of the non-log-linearity of the data, the Weibull model achieved the best fit as shown by the Akaike weights test between models ($P < 0.05$). The half-life estimations between models differed substantially, especially at high temperatures. Weibull half-life estimations were 268 h, 2.9 h and 3.5 s at 4, 22 and 56℃, respectively. In contrast, half-lives I calculated with the exponential model were 275 h, 42.9 h and 1.72 min, respectively (Figure 3.2).

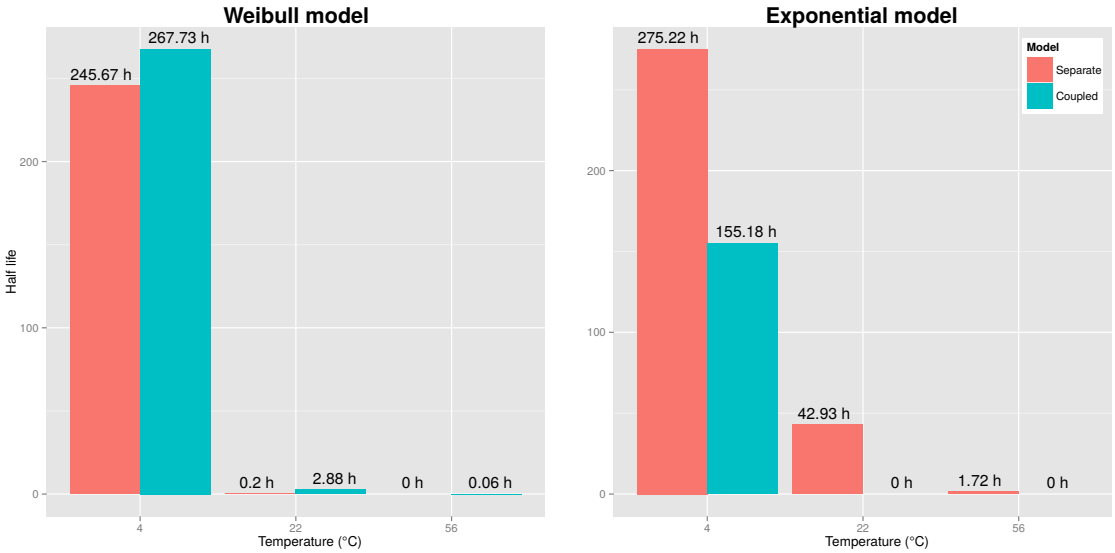

Figure 3.2: Half-lives calculated for each temperature: Weibull model versus exponential model. The estimations between the separate models for each temperature differ less with respect to the time–temperature coupled model in the Weibull model than in the exponential model.

Parameter estimates

The Weibull model parameters that control the shape of the decay curve were different from 1 for all temperatures. This was replicated with the time-temperature coupled model. This means that decay is non log-linear, and for this reason the Weibull model achieved a better fit than the exponential model. Parameters of fitted models in table 3.2.

Table 3.2: Parameter values of the Weibull model. T is the value of T-student statistic and P is the significance of the parameter estimate

	Parameter[a]	Value	S. E.	T	P
Weibull	α_ρ	-1.79604	0.25027	-7.176	1.81e-05
	β_ρ	0.23172	0.01014	22.846	1.28e-10
	α_κ	0.46812	0.03869	12.099	1.07e-07
	β_κ	-0.20464	0.12488	-1.639	0.13
Exponential	α_ρ	-0.3786051	0.1221587	-3.099	0.008
	β_ρ	0.0027711	0.0000467	59.333	$<$ 2e-16

[a] ρ subscripts indicate regression parameters affecting the rate parameter of the Weibull or exponential distributions. κ subscripts indicate regression parameters affecting the shape parameter of the weibull distribution.

Survival rates calculated with air temperature

The amount of virus surviving 24 h ranged from 2% (0.04–6.7% with SE of estimated parameters) in the northernmost location (Cairns) to 10% (1.6–18% SE) in the southernmost location (Kempsey) during summer. In the coldest month of winter, the amount of virus surviving was 12% (2.4–21.2% SE) in Cairns and 33.1% (20.4–40.4 SE) in Kempsey (Figure 3.3). Survival rates at 24 h were highly variable amongst years; however, variability within months could be greater than pooled variability between years as evidenced by the smaller 95% confidence intervals (95% C. I.s) of air temperature variability (Figure 3.5). Regarding the two major spillover clusters to date, 2011 [southern Queensland and northern New South Wales (NSW)] and 2012 (northern Queensland; Figure 3.1), the events in 2011 had a average survival slightly higher than the 1993–2012 mean temperatures, but within normal variability. Events from the 2012 cluster had survival rates very close to the mean for each location. The mean survival of 2012 locations was lower than the mean survival of 2011 location. These inconsistencies regarding survival and spillover occurrence suggest that clustering in both cases was not driven by conditions that promoted survival (fig 3.3).

Predictive ability of survival rates in space and time

The survival model was projected to three sets of layer; a set of layers of interpolated air temperature, and two sets of soil temperature at zero depth under 0 and 50% shade (microclim sets, Kearney et al., 2014). Soil temperature simulations were only performed 12 h after excretion because longer simulation times resulted in very low survival estimates that limited the partial ROC analysis. The difference between air and soil temperature was very large, which resulted in much lower survival estimates for both series of simulations at 0 and 50% shade at soil level than with air temperature. For instance, the highest survival rate 12 h after excretion at spillover locations under 50% shade in winter was 10% compared with 54% at 24 h with air temperature. Furthermore, surviving fractions at soil temperature implied that in most of the cases there was no virus left at 12 h, even under 50% shade in winter conditions. With soil temperature, more events occurred where 12 h survival was almost zero. The results described below correspond to simulations under air temperature, which likely represented the best case scenario for virus survival.

According to air temperature, most spillover events occurred where 24 h survival was estimated to be ~40% (Figure 3.4). Summer and spring spillover events occurred when and where virus

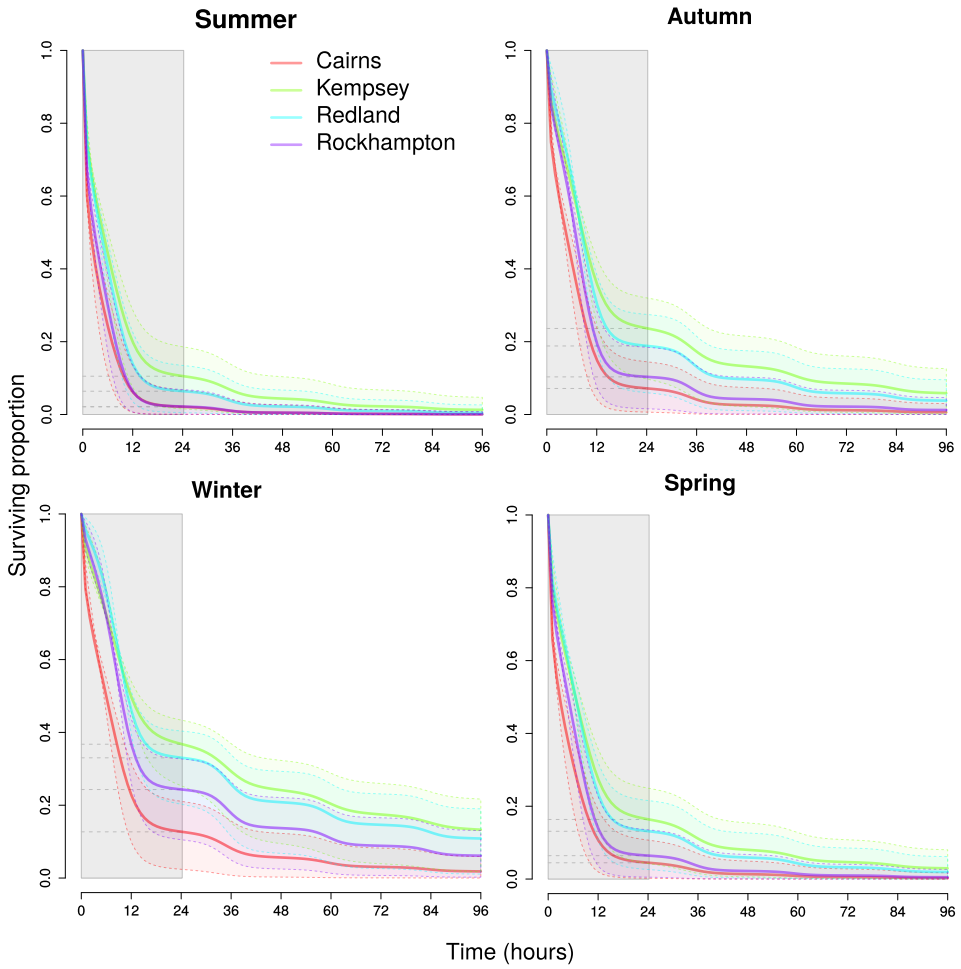

Figure 3.3: Simulated virus decay curves for 96 h after excretion at 3:00 a.m. Summer conditions are represented by the mean temperature of the hottest month and winter conditions are represented by the mean temperature of the coldest month. Autumn and spring are represented by the mean temperature of the first month of the season. The dashed lines represent the simulations with upper and lower standard errors of estimated parameters. The grey shaded area on the left side of each graph highlights the survival curve over the first 24 h.

survival was lowest across the current geographical distribution of spillover (Figure 3.6). The mean 24 h survival of these events was 3.5% (n = 6, 95% C. I. 1.5–5.2%) and the mean survival in buffer zones of 80 km (background survival) was 4.1% (95% C. I. 0.2–7.8%). For autumn events, mean survival was 6.8% (n = 2, 95% C. I. 2.0–11.0%) and background survival was 10% (95% C. I. 4.1–16%). In winter, mean survival at location of spillover was 34.7 (n = 32, 95% C. I. 19.8–49.7%) and background survival was 38.8% (95% C. I. 15.0–62.5%). Finally, in spring, mean survival was 9.6% (n = 8, 95% C. I. 0.0–20.0%) and background survival was 12.5% (95% C. I. 0.6–24.4%).

Estimated viral survival rates during spillover events were close to the mean survival for those

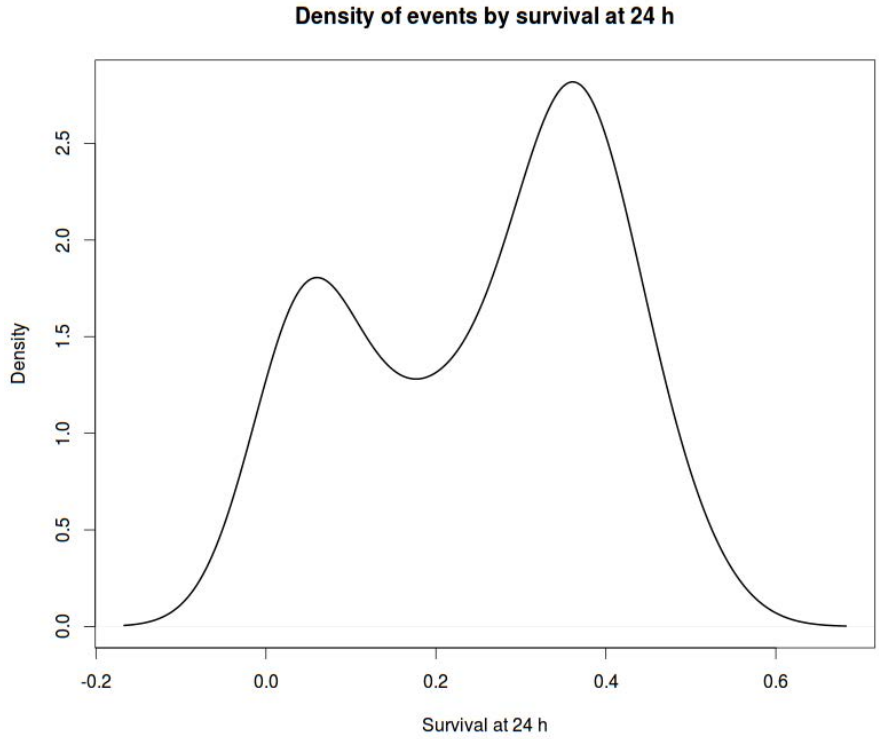

Figure 3.4: Density of HeV average potential survival in the locations of spillover at the month of occurrence.

areas both within and between years (Figure 3.5). Therefore, spillover events mostly occurred at times of intermediate virus survival. However, the distribution of virus survival amongst locations of spillover was bimodal (Figure 3.4). This means that when temperature conditions were cold, spillover tended to occur in cold areas; when temperatures were higher, spillover occurred in warm areas. Similarly, spillover occurred close to the coastal line, where temperatures were higher than immediately farther inland (Figure 3.6).

The distribution and timing of spillover events was unlikely to be strongly influenced by virus survival rates 12 (soil temperatures) and 24 h (air temperatures) after excretion. The survivorship models did not perform significantly better than random predictions of spillover [area under the curve (AUC) ratio not significantly > 1] in space and time. Furthermore, Kolmogorov–Smirnov tests suggested no significant difference between viral survivorship at the location of spillover events with randomly selected background (non-event) survivorship samples in summer. In winter, however, the empirical CDF of the events was significantly smaller ($D(34) = 0.79$, $P = 1.36 \times 10^{-8}$). This association of higher mean survivorship at spillover locations in winter was caused by the positive correlation of temperature with latitude in the southern hemisphere. The majority of

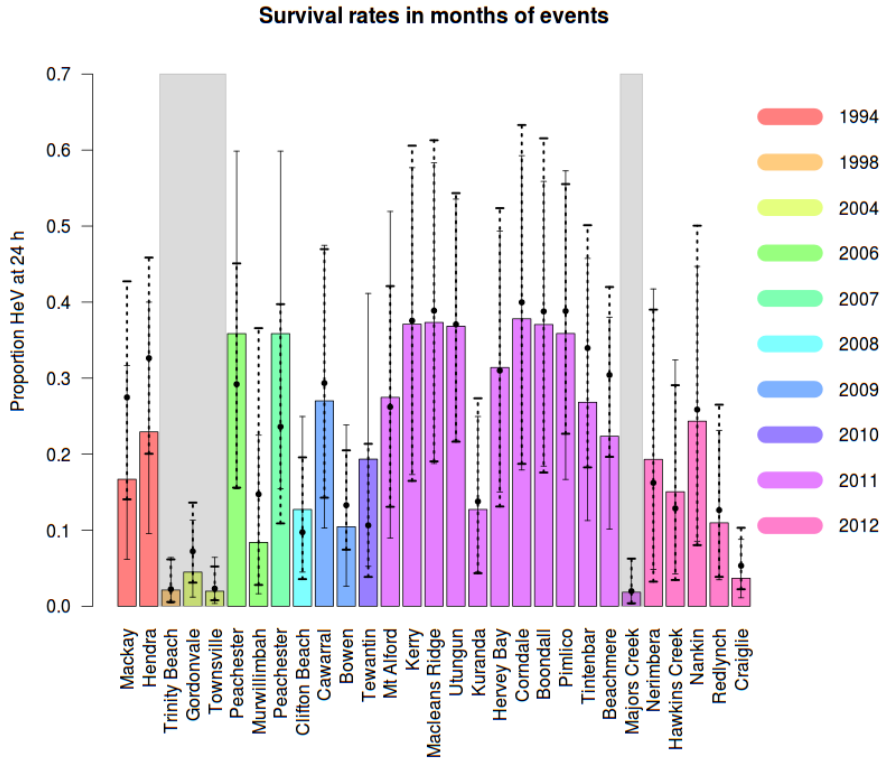

Figure 3.5: Comparison of the proportion of HeV surviving 24 h after excretion at the month of spillover with the 1993-2012 average survival at each of the spillover locations. Coloured bars are the 1993-2012 average and the thin continuous error bars show its 95% confidence intervals. The black points and dashed error bars show average and 95% C. I.s of HeV survival for the month of spillover occurrence in that location. Location of the point with respect to the thin error bars indicates how different the month of spillover was from the most common conditions (coloured bars). The grey shaded areas indicate the events that occurred in summer. Results are only shown for locations where reliable temperature data were available from a meteorological station.

the detected spillover events in winter/autumn occurred in the southernmost part of the black flying fox (spillover) geographical range (Figure 3.6). When I restricted sampling of non-events to a buffer zone of 40 km around each spillover event, the difference between survival at events versus non-events was not statistically significant ($D(34) = 0.14$, $P = 0.5$).

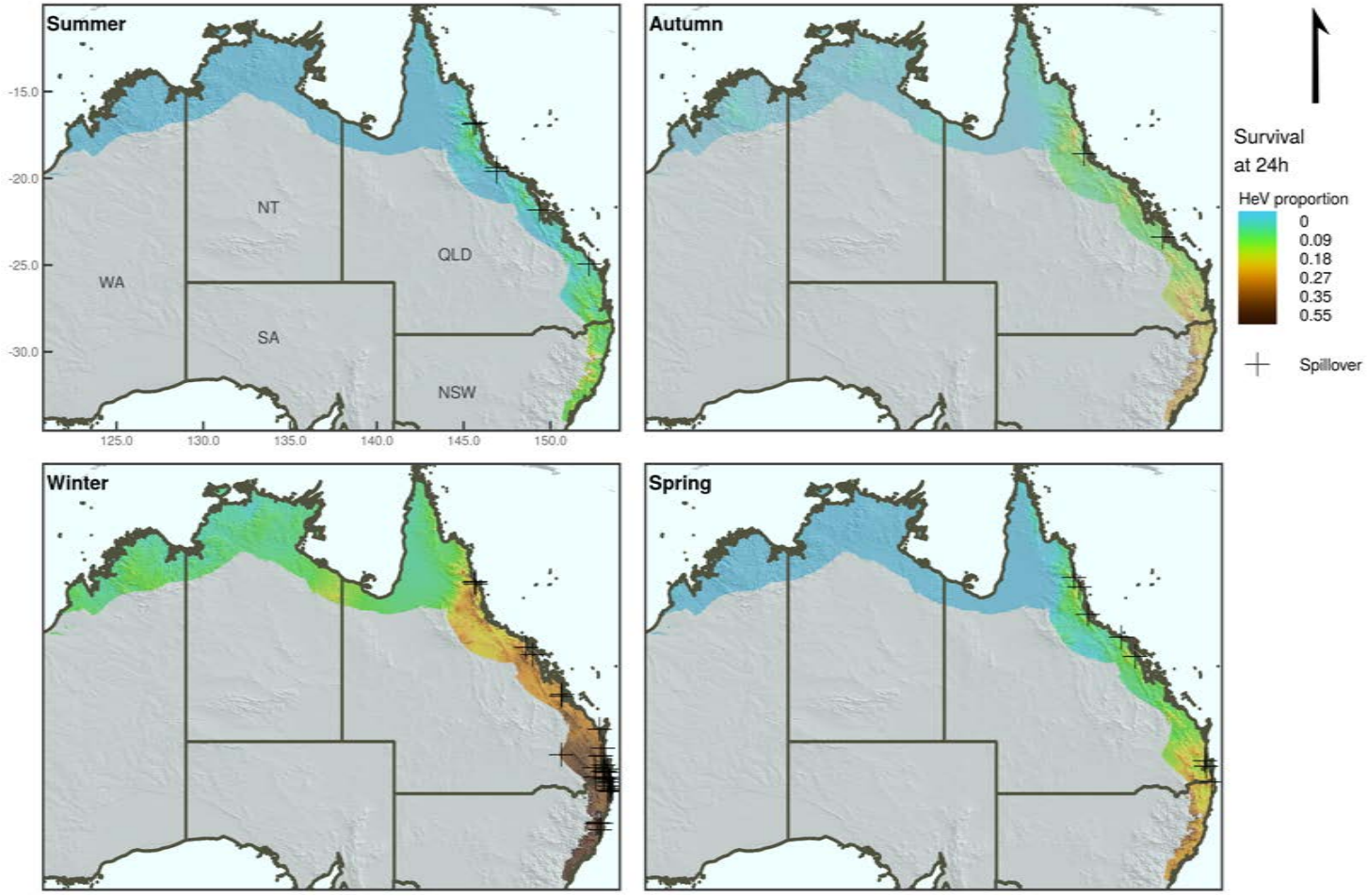

Figure 3.6: Maps showing the amount of HeV surviving 24 h after being excreted whilst temperature is the mean minimum for each season. Crosses show the locations of spillover events and circles correspond to the buffers used in the statistical analyses. Events were divided into season of occurrence. Western Australia (WA), Northern Territory (NT), South Australia (SA), Queensland (QLD) and New South Wales (NSW). The x- and y-axes show longitude and latitude, respectively.

Discussion

HeV transmission may need to occur shortly after the virus is excreted by bats and probably requires that horses directly contact fresh bat excreta. The spatial simulations with the microclim dataset (Kearney et al., 2014) suggest that HeV potential survival in the soil is much shorter than previously estimated with air temperatures. I conclude this based on the higher rate of HeV mortality immediately after excretion, the very low survival rates 12 h after excretion in soil microclimates and the lack of explanatory power of the pattern of spillover by virus survival, with both air and microclim temperatures.

Additional supporting evidence that HeV survival is likely lower than that predicted by Scanlan et al. (2014) is the non-log-linear relationship between $\ln S$ and time. This kind of relationship can result from heterogeneous susceptibilities of individual viruses or heterogeneous conditions in the experimental substrates (Peleg, 1996; van Boekel, 2002). It is likely that, in a natural setting, the resistance of free particles and the environmental conditions are more heterogeneous than under laboratory conditions. Therefore, the resulting decay rates might be greater, resulting in shorter lifespans. Low survival will be exacerbated by additional stresses, such as desiccation (Fogarty et al., 2008) and UV radiation. UV radiation is very effective at killing other viruses (Murray and Jackson, 1993; Weber and Stilianakis, 2008), but has not been tested for HeV. HeV is an enveloped virus (Paterson et al., 1998) and therefore could be highly sensitive to UV radiation, which will additionally reduce survival after sunrise.

Heterogeneous conditions might also be caused by microclimates, which in this context differ from the term microclimate used before in this same chapter. Microclimates as previously used refers to the temperature conditions at different heights or depths above or below ground under different levels of shade (Kearney et al., 2014). In this context microclimates are the conditions that occur in smaller spatial scale, whose variability with respect to macroclimate is explained by the conditions formed by vegetation or topography. Microclimates in this sense can differ from the macroclimate, decreasing maximum temperatures, increasing moisture, decreasing desiccation rates and creating a refuge from UV radiation (Chen et al., 1996). The effect of microclimates on temperature may be applicable to this study. A downscaling of interpolated air temperature from the macroclimate will not be representative of microclimates because soil characteristics are important determinants of temperature at ground level (Kearney et al., 2014). For instance, Scanlan et al. (2014) assumed that a microclimate is a colder version of the macroclimate by up

to 5℃, whilst a common effect of microhabitats is an increase in minimums (Chen et al., 1996), which may result in decreasing survival. I have shown here that soil level conditions dramatically decrease the survival of HeV even under 50% shade compared with air temperature (Kearney et al., 2014). Therefore, a homogeneous reduction in temperatures is not representative of microclimates. Microclimatic effects should be represented by direct measurements, and would benefit from consideration of the joint effects of moisture, temperature and desiccation on virus survival.

My analyses suggest that HeV survival in the environment is likely to be short. The ability of a pathogen to survive outside its hosts is indicative of the possible transmission pathways between hosts. For instance, influenza viruses may survive up to 2 months in water, and therefore can be transmitted by direct and indirect routes (Domanska-Blicharz et al., 2010). Less resistant, non-vector-transmitted pathogens such as human immunodeficiency virus (survival up to 1 week on smooth surfaces) are usually transmitted directly, whilst indirectly transmitted pathogens such as poliovirus survive for up to 2 months (Kramer et al., 2006). The ability of a pathogen to survive in the environment can be an evolutionary consequence of virulence/transmission trade-offs (Walther and Ewald, 2004). Consequently, the environmental susceptibility of HeV might be a consequence of evolutionary trade-offs that occurred within flying fox populations over long periods of time. For example, the clustering of bats in tree canopies, and subsequent exposure of many individuals to a mist of aerosolised urine, might favour transmission routes that do not require long environmental survival (Markwell and Shortridge, 1982; Plowright et al., 2015). The sit-and-wait strategy of highly resistant pathogens such as the causative agents of polio, smallpox and tuberculosis in humans (Walther and Ewald, 2004) may not be necessary for HeV transmission amongst flying foxes. Therefore Transmission routes to horses may be similar to some of the transmission routes between flying foxes.

The precise route of viral entry and infectious dose of HeV in flying foxes and horses are unknown. Some other animal viruses enter through nasal and corneal routes at lower minimum infectious doses than required for oral routes of infection (Ward et al., 1984). For example, experimental nasal inoculation of NiV in pigs and hamsters leads to central nervous system disease (Munster et al., 2012; Weingartl et al., 2005). Experimental infections with HeV in horses successfully reproduced disease with oral and nasal inoculation; however, doses were relatively large (2×10^6 and 5×10^4 $TCID_{50}$, respectively) and were therefore unlikely to represent natural conditions (Marsh et al., 2011). Other experimental studies failed to reproduce transmission from flying foxes to horses by ingestion of contaminated feed (Williamson et al., 1998). Whilst

oral transmission of HeV would require contaminated feed or water, nasal transmission may occur through inhalation of aerosolised fluids, droplets or loose contaminated particles in the air (Weber and Stilianakis, 2008). As HeV survival in feed might resemble survival under desiccation, transmission would have to occur very shortly after excretion. For example, time to death of 90% of HeV (1 log reduction) changed from 24 h in urine to 1 min under desiccation at 22℃ (Fogarty et al., 2008). Similarly, the low survival under desiccation makes inhalation of contaminated dust less likely to be a feasible route of transmission. Generally, non-smooth, dusty and dry environments further reduce the survival of pathogens (Wagenvoort and Penders, 1997). Given the above, and that urine is probably the most important route of HeV excretion (Williamson et al., 1998, 2000), I suggest that direct exposure to infectious flying fox urine may be an important transmission pathway. However, I cannot completely rule out indirect exposure through contaminated feed during some of the spillover events, especially where predicted 24 h virus survival and moisture are high. A special circumstance is present when water troughs are placed under trees, which reduces the likelihood of death of viruses by desiccation.

Given that virus survival driven by temperature is unlikely to be a major driver of the spatio-temporal pattern of spillover, there must be other factors limiting transmission in seasons and areas with higher viral survival but no reported cases. These factors must occur with periodicity in southern Queensland and northern NSW in order to explain the seasonal clustering of events in winter. These factors may be less variable in the north where events are more evenly spread throughout the year. For instance, flying foxes may spend more time feeding in agricultural landscapes (e.g. horse paddocks) in winter in the subtropics due to loss of winter feeding habitat, increasing the opportunities for horse exposure; this seasonal dietary shift may not be as apparent in the northern tropics (Plowright et al., 2015).

Scanlan et al. (2014) developed a viral survival model based on similar experimental data to that used here. The overall structure of their model and methods were similar; however, their results and conclusions differ from mine. They stated that HeV survival is a major driver of transmission and seasonality, and that the absence of detected events in the south during summer is driven by chance. In contrast, I found that virus survival did not influence the pattern of spillovers. I identified three main reasons for the different results. First, Scanlan et al. (2014) include recording error. The interval between virus titrations during the survival experiment at 56℃ was 10 min. Scanlan et al. (2014) reported this to be 10 h, and based their half-life estimates and subsequent regression analysis on this unit of measurement. The second reason is the use of

different models; Scanlan et al. (2014) used an exponential model compared with a Weibull model used here. As mortality rates are usually not constant over time, there is little support for the use of the exponential model in survival studies (McCallum, 2000; Peleg and Cole, 1998). To account for such an effect, other models and distributions (e.g. Gompertz, Gamma or Weibull) are usually more appropriate (Gil et al., 2011; van Boekel, 2002). The Weibull is simple and flexible enough to account for constant, accelerating or decelerating rates. This is possible thanks to the shape parameter κ, which modifies the instantaneous hazard of death. In fact the exponential model is a special case of the Weibull model when $\kappa = 1$, such that the instantaneous hazard of death is constant through time (McCallum, 2000). The third reason is the use of additional data points taken from experiments not designed to measure the effect of temperature (Fogarty et al., 2008). These data points alter the relationship between half-life and temperature. Another contributing factor is that the model used to estimate half-life in Fogarty et al. (2008) (one-phase exponential decay) was different from that used by Scanlan et al. (2014) (linear regression between ln $TCID_{50}$ and time). Consequently, half-lives used do not correspond to measurements of the same processes with equivalent models. Rather, they are a mixture of half-lives of survival experiments under urine interpolated with a one-phase decay model and survival experiments in EMEM interpolated with the classic exponential model.

Although I was unable to find a substantial effect of temperature on the epidemiology of HeV through virus survival, there are other ecological processes involved that are influenced by temperature. For instance, present and past temperatures affect the flowering status of many native *Eucalyptus* species (Hudson et al., 2010), which then influences the distribution and abundance of flying foxes, the reservoir hosts. Temperature also influences pasture quality and the feeding behaviour of horses(Plowright et al., 2015). I also have to consider that absolute abundance of HeV is not only a function of its mortality, but of the excretion rate and the number of infected flying foxes (Field et al., 2011). For example, with more infected flying foxes, more fruiting or flowering trees attracting more flying foxes can increase environmental loads of HeV. It has been shown recently that black and spectacled flying fox densities are higher in areas where spillovers occur (Smith et al., 2014). On the horses side, conditions that increase the time horses spend under trees, basic management practices such as feeding horses and placing water troughs under trees may increase opportunities for horse exposure to the virus (Plowright et al., 2015).

Despite the advantage of the wide range of temperatures in the experiments, there is no information to validate my simulations because the response of HeV is probably different under

changing temperatures. Another limitation is that the interval between measurements is too wide to precisely estimate half-lives. Thus, I recommend that future survival experiments be performed over shorter time periods that allow more confidence for interpolation. Experiments should also include the effect of other potential processes that affect HeV survival, such as desiccation and UV radiation (Zhao et al., 2012).

I conclude that the timing and geographical distribution of HeV spillover events cannot be explained by virus survival in the environment. Spillover events occurred when the suitability of temperatures for survival was intermediate to very low. Transmission routes requiring short periods of virus survival, such as direct contact with fresh bat excreta, are likely to be important, whilst routes of transmission requiring longer survival, such as consumption of contaminated feed, may be less important. The winter-dominant seasonal pattern of HeV transmission to horses in southern Queensland and northern NSW is likely driven by an additional seasonal factor (not virus survival alone), such as the relative availability of food for flying foxes in horse paddocks. In summary, virus survival in the environment is unlikely to be the driver of the pattern of spillover events. I must explore other seasonal risk factors that occur periodically at southern latitudes but are relatively constant in the tropics. Behavioural studies of the interactions between flying foxes and horses are needed to determine the route of HeV transmission.

Chapter 4

Microclimates rarely allow indirect spillover of the bat-borne zoonotic Hendra virus

The previous chapter describes how spillover is affected by potential survival of HeV in the environment. I demonstrated how the poor predictive capacity of environmental survival of HeV indicated that transmission could be relatively direct from flying foxes to horses. Relatively direct transmission indicates, however, that the virus in some circumstances is capable of surviving in the environment until contact with a susceptible horse occurs.

The HeV survival estimates in Chapter 3 (Martin et al., 2015) were obtained with air temperatures. Most of HeV excreted in paddocks occurs under the trees where flying foxes feed (Field et al., 2011). The microclimatic conditions that occur in these areas are unlikely to be similar to air temperatures as measured in meteorological stations, because temperature and evaporation rates in the soil result from different physical processes due to the structures that surrounds them (Kearney et al., 2014). To obtain more reliable estimates of HeV's potential survival I sampled the microclimatic conditions that occur under trees in horse paddocks in the area of Townsville.

To measure the effects of the microclimatic conditions on HeV survival I used Bayesian mixed effects models, and re-fitted a modified version of the survival model from Chapter 3 (Martin et al., 2015). The Bayesian models predict microclimatic conditions using meteorological station data, and can therefore be used for other more general purposes than for just understanding HeV survival. I used the predictions of the microclimate models to create different indicators of HeV survival capacity under these conditions. In addition, based on the lower survival of HeV under desiccation (Fogarty et al., 2008) I developed a measure of how likely survival estimates with temperature are lowered due to desiccation, by calculating the probability that there will be evaporation.

In relation to the conceptual spillover framework described in Chapter 2, I studied in what circumstances the layer *pathogen survival outside hosts* could be present. Therefore, finding the environmental characteristics that increase the chances of contact between horses and HeV.

This chapter was published in Microbial Ecology (Martin et al., 2017):

- Gerardo Martin, Rebecca J. Webb, Carla Chen, Raina K. Plowright, and Lee F. Skerratt. Microclimates Might Limit Indirect Spillover of the Bat Borne Zoonotic Hendra Virus. *Microbial Ecology*, pages 1–10, 2017. ISSN 0095-3628. doi: 10.1007/s00248-017-0934-x. URL http://link.springer.com/10.1007/s00248-017-0934-x

ABSTRACT

Infectious diseases are transmitted when susceptible hosts are exposed to pathogen particles that can replicate within them. Among factors that limit transmission the environment is particularly important for indirectly transmitted parasites. To try and assess a pathogens' ability to be transmitted through the environment and mitigate risk we need to quantify its decay where transmission occurs in space such as the microclimate harbouring the pathogen. Hendra virus, a Henipavirus *from Australian Pteropid bats spills-over to horses and humans, with apparently high mortality rates. While a vaccine is available, its limited uptake has reduced opportunities for adequate risk management to humans, hence the need to develop synergistic preventive measures, like disrupting its transmission pathways. Transmission likely occurs shortly after virus excretion in paddocks, however no survival estimates to-date have used real environmental conditions. Here I recorded microclimate conditions and fitted models that predict temperatures and potential evaporation, which I used to simulate virus survival with a temperature-survival model and modification based on evaporation. Predicted survival was lower than previously estimated and likely to be even lower according to potential evaporation. Our results suggest that relatively direct transmission is more likely under average conditions, however, indirect transmission may occur within a narrow range of microclimate circumstances. I recommend restricting horses' access to trees during night time and reducing grass under trees to reduce virus survival.*

Introduction

Infectious diseases are transmitted when viable infectious agents are successfully introduced and are able to reproduce in the body of a susceptible host (Ewald, 1987). Factors that have the

potential to reduce or increase the likelihood of transmission include, but are not limited to; reservoir host immunity, excretion routes, the environment (temperature, humidity, wind speed) (Sultan et al., 2005; Shaman et al., 2010), presence of vector hosts, the immune system of the receiving host and the target organs of infection. The effect of these factors will differ depending on the mode of transmission of the parasite (whether it be vector, direct or indirect). For instance the ability to survive in the environment is particularly important for indirectly transmitted parasites (Walther and Ewald, 2004). This parasite-environment interaction can determine the magnitude of the transmission rate among individuals (McCallum et al., 2001). Consequently the ability to be transmitted indirectly might depend on the predominant environmental conditions that the parasite experiences while awaiting contact with a susceptible host. Therefore, to try and infer the most likely transmission route of a parasite in order to disrupt it and mitigate its impact, we need to understand the consequences of its interaction with the environment.

Accurate environmental data is essential to predict the decay of a parasite population in that environment. When microorganisms are excreted on to the ground they experience several different micro-climatic conditions.Microclimates essentially differ from macroclimates in the spatial scale of their variability. Microclimates in the context of this study are the environmental conditions in small areas that are influenced by its prevailing substrate, topography and vegetation structures that surround them (Chen et al., 1996). While macroclimates change more gradually in space. There are existing models to predict the air temperatures at different heights above ground that might result from interactions of solar radiation and wind with shade and type of soil (Kearney et al., 2014). However, these models are uninformative of the potential variability of structures that make up the conditions at a scale that is relevant for a microorganism's survival. Hence, we need a framework that allows us to understand and easily predict the range of conditions that occur in the structures where hosts and parasites are more likely to contact each other.

Hendra virus (HeV), a Paramyxovirus of the genus *Henipavirus* was discovered in an outbreak involving the death of 14 horses and one human (Murray et al., 1995b). Its reservoir hosts are the four mainland Australian flying fox fruit bats (Chyroptera:Pteropodidae:*Pteropus*), although *Pteropus alecto* and *P. conspicillatus* seem to be the most important reservoirs (Smith et al., 2014; Edson et al., 2015; Martin et al., 2015). Transmission from flying foxes to horses is thought to occur after ingestion of urine contaminated feed. This hypothesis has been considered plausible given the ability of HeV to survive for up to 4 days in fruit juice and urine in laboratory conditions at 22 and 37 ℃, although HeV is extremely sensitive to desiccation at these temperatures (Fogarty

et al., 2008). Even under the best virus survival scenario represented by air temperatures, spillover has not occurred in areas with the highest possible survival during certain seasons (Martin et al., 2015). This suggests that survival as explained by air temperature is not important for spillover, and transmission is likely to be relatively direct. Regardless of these large scale patterns, which might be driven by other temperature related processes or heterogeneous HeV shedding patterns (Field et al., 2011), more accurate estimates of HeV survival are necessary to better understand its transmission to horses. Therefore we need to more closely investigate and estimate the survival of HeV in the environment using accurate microclimatic measurements.

Here I studied the microclimates where HeV is excreted and developed a series of models that predict these conditions using data from meteorological stations. I used the microclimate models' predictions to estimate survival re-parametrising a published HeV survival model (Martin et al., 2015). The main reasons for using a laboratory based model were that performing HeV survival experiments in the field replicating the conditions it experiences in paddocks would be unethical given its BSL4 classification. In addition, using other viruses like Cedar (Marsh et al., 2012), does not guarantee equivalence, and recovery of the viruses from the relevant substrates could be very problematic (Fogarty et al., 2008). Because HeV is highly sensitive to desiccation, using a model of potential evaporation (Fogarty et al., 2008) I calculated the probability that survival is shorter than estimated with the temperature only model due to evaporation.

Methods

The study system

Air or bare soil temperatures alone are not widely representative of the climatic conditions experienced by HeV excreted in horse paddocks, but to date they are the only climatic variables used to model HeV survival (Martin et al., 2015; Scanlan et al., 2014).To estimate HeV survival under the conditions the virus more likely experiences in paddocks I sampled microclimates. I generated a series of statistical models that predict microclimatic conditions using data from meteorological stations and measures of physical structures that surround microclimates (grass length and canopy openness) as explanatory variables of the measured microclimates.

I generated estimates of HeV survival in microclimates coupling a temperature-virus survival model with the microclimate temperature predictions of two temperature models; one for minimum and another for maximum temperature. HeV survival in response to constant temperatures

was estimated from laboratory data with the Weibull model (Martin et al., 2015):

$$S(t) = \exp\left(-\rho t^{\kappa}\right) \tag{4.1}$$

Equation 4.1 means that the proportion of virus surviving S is a function of time t that decays at a rate ρ. The instantaneous rate of decay can in addition decrease or increase with time depending on the size of the shape parameter κ. If $\kappa < 1$ the immediate rate of decay decreases with time, when $\kappa = 1$ it is constant, and when $\kappa > 1$ it increases with time (McCallum, 2000; van Boekel, 2002). I modified Martin et al. (2015)'s (Chapter 3) model to make it more numerically stable. The original model transformed both parameters ρ and κ in functions of temperature because both are temperature (T) dependent according to the survival data (Appendix 9.6.3.2). In the original formulation $\kappa(T) = \alpha_{\kappa} + \exp(\beta_{\kappa} T)$. One problem with this formulation is that it only makes sense if $\alpha_{\kappa} \geq 0$. To fix this I used $\kappa(T) = \exp(\alpha_{\kappa} + \beta_{\kappa} T)$ hence the modified model in equation 4.2 (keeping the original formulation for $\rho(T)$):

$$S(t, T) = \exp\left[-\exp\left(\alpha_{\rho} + \beta_{\rho} T\right) t^{\exp(\alpha_{\kappa} + \beta_{\kappa} T)}\right] \tag{4.2}$$

All the models were fit in a Bayesian inference framework using JAGS (Plummer, 2003) for Markov chain Monte Carlo (MCMC) simulation and sampling. The temporal scale of the HeV survival data was modified to hours to match the scale of the recorded microclimate data.

I used these models to estimate the potential range of HeV survival 12 h after excretion, the time elapsed to death of 90% of the virus and the probability that the proportion of viable HeV in paddocks is greater than 0.01 24 h after excretion. I chose these thresholds because 1) HeV survival was previously reported to be very low 12 h after excretion in soil conditions (Martin et al., 2015), 2) to have a time scale measure of potential survival capacity and 3) to assess if there is potential for HeV accumulation over successive days of excretion. In order for accumulation to occur, the proportion of viable HeV has to be greater than sterility conditions (10^{-4}, van Boekel, 2002) once virus excretion is resumed (24 h later).With the analyses of potential evaporation, I estimated the probability that survival is lower than estimated with the survival model based on temperature alone.

Sampling the microclimates

I measured temperature and relative humidity of microhabitats with Hygrochron iButton© data loggers at 15 minute intervals during day and night from September 2014 to August 2015. I

used the 15 min interval to maximise the likelihood of registering temperature and humidity extremes used for data analysis, while still being able to record data for a long period. Loggers were deployed in four different paddocks up to 20km north and south of Townsville, Queensland, Australia, which lies within the known distribution of spillover of Hendra virus. The criterion to select study sites in which to deploy the data loggers was: 1) properties had to have paddocked horses, 2) paddocks had to have at least three trees with various degrees of canopy openness and grass of variable length, 3) paddocks had to be within the distribution of *P. alecto*, 4) access had to be granted by owners after signing a confidentiality agreement. In each property I selected at least three trees with different degrees of canopy openness, and three grass/ground vegetation heights to cover the range of microclimates that potentially exist in paddocks that are relevant for HeV survival (Field et al., 2011, Figure 4.1).

I measured canopy openness with hemispheric photographs with a Vivitar 0.21× fisheye converter lens attached to a 14-42 mm Panasonic lens. Pictures were processed with the Gap Light Analyser (GLA, Frazer et al., 1999). I took all photographs at dawn, dusk or on cloudy days so that the background was brighter than foliage and branches that make up the canopy structure. This was necessary because GLA requires high contrast images between foliage and sky to calculate the area open to direct sunlight. Because some of the Eucalyptus species have very light coloured bark, their canopy pictures had to be pre-processed manually to darken the bark.

I measured grass height with a measuring tape from the position of the data logger to the tip of the leaves of the main mass fo grass that was covering the data logger. The long and medium grass treatments were enclosed in a 15cm diameter circle with chicken wire and secured to the soil with turf pegs and plastic coated wire. This protected the grass from being eaten by horses and helped to keep the microclimate in more constant conditions.

Data were downloaded from data loggers every 21-42 days whenever possible within this interval because by day 42 the memory of the data logger was full. Sampling the height of vegetation or downloading the data within the mentioned period depended on access to the property where loggers were deployed. I measured grass length continuously with a measuring tape, from the ground level to the tip of the leaves that made up the principal mass, ignoring the long leaves that frequently stand out but contribute very little to the total mass. I adjusted the length where necessary if grass had grown, been eaten or completely disintegrated after drying out. For those intervals where grass was growing/decreasing fast and continuously such that there was not enough grass length data, I interpolated the height linearly between the beginning

and end of the data recording period. In cases where the grass was mowed I identified the date of mowing and registered the height before and after the mowing date and used those measurements in the analyses. To maintain the grass levels of the sampling design I moved the logger to the nearest patch of grass with the correct height.If the change of position resulted in significantly new conditions, apart from the new grass height, I recorded the new canopy openness for use in the statistical analyses.

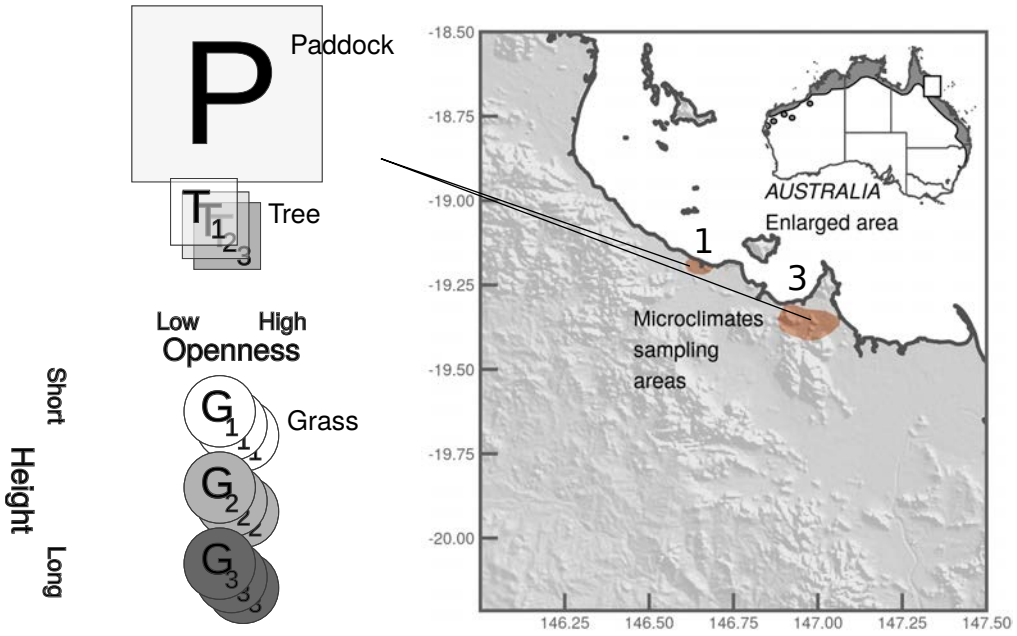

Figure 4.1: Geographic location of the areas where microclimates sampling took place and the sampling design used in the four different paddocks. *P* paddock, *T* tree, *L* logger, *G* grass. The number in the map indicates the number of paddocks in each of the sampling areas.

Analyses

I analysed all data with Bayesian models using a MCMC sampler for inference implemented in JAGS 4.0 (Plummer, 2003) interfaced in R (R Core Team, 2016) with the R2jags package. I estimated parameters for the survival model in equation 4.2 using flat priors with 10^{-4} precision for all parameters, 10M iterations, a burn-in rate of 3M and a thinning rate of 10K.

From the recorded temperature and humidity data I only used the daily minimum and maximum temperatures and relative humidity to fit models. This was necessary as only minimum and maximum air temperatures were available from meteorological stations. I transformed relative humidity to absolute humidity and/or potential evaporation as described in the following subsec-

tion. Before fitting the microclimate models, I performed an exploratory analysis to identify the type of correlations and variance structures between and within explanatory (macroclimate and vegetation) and response variables (microclimate), and assessed visually the type of statistical distribution of the response variables. Macro climate data was obtained from the bureau of meteorology of Australia [1].

For each microclimatic variable I fitted a series of models with combinations of all explanatory variables and their plausible interactions. In addition to these main effects I included a random effect for paddocks. In all cases I used non-informative normal priors with 10^{-4} precision to let data dominate the posterior distributions. Each model was fit with 3 chains of 50K iterations, a burn in of 10K and a thinning rate of 30. To select models I compared their convergence and deviance information criterion (DIC), and selected the model with the smallest DIC value. DIC is a fully Bayesian measure of goodness of fit, relatively equivalent to the Akaike information criterion used in frequentist statistics (Spiegelhalter et al., 2002). Then I performed a posterior predictive check of the selected models, looking for a prediction rate as close as possible to 50%. This means that data has to resemble approximately 50% of the posterior samples (the mean of the posterior samples, Gelman et al., 2013). These checks were only done with the temperature and humidity models, as there is currently no HeV survival data to validate predictions of survival in paddocks.

Analysis of the humidity data

The recorded relative humidity data was transformed into absolute humidity and potential evaporation (Myatt et al., 2010; Zhao et al., 2012). Humidity at minimum temperature was analysed as absolute humidity, and humidity at maximum temperature was analysed as potential evaporation. The procedure followed to transform data is described in the supplementary materials.

Survival simulations

I simulated HeV decay by coupling the survival model with the predictions of the temperature models. With these simulations I generated a timeline of the expected amount of virus remnant 12 hours after excretion, time lapsed until 0.1 of the virus was left and the probability that the surviving proportion is greater than 0.01 24 h after excretion. These simulations assume that excretion only occurs once in the night while temperature is at its minimum, to avoid having to

[1] http://www.bom.gov.au

cumulatively calculate several different survival curves. This approach represents the optimal scenario for virus survival because HeV decay is highest during the first moments after excretion, and so its highest rate of decay would occur during the lowest temperatures. In addition at higher temperatures the immediate rate of decay is faster and the shape parameter gradually increases towards 1 which means it does not decelerate as much as it does at lower temperatures (Martin et al., 2015).

To prepare data for simulation I used a random subset of 2500 parameter combinations out of the nearly 4.66 billion possible combinations between the survival and temperature models' parameters. This combination results from the posterior parameter estimates for each model (4002 $_{min}\times$ 4002 $_{max}\times$ 2910 $_{survival}$). A list of parameters and their values is given in supplementary information. For each simulation run I accounted for temperature changes over time with a cosine wave. I calculated the probability of observing a reduction in calculated survival rates based on the simulated potential evaporation per day. To indicate potential extent of virus survival reduction I generated a timeline of potential evaporation in the soil. I ran these simulations in two contrasting scenarios, one with short grass and high canopy openness (5 cm and 77%), and another with long grass and low canopy openness (40 cm and 5%).

Results

Virus survival simulations

Virus surviving 12h after excretion was higher in the scenario with long grass and low canopy openness compared with short grass and high canopy openness (40 cm grass – 5% openness vs 5 cm – 77.6%, Figure 4.2). When I estimated the time elapsed until death of 90% of the virus (Figure 4.3) a difference of up to 24 hours (upper 95% credible interval) between scenarios was observed in winter when minimum soil temperature was 10℃ (Figure 11, Appendix 9.6.3.2). The greatest difference between scenarios was seen in the probability that survival rates were greater than 0.01 24h after excretion (Figure 4.4). In short grass (low probability scenario), the probability that more than 1% of the virus is left is almost zero all year long, except for winter where it is nearly 0.15. However, in long grass, (high probability scenario), it rarely falls to 0.5, and mostly stays close to 1. But, survival rates are also likely to be lower than 10% of excreted virus.

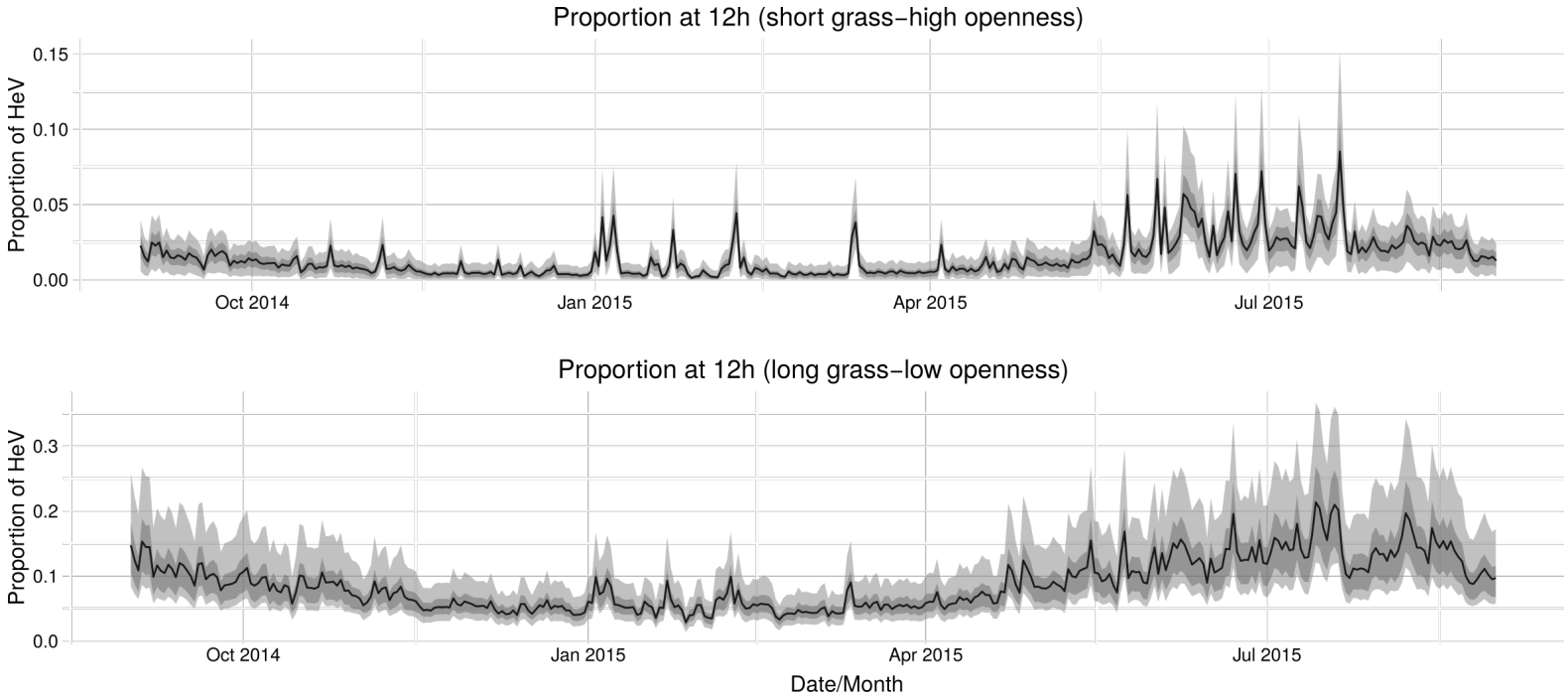

Figure 4.2: Simulated survival between two contrasting scenarios. Light gray ribbons show the upper and lower 95% credibility intervals.

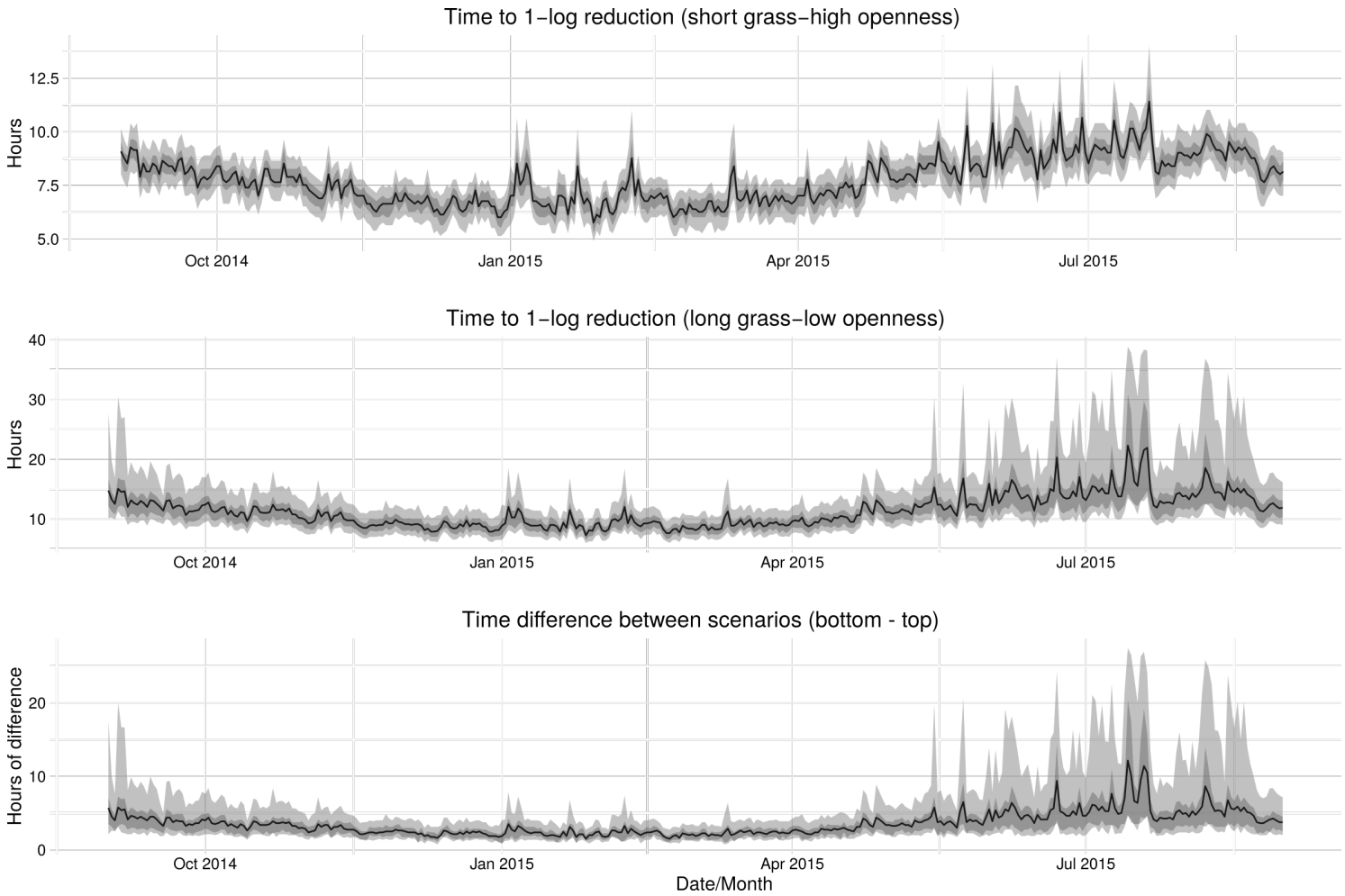

Figure 4.3: Simulated timeline of hours to death of 90% of the free virus. Bottom panel show the difference between scenarios, therefore, the greatest difference occurs in July/August where there is a maximum ca. 24h difference (95% Cr. I.).

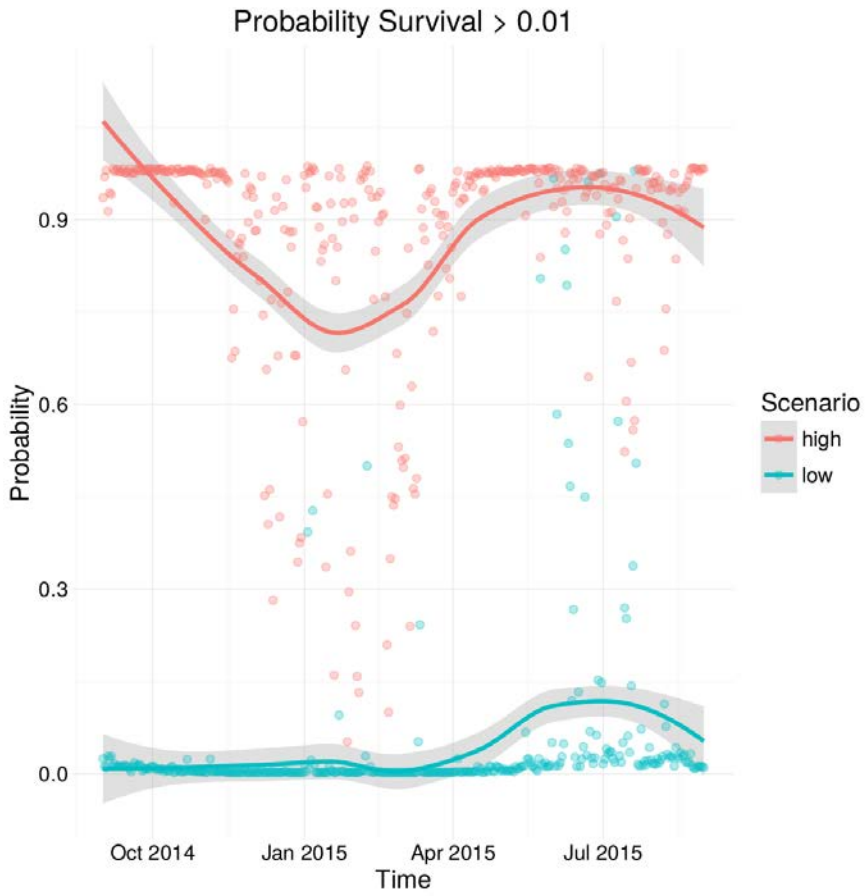

Figure 4.4: Probability that survival rates 24h after excretion are greater than 1%. Lines are the smoothed trend and points are the probability estimates in time. Low = low grass/high canopy openness, High = high grass/low canopy openness.

Microclimate temperature models

The microclimate minimum temperature model was the simplest because minimum temperature in the soil is highly correlated with air minimum temperature. Of all explanatory variables, air minimum temperature explained the most variance, followed by canopy openness. This model had a DIC=35554.9 and R^2=0.856. Despite this high correlation with air temperature, grass and openness had small negative effects on ground level temperatures and removing these variables increased the DIC (Table 2). Minimum temperatures in long grass tend to be less than one degree higher than in short grass and low canopy openness, with P=0.25 of being higher. This temperature difference between minimum temperature scenarios results in immediate shorter half-life in long grass (Figure 12).

Both variables had a positive effect on temperature variance. The posterior predictive checks resulted in prediction rates of 47.64%. Structure of the final model:

$$\mu_{\text{soil}_{min}} = \alpha + \beta_1 Temp_{\text{air}_{min}} + \beta_2 Grass + \beta_3 Open + \gamma_{\text{property}} \tag{4.3a}$$
$$Temp_{\text{soil}_{min}} \sim \text{normal}(\mu_{soil_{min}}, \tau \cdot 1/(Grass + Open))$$

Where $Temp_{\text{soil}_{min}}$ is the minimum temperature recorded in the data logger, $Temp_{\text{air}_{min}}$ is the minimum air temperature and *Grass* and *Open* are the grass and canopy openness measurements. Parameters that were estimated were α the intercept, subscripted β are the effects of each variable, τ is the precision (inverse of variance) which was affected by grass length and canopy openness, and γ is the random effect per property.

Microclimate maximum temperature is more variable and consequently its model was more complex, including two interaction terms, between Openness and Sunshine and Grass and Openness. Its DIC = 68818.8 and R^2=0.485 (0.479-0.487, 95% Cr.I.). In this model, the variables that explained more variance in decreasing order were Openness, the interaction between Grass and Openness and Air maximum temperature. Both Grass and Openness on their own have positive effects on temperature but their interaction has a negative effect (Table 3). The posterior predictive checks show a 50.71% prediction. A timeline of predicted maximum and minimum ground temperatures of Townsville is shown in Figure 11.

$$\begin{aligned} \mu_{\text{soil}_{max}} =& \alpha + \beta_1 Temp_{\text{air}_{max}} + \beta_2 Grass + \beta_3 Open + \beta_4 Sun \\ &+ \beta_5 Open \cdot Sun + \beta_6 Grass \cdot Open + \gamma_{\text{property}} \\ Temp_{\text{soil}_{max}} &\sim \text{normal}(\mu_{\text{soil}_{max}}, \tau \cdot 1/(Grass + Open)) \end{aligned} \tag{4.4a}$$

Where $Temp_{\text{soil}_{max}}$ is the recorded soil maximum temperature, $Temp_{\text{air}_{max}}$ is the air maximum temperature from the meteorological station, and *Sun* is the hours of sunshine from the meteorological station.

Maximum temperature in short grass was always higher than temperatures in long grass and low canopy openness. The temperature difference between these scenarios was close to 20℃ (Figure 11).

Microclimate evaporation and humidity models

Microclimate humidity at minimum temperature was transformed to Absolute humidity for analysis. Its final model included four explanatory variables, Grass, Openness, Absolute humidity

of air and the interaction between Absolute humidity of air and Grass. Of these, the variable explaining more deviance was Absolute humidity of air, followed by Grass. This model's DIC=-26623.1 and R^2=0.755 (0.754-0.755). As determinants of microclimate absolute humidity, openness and grass have negative and positive effects respectively, that is, higher openness decreases absolute humidity and longer grass increases it. The interaction between grass and air absolute humidity had a negative effect, probably due to the negative effect that grass has on temperature (see above results on minimum temperature) (Table 4).

$$\mu_{H\ \mathrm{soil}_{max}} = \alpha + \beta_1 AH_{\mathrm{air}_{max}} + \beta_2 Grass + \beta_3 Open + \beta_4 Grass \cdot AH_{\mathrm{air}_{max}} + \gamma_{\mathrm{property}} \tag{4.5a}$$

$$AH_{\mathrm{soil}_{max}} \sim \mathrm{normal}(\mu_{H\ \mathrm{soil}_{max}}, \tau \cdot 1/(Grass + Open))$$

Minimum microclimate humidity (humidity at maximum temperature) was modelled as potential evaporation. This model was more complex than the model of maximum microclimate humidity. It contained two interactions between Sunshine and Openness and between Grass and Air potential evaporation. The variables explaining more deviance were the interaction between Sunshine and Openness and Air temperature, which had a positive and negative effect respectively (Table 5). The posterior predictive checks rendered 48.97% prediction, and the DIC=-3510.2, R^2=0.786.

$$\begin{aligned} \mu_{Evap\ \mathrm{soil}_{min}} =& \alpha + \beta_1 Temp^2_{\mathrm{soil}_{max}} + \beta_2 Evap\ pot_{air_{min}} + \beta_3 Temp_{\mathrm{air}_{max}} \\ &+ \beta_4 Sun \cdot Open + \beta_5 Grass \cdot Evap\ pot_{\mathrm{air}_{min}} + \gamma_{\mathrm{property}} \\ Evap_{\mathrm{soil}_{min}} &\sim \mathrm{normal}(\mu_{Evap\ \mathrm{soil}_{min}}, \tau \cdot 1/(Grass + Open)) \end{aligned} \tag{4.6a}$$

Evaporation, both at minimum and maximum temperature is consistently higher in short grass/high openness compared with long grass/low openness (Figure 4.5). The probability that evaporation is higher under short grass/high openness than evaporation in long grass/low openness is ≈1.

Virus survival model

The model converged with 10M iterations, and I obtained the following half-life (HL) estimates for the experimental temperatures; HL_4=2.64 h (0.28-7.44, 95% credibility intervals), HL_{22}= 0.52 h (0.14-1.06), HL_{56}=0.02 h (0.021-0.028, Figure 8). Response to each of the fitted temperatures and the surface of the model are shown in Figure 9. I compared estimates of this fitted model with that

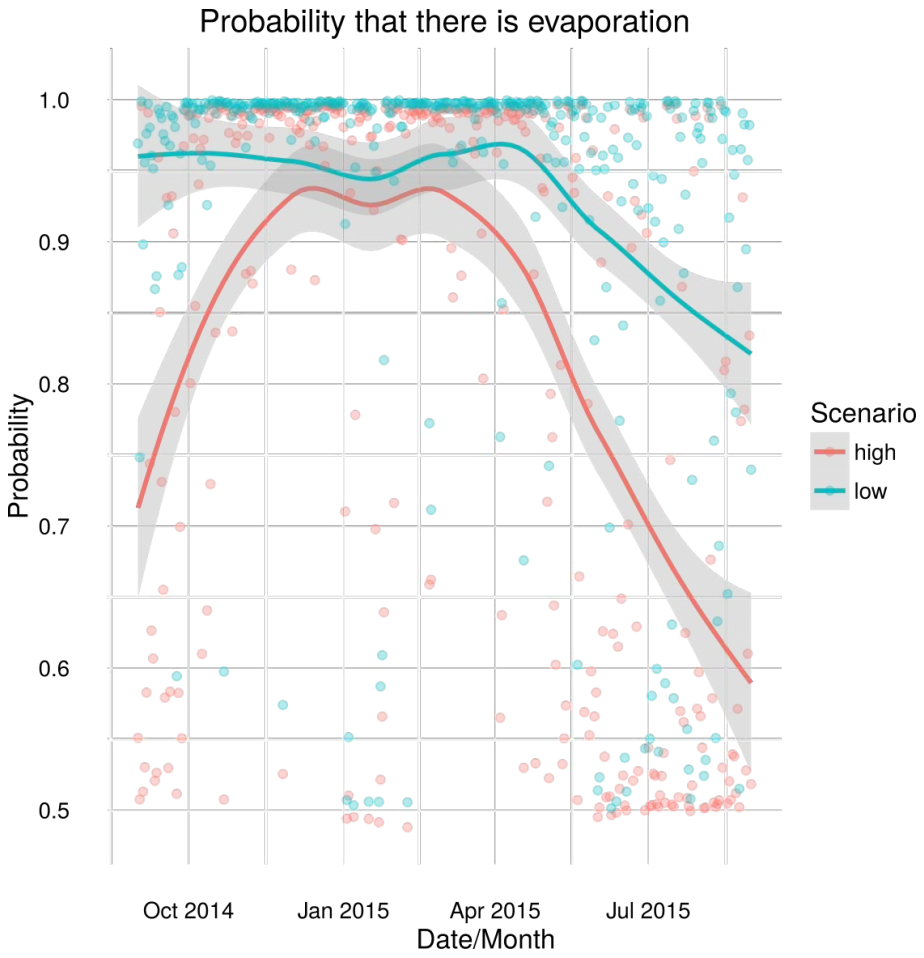

Figure 4.5: Smoothed probability that evaporation occurs in two contrasting scenarios. Low = low grass/high canopy openness, High = high grass/low canopy openness. Assuming that potential evaporation drives death by desiccation, the occurrence of evaporation can be interpreted as probability that survival is lower than estimated under the temperature conditions of the simulations.

of Martin et al. (2015), and did not identify major differences. Although, when I fitted the model using the first eight data points for each temperature, the half life estimates were noticeably lower than those of Martin et al. (2015). As a result, I kept the model parameters estimated with the first five data points (results not shown). The effect of removing those points has no effect on the quality of analyses since the removed data points correspond to virus titrations at times that far exceed the time used to evaluate survival here.

Temperature has an effect on both shape and rate parameters of the Weibull distribution, κ and ρ respectively. These parameters control how decay changes with time (κ) and how steep decay is (ρ). In the case of HeV, both parameters are controlled by temperature. Given parameter estimates, decay rate decreases with time ($\kappa < 1$). The effect of temperature on this parameter indicates that at higher temperatures, immediate rates of decay are higher. That is, at higher temperatures, greater proportions of HeV die immediately after excretion because $\kappa(56) = 0.44$ $(0.21 - 1.02, 95\%$ Cr. I.), $\kappa(22) = 0.53$ $(0.3 - 0.89)$, and $\kappa(4) = 0.58$ $(0.36 - 0.83)$.

Discussion

Estimated survival rates of HeV were consistently higher in long grass and low openness compared with short grass and high openness. Differences were consistent among all monitored thresholds, survival 12h after excretion, time elapsed until death of 90% of the virus and probability that survival rates were greater than 0.01 24h after excretion. Overall survival estimates based on temperatures suggest that potential for accumulation is higher in long grass during winter and evaporation increases this disparity all year round. These estimates, based on the most likely temperature conditions experienced by HeV excreted in paddocks, can be used to make informed decisions for active preventive management of HeV spillover in paddocks. Furthermore, the microclimate temperature and humidity models can be used for improving understanding of the effects of microclimates on the transmission of viruses and their environmental survival in general.

Previous estimates of HeV survival predicted an ability to survive for much longer than 24 h, suggesting great potential for accumulation if live HeV was excreted on successive days (Scanlan et al., 2014), Here I demonstrate that under the real temperature conditions experienced by the virus in the environment, survival for more than 24h is feasible under very specific circumstances; long grass/low openness and no evaporation, although at much lower levels than the mentioned study and likely at biologically insignificant levels. Studies of bat movements indicate that bats

return to feed in the same tree on consecutive nights. Therefore, there is potential for an infected bat to excrete virus repeatedly in the same tree for the length of its infectious period (Plowright et al., 2015). However, the necessary temperature, humidity, grass length and canopy cover conditions for significant virus accumulation over a period of days leading to an increase in spillover risk might not generally present, although this could be different in subtropical wet areas.

Based on the current knowledge of HeV survival capacity I cannot predict the exact evaporation dependent rates of decay. I infer that decay should increase monotonically with potential evaporation because Fogarty et al. (2008) calculated a 1200 times reduction of half-life between survival with and without desiccation at 37℃ and evaporation is temperature and humidity dependent (Myatt et al., 2010; Zhao et al., 2012). Hence, the predicted survival rates at 12h shown in Figure 4.2 could decrease in a magnitude proportional to what is shown in Figure 12 (potential evaporation, Appendix 9.6.3.2). The effect of humidity on survival and transmission seems to differ among viruses. For instance, higher absolute humidity decreases influenza transmission and survival of influenza in the air (Shaman and Kohn, 2009; Myatt et al., 2010), while Gumboro virus survival increases with relative humidity (Zhao et al., 2012). Additional factors that can further decrease HeV survival in microclimates are UV and dust (Chang et al., 1985; Kramer et al., 2006). To date, the effects of UV on HeV have not been tested, but it is an effective germicide, and enveloped viruses like HeV are usually highly sensitive to it (Chang et al., 1985). Furthermore, desiccation, exposure to UV radiation and dust, are likely to change the HeV response to temperature, accelerating the rate of decay in time through cumulative damage, a known phenomena in populations of free living microorganisms (van Boekel, 2002). In support of this, some of the HeV survival experiments of Fogarty et al. (2008), appear to show concave or convex non log-linear survival responses between substrates.

Previous attempts to quantify HeV survival rates in microclimates assumed that soil temperatures were up to 5 degrees lower than air temperature (Scanlan et al., 2014), or broad scale measurements of types of bare soil temperatures were used under different levels of shade (Martin et al., 2015). None of these studies have used the specific conditions that occur where HeV is excreted as I have done here. My results, not surprisingly, differ. On one hand I believe Scanlan et al. (2014) overestimate survival, because their microclimatic conditions represent a better survival scenario than air temperatures. On the other, Martin et al. (2015) underestimate survival because some of the temperatures used correspond to bare soil, sand or rock, which represent the

worst survival scenario. Our data suggests that HeV survival rates in most cases are probably lower than under air temperatures and higher than estimated at bare soil temperature.

I used the models with macroclimatic data from other regions to predict microclimatic conditions, however these predictions have not been validated. While temperature estimates seem reasonable given our current knowledge, there are other complexities I did not account for. For instance, sunshine hours is used to represent solar radiation, however radiation changes latitudinally, hence the effect of sunshine hours would be different farther south than in Townsville. In addition, topographic shading can result in further microclimatic differences, even in areas with similar macroclimatic conditions (Morecroft et al., 1998). These extrapolated predictions generated from Brisbane and Cairns (Appendix 9.6.3.2, Figures 14 - 20), and the resulting survival rates do not differ greatly from Townsville. These simulations show a similar pattern of lower survival than with air temperatures and higher than bare soil (Martin et al., 2015). For the reasons mentioned above, these simulations still need to be validated and their purpose is to show what survival might be like.

Martin et al. (2015)'s conclusion that virus transmission is likely to follow relatively direct routes is supported. This is because I found that evaporation and the consequent probability of survival reduction are relatively high at all times. However, I found that virus survival under the optimum microclimate temperature conditions experienced by HeV excreted in paddocks can be as long as 20 h, assuming that a 99% decay is required to significantly reduce risk to horses. In this case, 20h is certainly long enough for indirect contact to occur. Determining the length of time for optimal survival for spillover depends mainly on the minimum infectious dose and the amount of virus excreted by flying foxes. Consequently, indirect transmission during the night is more likely because HeV loads are higher, and during the day evaporation and UV radiation will very likely further increase temperature dependent decay, making virus transmission during the day and virus accumulation on successive days of excretion even less probable.

The experimental data used here was generated under tightly controlled laboratory conditions. What the data actually represents is the decay of a HeV population in EMEM culture medium (Scanlan et al., 2014) under constant temperatures. The first step taken to run these simulations was transforming the temperature into a function of time. I currently ignore how HeV actually responds to varying temperatures over time; the cumulative damage of different temperatures through time could result in different decay rates compared with constant temperatures. One feature of the HeV survival data that indicates that decay under varying temperatures would be

different is the lack of log-linearity. Log-linearity generally results from immediate response to an external factor like temperature when is there is no effect of the time of exposure (Peleg et al., 2005). In the case of HeV, its decay slows down with time. Consequently, there is an effect of the time of exposure to temperature, and the only way to assess the effect of exposure to varying temperatures is experimental validation.

The modification of the Weibull survival model with respect to Martin et al. (2015), resulted in shorter half-life esti- mates, especially at 4 °C. However, when survival simulations were performed, the difference between models given the range of termperatures used was negligible. Similarly, Scanlan et al. (2015), argue that the recording error in Scanlan et al. (2014), had no sensible effect on survival estimates due to the prevailing temperatures used in simulation of HeV decay. However, as with any empirical model, extreme care should be taken when they are used under conditions that are outside the range used to fit them. In sight of this I recommend that when the microclimate temperature models are validated, thorough comparisons of model predictions should also take place. Therefore the unvalidated nature of these studies should also serve to guide future research (Restif et al., 2012) towards refining mitigation strategies and incorporate into spillover risk meta-models.

Conclusions

I identified scenarios where small changes in conditions could lead to large changes in the amount of virus available to horses. These changes are caused by long grass and low canopy openness. Therefore, the reduction of pasture under trees can be an effective preventive strategy for indirect HeV transmission. However, restricting access to trees during the night is likely to reduce risk more effectively because transmission can be relatively direct. Further manipulation of microclimates might involve increasing canopy openness when feasible to increase the radiation that reaches the soil. These measures will likely reduce the probability that horses contact viable viruses either by in- creasing the decay rate of the virus or reducing the likelihood of horses feeding on Hendra virus contaminated areas of the paddock. I recommend that further research focuses on validating the predictions I produced for the northern and southern extremes of the distribution of HeV spillover, and that more accurate estimates of HeV survival in response to evaporation are obtained under laboratory conditions.

Part III

Reservoir host distribution: studying the effects of climate on Hendra virus spillover risk

Chapter 5

Climatic suitability influences species specific abundance patterns of Australian flying foxes and risk of Hendra virus spillover

The first condition for spillover to occur is the presence of reservoir hosts (Chapter 2, Plowright et al., 2015). Within the areas inhabited by reservoir hosts, HeV levels shed into the environment vary according to their own dynamics in the reservoir host (i.e. prevalence and intensity of infection), and how the reservoir hosts use the available space. Consequently spillover risk varies in space alone due to the distributional pattern of the reservoir hosts. When I started this study it was not known which of the four flying fox species that had been found with antibodies against HeV were more likely to be involved in spillover.

Here I used two ecological concepts to find which Australian flying fox species were more likely transmitting HeV to horses; the ecological niche and distance to the niche centroid of species. First an ecological niche is the set of environmental conditions that allow an organism's populations to breed and persist, by means of its effects on the organism's physiology (Soberon and Nakamura, 2009). The responses to each of the different environmental dimensions (temperature, rainfall humidity, etc.) can be used to relate them to the organism's geographic distribution. The process of finding the responses to the environment and relating them to space is known as ecological niche modelling (Owens et al., 2013). The resulting predicted geographical distributions depend mainly on the nature of data and the statistical or mathematical method used to estimate the niches, and its meaning is always subject to interpretation (Soberón and Peterson, 2005). Ecologically, realised distributions are the product of the intersection between the geographical space available for the species to move (M), areas where interactions with other organisms allow its survival (B, from

biotic) and geographical areas where its climatic characteristics (A, from abiotic) are tolerated by the species (Soberón and Peterson, 2005). The interaction between these tree factors results in realised distributions. However, including B, A and M is very difficult, especially B. Therefore, distributions are usually estimated based on A sampled from M (the area where the species selects its climatic niche) (Soberón and Peterson, 2005). This leads to distributional estimates based on the occupied climatic niche, and are smaller than those entirely based only on climatic tolerance (A), which is the fundamental niche. Such estimates are rarely met as only a subset of the entire scope of a species' climatic tolerances might exist, therefore estimates of the fundamental niche are termed the existing fundamental niche (Townsend Peterson et al., 2011). Consequently, distributional estimates sampled from A are intermediate estimates between the realised and the potential distribution.

The niche centroid, is given by the arithmetic mean of each dimension occupied by the species, and is regularly interpreted as the optimum set of conditions for the organism. Distance to this centroid therefore represents similarity with the optimum and can be calculated with any distance measuring method depending mainly on the correlation structure between the dimensions. This measure in many cases is negatively correlated with the organism's spatial abundance patterns (Martínez-Meyer et al., 2013). I used the ecological niche concept to identify the areas where the four flying fox species can survive, breed and persist (Hutchinson, 1957), and the distance to the niche centroid to find how population density of each flying fox species varied within their distributional areas (Martínez-Meyer et al., 2013).

Thanks to this study, there is today compelling statistical (Smith et al., 2014), epidemiologic (Edson et al., 2015) and ecological evidence (this study) to narrow down the main reservoir hosts of HeV to two of the four flying fox species, black and spectacled flying foxes, despite the frequent findings of HeV infection in all four species.

Below I describe the methods that I used to predict the potential distribution of the four flying fox species and how I modelled their abundance within these geographical distributions. Finally I describe how I related these large scale processes driving flying fox abundance in the landscape to HeV spillover.

This chapter has already been published as (Martin et al., 2016):

- Gerardo Martin, Carlos Yanez-Arenas, Billie J. Roberts, Carla Chen, Raina K. Plowright, Rebecca J. Webb, and Lee F. Skerratt. Climatic suitability influences species specific abundance patterns of Australian flying foxes and risk of Hendra virus spillover. *One Health*, 2:115–121, 2016. ISSN

23527714. doi: 10.1016/j.onehlt.2016.07.004. URL http://dx.doi.org/10.1016/j.onehlt.2016.07.004

ABSTRACT

*Hendra virus is a paramyxovirus of Australian flying fox bats. It was first detected in August 1994, after the death of 20 horses and one human. Since then its spillover has occurred regularly within a portion of the geographical distribution of all Australian flying fox (fruit bat) species. There is, however, little understanding about which species are most likely responsible for spillover, or why spillover does not occur in other areas occupied by reservoir and spillover hosts. Using ecological niche models of the four flying fox species I was able to identify which species are most likely linked to spillover events using the concept of distance to the niche centroid of each species. With this novel approach I found that 20 out of 27 events occur disproportionately closer to the niche centroid of two species (*P. alecto *and* P. conspicillatus*). With linear regressions I found a negative relationship between distance to the niche centroid and abundance of these two species. Thus, I suggest that the bioclimatic niche of these two species are likely driving the spatial pattern of spillover of Hendra virus into horses and ultimately humans.*

Introduction

Spillover of wildlife pathogens is a recurrent and often unpredictable phenomenon with important consequences for human and domestic animal health. Bats (Mammalia: Chiroptera) have been focus of considerable attention for their seemingly disproportionate diversity of viruses that are pathogenic to other mammal orders (Calisher et al., 2006). A few well known bat borne zoonotic viral diseases include Ebola, Marburg virus disease and SARS (Leroy et al., 2005; Swanepoel et al., 2007; Wang and Eaton, 2007). Despite their importance, spillover of these viral diseases is difficult to predict (Peterson, 2007; Peterson et al., 2004; Peterson, 2006; Pigott et al., 2014), partly due to the poor understanding of the viruses in their specific reservoir hosts and the ecological interaction of these hosts with the spillover hosts.

The abundance of reservoir hosts is an important determinant of the risk of pathogen spillover as it is a key driver of pathogen prevalence and disease transmission (Anderson and May, 1992; Keeling and Rohani, 2007). Spatial patterns of species abundance can be influenced by the climatic characteristics of the geographic areas inhabited by species (Martínez-Meyer et al., 2013). At the

very least, climate can predict where abundance is more likely to be higher (VanDerWal et al., 2009).

Ecological niche modelling (ENM) is a field of ecology that studies the environmental requirements of species. By using spatially referenced environmental and climatic data ENM is frequently used to identify geographic areas where species can survive and persist (Soberon and Nakamura, 2009; Owens et al., 2013). The abundance patterns of species within the predicted geographic ranges are often related to its location within the ecological and climatic niche (Martínez-Meyer et al., 2013). The different locations within climatic niches can be estimated by finding its multivariate centroid, which is formed by the mean of each environmental/climatic dimension of the niche. For instance the average of the maximum temperature or rainfall of wettest season across a species geographical range might represent a bi-variate niche centroid. Departures from the centroid in any direction are measured as environmental distance from the niche centroid (DNC). Consequently the DNC of reservoir host species could be used to better understand and predict the risk of spillover of emerging zoonotic pathogens.

One of these emerging zoonoses is HeV, belonging to the genus *Henipavirus* (Paramyxoviridae). It was discovered in Australia in 1994 after a respiratory disease outbreak involving the death of 20 horses and one human (Murray et al., 1995b). Hendra virus has been found to naturally infect the four Australian fruit bat species (genus *Pteropus*, also known as flying foxes, FF)2, the black flying fox, *P. alecto*; grey headed flying fox, *P. poliocephalus*; spectacled flying fox, *P. conspicillatus*; and the little red flying fox, *P. scapulatus* (Halpin et al., 2011). To date, infection in horses is rare and sporadic. Fifty-one spillover events have been recorded since September 1994, spanning nearly 1500 km of the east coast of Australia. The case fatality rates in horses and humans are approximately 75 and 50%, respectively (Geisbert et al., 2012).

Recent analyses suggest that black (*P. alecto*, BFF) and spectacled FF (*P. conspicillatus*, SFF) are more likely to be responsible for the HeV spillover events. This is based on the observation that the density of records of these two species is higher in areas where spillover has occurred (Field et al., 2011; Smith et al., 2014), and that HeV is more likely to be detected in these species (Edson et al., 2015; Goldspink et al., 2015).

Spillover events seem to be progressively expanding south, coinciding with the southwards expansion of *P. alecto* during the last few decades (Roberts et al., 2012). Although these correlations are statistically significant, an ecological explanation is still missing. This is because the rate of expansion of the BFF is faster than the rate of observed climate change (Roberts et al., 2012).

Despite the apparent lack of association, it is well known that FF have limited thermal tolerance that differs among the four Australian species. The different tolerance to environmental factors indicates that their fundamental niche is a key component of their realised distribution, making climate an important factor limiting their geographic distribution (Welbergen, 2008; Kearney and Porter, 2009). For instance, the range of overlap between the range of preferred rainfall levels results in the occasional overlap of *P. poliocephalus* and *P. conspicillatus* in the northern and southern limits of their respective known distributions (Parsons et al., 2010). Therefore it is unclear if the southwards increase of spillover is the result of the expanding range of *P. alecto* driven by climate of areas that could already be suitable for this species, or confounded by improved reporting and surveillance after the first New South Wales spillover case was detected in 2006 (McFarlane et al., 2011). One way to address the uncertain role of the four FF species is to look at the ecological suitability of spillover sites for each of the four potential reservoir host species.

One of the key determinants of ecological suitability for FF are their preferred food resources, which are dependent on climate. For example, the flowering status of several Eucalyptus species, the main food source for FF, is determined by climatic factors (Hudson et al., 2010). In addition, the spillover pathway of Hendra virus from FF to horses is directly linked to FF food resources, as transmission appears to be due to FF shedding virus in trees inside horse paddocks while foraging (Martin et al., 2015; Plowright et al., 2015). This provides an ecological basis for investigating the spatial suitability and abundance patterns of FF in relation to climate with correlative methods. Moreover,

Three previous studies have modelled the distribution of henipaviruses, first Peterson (2013) sought to identify conditions that allow transmission and persistence of Nipah virus (NiV) among hosts. Second, Daszak et al. (2013) modelled the present and future potential distributions of *Henipavirus* hosts; and, Smith et al. (2014) identified geographical correlates of HeV spillover. Other studies of bat borne zoonotic viruses have focused strictly on finding geographic areas of risk to human populations (e.g., Pigott et al., 2014, 2015). In this study I modelled the climatic requirements of HeV reservoir hosts. The models were then used to establish a relationship between suitability for FF and risk of HeV spillover based on the observed geography of spillover. Our results provide further evidence of the association of FF species with HeV spillover and potential drivers of the spatial pattern of spillover.

Methods

Predictions from niche models are a series of smoothed surfaces in the form of maps whose accuracy depends largely on the input explanatory environmental variables and their accuracy (Peterson, 2006; Owens et al., 2013). Correlative niche modelling relies on statistical relationships between environmental characteristics and geographical records of species presence (Phillips et al., 2006). In many cases reliable records of species absence are not available which has led to the development of algorithms that use presence only data, like Maxent (Phillips et al., 2006). Similarly, validation techniques have been adapted to this kind of presence only data. For example some model testing methods use the proportion of the study area predicted to be occupied by the species and the proportion of predicted presences; like the Partial ROC and Jacknife test (Peterson et al., 2008; Pearson et al., 2006). These methods compare prediction rates of the model on testing data by comparing prediction rates with a random spatial predictor (proportion of area predicted to be occupied). Maxent is a machine learning algorithm based on maximum entropy, that is similar to a Poisson regression (Renner and Warton, 2013), but has a logistic-like output and is capable of fitting non-linear relationships. The result is a series of response functions that provide an estimate of probability of species presence in relation to the assumed proportion of grid cells occupied by the species (Elith and Leathwick, 2009). Below I describe the methods I used to select the variables to model the niche of each FF species, validate the models and calculate the DNC of FF species of all pixels across the area where HeV spills over to horses and determine its relation to HeV spillover.

Niches of flying foxes

I obtained flying fox presence localities from the global biodiversity information facility database[1], the Atlas of Living Australia[2] and Roberts et al. (2012). The three databases were combined to maximise the number of records. Then I used an iterative method to eliminate localities within a pre-specified threshold distance to reduce spatial autocorrelation (Veloz, 2009; Elith and Leathwick, 2009), . This method first calculates the distance between pairs of points and identifies the pair that is closest. Then it eliminates the first point of the pair in the database, and the process is repeated until all remaining points are farther from each other than the specified threshold. The criterion to select the threshold distance was the maximisation of the model's performance on

[1] http://www.gbif.org
[2] http://www.ala.org.au

independent data, therefore I tried thresholds from 0.1-1 °. The filtered presence localities were then used to sample climatic raster data from the Worldclim[3] bioclimatic variables (Hijmans et al., 2005). In addition, points that were dubious or very far from the known distributional limits were removed, because niche models should only contain records of localities that are suitable for the species to breed and persist. Therefore, because the finding of individuals of highly mobile and abundant species, like flying foxes, very far from their known breeding habitat is not uncommon (Elith and Leathwick, 2009). For instance, the *P. poliocephalus* dataset, had presence records in New Zealand, which beyond any doubt has not had a strong effect on this species' recent evolution. For each bat species I selected a set of layers based on pairwise correlations between climatic variables and how the presence points were distributed within each plot of variable pairs (Owens et al., 2013). I sought to include the variables where presences had a unimodal distribution and occupied a limited range within the scope of possible values of the variable. These type of presence/background relationships result in model responses that are more adequate for climate change predictions, because models are less likely to misbehave when facing extraneous conditions in the prediction data ((Owens et al., 2013), I used these change predictions in Chapter 7).

To validate models by means of measuring its performance on independent data I selected training and testing data spatially. With this step I minimised the chances of testing the model with data that is spatially autocorrelated with the training data, which tends to inflate model performance (Veloz, 2009). To do so I created a chess board grid with squares of 40,000 km^2 approximately, and 200 km wide horizontal and vertical bands (along longitude and latitude, Appendix 9.6.3.2 Figure 21). I used points lying within contiguous bands or squares for training and testing with a partial ROC analysis (Peterson et al., 2008; Barve, 2008). Given that I did not verify flying fox occurrence records for accuracy I allowed a 50% omission rate of testing points for the partial ROC analysis. Because the final data set for *P. conspicillatus* contained less than 30 occurrence records, I validated this model with a Jacknife test (Pearson et al., 2006). For the Jacknife test I calibrated $N - 1$ models (N=number of presence localities), leaving one of the presence localities out in each model run. Then from the scores assigned by the algorithm to each locality I used the minimum of these values as a threshold to see if the omitted locality had been predicted as present (had a probability of occurrence $\geq$ threshold). The predictions/non-predictions and thresholds were used as probabilities to run the validation test with the "pValueCompute" tool

[3] http://www.worldclim.org

from Pearson et al. (2006).

Because niche models should only encompass the areas where species can move (areas colonisable by species = M [Movement]) (Soberón and Peterson, 2005; Barve et al., 2011), I assumed that the climatic regions of Australia (Bureau of Meteorology of Australia [4]) occupied by each FF species are the boundaries of the areas accessible to colonise. A practical justification for this step is that the absence of sensible limits to the area used for model projection can inflate validation statistics by means of comparing the models' predictions with areas that have little value for the species' persistence (Barve et al., 2011). The same assumption helped identify the HeV M area. All climatic regions containing at least one presence point of the final presence database were combined to mask the climatic variables for each species. All the FF niche models were generated with Maxent without clamping and extrapolation (Phillips et al., 2006). To generate the binary models necessary for the subsequent analyses I applied a threshold corresponding to the 50^{th} percentile of model scores at presence localities, which represents the same criterion used in model testing. The resulting binary maps represent areas where each FF species has a probability ≤ 0.5 of being present. All models and analyses were performed with the statistical programming language R 3.1.1 (R Core Team, 2016) with package dismo and raster (Hijmans et al., 2013; Hijmans, 2013).

Proximity of HeV spillover events to the centroid of flying foxes

To calculate the centroid I extracted the variables' values contained within each of the FF predicted distributions that overlap with the HeV spillover M area (Martínez-Meyer et al., 2013). The centroid of all the climatic dimensions is found with the arithmetic mean of each variable. Then I calculated the Mahalanobis distance (Euclidean times covariance matrix, to correct for variable's correlations) from each pixel within the HeV M area to the centroid of each bat species. In other words, the centroid was obtained with the climatic data after I removed the FF areas that do not overlap with the HeV M area. In doing this I assumed that FF have multiple centroids and that the centroids within the HeV M area are independent from the centroids from the areas that were not included. This assumption was based on other climatic envelope modelling algorithms that assume that all presence localities represent optimal conditions (Farber and Kadmon, 2003; Busby, 1991). Finally I extracted the resulting distances to each FF species' centroid at the location of spillover events. To avoid comparing DNC at different scales, distances to FF species centroids were calculated

[4] http://www.bom.gov.au

using the same set of climatic variables selected with the procedure described in the previous section using the HeV presence records.

To confirm that distances to the niche centroid at the location of spillover differed between the four bat species I performed a Kruskal-Wallis test. To assess if the frequency of occurrence within each of the calculated centroid distances departed from random expectations I identified which FF species centroid was closer to each spillover location. To calculate the expected frequencies, the maximum value from all these minimum DNC scores was used as a threshold to calculate the proportion of pixels occupied by each FF species within an equal or smaller distance to the centroid. With these values I calculated the probability of finding each species using the proportion of pixels predicting its presence with respect to the total number of pixels occupied by all FF species. These probabilities were used as the expected frequencies of any species' DNC being lowest in the location of spillover. I used a chi squared test to compare expected and observed frequencies (number of times each species had the minimum DNC at the location of spillover). I assumed that all spillover localities were independent from each other after filtering for spatial autocorrelation of spillover events. The independence assumption might not be true, however after using the distance threshold of 0.5° I was left with 27 presence records, and I did not want to lose any more statistical power.

Finally to determine if the selected FF species occur at higher densities in areas closer to the niche centroid, I registered the coordinates and all the abundance categories for each flying fox roost site (camp) in the National FF monitoring program of Australia[5] using the interactive FF web viewer. Then I performed linear regressions between the average abundance category, the maximum category for each camp and the standard deviation. Additionally I performed a kernel density estimation weighted by the maximum abundance category for each camp. I then ran a correlation test between these density models and the DNC models.

Results

I was able to calibrate at least one model that performed better than random (Appendix 9.6.3.2 Table 7) for each FF species (Figure 5.1). Although the model for *P. conspicillatus* could only be validated with the Jacknife test, it also performed better than random. Variables describing niches differed across species and are listed in Appendix 9.6.3.2 tables 6 and 9. As for the DNC models, I found that sixteen out of 27 HeV spillover events that remained in the data set after filtering

[5] http://www.environment.gov.au/node/16393

were closer to the niche centroid of *P. alecto* than to the centroid of the other three species. In 7 events, the distance was smaller to the centroid of *P. scapulatus*, and for the remaining four events, the distance was smaller to the centroid of *P. conspicillatus*. The DNC at spillover sites were significantly different among species (one way Kruskal-Wallis, χ^2=43.31, d.f.=3, P=2.11×10^{-9}; Figures 5.2 and 5.3), indicating that some species are more likely involved in spillover.

Table 5.1: Relationship between distance to the niche centroid and size categories of flying fox camps. The categories used were: 1 (1 – 499), 2 (500 – 4,999), 3 (5000 – 9,999), 4 (10,000 – 19,999), 5 (20,000 – 49,999) and 6 (>50,000). Average is the average camp size, Max is the maximum camp size and S.D is the standard deviation of camp size.

P. alecto	*P. conspicillatus*
$\text{Average} = 0.37 - 0.15 \times DNC$	$\text{Average} = 1.13 - 0.22 \times DNC$
$R^2 = 0.03, P = 0.01$	$R^2 = 0.09, P = 0.2$
$\text{Max} = 0.94 - 0.15 \times DNC$	$\text{Max} = 1.12 - 0.05 \times DNC$
$R^2 = 0.08, P \ll 0.05$	$R^2 = 0.06, P = 0.7$
$\text{S.D.} = 0.87 - 0.11 \times DNC$	$\text{S.D.} = 1.10 - 0.013 \times DNC$
$R^2 = 0.05, P \ll 0.05$	$R^2 \approx 0, P = 0.9$

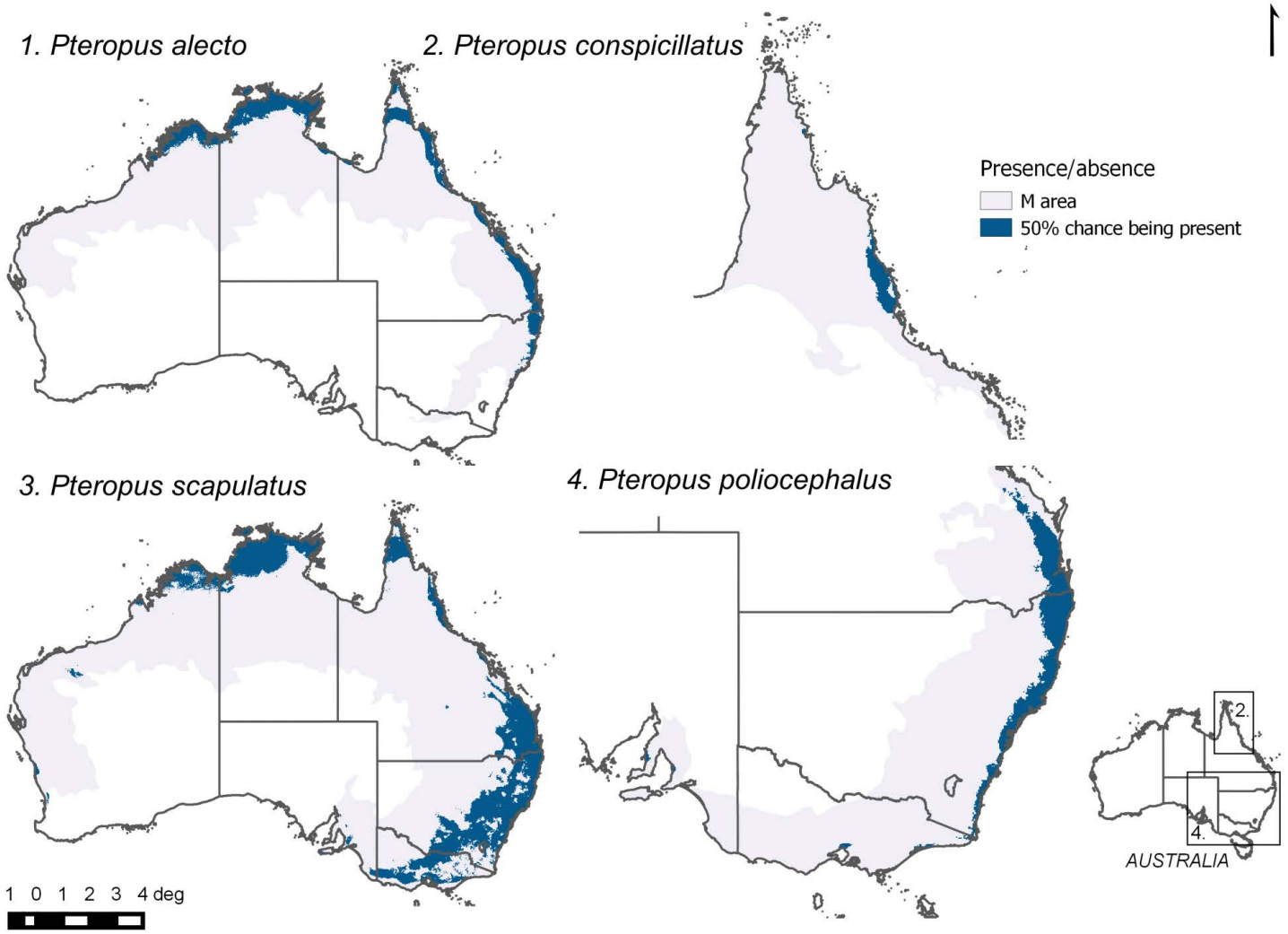

Figure 5.1: Maps of predicted potential distributions of the four Australian flying foxes. Dark blue indicates areas where each species has at least a 0.5 probability of being present. Grey shaded areas correspond to the available geographic space for each species (M areas)

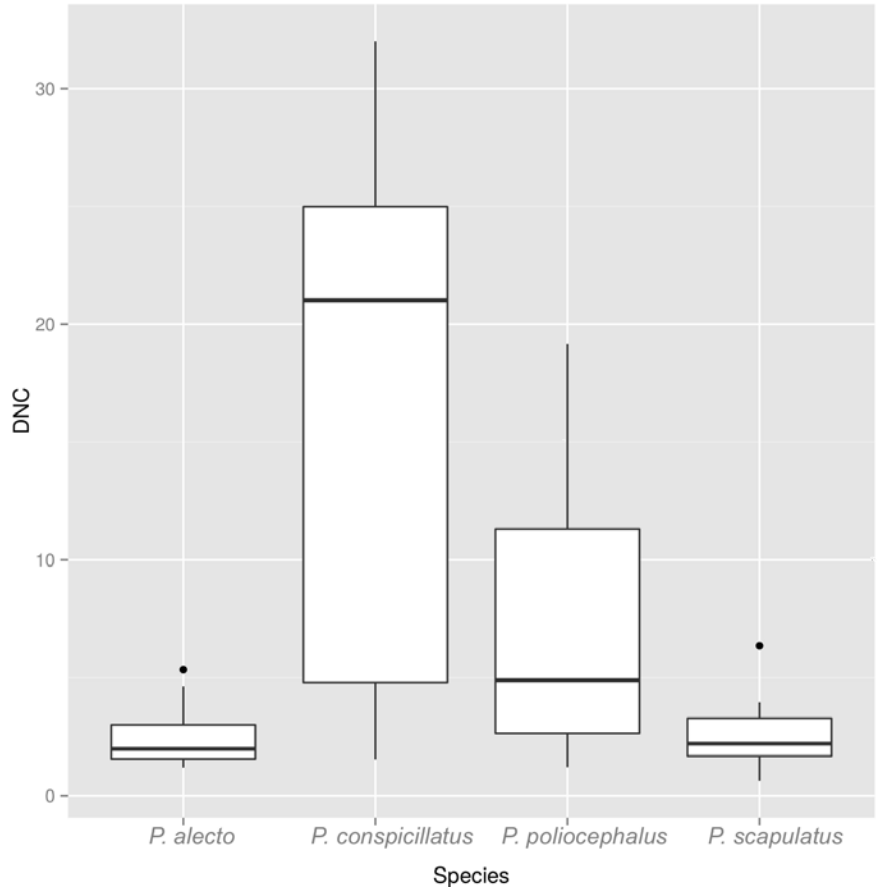

Figure 5.2: Box plots of the Mahalanobis distance to the centroid of each species from the locations of spillover events.

Because most of the events (16/27) have occurred closer to the niche centroid of *P. alecto*, I tested this association with the chi squared test which was highly significant (χ^2=49.9, d.f.=3, P=8.09×10^{-11}). The probability of randomly selecting a pixel with conditions suitable for *P. alecto*, *P. conspicillatus* and *P. scapulatus* in the geographic space of the HeV M area was 0.26, 0.016 and 0.61, respectively . The linear regressions confirm a decreasing trend of abundance with DNC only for *P. alecto* especially the maximum camp size (Table 5.1). Similarly the correlation between weighted density of *P. alecto* and *P. conspicillatus* and DNC were -0.28 (P <0.05) and -0.39 (P <0.05) respectively (Figure 5.4).

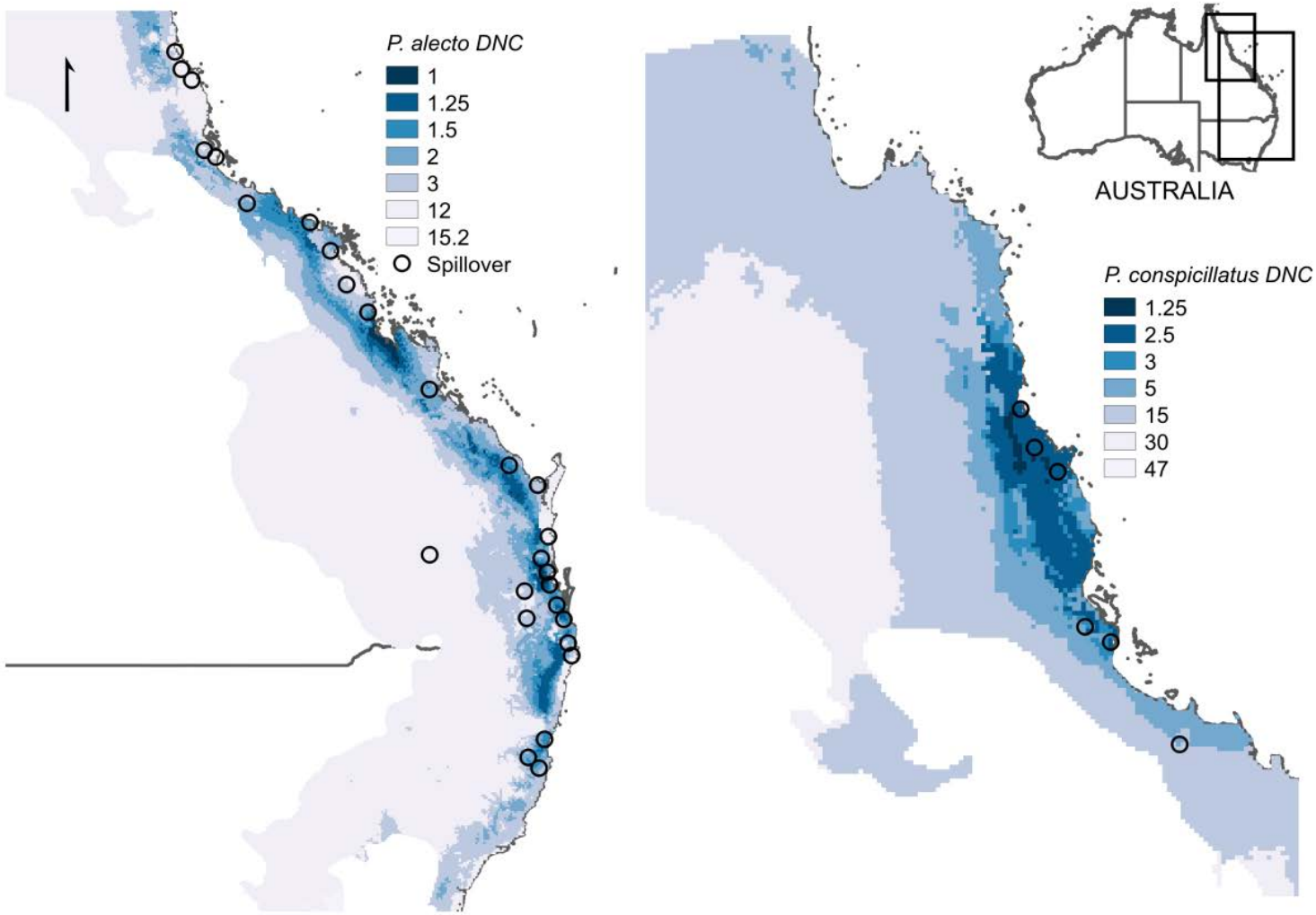

Figure 5.3: Map of distance categories to the niche centroid of *P. alecto* and *P. conspicillatus* and spillover events. According to the distribution of distance to niche centroid categories and hence abundance in space of flying foxes, spillover events have occurred closer to these two species compared with *P. poliocephalus* and *P. scapulatus*.

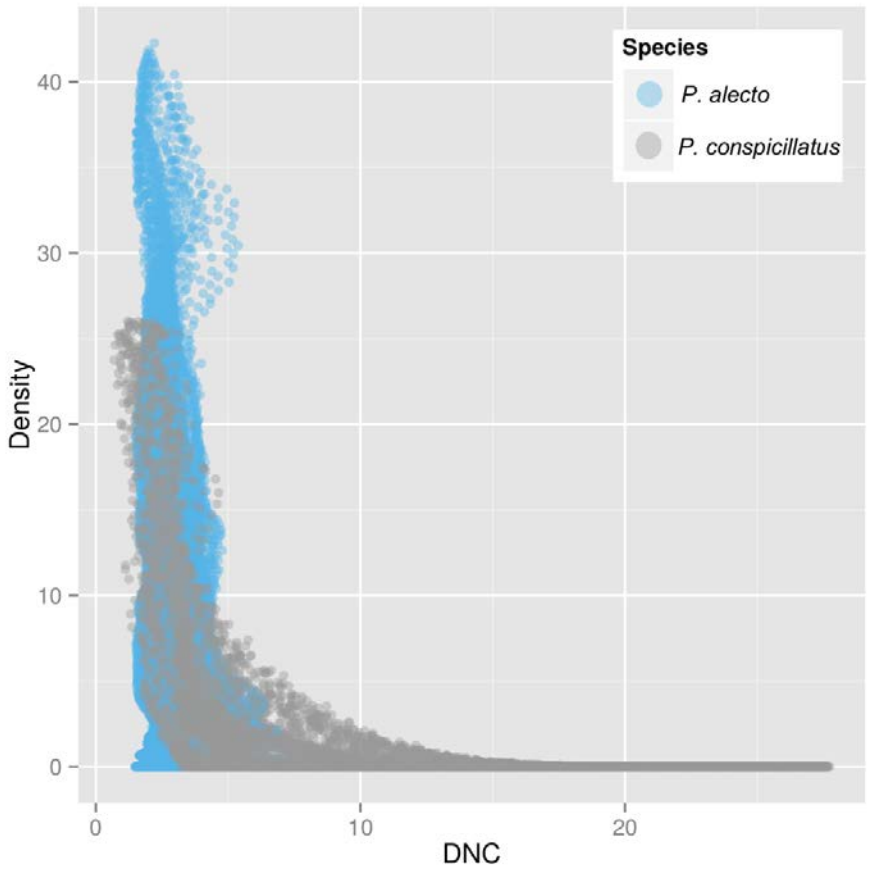

Figure 5.4: Scatter plot between weighted density and distance to niche centroid of *P. alecto* and *P. conspicillatus*. Despite the lack of a significant relationship between *P. conspicillatus* and the abundance categories in Table 5.1, there is a significant negative correlation between distance to niche centroid (DNC in the figure) and weighted density.

Discussion

The climatic characteristics of HeV spillover locations are similar to the conditions suitable for *P. alecto* and *P. conspicillatus*. In areas where conditions permit the presence of other species, spillover events have occurred mostly in areas closer to the centroid of *P. alecto*. Density of *P. alecto* and *P. conspicillatus* records are higher in areas where spillover to horses has occurred, suggesting these species were more likely to be responsible for spillover than *P. poliocephalus* and *P. scapulatus* (Smith et al., 2014). None of the events occurred closer to the centroid of *P. poliocephalus* than to the centroid of other species, and the presence of spillover closer to seven out of 27 events to the niche of *P. scapulatus* is possibly because it has the widest distribution of all

FF species. Hence, the majority of the Hendra M area was suitable for them. *Pteropus scapulatus* are highly mobile and unpredictable, they are nectarivorous and thus rely strictly on flowering trees (Plowright et al., 2008; Vardon et al., 2001). HeV antibodies are distributed throughout *P. scapulatus* populations (Plowright et al., 2008). Yet, no spillover events have been reported in areas where *P. scapulatus* is the only species present, and *P. alecto* has been consistently found in proximity to spillover events (Field et al., 2011). Nevertheless, their intermittently combined densities have important implications for spillover (Field et al., 2011; Smith et al., 2014).

An important feature of HeV spillover is the timing of events. Spillover tends to cluster in space and time, most events usually occur in winter in the southernmost part of the distribution of *P. alecto*. The reasons for this are still unknown, and are probably multifactorial ((Plowright et al., 2015). Given the movement patterns of *P. poliocephalus*, it is possible that they play a role in spillover because they tend to move towards the northern areas of their distribution during the southern hemisphere winter (Eby, 1991), which will create higher concentrations of FF in areas highly suitable for *P. alecto* according to our models.

To confirm the climatic suitability-abundance correlation for FF I was able to demonstrate a negative relationship between DNC and maximum abundance of FF. Furthermore, the negative relationship between the standard deviation of the camp size and DNC provides more support; meaning that the higher the DNC the smaller and less variable with respect to maximum size the camp sizes tend to be through time. In the case of *P. conspicillatus*, the regressions were not significant, however the significant negative correlation between the weighted kernel density model and DNC suggests that the relationship is negative (Figure 5.4). Our results show stronger relationships between climatic suitability and maximum size of populations (number of FF in camp sites), a phenomenon observed in several different species (VanDerWal et al., 2009). This indicates that the areas closest to the smaller DNC have greater potential to harbour either large or several FF camps, and hence timing of such densities might be a key determinant of risk of spillover.

Throughout this study I made two key assumptions: 1) FF do not have a single range-wide DNC that influences abundance patterns, but multiple independent DNCs; and 2) that spillover cases used in analyses are independent from each other and from the FF camp records used to train the models. The assumption of local DNC independence from a range-wide DNC is based on similar assumptions made by some modeling algorithms. For example, the Mahalanobis distance algorithm (Farber and Kadmon, 2003) and BIOCLIM (Busby, 1991) assume that all localities used in

model training are as suitable as is the niche centroid. The second assumption appears reasonable given that spillover events appear to be independent of one another and FF localities.

There are obvious limitations in our methods. First, climatic data used by our niche models are averages over space and time rather than the specific conditions that occur at the time and place of a spillover event. Second, presence records of FF mostly reference the location of bat roosting sites, whereas HeV spillovers usually occur where FF forage. Therefore, there is a spatial lag between the areas chosen by FF to camp and the areas where HeV is transmitted to horses. These areas could well be outside of the preferred conditions by *P. alecto* to establish a colony (Vardon et al., 2001) but within the preferences of other FF species that could be present. Despite this shortcoming, the aim of the study is to identify where climatic characteristics allow the presence of larger flying fox populations. Given the methods I used, I do not aim to understand small scale interactions such as choosing to camp in a specific tree and forage in another (Soberon and Nakamura, 2009). A clear example of the implications of climate on persistence of species are the heat waves that exceed the limits of the temperature tolerance of FF (Kearney and Porter, 2009; Welbergen, 2008). For example, *P. scapulatus* has lower evaporation rates and higher thermal tolerance than *P. alecto* and *P. poliocephalus*, which explains its wider distribution into drier and warmer areas (Vardon et al., 2001, Figure 5.1). These relationships represent the ecological scale of organisation on which our results should be interpreted (Soberón and Peterson, 2005). Therefore, the DNC models do not represent areas where FF are constantly more abundant, but are areas with certain climatic characteristics that have greater potential to harbour larger populations given the temperature tolerance and preference of the species and its food resources (VanDerWal et al., 2009).

The relationships between climatic suitability and abundance are typically weak as I found here. Additional factors contribute to abundance patterns such as geographical barriers, biotic interactions and ecological changes (Martínez-Meyer et al., 2013; VanDerWal et al., 2009). In the specific case of FFs, density is affected by the presence of food resources (biotic interactions) that can be spatio-temporally sporadic (Eby, 1991). In addition, sampling bias can greatly affect the strength of the DNC-abundance relationship. In particular, the timing of a census is important for highly mobile and gregarious species. We suspect that the DNC-abundance relationship was altered by the increasing width of the abundance categories in the national FF monitoring program. The higher the category reported the broader the difference between the upper and lower limits. However, the non-random distribution of spillover among FF niches suggests there is

a strong relationship between spillover and *P. alecto* and *P. conspicillatus* numbers and/or presence. Further analyses of habitat suitability and abundance should be performed with raw values of FF abundance that better account for variability than categories of abundance.

Our modelling suggests that there is a bioclimatic effect driving the spatial patterns of *P. alecto* and *P. conspicillatus* abundance. The location of urban settlements in geographical proximity to the niche centroid of *P. alecto* may contribute to urban habituation of this species. Our models can be used for guiding future research, to address key questions in understanding the dynamics of spillover. The effect that climatic variations in areas close to the niche centroid have on HeV dynamics and FF population levels could be investigated to better understand the risk of HeV spillover to horses.

Conclusions

According to the DNC analyses, *P. alecto* and *P. conspicillatus* are more likely to have been present in proximity to spillover events and therefore responsible for transmission of HeV to horses. Our results indicate that the bioclimatic suitability for *P. scapulatus* is very high in almost 25% of HeV spillover events, which requires further investigation.

Chapter 6

Spatiotemporal patterns of Hendra virus spillover risk: distribution and climatic correlates

In Martin et al. (2016) (Chapter 5) I investigated the effects of climate in determining which species are more relevant for HeV spillover to horses. The spatial variability of flying fox carrying capacity was explained partly by the distance to their niche centroids. HeV spillover risk within these areas varies across time. The biological mechanisms and climatic drivers behind this phenomenon are still unknown. Consequently, better understanding of the factors that influence the spatio-temporal spillover pattern would result in improved predictability, prevention and risk mitigation.

In this chapter I developed a statistical model that reproduced the spatio-temporal pattern of HeV spillover risk, within the areas where reservoir hosts are present. Compared with Chapter 5, this study specifically uses the spatial location of spillover events to create a distribution model in response to monthly climatic conditions.

With these analyses I identified the climatic factors that correlate with spillover risk variability between months, and provided insights to the biological mechanism that drives spillover seasonality.

The analytical methods that I used were a combination of machine learning, frequentist statistics, and geospatial modelling.

This chapter is in review in EcoHealth, submitted 27 July 2016 (Martin et al., b *in-review*):

- Gerardo Martin, Carlos Yanez-Arenas, Carla Chen, Raina K Plowright, Billie J Roberts, and Lee F Skerratt. Seasonal spillover of Hendra virus: distribution and climatic dirvers. *EcoHealth*, b

Abstract

Understanding the climatic and environmental factors driving spatiotemporal patterns of disease can improve our ability to anticipate and mitigate the risk that disease

*poses to populations. Hendra virus (HeV) was first described in Australia in 1994, after it spilled-over to horses and thence to humans from its bat reservoirs (*Pteropus sp.*). Events of HeV transmission from bats to horses so far occur during winter below latitude 22°south but is aseasonal north of this latitude. I generated a consensus statistical model of climatic and environmental drivers of HeV spillover per month. The model reproduced the spatiotemporal pattern of spillover risk seen from 1994 until 2015. The statistical model was generated with an ensemble of methods designed for presence-absence data including boosted regression trees, random forests and logistic regression. Spillover presence per spatial unit (2.7×2.7km pixels) was obtained with the spillover database of Biosecurity Queensland and absences were sampled with a horse census of Queensland and New South Wales. The most influential climatic factors were related to the seasonal amplitude of minimum temperature and rainfall. The bimodal responses to several variables included in the model suggest spillover involves two systems above and below latitude 22°south. The southern system could be driven by* P. alecto *and the northern by* P. alecto *and* P. conspicillatus*. I recommend enhanced preventive management for horses from Mar-Nov below latitude 22°south. Future research should look for immune and behavioural differences in response to food shortage in bats and horses in the two latitudinal regions.*

Introduction

Infectious diseases have temporal patterns of incidence, some of which might present as seasonal cycles (Fisman, 2007). However, incidence can also vary over space, resulting in spatiotemporal patterns (Ostfeld et al., 2005). These patterns have mostly been studied in single host-single pathogen systems, except for vector borne diseases (Ostfeld et al., 2005; Bacaër and Guernaoui, 2006; Altizer et al., 2006). The biological mechanisms regulating spatiotemporal patterns of incidence can result from interactions between the host, pathogen and climate (Dowell, 2001; Sultan et al., 2005; Fisman, 2007). Then, a typical consequence is the climatic regulation of incidence cycles that can result in longer and larger outbreaks when environmental conditions are more suitable for disease (eg. cholera, dengue and influenza) (Pascual and Dobson, 2005; Sultan et al., 2005; Grassly and Fraser, 2006; Cuong et al., 2013).

Spillover is a special case of disease incidence with spatiotemporal patterns involving several host species that has received little attention (Lo Iacono et al., 2016). It is generally regarded as the

transmission of a parasite from a reservoir host to a non-definitive host, either wild, domestic or human (Daszak, 2000). For spillover to occur and result in a diseased individual, several ecological processes at different scales of organisation need to converge (e.g. pathogen survival in the environment, presence of infectious reservoirs and presence and susceptibility of spillover hosts) (Estrada-Peña et al., 2014; Plowright et al., 2015). For this reason climate could be an overarching driver of spillover risk. Therefore, the climatic factors associated with spatiotemporal patterns of spillover might be used for risk prediction, mitigation and for guidance of further research. One of such diseases, is the bat borne Hendra virus (HeV) in Australia (Plowright et al., 2015).

Hendra virus is a Paramyxovirus, genus Henipavirus, first detected to infect and cause disease in horses and humans in 1994 (Murray et al., 1995b). In its spillover hosts, HeV causes severe respiratory and nervous system illness with mortality rates of 50% in horses and 75% in humans. Although the latter is uncertain given that there have only been seven cases since emergence. The four Australian flying fox bat species (*Pteropus alecto*, *P. conspicillatus*, *P. poliocephalus* and *P. scapulatus*) are the only wild animals that have been found with antibodies (Halpin and Field, 1996). Of the four bat species, *P. alecto* (black flying foxes) and *P. conspicillatus* (spectacled flying foxes) are the natural reservoir host and more likely to transmit HeV to horses. Firstly, because these species are statistically associated with the spatial pattern of spillover (Smith et al., 2014); secondly they are the only bat species where the virus has been isolated (Edson et al., 2015); and thirdly, spillover events consistently occur in the geographical areas that are climatically more suitable for these two bat species (Martin et al., 2016). These areas are the northern wet tropics inhabited primarily by *P. conspicillatus* and to a lesser degree by *P. alecto*, and from the dry tropics to the temperate wet forests of central New South Wales inhabited by *P. alecto* (Martin et al., 2016). None of the bat species develop or show signs of disease as a result of HeV infection (Williamson et al., 1998, 2000).

During the time frame since emergence, and particularly after a large cluster of spillover events, a spatio-temporal pattern of spillover became evident. HeV is transmitted to horses in eastern Australia, during the southern hemisphere winter between May and September below latitude 22° south (34 out of 55 spillover events). Above this line transmission has been recorded in all seasons (the remaining 21 events) (McFarlane et al., 2011; Plowright et al., 2015).

Several environmental factors could be related to the spatio-temporal patterns of spillover. Bats feed exclusively on nectar and fruit of native and introduced plants (Richards, 1990; Palmer et al., 2000). Nectar production by native Eucalyptus spp. trees depends on present and past climate

(Hudson et al., 2010), and the pulses of nectar production regulate the number of bats present in certain geographical areas (Giles et al., 2016); nutritional stress that could result in increased susceptibility to diseases in general (Eby, 1991) and to HeV infection in particular (Plowright et al., 2008) driven by low plant production, which is characteristic of winter seasons in subtropical areas (McFarlane et al., 2011). The temporal dynamics of food for bats in horse paddocks might also align with these climatically driven pulses of nectar production that occur at larger spatial scales. Climate also influences the geographical distribution and density of bats over the longer term (Martin et al., 2016). All of the ecological interactions between bats, climate and plants could have direct consequences on the dynamics of HeV in bats (Plowright et al., 2011, 2015, 2016). However it is is still unclear which climatic factors and biological mechanisms could regulate the observed seasonal pulses of HeV excretion and spillover risk (Field et al., 2015a; Plowright et al., 2015).

Transmission from bats to horses is thought to occur by contact with infectious bat excreta or possibly ingestion of urine contaminated feed in the environment (Edson et al., 2015; Plowright et al., 2015; Martin et al., 2015). Because the cumulative number of spillover events matched the seasonal survival pattern of HeV in the environment, spillover seasonality was thought to be caused by increased environmental survival of HeV (Scanlan et al., 2014). However an analysis of the spillover events in space and time found that HeV spillover did not occur when and where survival was higher (Martin et al., 2015, 2017, Chapters 3 and 4). These results suggest that long time to inactivation is not necessary for transmission and that spillover seasonality is unlikely to be caused only by increased in environmental survival.

A common approach to investigate disease seasonality consists of regression procedures to identify statistically significant correlations between disease incidence and an environmental or climatic factor. These associations between disease incidence and climate are often weak and relatively uninformative about the underlying mechanisms driving seasonality (Dowell, 2001; Pascual and Dobson, 2005). Therefore, I used alternative methods to account for other factors necessary for transmission and identify climatic correlates of HeV spillover risk. I investigated the spatiotemporal pattern of HeV incidence in horses in a niche modelling framework to identify environmental requirements for spillover occurrence in space and time with an ensemble of presence-absence methods (Marmion et al., 2009). To identify the requirements or climatic correlates I aimed to reproduce the observed spatiotemporal pattern of HeV spillover with a consensus statistical model. In the model I included the presence and abundance of bats and

horses which are key determinants of HeV spillover dynamics.

Methods

I developed a model that reproduced the monthly distribution of HeV spillover risk using presence-absence (case-non case) per spatial unit (raster pixels) data. Presences (cases or HeV events as they are generally called) represent approximately 2.7×2.7 km pixels where there have been laboratory confirmed cases of clinically ill horses with HeV, and absences (non cases) are the pixels where no HeV cases have been reported during the month of spillover, but are at risk of spillover given the presence of bats. Environmental data of the month and year of each spillover event was extracted from raster layers using the longitude and latitude coordinates of the events using the database maintained by Biosecurity Queensland. Absences were sampled within a series of minimum and maximum distances from the source spillover event using the coordinates of the centroid of horse paddocks from the horse census of Queensland and New South Wales of 2007 (Moloney, 2011). The extracted data was used to fit three models with different regression methods that were combined to generate a consensus model. The entire process is described in greater detail below.

Extracting data

Prior to extracting the environmental data, I thinned the dataset with the coordinates of the spillover events to reduce spatial autocorrelation from 55 spillover events to 42 (Hijmans, 2012). I used a recursive filtering algorithm based on a physical distance threshold of 0.05° between points (same method described in Chapter 5). This was necessary because point data and environmental rasters have a strong spatial dependence even more so in the presence of sampling bias which might be true for HeV spillover (Smith et al., 2016). Besides, autocorrelated datasets compromise the assessment of a model's performance on independent data (Veloz, 2009), and violate the assumption of independence between observations of the regression procedures. In addition to this adjustment, I assumed a two week delay between the registered date of the report and actual transmission, such that the climatic conditions were more likely to precede the actual transmission from a bat to a horse. The geographical coordinates and the delayed date of spillover of the filtered database were used to extract the values of monthly climatic variables from the pixels of the raster files where and when each event was located.

I selected explanatory variables according to our current knowledge of the HeV spillover

system; bat species (distance to bat camps or roosting site, and environmental distance to the niche centroid as surrogate of abundance, see supplementary materials), density of horses (number of horses per grid cell), and variables representative of climatic variability, corresponding to the average conditions of the recorded month of spillover compared with seasonal extremes. For instance, the variables minimum temperature difference from minimum temperature of coldest month (*mindif*, 6.1), maximum temperature difference from maximum temperature of warmest month (*maxdif*), rainfall difference from wettest month (*raindifwet*), and rainfall difference from driest month (*raindifdry*), represent the amplitude of seasonal variability.

The variables distance to closest bat camp and environmental distance to the niche centroid of bats were model generated (described in detail in the supplementary materials), with similarity index methods (Farber and Kadmon, 2003; Martínez-Meyer et al., 2013). Distance to the closest bat camp represents the physical distance (in a straight line) to a pixel with similar climatic characteristics to those occupied by bats. And climatic distance to the niche centroid is a measure of similarity with an optimum defined by the multivariate centroid of the climatic conditions occupied by bat roosts.

To generate the horse density model I repeated the coordinates of the property centroid by the number of horses reported. Then I introduced non-parameteric noise equivalent to half of the pixel size of the environmental data on each of the repeated property coordinates. After noising the coordinates, I counted the number of points per pixel and repeated the process 100 times. When iterations were completed I averaged the 100 raster layers to obtain the final horse density model. A more detailed description is given in Appendix 9.6.3.2.

While these types of analyses are correlative, the variables related to bat and horse presence and abundance could represent mechanistic relationships. The variables of climatic variability were used to represent other biological phenomena that might influence spillover risk but for which I have no data, such as plant phenology, bat and horse behaviour and HeV levels in bats (Plowright et al., 2015).

Sampling absence (non-case) data

The process to obtain absence data comprised model validation simultaneously, although validation is described in detail below. To sample absence data I randomly selected the coordinates of the centroid of 18 properties per spillover event (756 in total) from the horse census database, assuming that the recorded spillover events are a representative sample of the areas at risk of HeV spillover.

From this database I randomly selected the coordinates of three to four absences per spillover event for the testing/validating data set. The final dataset used to fit the models comprised 600 absences (15-16 per spillover event). This ratio of absences/presence is the minimum of the recommended range of ratios for generalised linear models, boosted regression trees and random forests for use in species distribution models (Barbet-Massin et al., 2012). All sampled absences lied within two buffers of different radius size around each spillover event. One radius was used to limit the minimum distance allowed around the spillover event (10-20 km) and the other buffer was used to limit the maximum distance (50-250 km). Then I implemented an iterative process that consisted of (1) increasing or decreasing the size of both buffers, (2) randomly sampling environmental data lying between the two buffers, (3) fitting the models with the sampled data and (4) testing the fitted model's performance on independent data 6.1.

To test the model's performance (validation) in each iteration I (1) partitioned the dataset into 8 subsets for testing and training such that every event was used in either training or testing; (2) assessed its discriminative ability between presences and absences with the area under curve (AUC) of the receiver operator characteristic (ROC, specific details on model testing are given below), using the 150 absences that were sampled previously; and (3) assessed whether the model had reproduced the observed spatio-temporal pattern of spillover risk (figure 6.1). To do the latter, models fitted in each iteration were projected to the average conditions of the months between discovery in 1994 and 2015 where spillover has been recorded (e.g. average conditions for each January from 1995 to 2015). Then the predicted suitability for each month was averaged by rows of pixels by using only the pixels that were 75 km or closer from the coast. The resulting averages by rows of the projected maps were stacked together and compared with a kernel density estimation of spillover event densities by month and latitude (Plowright et al., 2015). Finally, I kept the absences sampled within the the buffer sizes that maximised the AUC and allowed reproduction of the spatiotemporal pattern.

Fitting the models

Consensus or ensemble methods are algorithms that combine the predictions of a series of models fitted with different methods. The resulting distribution models after combining the different methods can exceed the performance of models generated with a single method depending on the combining algorithm (Marmion et al., 2009). Here I modelled the spatiotemporal pattern of HeV spillover risk with three regression methods, boosted regression trees, random forests and

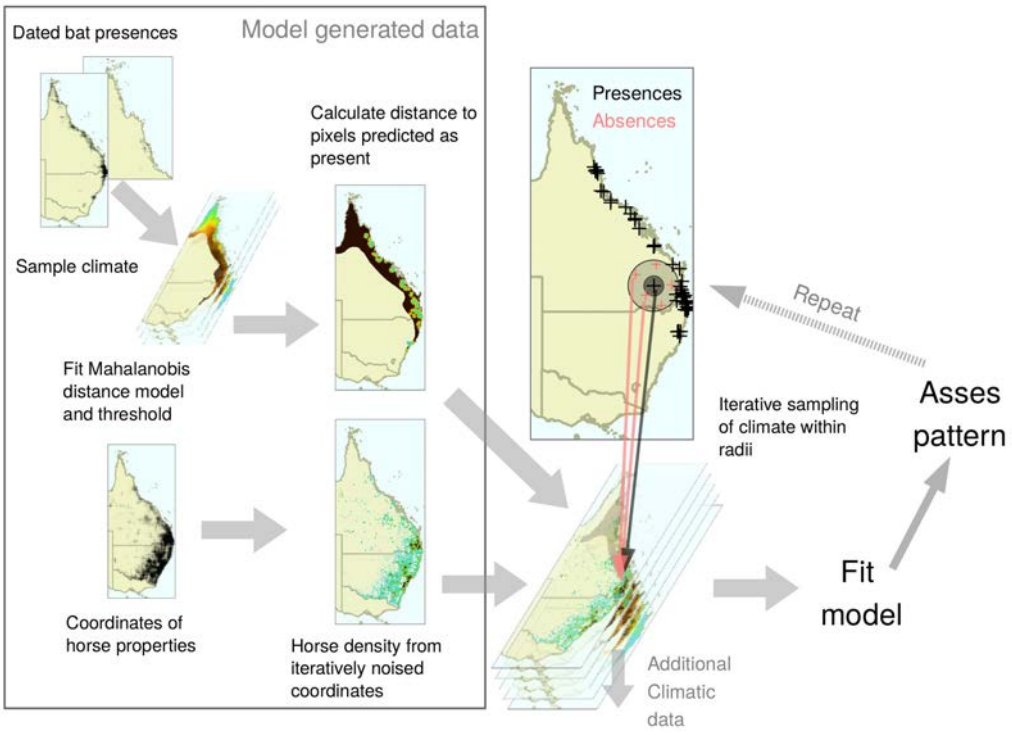

Figure 6.1: Workflow followed to generate data and fit the model that reproduced the spatio-temporal pattern of spillover. The variables that were model-generated can represent causal associations because they are conditional for spillover (presence of reservoir and spillover hosts). Additional climatic data influence variability of spillover risk.

logistic regression, to create a consensus model with the AUC-weighted average of each model's predictions. All regression methods were implemented in R 3.1.1 (R-Development-Team, 2014) (R-Development-Team 2014), using packages `gbm` and `RandomForest`.

Boosted regression trees and random forests are extensions of classification and regression trees, which consist of the combination of multiple simple trees fitted to subsets of the data (bagging). The main difference between them is a process called gradient boosting, performed by boosted regression trees. Gradient boosting consists of sequentially adding simple regression tree models that are fitted to the residuals of previous models. When the sequential models are combined the different splits give rise to smooth surfaces similar to those from traditional regression methods Elith et al. (2008). I used these three methods because boosted regression trees and random forests have very high predictive accuracy (Breiman, 2001; Elith et al., 2008); logistic regression is a transparent, well understood and robust methodology, and because I could analyse presence-absence data with a logistic response with each of the methods.

The response variable for regression was presence or absence of spillover (logistic response).

Each observation (presence or absence) was explained by additive terms of the variables listed in table 6.1. I only used additive terms because boosted regression trees and random forests automatically determine the most relevant variable interactions (Breiman, 2001; Elith et al., 2008), and because including interactions in the formulas of generalised linear models to generate species distributions, does not usually improve their predictive performance (Thuiller et al., 2003).

Validating the models

I validated models fitted with individual methods with an AUC analysis at the same time that absences (non-cases) were being sampled. This method measured the model's ability to discriminate presences from absences (cases from non-cases), such that an AUC = 1 indicates perfect discrimination between presences and absences. Model's AUC scores on independent data were obtained by cross validation; each of the eight partitioned datasets (described above) comprised of subsets of 70% of the presence data used to fit the model and then obtained the AUC with the remaining 30% of the data left behind. For each of the partitions of presences I used the same 150 randomly sampled absences (3-4 absences per presence) to generate the AUC. The statistical significance of these performance tests was assessed by comparing the model's highest AUC with a distribution of AUC scores of 1000 null models fitted with 1000 sets of randomly fabricated presences and absences that were partitioned to generate the AUC (Raes and Ter Steege, 2007). After obtaining the distribution of AUC values of the null models I calculated the probability that the AUC of the tested model was significantly better than random by finding the proportion of null models that had a lower AUC.

The final model testing stage consisted of assessing the performance of the spatial projections of the model, for which I used the partial ROC test (Peterson et al., 2008). This modification of the traditional AUC analysis consists of calculating the area of a polygon formed by the proportion of the predicted geographical area (within a threshold of model predicted values) versus the proportion of predicted presence points. The calculated area under the polygon formed by the different fractions of predicted area and predicted points is then divided by the area under a random predictor based on the proportion of the geographical area predicted by the model. For this reason the maximum value of this performance metric is 2. AUC ratios of 1 occur when the area under the polygon of proportion of area predicted vs proportion of predicted presences equals the area under the random prediction (model predictions are not better than random) (Peterson et al., 2008). These model tests were accompanied by an extrapolation analysis that

allowed us to identify geographical areas and points in time where the model predictions were affected by the projection data.

Extrapolation analysis

To make sure that model predictions were as artefact free as possible I sought for differences between fitting and projection data with an extrapolation detection analysis using ExDet [1] (Mesgaran et al., 2014). When statistical models are used for prediction they can face projection data that is different from the data used to fit the models. The differences between fitting and projection data can be values out of the range in the fitting data (type 1 extrapolation) or different correlation structures between variables (type 2 extrapolation, Owens et al., 2013; Mesgaran et al., 2014). These differences can result in prediction artefacts of the model. Hence I identified geographical areas in the raster maps generated with the models that could be spurious predictions based on the differences between fitting and projection data.

Interpreting the model

I used two approaches to interpret the consensus model, variable partial effects curves derived from the consensus model and a similarity index model using only climatic variables (Table 6.1) from the Bureau of Meteorology (BOM) [2] generated with the Mahalanobis Distance algorithm (Farber and Kadmon, 2003).

Variable partial effects curves show how predicted suitability responds to increases of an explanatory variable, while the remaining variables are kept constant at their mean value. More detailed information about the methods used can be found in the supplementary materials.

Results

The final consensus model successfully reproduced the spatiotemporal pattern of spillover seen from 1994 until 2012 (Figures 6.2 and 6.3). This occurred when absences were sampled within a buffer of 20 – 250 km around spillover events. The spatiotemporal pattern consisted of relatively constant risk of spillover in northern latitudes throughout the year, whereas below the tropics higher risk was during winter and early spring. At the time of these analyses, 32 events have occurred below 22° south latitude, all in winter and early spring (April-October), and above this

[1] http://www.climond.org
[2] http://www.bom.gov.au

latitude 23 events have been evenly distributed across seasons. Given the spatial autocorrelation of some events, the final dataset for analysis contained only 42 events.

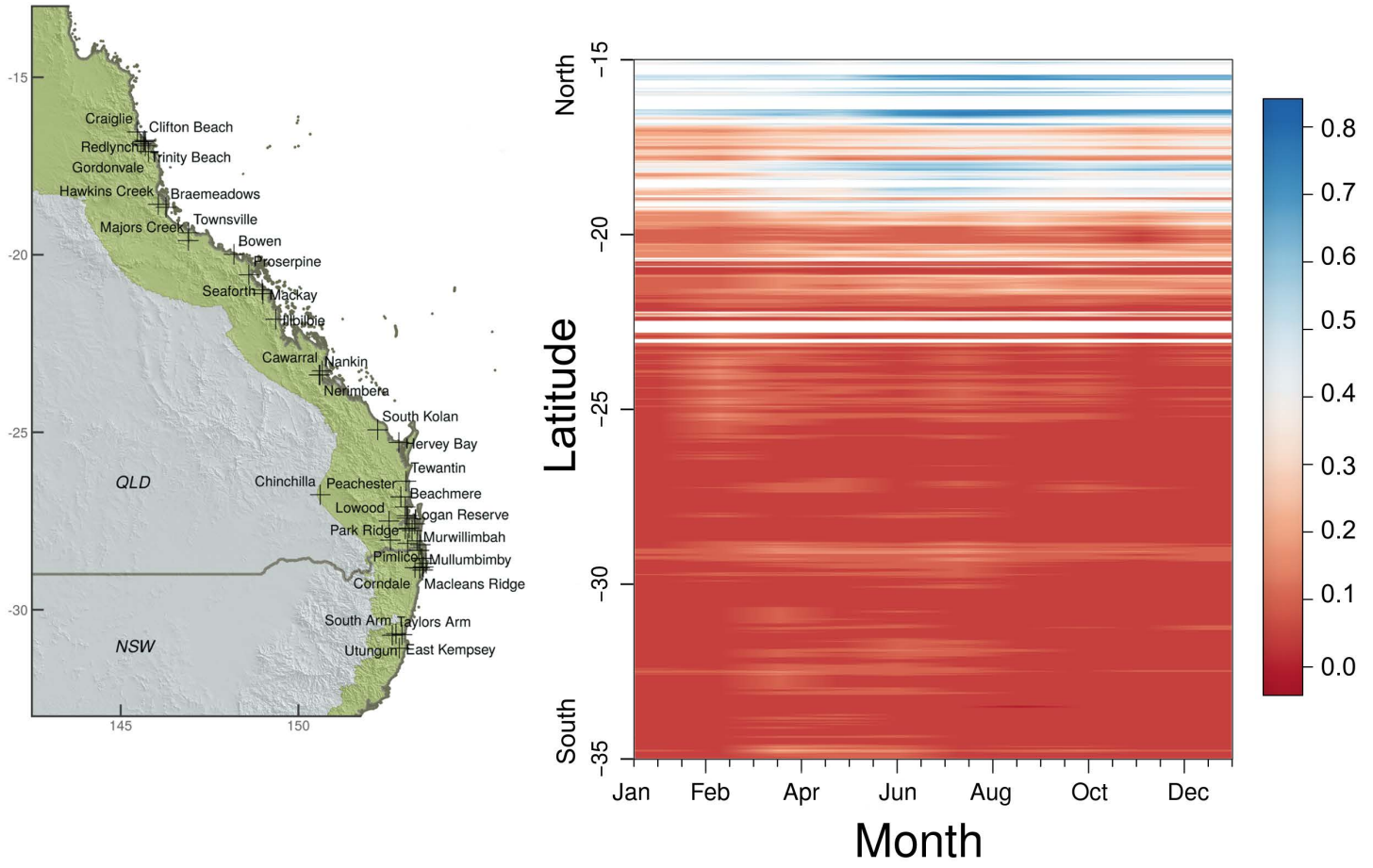

Figure 6.2: Spatio-temporal pattern of predicted suitability of spillover averaged across longitude by up to 75 km inland at each month. Probability of spillover occurrence increases at lower latitudes from March and peaks in June at 28° south. In contrast, likelihood of spillover is more constant (white-blue tones) in higher latitudes across the year. The blank spaces correspond to areas with no horses registered, which appear consistently with between months. The map of the Australian east coast on the left side is a reference for the reader.

The largest seasonal differences occurred above and below latitude 22° south (Figure 6.2) and between January and July (Figures 6.2 and 6.3). Suitability for spillover occurrence increased at lower latitudes from March and peaked in June at 28° south. In contrast, likelihood of spillover is more constant (white-blue tones in Figure 6.2) in higher latitudes across the year. The apparent lower overall risk below 22° south in Figure 6.2 is caused by the averaging across longitude necessary to produce the plot, and the negative effect that horse density has on spillover risk (see below and Appendix 9.6.3.2 Figure 22).

The Mahalanobis distance model (fitted with climate data only, without horses and bats) also reproduced the spatio-temporal spillover risk pattern. Its spatial projections show the change of the size of areas to be at risk of spillover (Figure 6.4). This model also allows better visualisation of the overlap in risk between months (areas that remain at risk in successive months, Figure 6.4).

Minimum temperature difference from minimum temperature of coldest month (*mindif*, Table 11) and horse density were the most influential variables in the consensus model. These two variables had a negative effect and accounted for 32% of explained variability. However horse density had a negative effect, which reached a minimum at 200 horses per pixel, then increased and remained stable at 220 horses and above at about 50% of the maximum suitability reached at 1 horse per pixel (Appendix 9.6.3.2 Figure 22). Rainfall difference from the wettest month (*raindifwet*, Table 6.1) had a negative effect. Risk reached a minimum at -400 mm (drier conditions), then increased to a stable point at 250, which was the maximum for positive values of *raindifwet*. Average minimum temperature had a positive effect, and together with *raindifwet* explained 26% of explained variability. The remaining variables had little explanatory power. A common feature among variables was the occurrence of bimodal responses (Figure 22).

From the four most influential variables mentioned above, *mindif* and *raindifwet* are the two climatic factors that had the most importance in the consensus model. The average value of *mindif* and *raindifwet* is lower among presences (events) than controls (absence of events), hence the negative relationships (density curves, Figure 6.5). Distance to the niche centroid was positively correlated with risk of spillover in the consensus model (Figure 22).

Table 6.1: Variables used for Hendra virus spillover distribution models.

Variable	Short name	Source
Distance to flying fox camps	*distbats*	Model generated
Distance to the niche centroid of flying foxes	DNC	Model generated
Horse density	*horsedens*	Horse census
Normalised difference vegetation index average (month)	NDVI	BOM
Average minimum temperature (month)	*mintemp*	BOM
Temperature range (month)	*mintemp*	Generated from BOM data
Rainfall	rainfall	BOM
Temperature minimum - minimum temperature of coldest month	*mindif*	Generated from BOM data
Temperature maximum - maximum temperature of hottest month	*maxdif*	Generated from BOM data
Rainfall - average rainfall of the wettest month	*raindifwet*	Generated from BOM data
Rainfall - average rainfall of the driest month	*raindifdry*	Generated from BOM data
Solar exposure	*solex*	BOM

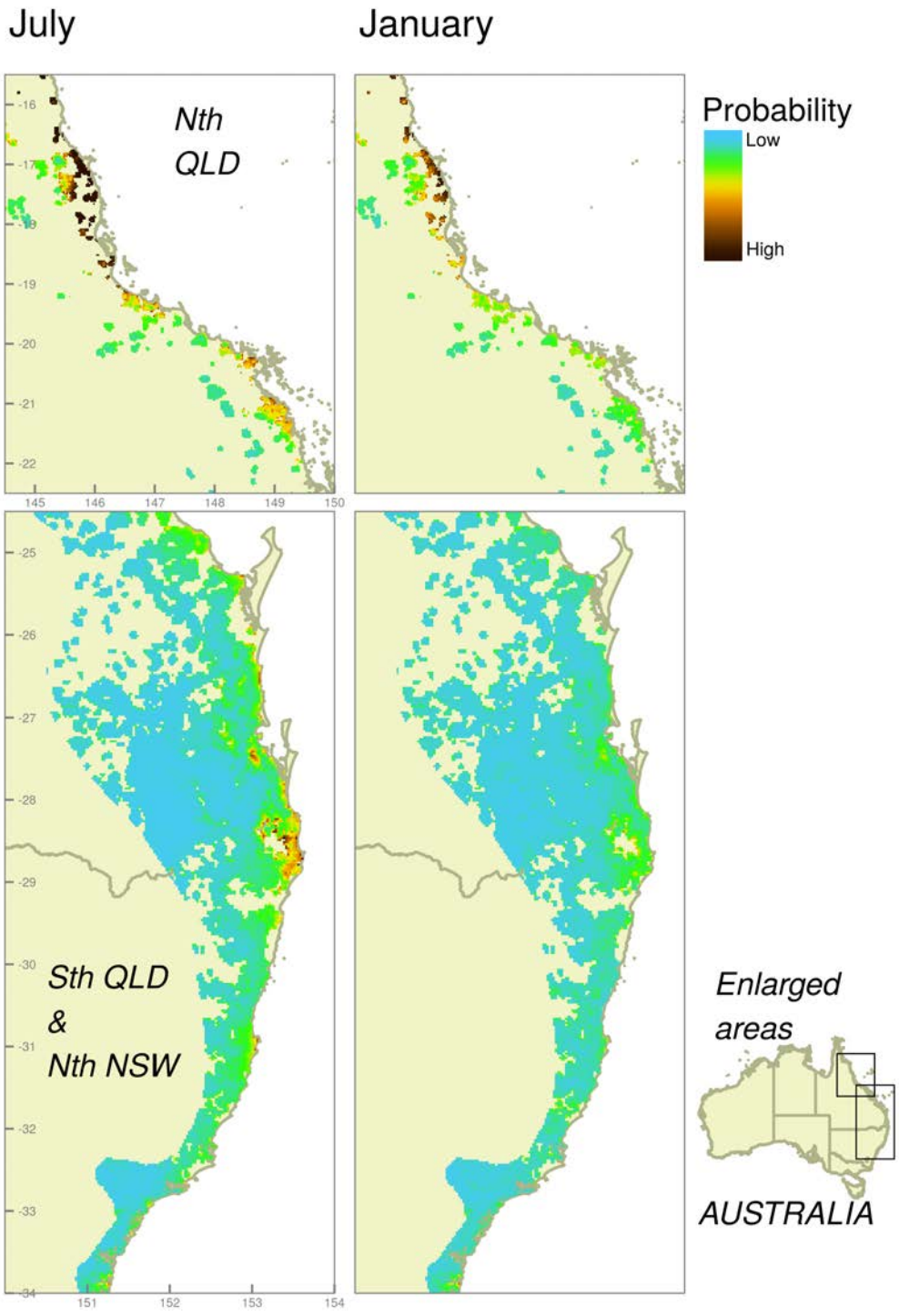

Figure 6.3: Models projected to the average conditions of July and January between 1994 and 2014 in areas occupied by horses. Darker pixels indicate better suitability for spillover according to the horse density, distance to flying fox camps and environmental conditions. The lower suitability in areas close to the border between Queensland and New South Wales (more cyan colour) for January represent the seasonal fluctuations. The dark pixels in the southernmost locations are due to type 1 extrapolation. The dark pixels in southern Queensland in the January projection are due to high environmental similarity.

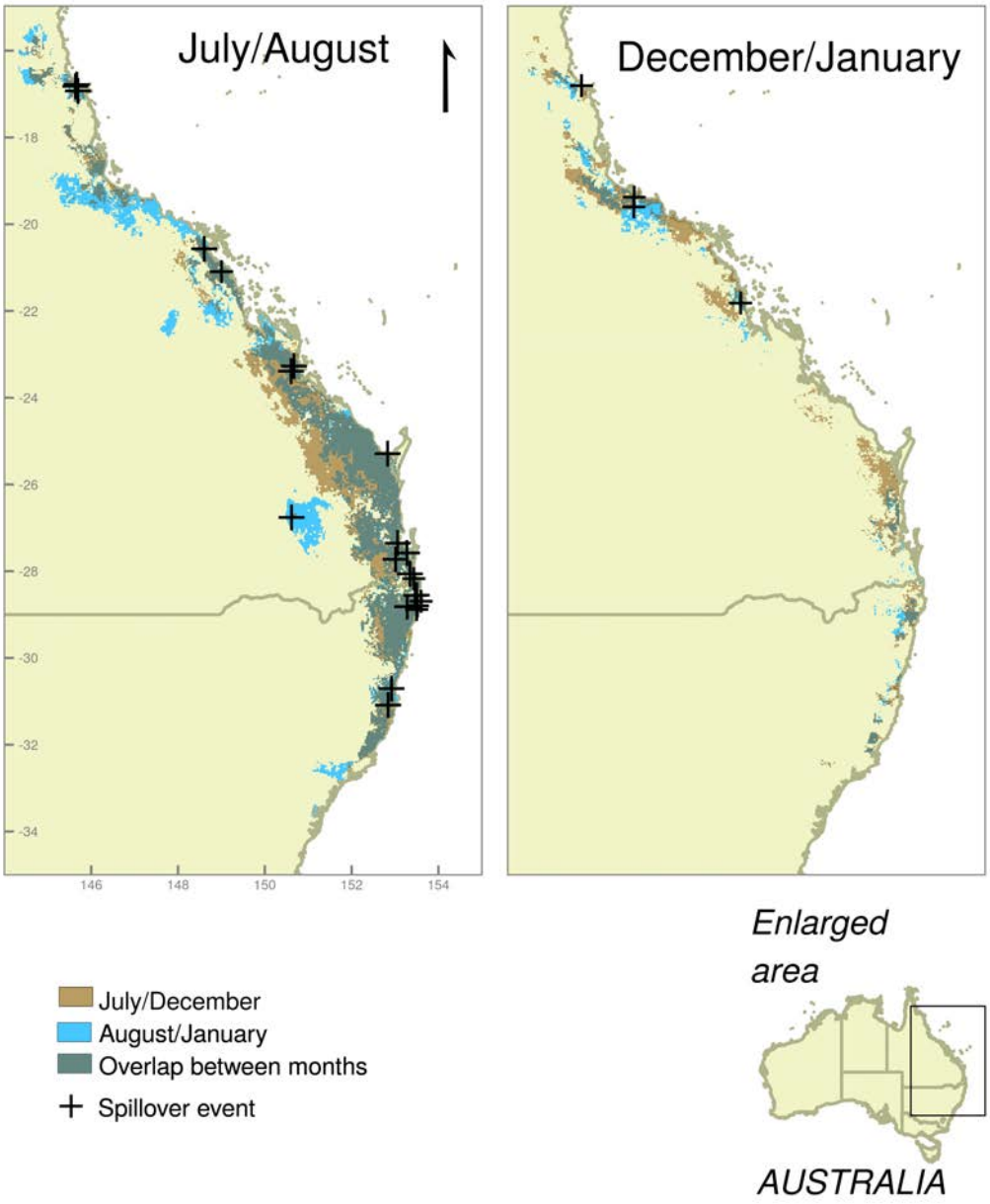

Figure 6.4: Predictions of suitability according to the Mahalanobis distance model with climatic data only. Colours represent the month where areas at risk occur. In the left side June (beige) and August (blue), in the right side December (beige) and January (blue), and the overlap in risk that occurs between months (grey). Spillover localities correspond to those reported in July, August, December and January.

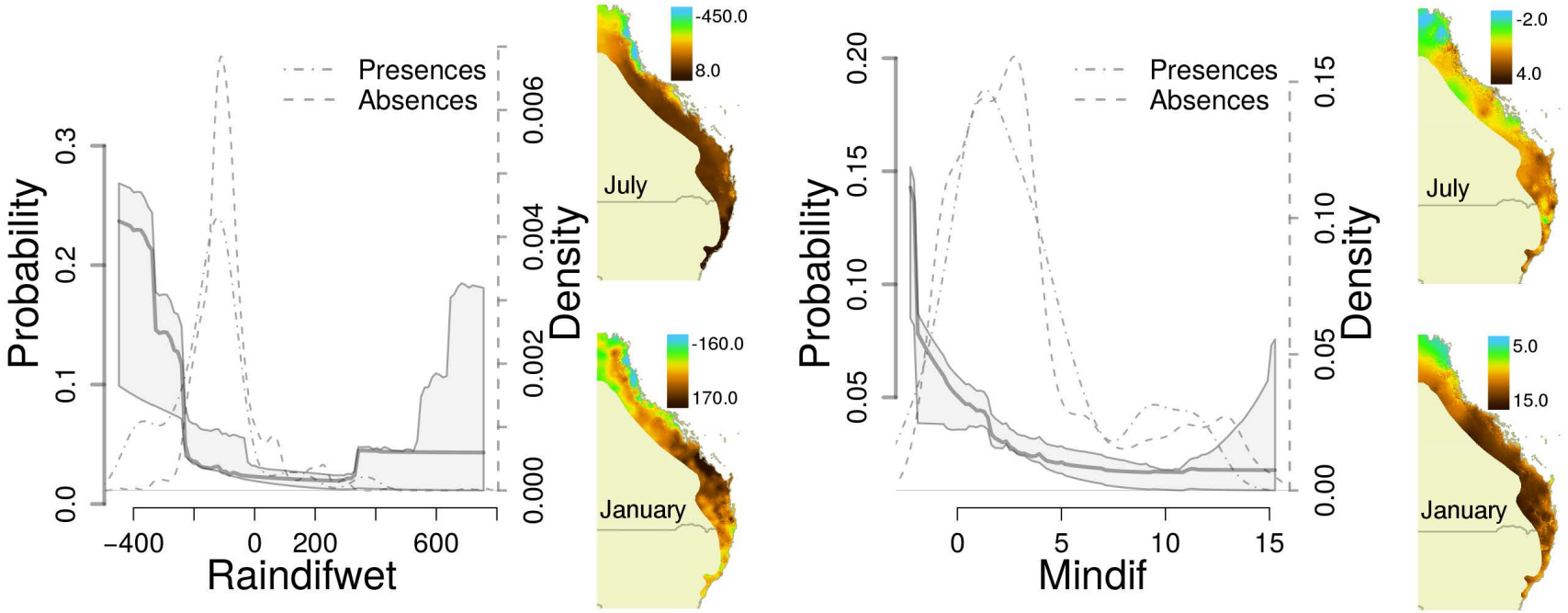

Figure 6.5: Bold lines represent the partial dependence plots for the average weighted model for two variables, *raindifwet* and *mindif*. The grey shaded areas represent the average ± 1 weighted standard error of model predictions. The dashed lines are the density of the variables among presences and absences. Both variables, *raindifwet* and *mindif*, have higher average values among absences than presences, which results in negative relationships between the variables and probability of spillover. The maps on the right side of each graph show the values of both variables in two contrasting months, July and January, the values of *raindifwet* and *mindif* are higher in southern locations in summer months (January), which is correlated with spillover seasonality.

Individual models

All individual models that were combined in the consensus model had a high discriminative ability, AUC = 0.936 (+/- 0.01), and performed significantly better than random when compared with the AUC of 1000 null models ($P < 0.05$). The logistic regression model had the highest AUC and explained 23% of the deviance. Of all variables, *mindif* (minimum temperature difference from the minimum temperature of coldest month) explained most of the deviance with a negative relationship. *mindif* was followed by horse density (negative relationship) and minimum temperature (positive). The boosted regression trees model had the second highest AUC (= 0.935). *Raindifwet* (rainfall difference from wettest month), distance to the niche centroid of bats and horse density explained most of the variability. The random forest model had an AUC = 0.92. It also found *raindifwet* was the most important variable in describing spillover events, followed by minimum average temperature, and distance to bat colonies. In contrast, the Mahalanobis distance model with climate-only data had the lowest performance with an AUC = 0.73 ($P = 0.01$), and was not included in the consensus model because it only included the climatic variables. The AUC scores of the models in relation to the distribution of the AUC scores of the null models are in Appendix Appendix 9.6.3.2 (Figure 23).

The algorithm or combination of algorithms that had the best performance in space of all according to the AUC ratio of the partial ROC test was the average of random forest and boosted regression trees ($1.72, P < 0.05$, P value indicates the probability that the calculated ratio is ≤ 1). As for individual models, random forest ($1.64, P < 0.05$) had a AUC ratio slightly higher than logistic regression ($1.64, P < 0.05$) and boosted regression trees ($1.62, P < 0.05$). The weighted average model that resulted from these three algorithms also performed better than a random prediction ($1.58, P < 0.05$) and clearly shows the lower suitability for spillover in southern regions during summer. The algorithms were slightly different in terms of how variability was explained by environmental factors but their explanatory performance was very similar. For these reasons the consensus model consisted of all three regression methods.

Extrapolation analysis

I identified an area where the consensus model faced extrapolation. This was located in the southernmost limit of the model projection. The type of extrapolation changed between months (extended variable range or inverted variable correlations) and in all cases increased the predicted

spillover suitability. The only month in which the model did not face novel conditions in this area was February, and it predicted low suitability (Figure 6.2). A comparison of these projections with the Mahalanobis distance model shows that the environmental conditions of this southern area are not similar to any of the conditions of the spillover events. In contrast, the small areas close to the border between Queensland and New South Wales that remained with higher probabilities of spillover during summer have similar environmental conditions to other events (Figures 6.3 and 6.4).

Distance to bat camps and horse density

All the projections of the distance to bat camp models after 2007 were predictions of the trained model. All of those models for which I had data for validation performed better than random with AUC ratios greater than 1.5 (maximum possible of 2). An example of the validated models is shown in Appendix 9.6.3.2 Figure 24.

Discussion

The model reproduced the observed spatiotemporal pattern of HeV spillover (Plowright et al., 2015), although there were clear differences. The first was the inverse estimates of suitability with respect to spillover events density; second the prediction of areas at risk during summer below latitude 22°south. These differences are discussed in more detail below. The pattern captured by the model suggests that the higher risk period below latitude 22°south is from April to October. While no events have been reported to occur in April below this latitude, the longer predicted high risk season may be explained by a delay between transmission of HeV from bats to horses and reporting of the clinical case of the disease. Above 22°south, higher spillover suitability is more constant among months (Figures 6.2 and 6.4). The climatic sources of the pattern are most likely related to the difference in minimum temperature from the minimum temperature of the coldest month (*mindif*), and difference of rainfall from rainfall of the wettest month (*raindifwet*). These two climatic factors explained the majority of variability in the data. Minimum temperatures change more dramatically between seasons below latitude 22°south (Figure 6.5) than above this line.

Bimodal responses to rainfall levels (*rainfall* and *raindifwet*) indicate that either wet or dry conditions increase spillover risk. These contradictory relationships suggest that a set of optimal conditions for spillover does not exist. The lack of a single set of optimal conditions for spillover

to occur could indicate that spillover risk is better represented by two systems, one in the north and another in the south. These two systems might well exist as a result of two different bat species likely involved in spillover, *P. conspicillatus* and *P. alecto* (Smith et al., 2014; Edson et al., 2015; Goldspink et al., 2015; Martin et al., 2016). The southern system could be driven by *P. alecto* and the northern by both *P. alecto* and *P. conspicillatus* and involve interactions with different plant communities.

Migration of reservoir hosts could be one of the biological mechanisms driving spatiotemporal patterns. In other bat virus spillover systems, spillover seasonality is caused by greater numbers of microbats migrating to greener areas during winter (Escobar et al., 2013). However, the data I used to calibrate the distance to bat camp models indicates that there are bats still present in areas and seasons without recorded spillover events. In fact, recent analyses indicate that spillover has occurred when bat densities are low due to emigration in response to low food availability (Giles et al., 2016). Although the effects of food shortage in bats are not fully understood, nutritional stress has been associated with increased HeV seroprevalence (Plowright et al., 2008). Nutritional stress in that case was caused by flowering cessation of native plants after a cyclone. However, the relationship between seropositivity and HeV infectious status is unknown (Plowright et al., 2008; Field et al., 2011). In general, HeV spillover has been related to low plant and crop productivity (McFarlane et al., 2011). Consequently some of the potential scenarios by which bat-plant interactions could influence seasonal spillover risk below latitude 22° are: 1) poor nutrition leading to higher infection susceptibility which could lead to higher HeV infection levels and transmission among individual bats; 2) higher densities of bats feeding in more urbanised or agricultural landscapes when native plants are not in bloom (Plowright et al., 2015); or 3) a mixture of infection susceptibility and switching of foraging habitat. Of these processes, there is stronger evidence for infection susceptibility because throughout the distribution of *P. alecto* there is a seasonal gradient, peaking in winter, of HeV excretion (Field et al., 2015a). Although, there are multiple alternative mechanisms that could be influencing seasonal excretion patterns (Plowright et al., 2016).

The negative response of spillover risk to horse density that I found contrasts with previous analyses that failed to demonstrate an effect of horse density (McFarlane et al., 2011; Smith et al., 2014). This effect might occur as a consequence of several different processes, ranging from bat foraging habitat availability to husbandry practices in professionally managed properties associated with higher horse densities. Although not considered here, there could be a relationship

between number of horses per pixel and availability of bat food trees and the type and quality of management practices. This deserves further research to show how paddock management and structure might influence susceptibility to or likelihood of contact with HeV, because it could be one of the mechanisms influencing the spatiotemporal pattern of spillover. In other pathogen spillover systems the same effect of apparent competition between host species arises when the spillover host is negatively affected by the pathogen (Holt and Pickering, 1985; Power and Mitchell, 2004). Horses are affected by HeV, but HeV spillover is too rare to reduce horse density. However, the same effect would arise from ecological competition between bats and horses (Power and Mitchell, 2004). It is possible that domestic horses compete for habitat with bats because horses are linked to land clearing for grazing whereas bats rely on flowering trees for food. Consequently two factors could potentially create the relationship seen here; a negative effect of horses on bats' foraging habitat and a correlation between horse density and professionally managed properties which could have higher horse densities than "hobby farm" properties. Regardless of the underlying cause, the resulting effect is lower spillover risk per horse as density increases.

The consensus model fitted a positive response to distance to the niche centroid of bats, the surrogate measure of bat abundance. The relationship between bat abundance and distance to the niche centroid is generally negative (Martin et al., 2016), hence, greater environmental distances from the niche centroid result in potentially smaller numbers of bats per pixel (Martínez-Meyer et al., 2013). This seemingly accurate prediction given Giles et al. (2016)'s recent findings of spillover occurring during low abundance of bats is, nevertheless, spatially confounded. This is because spillover occurs in foraging areas which are generally physically and environmentally distant from camp sites where bats are most abundant (Vardon et al., 2001).

The differences between the climate-only Mahalanobis distance and the consensus model could be explained by the absence of the factors that are conditional for spillover like the presence of bats and horses. In addition environmental envelope methods' distributional estimates, like those of Mahalanobis distance, are closer to the potential distribution than presence-absence methods that estimate the realised distribution (Jiménez-Valverde et al., 2008; Soberón and Peterson, 2005) Alternative explanations for the wider areas predicted in the climate-only model could be related .to the spatial resolution of the environmental data. It is possible that the spatial scale at which climate influences the biological mechanism driving the spatiotemporal spillover pattern is greater than the 2.7×2.7 km pixels used here. This is a common issue in species distribution and ecological niche modelling studies; ideally the size of spatial units or map pixels should match the scale at

which species select their habitat (Peterson, 2006). For instance it has been suggested that the minimum area for a bat population to persist is 5000 km^2 (Vardon et al., 2001), and the foraging habitat of a bat camp is up to 40 km wide (Field et al., 2015b). Therefore, the spatial scale at which climate influences risk of HeV spillover could be different than the one used here.

My analyses have obvious limitations: 1) the absence of a strong link between climatic factors and a specific biological mechanism precludes the identification of the factors driving seasonality; 2) a poor understanding of bat foraging patterns and HeV transmission pathways to horses may result in misclassification of non-case properties; and 3) the potential errors in the model generated variables (distance to bat camps and DNC), regardless of their high performance, could accumulate uncertainty in the final spillover model.

The higher risk season of HeV spillover below latitude 22° south is from April to October. Whether this seasonal pattern is caused by immigration or emigration of bats is unclear. The number of bats in such areas depends mainly on food abundance, which has been previously suggested as a cause of increased susceptibility to HeV (Plowright et al., 2008). In the context of these observations, it is justified to speculate that the models could well be detecting these signals and the underlying mechanisms of seasonal spillover below latitude 22° south may be a mixture of seasonal movement and feeding of the reservoir host in horse paddocks (Pascual and Dobson, 2005; Grassly and Fraser, 2006). Impairment of the immune function of both reservoir and spillover hosts is also possible and could act in synergy with behavioural changes.

Determining how the components of the HeV spillover system are affected by climate is beyond the scope of this analysis. Thus further research is needed to understand the effects of climate on food availability and the consequent effects on bats and horse interactions and immune function. However, good husbandry practices like restriction of access of horses to trees (where flying foxes feed and excrete HeV) and vaccination against Hendra virus can override the effect of many environmental factors (Haining, 2003). I suggest that these practices should be more rigorously considered and followed in the areas and seasons that are at greater risk of Hendra virus spillover.

Conclusions

The mechanisms driving seasonality of HeV spillover are likely influenced by the seasonal amplitude of minimum temperature and rainfall. These climatic extremes are often associated with food shortages. Therefore, I suggest that future research focuses on determining how behaviour and immune function of both horses and bats change in response to food shortage driven by

climate. Behavioural and immunological changes might be more evident in areas north and south of latitude 22° south, which is where the major differences seem to occur between summer and winter. Although I suggest that the high risk season below the latitude 22° south goes from May to October, considering a longer risk season such as from March-November could result in improved risk mitigation. Properties within and around the areas I have found at high risk should be encouraged to improve mitigation by vaccination and following the prevention guidelines of the Australian Veterinary Association [3], namely: removing feed and water troughs from under trees, restricting access to trees, at least during the night, and removing grass or tall vegetation that might provide better conditions for HeV survival and transmission in the environment.

[3] http://www.ava.com.au/hendra-virus

Chapter 7

Climate change will increase the extent of areas at risk of Hendra virus spillover

In Chapter 5 I showed that the spatial pattern of spillover is mainly driven by the presence of *P. alecto* and *P. conspicillatus*. Risk within the distribution of these species is weakly correlated with a single climatic driver, instead multiple factors act in synergy (Chapter 6). Temporal patterns of risk are likely influenced by flying fox species specific traits along the latitudinal gradient in response to these drivers. Based on these results I generated two models that predict risk according to each flying fox species involved in spillover.

This chapter is the first attempt to predict risk of HeV spillover. By modelling spillover in space under the current potential distribution of its reservoir hosts I predicted spillover risk in response to climate change.

The methods used for these analyses were fully Bayesian hierarchical geo-spatial models. They, compared favourably with methods in Chapters 5 and 6, controlled for spatial autocorrelation and included the effect of the underlying horse population at risk. The resulting spatial models include wider areas, and could be interpreted as the probability that there are adequate climatic conditions for the occurrence of HeV spillover events given that its reservoir and spillover hosts are present.

Climate change projections that result from the different general circulation models carry considerable uncertainty (Stainforth et al., 2005). Because explaining the sources of such uncertainty and reducing its effects on HeV epidemiology is beyond the scope of my project I generated a consensus scenario model, where I show the spillover predictions under all general circulation models available in the Worldclim database (Hijmans et al., 2005).

In terms of the HeV spillover system, this chapter has made substantial contributions towards

mitigation and research agendas. The predictions of these models contribute not only to improve mitigation of HeV's impacts on public health, but on the effects of climate change on biodiversity conservation.

This chapter is in review in EcoHealth, submitted 10 February 2017 (Martin et al., c *in-review*):

- Gerardo Martin, Carlos Yanez-Arenas, Carla Chen, Raina K Plowright, Rebecca J Webb, and Lee F Skerratt. Climate change will increase the extent of areas at risk of Hendra virus spillover. *Emerging Infectious Diseases*, c

ABSTRACT

*When Hendra virus (HeV) spills over from bats to horses and occasionally from horses to humans case fatality rates can be as high as 75%. Therefore, predicting spillover is important to prevent and mitigate its impacts. Given our currently limited predictive capacity, ecological niche modelling is one of the few tools available to forecast estimates of HeV spillover risk at its most fundamental level determined by the climatic suitability of its reservoir hosts. Ecological niche models can produce risk maps which represent the likelihood that environmental characteristics are suitable for the phenomena of Hendra virus spillover. We produced two models to represent risk of HeV spillover in Australia with respect to its two reservoir hosts, the black (*Pteropus alecto*) and the spectacled (*P. conspicillatus*) flying foxes. Using Bayesian hierarchical models with a Log-Gaussian Cox process I maximised available data and generated probabilistic maps for current and future climatic scenarios. With these methods I included a horse population at risk offset to correctly estimate the influence of the climatic suitability of the reservoir host and other climatic factors on HeV spillover risk. We found that current areas at risk are wider than recognised, by the Australian public and stakeholders. Absence of spillover in these areas may be due to the very low density of horses. In response to climate change, suitability for spillover was predicted to increase southwards due to the expansion of the potential distribution of the black flying fox (*P. alecto*), which could result in 110,000-165,000 (175-260% increase) more horses at risk from the 64,000 horses at risk under current climatic conditions. Future suitability for spillover in the northern limits of the distributional range is highly uncertain because models faced extreme extrapolation in this region. However, HeV spillover as explained by the distribution of* P. conspicillatus *is likely to shrink. We recommend that HeV monitoring in bats and HeV prevention in horses be enhanced in areas predicted to be at spillover risk.*

Introduction

Emerging zoonotic diseases account for close to 13% of known human pathogens (Taylor et al., 2001; Woolhouse and Gowtage-Sequeria, 2005). These diseases among other emerging pathogens that affect crops and domestic animals can have deep socio-economic consequences (Jones et al., 2008), especially when they adapt to the new hosts (Taylor et al., 2001). Four diseases that have spilled over from wildlife hosts to humans that have resulted in epidemics are Ebola and Marburgh viruses in Africa (Leroy et al., 2005) and SARS *Coronavirus* and Nipah virus in east Asia (He et al., 2004; Chua, 2003). The consequences of these outbreaks are not only the loss of human lives, but in some instances the collapse of public health systems that control and provide treatment for other diseases (Chang et al., 2004; Plucisnki et al., 2015). What these diseases have in common is not only its high virulence in humans, but its wildlife origin in bats, mammals of the order chiroptera (Li et al., 2005; Leroy et al., 2005; Wang and Eaton, 2007).

Once the aetiologic agents of diseases and its reservoir hosts are defined, prevention of spillover depends on our understanding and consequent ability to predict it. Mechanistic models of infectious diseases have proven useful frameworks to make informed decisions towards controlling and mitigating the impacts of epidemics (Wickwire, 1977). However, these methods require large amounts of high quality longitudinal data rarely available for pathogens of wild animals. However, prediction can be made at lower spatial and temporal resolutions, that are based on different biological mechanisms that require other types of readily available data.

Hendra virus (HeV) is a Paramyxovirus of the genus *Henipavirus* discovered in 1994 in a Brisbane suburb in Queensland (QLD), Australia. Hendra virus spills over to horses and thence to humans from two of the four Australian mainland flying fox species, *Pteropus alecto* and *P. conspicillatus* (Halpin et al., 2011; Smith et al., 2014; Edson et al., 2015; Martin et al., 2016). Nipah virus, a closely related *Henipavirus* from Pteropid bats of east Asia spills over to pigs and humans, where it has been able to cause epidemic disease outbreaks with case fatality rates close to 41% in humans (Chong et al., 2002; Chua, 2003). In Bangladesh, however, spillover occurs directly to humans with even higher mortality rates (Hossain et al., 2008). The proven ability of henipaviruses to cause epidemic outbreaks and the case fatality rates of HeV infection of 50-75% in spillover hosts (although the number of human infections, 7, is very small) make spillover prediction highly necessary. However the unpredictable nature of flying fox movements, the poor understanding of HeV dynamics in bats (Plowright et al., 2015) and the relatively small number of HeV spillover

events in horses, limit our ability to predict its levels in those populations. Consequently, disease risk mapping is one of the few tools available to coarsely forecast HeV spillover and identify populations at risk.

A potential approach to map the risk of disease spillover is by modelling the zoonotic ecological niche of the causal agent and its reservoir (Pigott et al., 2015). Ecological niche modelling, is frequently used to predict species' geographic distributions. The process of niche modelling relates the environmental conditions of locations where species are able to breed and persist, to the prevailing environmental conditions where species can occur (Soberón and Peterson, 2005). The environmental data are then used to fit a statistical model to represent a measure of environmental suitability in spatially referenced data that can be represented as maps (Peterson, 2006). Assuming that the organisms being modelled do not undergo an environmental niche shift, models can then be used to predict future distributions under climate change scenarios (Pearman et al., 2008). For instance using these methods many diseases have been predicted to impact wider areas, expanding or shifting from tropical to subtropical areas (Lafferty, 2009). Therefore, anticipating the potential impacts of climate change on HeV zoonotic niche is critical to adequately allocate resources and mitigate risk. Previous ecological niche modelling studies of *Henipavirus* spillover systems focused on answering ecological and epidemiological questions (Hahn et al., 2014; Martin et al., 2016); or generate broad predictions from its putative reservoir hosts (Daszak et al., 2013). While its contribution towards improving our understanding is valuable, none of them have strictly focused on prediction of spillover.

Empirical evidence suggests that HeV is related to climate by several different mechanisms. The spatial and temporal abundance patterns of flying foxes are related to climatic suitability (Martin et al., 2016). The spatial dynamics of bats are largely governed by food resources that are dependent on climate (Giles et al., 2016). There have been suggestions that HeV shedding can be linked to low food productivity and availability after severe weather events (McFarlane et al., 2011; Plowright et al., 2008; Field et al., 2011). In addition, changes in virus survival in microclimates might facilitate transmission (Martin et al., 2015). In light of this, I present a series of models of the zoonotic niche of HeV spillover to horses under current and future climatic conditions.

Methods

Ecological niche models often use presence only data which has led to the extensive use of algorithmic modelling (Elith et al., 2011). A well known disadvantage of these methods is their

potential for use as black boxes given their complexity. Recent efforts have made possible the application of better understood techniques like generalised linear models for presence only data, in the form of Poisson point process models (Renner and Warton, 2013; Renner et al., 2015). Taking advantage of these, now widely available, statistically transparent frameworks I modelled the risk of HeV spillover as a Log Gaussian Cox process in a Bayesian hierarchical inference framework. These models incorporate a Gaussian field to model spatial dependence between point observations which allowed us to use all the spillover records registered to date without the need of thinning to reduce spatial autocorrelation. Instead I modelled spatial dependence with a pre-specified covariance function. The resulting models were used to forecast future risk of HeV spillover with a series of climate change scenarios.

We assumed that risk of HeV spillover comprises two separate reservoir host systems, as suggested by the results in Chapter 6. Each system is limited to the areas assumed to be colonisable by the two key reservoir host species, *P. alecto* and *P. conspicillatus* (Martin et al., 2016; Soberón and Peterson, 2005). Each of the colonisable areas was assumed to be the climatic regions of Australia obtained from the bureau of meteorology[1] that contained at least one presence record of each of the flying fox species. The expected intensity of spillover cases was explained by a series of Worldclim bioclimatic variables (Hijmans et al., 2005) and the climatic suitability for the two key reservoir hosts previously modelled with Maxent (Martin et al., 2016; Phillips et al., 2006, Chapter 5). These models were built in a similar fashion as described below, save for the model fitting procedure. To select the relevant bioclimatic variables for each system, I performed a Niche views procedure. It consists of an analysis of the correlations between pairs of explanatory variables and the location of the presence points within the bivariate clouds of data points (BIO1-18 and *P. alecto* or *P. conspicillatus* models, Owens et al., 2013). The variables selected should have the presence points lying close to the centre or relatively far from the margins of the range of values within the bivariate cloud of data (Owens et al., 2013).

To assign spillover events to either system (*P. alecto*, north and south, and *P. conspicillatus*, strictly north, Figure 7.1), I extracted the Maxent relative probability of presence of the two flying fox species at the location of spillover. The spillover location points were assigned to their corresponding host reservoir system depending on which species had the maximum probability value, assuming that transmission to horses occurred from the reservoir host most likely to be found in that area. To this data, I added the location points to each host reservoir system that

[1] http:www.bom.gov.au

had lower maximum probability values than for the other reservoir host species for that point but were within the top 5% of probabilities of occurrence for that species at spillover locations, mimicking the standard statistical significance threshold, to allow some ambiguity of transmission source.

Parameters for the Poisson model representing the intensity of spillover event points per area unit and spatial autocorrelation with a Log-Gaussian Cox process, were estimated by Markov chain Monte Carlo (MCMC) with a Metropolis-adjusted Langevin sampler implemented in the R 3.2.3 `lgcp` package (R Core Team, 2016; Taylor et al., 2013). Model selection was performed a priori with a down weighted Poisson regression. This method consists of assigning very small uniform weights to the spatial units with presences and weights equivalent to the area of spatial units to the spatial units without spillover events recorded (quadrature points or background in Maxent Renner and Warton, 2013). The weights were 1×10^{-6} for units containing spillover events and the area measured in km^2 of the cells for quadrature points (Renner and Warton, 2013). The optimal grid size for the point processes was estimated with a minimum contrast method. We began selection of the down weighted Poisson model with four model structures with the variables selected in the process described above (Renner et al., 2015); interactions between all explanatory variables; with linear, quadratic and cubic terms; linear and quadratic terms and a series of interactions between linear, squared and cubed terms. Each model was then subject to automated step-wise variable deletion until I obtained the model with the lowest AIC. The variables that were kept in the model with the lowest AIC were then included in the final model to be fit as a Log-Gaussian Cox process. Further refinements to the model structure were carried out after assessing the predicted spatial patterns and the convergence behaviour of the Metropolis sampler (Taylor et al., 2013).

To find the appropriate spatial covariance function I fitted several models with short chains of 5000 iterations of the MCMC sampler, with 500 burn-in iterations and thinning rate of 15 with the exponential and spiked exponential covariance functions. The chains were run with a range of priors and number of neighbouring cells to compute the covariance function. When the short MCMC chains appeared to be well mixed, with lower values of autocorrelation and no rejected samples during the 'run' phase, I ran the full MCMC chains. The final size of the chains was chosen upon the behaviour of the h parameter. For runs with $h \approx 0.3$ I used 5M iterations, but in cases where h decreased the number of iterations was increased to up to 20M. Models with any $h < 0.1$ at the end of the 5K iteration chain were rejected. The burn-in phase included 10% of the

number of iterations and the thinning rate was set up to keep 1% of the posterior samples (Taylor et al., 2015). To have a model that represents the underlying risk, regardless of the underlying population at risk, I corrected for the effect of horse population on spillover intensity per unit area, with a horse population density model as an offset. In the absence of more data regarding horse densities than the 2007 horse census (Moloney, 2011), a critical assumption is that horse population of 2007 is still correlated and broadly representative of the horse population during the time when HeV spillover events have occurred, at the spatial scale of the model. Hence the Poisson component of the model with population offset and spatial covariance results in the Bayesian model of equations 7.1a and 7.1b:

$$\begin{aligned} \mu(s) &= \exp\left(\beta Z(s) + Y(s)\right) \\ R(s) &= C_A \lambda(s) \mu(s) \\ X(s) &\sim \text{Poisson}\left(R(s)\right) \end{aligned} \tag{7.1a}$$

$$\begin{aligned} \text{cov}\left[Y(s_1), Y(s_2)\right] &= \sigma^2 r\left(\|s_2 - s_1\|; \phi\right) \\ r(s) &= \exp\left(-s/\phi\right) \\ s &= \text{euclidean}(s_2, s_1) \end{aligned} \tag{7.1b}$$

Parameter priors:

$$\begin{aligned} \beta &\sim \text{normal}(0, 10^6) \\ \log(\phi) &\sim \text{normal}(\log(500), 2) \\ \log(\sigma) &\sim \text{normal}(\log(1), 0.15) \end{aligned}$$

Where β is the vector of effects of environmental covariates $Z(s)$; $Y(s)$ is the bivariate (s_1, s_2) covariance function, C_A is the spatial grid cell size, $\lambda(s)$ is the horse population density, $X(s)$ is the point intensity data, and σ and ϕ are the exponential covariance function ($r(s)$ in equation 7.1b) parameters (Taylor et al., 2013; Diggle et al., 2013).

The horse population density model was built with the horse population census of 2007 (Moloney, 2011). This horse density model was created by introducing non-parametric noise to the geographical coordinates of the horse properties, equivalent to 50% of the cell width of the environmental data. The number of horses per grid cell after noising the coordinates was rasterised, and the process was repeated 100 times. When iterations were completed the 100 raster layers were averaged to create the final horse density model (Figure 7.1). This method allowed us to account for the effect of properties spanning more than one grid cell but whose centroid lied within a single pixel.

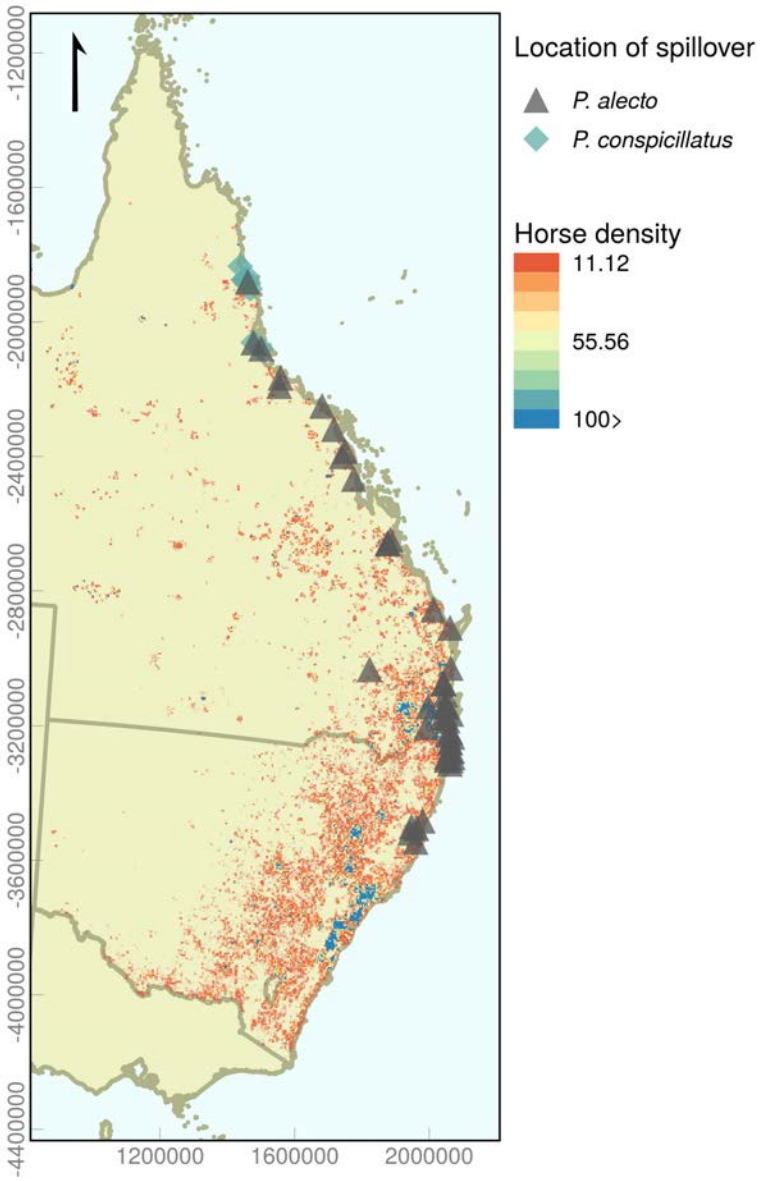

Figure 7.1: Location of spillover events over the horse density model. The symbol for spillover events represents the species that each event was attributed to with the method described.

Once I obtained the converged MCMC chains, I used the posterior estimates of the environmental covariates to project the median point intensity of spillover per unit area in geographic and environmental space. Using the posterior distributions of intensity per unit area I calculated the probability that the predicted intensity exceeds the lower 20th percentile of the median intensity estimated for the locations with spillover events. This threshold was chosen because the database contains location uncertainty in nearly 20% of the spillover locations. Then to simulate the future scenarios of spillover, I compared the data used for model fitting with the prediction data with

an extrapolation analysis using the extrapolation detection tool (ExDet, Mesgaran et al., 2014). This is necessary because statistical models can result in spurious predictions when they face data different from that used to fit the model. For instance prediction data can differ in the range of values used to fit the model (type 1 extrapolation) or have different correlation structures between co-variables (type 2 extrapolation). The analysis was used to identify the geographical areas where the model faced extrapolation conditions in the climate change scenarios. We used these results to remove all areas of predictions where models faced extrapolation due to novel climatic conditions. We used the 16 climate change scenarios under two different greenhouse gas representative concentration pathways (RCP 45 and 85, Hijmans et al., 2005). Concentration pathways are a series alternative trajectories that greenhouse gas concentration might follow depending on a series of ecological, technological, socio-economic, political and demographic factors that could result in different degrees of climate change. The number that accompanies the acronym RCP indicates the severity of greenhouse gas concentration (van Vuuren et al., 2011).

To allow visualisation of the potential consequences of climate change I generated a consensus view of climate change projections. To do so I applied an exceeding probability threshold to all climate change projections. The resulting map highlights areas where risk could remain, areas where risk could increase and areas where risk could decrease. This was done with a series of modifications to the layers' binary values such that when they were added all areas under similar levels of current risk have positive values, areas where risk could increase have negative values and areas with lower risk had values closer to 1.

Combining the layers for the consensus climate change model We began by setting areas that contained model extrapolating conditions to 0 from each exceeding probabilities projection in climate change scenarios. Then I thresholded all models with the same cut-off value of 0.2 used to test the models' performance (20% omission rate). After applying the threshold to the exceeding probabilities models, the areas predicted to be at risk contained values of 1 (present > 0.2), and areas at lower risk contained values of 0 (absent ≤ 0.2). The areas predicted absent in the model projection under current climatic conditions were set to -1 (presence = 1, absence = -1). Then, each of the thresholded climate change projections had 1 added, so that areas predicted absent = 1, and areas predicted present = 2. All these new binary layers were then added into a single layer. Finally, I multiplied by the present risk scenario (presence = 1, absence = -1), so that all areas that were predicted present in future climatic conditions but were absent in today's conditions

became negative (increased risk). All areas that were predicted present had positive values; and the areas that became unsuitable after climate change had values closer to 1 (presence today × absence future = 1). Future absence in the areas represented by these calculations can be caused by areas remaining in the same state as in current conditions, areas becoming unsuitable, or by being unable to predict anything due to extrapolation. To help readers identify areas I was unable to predict due to extrapolation I provide the map of extrapolation conditions, which is an average of the binary layers with extrapolation conditions for each climate change scenario.

The climate change consensus scenarios were used to calculate the number of horses, based on the 2007 horse population census, that would be contained in the areas to be come at risk. In any case I report the maximum number of horses that could become at spillover risk.

Models' predictive performance was measured with the partial ROC with a 20% omission rate (Peterson et al., 2008) for the*P. alecto* system, and with a Jacknife test (Pearson et al., 2006) for the *P. conspicillatus* system, because the sample size (9 events) limited the use of other validation methods. We partitioned the *P. alecto* system data in four sets and cross validated their predictions with models fit in one chain of 5M iterations, burn-in of 500K and thinning of 4.5K. We allowed the partial ROC test a 20% omission of the test points to represent the 20% uncertainty in spillover location according to the Biosecurity Queensland dataset. While desirable, a higher number of partitions was not possible due to the high computational intensity these analyses. For the *P. conspicillatus* system, I fitted 8 models, each one omitting one of the spillover presence points. Then I calculated the minimum thresholds and its corresponding percent of area predicted for the Jacknife test.

Results

Model projections

The predicted spatial patterns of risk under present climatic conditions for both reservoir host systems are consistent with the distribution of spillover events since 1994. Current risk as explained by *P. alecto*, comprises most of the east coast of Australia, from northern QLD to central New South Wales (NSW). Additional areas spanning farther north than the northernmost known spillover event were also predicted (Figure 7.2). Risk driven by *P. conspicillatus* resulted in novel areas predicted to be at risk of spillover, located in the northernmost location within Australia(Figure 7.3).

In the *P. alecto* HeV spillover system, when I projected the models to future climate change scenarios in 2050, all 16 scenarios agree that there will be an expansion of risk towards the south and slightly farther inland (red areas in left panels of Figure 7.4). This expansion could result in 112 914 more horses (175% increase at 2007 levels) at risk under the greenhouse gas representative concentration pathway (RCP) 45, and 164 391 for RCP85 (260% increase). The majority of horses in areas at increased risk occur over 390 and 425 km respectively along the coastline south of the southernmost known spillover event. Expansion in both RCPs reaches an area called the Hunter Valley in NSW, which has a high density of horses. The climate change scenario agreement in this area is very high. Despite the increased geographical extent of spillover risk, model projections predicted average lower probability of exceeding the specified intensity threshold for spillover to occur (20^{th} quantile of median intensity at spillover locations) compared with current conditions.

While there is consensus that novel areas will be at risk in northern locations in the *P. alecto* spillover system, these areas will face novel climatic conditions that result in model extrapolation, which increases uncertainty (top right corner of right panels in Figure 7.4). We could not identify areas that became completely unsuitable for spillover (highlighted in green). The only areas with 100% agreement to become completely free of risk are most likely over-predictions, because they lie very far from the know distribution of spillover and *P. alecto*.

The effect of the greenhouse gas representative concentration pathways is probably a greater inland expansion of risk in RCP 85 compared with RCP 45, based on *P. alecto*. This means that in the more severe climate change scenario in response to green house gas accumulation, risk will increase farther inland.

With respect to *P. conspicillatus*, models predicted both expansion and contraction but with low agreement between climate change scenarios (left panels Figure 7.5). The northernmost end of modelled areas were predicted to shrink in risk in both concentration pathways, although these areas were affected by extrapolation. Other small areas were predicted to become unsuitable in RCP 85 that were not affected by extrapolation. Both scenarios, RCP 85 and 45, predict lower probabilities of exceeding the intensity threshold, compared with current climate scenarios (right panels in Figure 7.5). The areas that experienced no change for *P. conspicillatus* were small, and compared with *P. alecto*, they experienced either no change or expansion (darkest blue figures 4 and 5). This indicates that *P. conspicillatus* habitat is likely to shrink, and become more suitable for *P. alecto*, which raises concerns over *P. conspicillatus* conservation measures that might also affect HeV epidemiology.

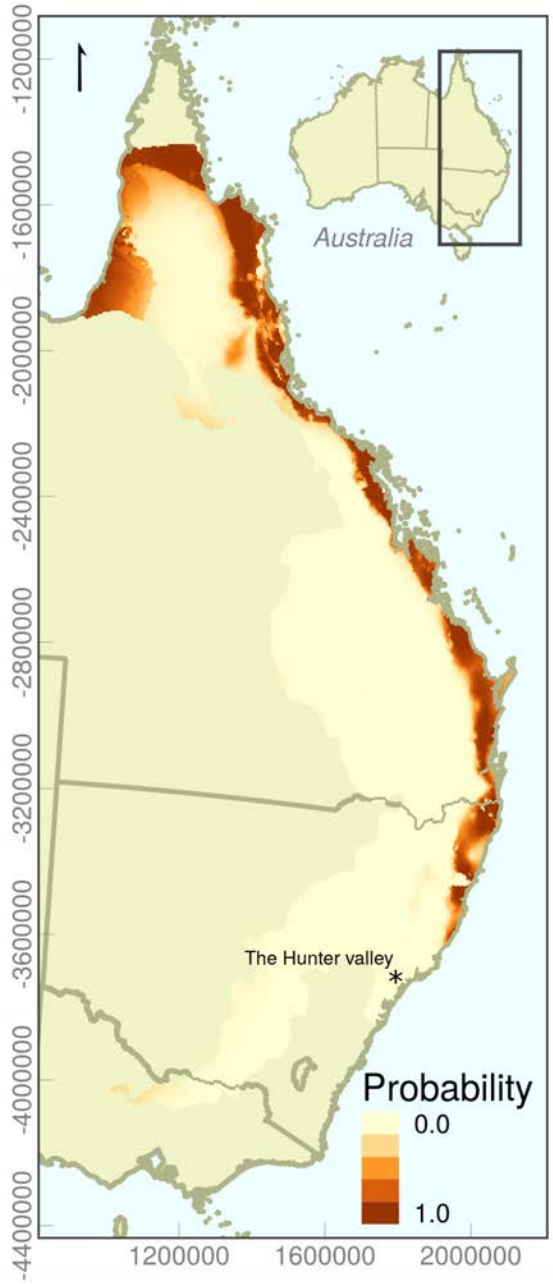

Figure 7.2: Present risk of HeV spillover as explained by the distribution of *P. alecto*. The Hunter valley mark is a high horse density area.

Model fit and performance

The model selection procedure resulted in retention of the variables and interactions in tables 7.1 (*P. alecto*) and 7.2 (*P. conspicillatus*). For the *P. alecto* system I could successfully implement the best model according to the AIC of the downweighted Poisson regression. However, for the *P. conspicillatus* system all attempts to include linear and quadratic terms or their interactions

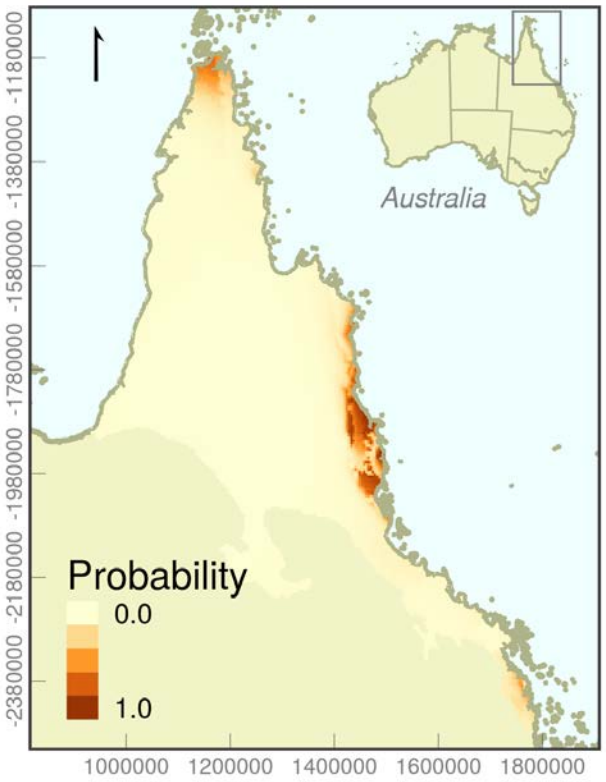

Figure 7.3: Present risk of HeV spillover as explained by the potential distribution of *P. conspicillatus*.

resulted in either singularity of the covariance matrix or in very long MCMC chains. As a result, I sought to keep a balance between AIC and the convergence properties of the MCMC chain which resulted in a simple model of linear terms of the climatic components and a cubic term of the *P. conspicillatus* Maxent model.

Both models converged with 10M iterations, burn in of 1M and thinning rate of 9K. Both models performed better than random based on its respective performance metrics. The *P. alecto* HeV spillover system had an area under the curve ratio of 1.47 that was significantly different from 1 ($P = 0.04$, 1 represents the random prediction threshold) with an omission rate of 20% consistent with the threshold to calculate the exceeding probabilities. The *P. conspicillatus* spillover system that was tested with the Jacknife test, also performed better than random with a prediction rate of 0.75 ($P = 2 \times 10^{-6}$). Given that I was looking for a 20% omission threshold and the small number of presence points in the *P. conspicillatus* data set, the prediction rate of 0.75 is acceptable.

The absolute effect of each of the variables included in the model of the *P. alecto* system, only bio15 (precipitation seasonality) and *P. alecto* had positive effects (Figure 25 in Appendix 9.6.3.2). Whereas variables in the *P. conspicillatus* system, only probability of *P conspicillatus* presence had

Table 7.1: Posterior parameter estimates of the *P. alecto* system model. β's represent the regression coefficients. Parameters σ and φ are the mean and variance of the spiked exponential covariance function. *bio5* = maximum temperature of warmest month, *bio9* = mean temperature of driest quarter, *bio12* = total (annual precipitation), *bio15* = precipitation seasonality (coefficient of variation), *Maxent.p.alecto* = relative probability of presence (climatic suitability).

	median	2.5%	97.5%
$\log(\sigma)$	3.817497×10^{-2}	-1.568415	7.081970×10^{-1}
$\log(\phi)$	1.588467	2.679587×10^{-1}	3.093003
$\beta_{Intercept}$	3.922981	-3.376057×10^{1}	3.852942×10^{1}
β_{bio5}	-9.316293×10^{-2}	-1.890911×10^{-1}	1.705975×10^{-2}
β_{bio9}	-8.620517×10^{-3}	-5.012380×10^{-2}	3.087590×10^{-2}
β_{bio12}	-1.710871×10^{-2}	-3.934777×10^{-2}	3.480018×10^{-3}
β_{bio15}	1.840011×10^{-1}	9.811339×10^{-2}	2.795649×10^{-1}
$\beta_{Maxent.p.alecto}$	-1.438959×10^{2}	-2.504255×10^{2}	-3.564127×10^{1}
$\beta_{I(Maxent.p.alecto^2)}$	5.913680×10^{1}	-6.198367	1.252079×10^{2}
$\beta_{bio5:Maxent.p.alecto}$	2.524097×10^{-1}	4.738640×10^{-2}	4.704084×10^{-1}
$\beta_{bio12:Maxent.p.alecto}$	9.334252×10^{-2}	2.171861×10^{-2}	1.726844×10^{-1}
$\beta_{bio12:bio15}$	-1.433364×10^{-4}	-2.197990×10^{-4}	-7.637361×10^{-5}
$\beta_{bio12:I(Maxent.p.alecto^2)}$	-7.449967×10^{-2}	-1.408666×10^{-1}	-1.353857×10^{-2}

a positive effect on the probability of exceeding the intensity threshold (Figure 26 in Appendix 9.6.3.2). Proof of model convergence is given in Appendix 9.6.3.2, figures 29-34.

Extrapolation analysis

All future climate scenarios result in novel conditions for the model especially in northern areas. Extrapolation affected mostly the projections of the *P. alecto* spillover system, because extrapolation occurred in the novel areas in northern QLD (top right corner of the right side panels Figure 7.4). All the climatic variables used in the model caused type 1 extrapolation in these areas. Type 1 extrapolation is an increased range of values than used in model training (Mesgaran et al., 2014). Additional areas of extrapolation occurred in southern locations along the coast.

Table 7.2: Posterior parameter estimates of the *P. conspicillatus* system. *bio2* = mean diurnal range (mean of max temp - min temp), *bio5* = maximum temperature of warmest month, *bio9* = mean temperature of driest quarter, *p.consp* = relative probability of presence (climatic suitability).

Parameter	Median	2.5%	97.5%
$\log(\sigma)$	0.2876164	-2.29218438	1.72870463
$\log(\phi)$	1.5956162	0.17490535	2.93283772
β_{bio2}	-0.3454483	-0.82917878	-0.06260373
β_{bio5}	0.1196481	-0.09607769	0.48394434
β_{bio9}	-0.1569954	-0.48183344	0.04463800
$\beta_{I(p.consp^3)}$	10.3125608	2.46454087	28.37984947

Because extrapolation in these areas was caused by the model of *P. alecto* distribution which can only have values 0-1 extrapolation artefacts are unlikely. We did not perform an extrapolation analysis for *P. alecto* models, but only compared the predictions of Maxent models fit with and without clamping and extrapolation and did not detect any difference.

Extrapolation in the *P. conspicillatus* system was mostly present in areas that are outside the range of *P. conspicillatus*. These areas were included as quadrature points because *P. conspicillatus* records reach some of the climatic regions that were assumed to constitute the areas available to colonise by the bat species. Therefore, predictions within these areas are least likely to affect predictions, save for the novel areas in the northernmost end of Australia. Some climate change scenarios, however, predict the occurrence of extrapolation type 1 and 2 through the current distribution of spillover likely caused by *P. conspicillatus*. Probability of extrapolation for this system is shown in the top right corner of the right side panels in Figure 7.5.

Discussion

When models were projected to climate change scenarios, I observed a southwards expansion of suitability, but high uncertainty in areas north of the current distribution. In addition to a southwards increase, some scenarios predicted an inland expansion in the *P. alecto* spillover system. However, while the total area at risk of spillover was predicted to increase, probability of spillover in these areas was predicted to slightly decrease, especially with respect to *P. conspicillatus*.

In areas at risk with respect to *P. conspicillatus*, risk with respect to *P. alecto* was predicted to remain relatively stable or increase. These expansions suggest that additional mitigation efforts should be allocated where risk has been predicted to increase (marked as red in the consensus maps in Figures 7.4 and 7.5). In addition, the further expansion of *P. alecto* into *P. conspicillatus* areas implies that *P. alecto* may replace *P. conspicillatus*. Regarding the potential frequency of spillover events I cannot make any statements because the seasonal patterns could change rather unpredictably (Chapter 6, (Pascual and Dobson, 2005)).

Regarding the biology behind the statistical associations in the models, there seem to be similarities with the consensus model in Chapter 6 in the *P. alecto* system. First, most of the variables' interactions that were kept in the model represent rainfall (*bio12*) and its seasonality (*bio15*). These two interact with the suitability for *P . alecto*, indicating that interactions between rainfall, its variability and the probable presence of this bat species are important for spillover. In fact, high suitability for *P. alecto* is not enough to explain spillover, because *Maxent.p.alecto* alone had a negative effect, which is reversed when it interacts with rainfall levels (Table 7.1). Of course it would be speculative to state which components of HeV spillover would be affected, bats, horses vegetation or the virus. What I could infer from these associations is that rainfall levels and its variability with respect to seasonal extremes could in fact be important drivers of spillover risk (Martin et al., b, *in-review*, Chapter 6). Whereas in the *P. conspicillatus* system, the small number of spillover events (9), limits the number of variables that could be included in the model and its interactions. From the structure I kept, only climatic suitability for *P. conspicillatus* had a significant effect. Given its cubic exponent and positive effect, I can infer that transmission from this species to horses could only occur in areas where climatic suitability for this species is very high.

The forecasted area of HeV spillover to horses is wider than the area of detected HeV spillover events. Based on both, *P. alecto* and *P. conspicillatus*, areas farther north than previously recognised were predicted to be at risk. Absence of spillover detection in these areas is probably due to the very low density of horses and potentially of humans (Figure 7.1). However it seems that low horse population densities are associated with higher spillover risk (Chapter 6, Martin et al *in-review*).

Previous niche modelling of *Henipavirus* hosts predicted broad areas at risk in Australia (Daszak et al., 2013). Our results differ from these predictions because I have included more detailed data regarding the causal associations between the reservoirs and spillover hosts. Before 2014 it

was unclear which bat species were more relevant for HeV epidemiology. Recent findings have provided statistical (Smith et al., 2014), epidemiological (Edson et al., 2015) and ecological support (Martin et al., 2016) for the involvement of *P. alecto* and *P. conspicillatus* as the main HeV reservoir hosts. Hence the narrower areas that I predicted to be at risk.

There was complete agreement among climate change scenarios that there will be a southwards increase of suitability for spillover caused by the response of *P. alecto* to climate change. However, the already observed southwards expansion of *P. alecto* is faster than predicted by changing climate (Roberts et al., 2012), suggesting that other factors are also affecting the presence and density of species (Soberón and Peterson, 2005). To date the southernmost recorded spillover events in Kempsey, north-central eastern NSW (figure 7.1), lie within the limits of the current potential distribution of spillover (blue areas in left panels of Figure 7.5). This shows that even when *P. alecto* is capable of occupying areas beyond its optimal niche, spillover occurs within the areas with the highest suitability in most cases, most likely due to higher densities of *P. alecto* (Martin et al., 2016). Therefore, as climatic suitability alone for *P. alecto* continues to increase southwards, spillover is likely to do so as well.

As mentioned above, the models predicted a southwards expansion of risk with high agreement between climate change scenarios; and farther inland with lower agreement. The cause of predicted expansions might be related to the higher temperatures expected at higher altitude and lower latitudes (Lafferty, 2009), particularly in Australia (Williams et al., 2003). This is consistent with the predictions of tropical diseases expanding or shifting into subtropical areas (Lafferty, 2009). The lower agreement on the inland expansion indicates that the effect of altitude is less clear among climate change scenarios. In fact, some of the scenarios indicate that there could be a contraction towards the coast. Consequently, to adequately assess if there will be expansion or contraction to and from the coast, flying fox monitoring programs might be of great value to establish which is the more likely scenario, that could result in a decrease of the horse population density at risk in central QLD.

The ultimate implications of the south and probable inland expansion could be a greater number of horses at risk of spillover, based on this study. Depending on the representative concentration pathway (RCP), there will be at least 112-165,000 more horses at risk out of a population of 64,000 horses currently at risk in eastern QLD and north-east NSW (175-260% increase) based on the 2007 horse census. Because there is considerable uncertainty around the potential outcomes in new areas, more research is needed, first to verify predictions of increased risk, second to

assess changes in horse population since 2007, and then to anticipate the consequences. One potential area of ecological and epidemiological research might involve the role of novel ecological interactions between flying foxes and other organisms that could experience distributional shifts. We need to understand if these novel interactions affect the dynamics of bat populations, HeV and spillover (Williams et al., 2003; Sala et al., 2009).

Our models predicted that spillover could decrease with respect to *P. conspicillatus* in response to climate change. However, with respect to *P. alecto* spillover was predicted to remain or increase within the areas suitable for *P. conspicillatus*. Therefore, these areas of tropical north QLD could experience a replacement of reservoir host species. We don't know if such replacement of reservoir hosts may result in epidemiological processes that would require different mitigation strategies. We recommend, as a result, that an area of research might involve the development of specific management strategies for the different flying fox species relevant to Hendra virus spillover to anticipate flying fox species' replacements.

The predicted shrink of *P. conspicillatus* potential distribution could also affect the dynamics of many ecosystem processes because flying foxes are effective pollinators and seed dispersers. The absence of such ecosystem services could result in further biodiversity loss. Such loss of ecosystem services occurs even before bats become extinct (McConkey and Drake, 2006). Consequently serious additional conservation issues may arise as result of *P. conspicillatus* decline that could also affect HeV epidemiology.

Predicting HeV spillover with the methods I used carries considerable uncertainty. Sources of uncertainty are likely related, but not limited to: 1) the type of presence only data used; 2) the effects of climate on HeV spillover act at several different levels of ecological organisation and are not well understood; 3) flying fox species distributions do not depend entirely on climate (Tidemann et al., 1999; Vardon et al., 2001); 4) the predicted distributions in response to climate change do not account for other organisms' shifting distributions that affect bats; 5) climate change could also affect horses' behaviour or susceptibility to diseases which could either increase or decrease spillover risk, however this aspect might also be affected by human intervention. Other organisms shifting distributions might give rise to novel and unpredictable interactions and effects on bat distributions. It is unclear whether the lower average probability of spillover that climate change scenarios predict will effectively translate in lower frequency of spillover. All of these issues, warrant further research to increase understanding of HeV epidemiology and bat virus spillover in general.

Spillover of diseases from wild to domestic animals and humans comprises several levels of ecological organisation. The first level includes the distribution of the reservoir host, and then the distribution of the causal agent within the reservoir host (Plowright et al., 2015). By including the additional layer of spillover host distribution as an offset during model fit, I have isolated the effect of climate (Taylor et al., 2015) on the biological processes that affect the reservoir and the causal agent and result in HeV spillover . Therefore, the models represent the underlying risk to any spillover hosts present in the areas predicted to be at risk. The 20% omission threshold indicates that within these areas at least 80% of spillover cases will occur. The precise location and timing of spillover cases will depend on processes that occur at smaller scales like the fraction of susceptible horses that are effectively exposed to surviving virus excreted in areas where infected flying foxes forage (Plowright et al., 2015). Consequently the models should be used to identify areas to allocate resources for mitigation and undertake research activities.

Conclusions

Our results indicate that current potential distribution of HeV spans farther north, but the absence of reported spillover events might be due to the very low horse density. Spillover will potentially increase towards the south, and inland. However, the latter expansion will have to be assessed by monitoring of flying fox populations. In northern QLD, the likely replacement of *P. conspicillatus* by *P. alecto* indicates that mitigation strategies may have to be adapted to mitigate risk of HeV spillover.

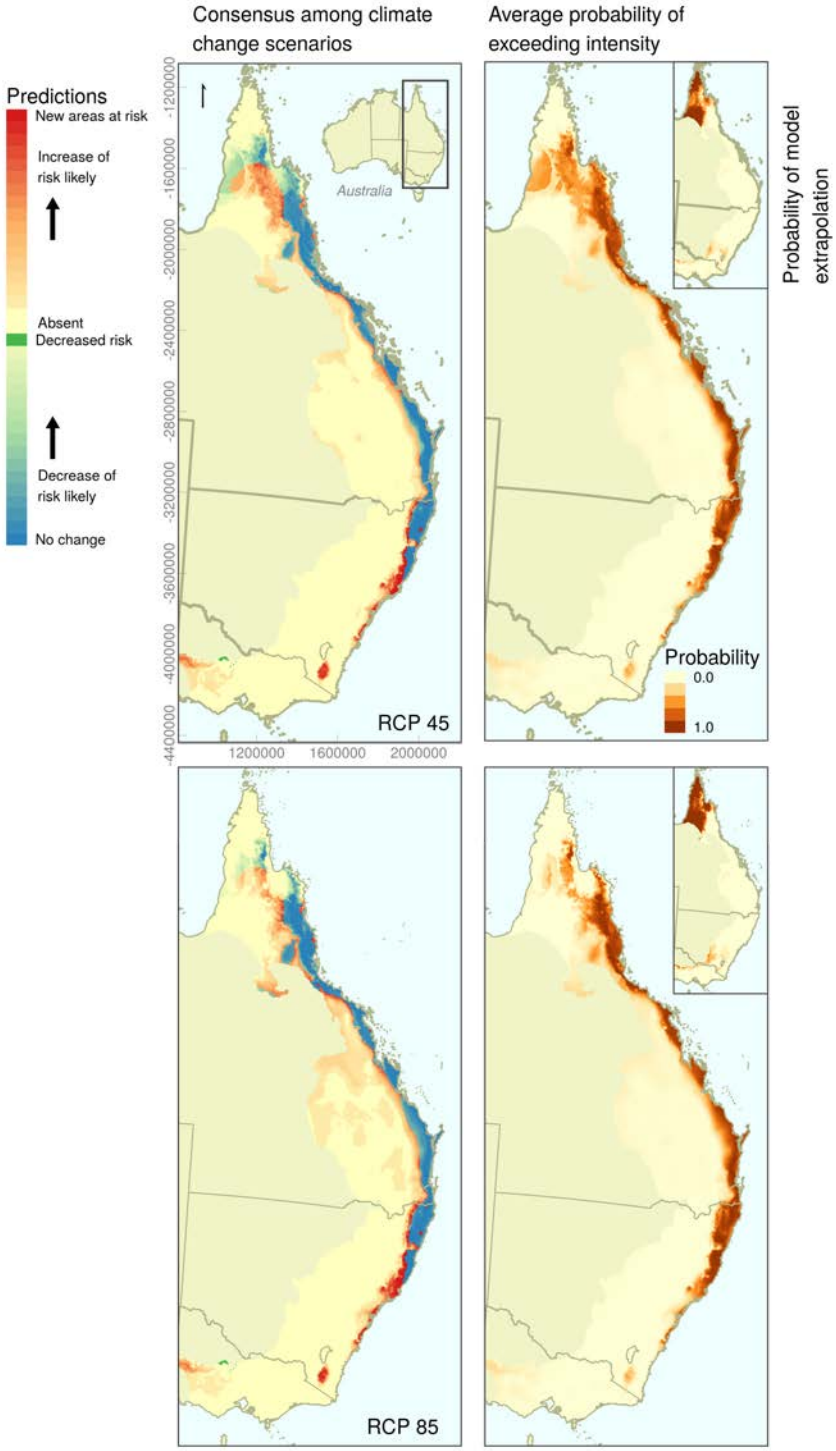

Figure 7.4: Predicted risk for 2050 in two greenhouse gas representative concentration pathways (RCP) for the *P. alecto* spillover system. Top RCP 45, and bottom RCP 85. Left panels show areas of expansion and contraction and the level of agreement between climate change scenarios. Right panels show the average predicted probability of spillover among climate change scenarios (main panels); top right corners show the probability of model extrapolation (pixel-wise proportion of scenarios that had either extrapolation type 1 or 2). The red and green areas in the bottom left of the agreement scenarios are most likely overpredictions, and shouldn't be interpreted as areas at increased risk.

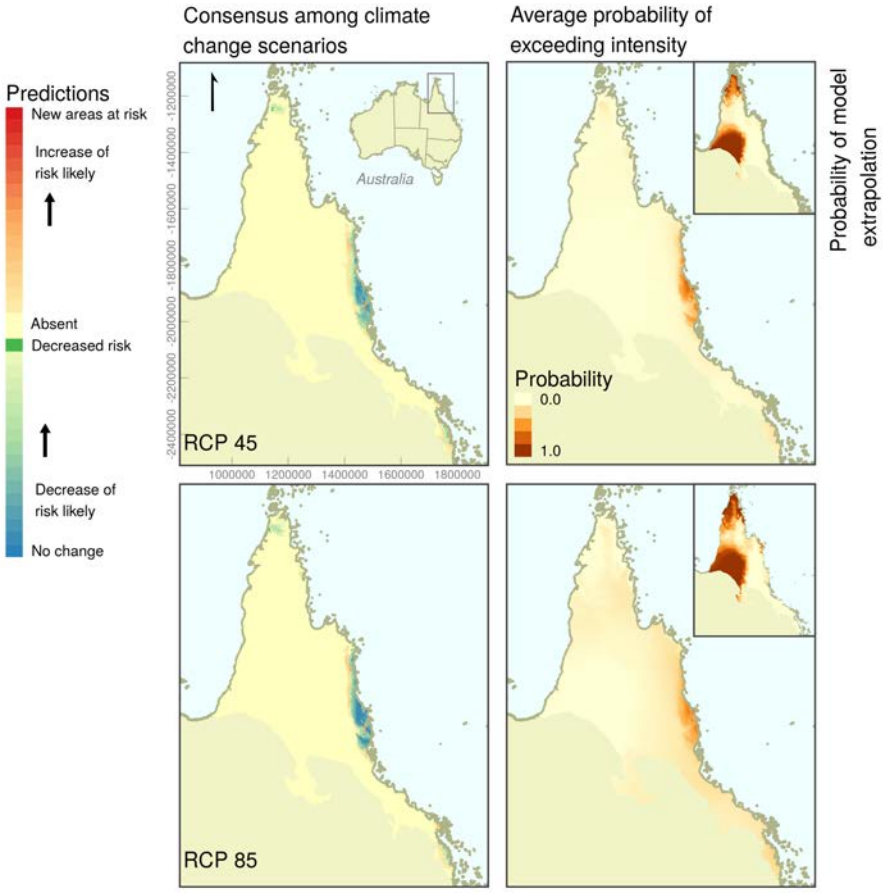

Figure 7.5: Predicted risk for 2050 in two greenhouse gas representative concentration pathways (RCP 45 and 85) for the *P. conspicillatus* spillover system. Left panels show the areas of contraction and expansion and the degree of agreement between climate change scenarios. Right panels (main) show the averaged probability of exceeding the threshold intensity. Top right corner of left panels shows the pixel-wise probability of extrapolation in the averaged model.

Part IV

The paddock environment and horse behaviour: influence of paddock on risk of contact with Hendra virus

Chapter 8

Tree cover in paddocks could be an important determinant of exposure to Hendra virus in horses

A necessary factor for spillover to occur is spillover host exposure to live viral particles (enabling conditions for spillover, Chapter 2, Plowright et al., 2015). Depending on climatic conditions, horse contact with HeV has to be immediately or soon after excretion for transmission to occur (Chapters 3 and 4). Consequently, the more time horses spend away from these areas the less likely they are to contact live HeV. The time that horses spend away from areas contaminated with HeV could be a result of husbandry, for instance, night time stabling, night time fencing of trees, or the absence of incentives to remain in these areas.

Currently, very little research has involved studying the behaviour of horses, and more specifically how their behaviour relates to areas where HeV is excreted, which comprises the areas covered by trees in a paddock (the *drip zone*; Field et al., 2011). To fill some of the gaps, I decided to track horse movements with GPS trackers in order to calculate how much time they spend in these areas. With the collected data I related the time horses spent under trees to a series of paddock characteristics, to identify general paddock characteristics that might encourage horses to spend time in the areas where HeV could be excreted.

The analytical methods that I used were Bayesian mixed effects models to try and correct for sampling artefacts and unaccounted effects like specific horse behaviour. I compared the observed data of time spent under trees with expectations from simulated data to see if horse movements in paddocks resulted in time spent under trees similar to that expected under random movement patterns. This allowed me to better understand the effect of some paddock attributes.

Overall I improved the knowledge of how horses behave in paddocks and the time they allocate to areas covered with trees. I refined some of the mitigation strategies for horse owners based on

potentially reducing the interactions between horses and HeV. In addition to improving mitigation, understanding the contact rate between HeV and horses could help to parametrise mechanistic models that can be used for spillover prediction.

This chapter has been submitted for publication in the Journal of Preventive Veterinary Medicine, 1 November 2016 (Martin et al., a *in-review*):

- Gerardo Martin, Rebecca J Webb, Carla Chen, Raina K Plowright, and Lee F Skerratt. Tree cover in paddocks is the main determinant of exposure to Hendra virus in horses. *Preventive Veterinary Medicine*, a

ABSTRACT

Hendra virus is a Paramyxovirus of the genus Henipavirus *of Australian flying fox bats that causes fatal disease when it is transmitted to horses and thence to humans. Transmission of Hendra virus to horses is most likely to occur under the trees where bats feed. Therefore, it is important to understand the environmental factors that result in horses spending more time under trees. To provide insights and generate management strategies I investigated the relationship between the proportion of time that horses spend under trees and characteristics of their paddocks. I deployed GPS trackers in ten paddocked horses and measured paddock proportion covered by trees, grass and weed height, size and number of horses among other attributes. To analyse the data I fitted Bayesian mixed effects models to account for variability of individual horse behaviour, sampling artefacts and the effect of temporal autocorrelation. I found that time spent under trees increases mainly with the proportion of the paddock covered by trees during both day and night, but is usually higher during the day. I did not find strong effects of any paddock characteristics on time spent under trees during the day or night. These results indicate that the most effective risk mitigation strategy could be restriction of access to trees. However, because I cannot discard that grass management would affect time spent under trees, reduction of grass under trees to reduce survival of excreted Hendra virus has to be assessed for any adverse effects on time spent under trees in places where restriction to trees is not possible.*

Introduction

Horses are highly selective foragers that preferentially use parts of the paddock habitat for their daily activities (Odberg and Francis-Smith, 1976; Fleurance et al., 2007). For instance, paddocks

that are grazed by horses have a typical heterogeneous vegetative structure comprising areas with consistently short or long grass as a result of feeding intensity (Odberg and Francis-Smith, 1976). Horses usually prefer to feed in areas with relatively short grass and recent growth (Fleurance et al., 2010). Where overall grass quality is lower, horses feed where grass is more abundant or taller (Edouard et al., 2009). These interactions between horses and vegetation contribute to determine overall availability of suitable grass within paddocks. Consequently the behaviour of horses may be influenced by the plant community, opening up possibilities for manipulation of horse behaviour by altering paddock structure.

Some infectious diseases are associated with types of habitat. For instance leptospirosis (a disease caused by infection with bacteria of the genus *Leptospira*) is largely associated with stagnant water bodies (Michel et al., 2001). Furthermore, some diseases are transmitted after interactions with certain landscape features; for example, speleologists are at greater risk of infection with *Histoplasma capsulatum* (Ashford et al., 1999; Taylor et al., 1999). For similar reasons some species are considered susceptible to certain diseases as a result of behavioural traits; stream dwelling frogs are generally more susceptible to infection with *Batracochytrium dendrobatidis* than terrestrial frogs (Murray and Skerratt, 2012; Rowley and Alford, 2007).

Hendra virus (HeV), a Paramyxovirus in the genus *Henipavirus*, was discovered in 1994 in Australia after a respiratory and neurological disease outbreak involving the death of 20 horses and one human. The reservoir hosts of HeV were found to be two of the four mainland Australian flying fox species, *Pteropus alecto* and *P. conspicillatus* (Halpin et al., 2011; Smith et al., 2014; Edson et al., 2015). Flying foxes are nocturnal and feed mainly during the night on nectar and fruits of native and some introduced plants. Due to the short survival time after the virus is excreted in the environment, transmission from bats to horses is thought to be relatively direct, such as bats urinating on horses or by ingestion of contaminated pasture under trees shortly after HeV is excreted (Field et al., 2011; Martin et al., 2015). The area where horses contact the excreted virus is known as the drip zone, which comprises the parts of a paddock covered by the trees where flying foxes feed and excrete virus (Field et al., 2011). Therefore, identifying the attributes of paddocks that influence the time horses spend under trees is of critical importance in order to better implement risk mitigation strategies to reduce the risk of contact with HeV and improve our understanding of the HeV spillover system (Plowright et al., 2015).

Here I investigated how paddock characteristics affect the proportion of time horses spend under trees (in the drip zone). I established relationships between time spent under trees and a

number of paddock attributes. From these I developed management recommendations to reduce the risk of HeV spillover.

Methods

Data collection

In order to asses how a series of paddock attributes affect the proportion of time that horses spend under trees I collected data on paddocked horse movements. To relate the proportion of time that horses spent under trees (quotient of total minutes spent under trees by total minutes tracked) to paddock characteristics I collected a series of variables that describe the paddock environment.

I selected four properties in the area of Townsville, QLD, Australia. The criteria to include them in the study was: 1) lie within the known distribution of reservoir hosts of HeV; 2) have at least one horse that depended on the resources that the paddock produced; 3) have a reasonable size that allowed us to measure the vegetation with transects, track the horses with the GPS tracker and made recovery of the trackers possible if they fell off the horse; 4) have trees; 5) that the owners agree to take part of the study and vaccinate the horses against HeV (required by the animal ethics committee).

The horses were eight thoroughbred, one hannover and one mixed brumby-thoroughbred. Of the four different properties, manure removal was only carried out in one, which was the smallest one that had two horses, a gelding and mare. This property had a shelter, although access was not 100% of the time. The largest paddock (ca. 7 ha), had five horses, of which I tracked only three, two thoroughbred (gelding and mare) and the brumby-thoroughbred mixed (6 mo at the beginning of the study). The remaining three thoroughbred horses were kept in paddocks of variable size and were two geldings (8 yo) and two mares (10 and 3 yo). Grass in this property was managed by rotation, so horses were moved to adjacent paddocks once resources were running low to allow recovery. The hannover gelding was kept in a single paddock of 2 ha and had constant access to food supplement. All the participating properties are located in the dry tropics and lie within the distribution of *P. alecto* and at the edge of the distribution of *P. conspicillatus* (Martin et al., 2016).

Once properties were selected the movements of 10 horses were recorded with GPS trackers built with arduino© components. I bought all the primary components of the trackers from adafruit[1]. The board to interconnect the GPS plate, power source, memory jack and arduino board

[1] https://www.adafruit.com/

was designed by Sam Foley, from the James Cook University's electronic engineering department. The board was programmed with the arduino language to store the geographical coordinates in the WGS84 coordinate system every minute.

Before I deployed the GPS trackers I assessed their accuracy and verified the battery duration, and if accuracy changed with time and battery charge. To do so I left all trackers that were going to be deployed under a tree for two weeks inside the same casing that I would use in the tracking session. After this time, I downloaded the recorded data and measured the diameter that contained 95% of the fixes and measured the minimum error by longitude and latitude. This process was repeated after the trackers were recovered from the horses to make sure trackers had not suffered damage and that battery life was still 10-11 days.

Each horse was fitted with a tracker for up to 11 consecutive days (due to battery life constraints). Horses were tracked once every one-three months between November 2014 and August 2015 to ensure the effects of all seasons were considered. Animal ethics for this procedure was approved by the James Cook University's animal ethics committee, for the period 28 May 2014 to 30 April 2016, under the project name "Models that predict risk of Hendra virus transmission from flying foxes to horses".

In each tracking session I sampled the vegetation of the paddocks where horses were being kept with measurement points evenly spaced every 10 metres along transects that uniformly covered the entire paddock area. I recorded the geographical coordinates of the measurement points with a hand held GPS. At each point, I obtained five measurements of vegetation height (cm) and classified the vegetation as grass or herb (weed). One vegetation measurement was taken at the GPS point and two on the left and right sides at one and two metres from the GPS point. The registered coordinates and vegetation heights were used to generate interpolated maps of vegetation average and standard deviation of height with a resolution equivalent to the GPS's theoretical accuracy of 5 m.

To calculate the proportion of time spent under trees I registered the coordinates of the trees in each paddock. Then I loaded the coordinates in Google Earth to create the polygons around each of the registered trees which I confirmed back in the paddocks. After this was accomplished I rasterised the polygons at the same resolution of the interpolated vegetation maps (5 m pixels). This resulted in binary layers of the areas covered/not covered. The proportion of time spent under these trees was obtained by extracting the GPS coordinates of the tracking session and obtaining the quotient of the total minutes spent under trees by the total minutes tracked.

To compile the final dataset for analysis, I generated summary statistics of the interpolated vegetation maps to use as explanatory variables. The datasets contained the daily number of GPS fixes that occurred under trees, the total number of GPS fixes that occurred per day and night along with the explanatory variables that describe the paddock environment. The response variable for analysis was therefore the number of minutes that horses spent under trees and the total number of minutes that the horse was tracked that day.

Statistical analyses

Because horses behave differently during the day and night (Houpt et al., 1986) there is a need to understand how paddock characteristics might affect the total and daily proportion of time that horses might spend under trees both during the day and night, and if there could be differences explained by paddock structure. Consequently, the purpose of the analyses was: 1) determine how the proportion of the paddock covered by trees affects the proportion of time spent under trees; 2) find paddock characteristics, other than the proportion covered by trees, that increase the proportion of time spent under trees, both daily and for the entire duration of the sampling period; 3) find paddock attributes that influence differences of time spent under trees between day and night , both daily and for the entire duration of the sampling period; 4) find paddock attributes that influence the proportion of time spent under trees during the day and during the night separately.

Consequently, the analyses were performed at two different temporal extents. In the analyses of total time under trees, I only used the data of the GPS trackers that worked for more than 24 h. For the daily time under trees only the data collected over 6 h or more was used. For instance if a tracker worked for 18h, this data was used in the daily time under trees analyses but not on the total time under trees analyses.

To analyse data I used generalised linear mixed effects models with continuous and the categorical variables time of day, which comprised two levels *day* (GPS fixes between 18:00 and 6:00) and *night*. The mixed effects included in all the models were used to control the effect of individual horses, the sampling session and time since deployment of the GPS tracker (included only in the models analysing daily time under trees). The potential confounders identified were mostly derived from collinearity between variables. For instance the amount of trees, grass, and weeds were all correlated with each other because plants in grasslands compete for space, light, and nutritional resources (Wilson and Tilman, 1991). A first step taken to reduce the effect of

the potential confounders was to eliminate all variables with a correlation coefficient $\rho > 0.75$. Secondly, to adequately interpret the models, the response of the observed proportion of time under trees to the different variables were compared with the responses of models fitted to simulated data of expectations of the proportion of time spent under trees if horses moved randomly (details below).

Modelling the proportion of time spent under trees

All data was analysed with Bayesian generalised linear mixed effects logistic models using JAGS 4.0 (Plummer, 2003) interfaced in R 3.2.3 (R Core Team, 2016) with the `r2jags` package for MCMC with Gibbs sampling. The general type of model fitted was:

$$\text{logit}(P_{\text{under trees},\,i}) = \beta_i \times \mathbf{X}_i + \gamma_{\text{horse}} + \gamma_{\text{session}} + \gamma_t t + \varepsilon \tag{8.1a}$$

$$N_{\text{GPS fixes under trees}} \sim \text{binomial}\left(N_{\text{Total GPS fixes}}, P_{\text{under trees},\,i}\right) \tag{8.1b}$$

Parameter priors:

$$\beta_i \sim \text{normal}\left(0, 10^6\right)$$
$$\gamma_{\text{horse, session},\,t} \sim \text{normal}\left(0, \sigma^2_{\text{horse, session},\,t}\right)$$
$$\sigma^2_{\text{horse, session},\,t} \sim \text{cauchy}\,(0, 25)$$

Where $P_{\text{under trees}}$ is the proportion of time that horses spent under trees; β_i are the covariables' effects, in the case of ANCOVA models with the categorical variables *day* and *night* the subscript $i = (1, 2)$, hence each β_i has two levels; γs are the random effects for *horse* sampling *session* and t (time elapsed since beginning of the sampling session) ; ε are the residuals assumed to be normally distributed; and $\mathbf{X}$ is the matrix of predictors: intercept, tree cover (C), paddock size (S), grass height (G), weed height (W) and time of day (categorical with levels *day* and *night*) and their products (interactions). All parameter priors were normally distributed with mean zero and variance 10^6 to let data dominate the posteriors (non-informative). However the variance of random effects (σ^2) had a half Cauchy prior. To fit these models I started running three chains of 100K iterations and then increasing the number of iterations until all parameters in all chains converged according to the Gelman and Geweke diagnostics (Geweke, 1992; Brooks and Gelman, 1998).

Model selection consisted of changing the elements of matrix $\mathbf{X}$. First including all the variables interacting with tree cover, and then incorporating other interactions between cover, size, grass,

weed and number of horses. The model matrix that minimised the deviance information criterion (DIC) whilst retaining the assumption of normal residuals (ε) was kept. As proof of adequate fit I performed posterior predictive checks, aiming for data to represent the median of model posteriors.

Comparing the responses of models with random movement expectations

The responses to the explanatory variables fitted by the models might reflect the degree collinearity between variables that I kept ($\rho < 0.75$). For instance, tree cover and grass correlate negatively, which might result in an apparently negative effect of grass on time spent under trees. To better understand the effects of variables on the proportion of time spent under trees I compared the responses of the models fitted to collected data with the responses of models fitted to the simulated proportion of time spent under trees expected if horses moved randomly in paddocks.

If horses move completely randomly across the paddock, the proportion of time spent under trees should be proportional to the proportion of the paddock covered by trees. To simulate a data set of expectations of the proportion of time spent under trees resulting from random movements I implemented a binomial process using the number of GPS fixes and the proportion of the paddocks covered by trees. First to simulate a sample size (N_{sim}), the number of GPS fixes of the collected data was used as the expectation of a Poisson process; second, the proportion of the paddock covered by trees was used as the probability of success (P_{succ}) of a binomial trial with sample size N_{sim}; finally a number of GPS fixes was generated using the two numbers P_{succ} and N_{sim}. The validation of this procedure is described below.

The simulated data was fitted to the optimal model for the collected data obtained with the selection procedure described above. To test the effect of the rest of the explanatory variables on the outcome of the simulated data, I fitted a simple model of simulated time under trees vs tree cover and compared the DIC of the full model vs the simple model. If the full model fitted to simulated data had a lower DIC than the simple model, then the collected data could be representative of a random movement scenario. Finally, to compare the effects of the variables on simulated data with the effects on the collected data I calculated the probability that horses spend more or less time under trees than expected if they moved randomly across the paddock, using the posterior samples of both models (fitted to collected and simulated data).

Validating the random movement expectations

To show that time under trees in a random walk approaches a binomial process, where proportion of tree cover is the probability of success in a binomial trial I simulated a series of random walks. I took the described approach because the location data of horses in relation to tree cover was collected binomially. To match the sample size of the collected data, the simulated walks were set to last 6 h to 11 days (6 h was assumed to be the minimum acceptable sample size to obtain a measure of time spent under trees independent of the starting point, and 11 days was the maximum lifespan of the GPS batteries). Simulations took place in a finite space of 1 ha that represented the paddock. To obtain estimates of time spent under trees I created a layer of tree cover by setting randomly the location of five trees. The proportion of the paddock covered by trees was generated using canopy sizes of 2-20 m. Each combination of settings (days sampled and canopy sizes) was run 100 times. With the simulated canopy coverage I generated a binomial process, using the length of the sampling period as the sample size, and the resulting number of successes was the number of times that horses occurred under trees in the simulation. Then I measured the correlation between the outcome of the binomial process and the time spent under trees in the simulated walk.

Results

The GPS trackers built with arduino components performed well according to the accuracy assessments through the study period. In all the trackers that I deployed in the field the accuracy under trees was ≈ 4 m. In limited occasions (< 1%) the error was up to 15 m, and the error rate did not increase significantly with proximity to the tree. This was not the case when the trackers were inside a building (this was merely observational and was not formally tested). In addition I did not detect any effect of the casing on accuracy. However I did detect that error rate increased between the fixes that were closer to the 10^{th} day. In these cases, errors in the date an time of the fix appeared in the dataset, and allowed us to eliminate dubious data points, which in many cases were also far from the paddock boundary. For these reasons, I did not take special precautions in addition to removal of obviously wrong fixes when calculating the proportion of time spent under trees. The error rate of the actual fixes was smaller than the theoretical accuracy of the trackers (5 m) which was the same resolution of the collected vegetation data. In addition variability of time spent under trees far exceeded the error rate of the GPS fixes, even in the simulated data of

time spent under trees.

Collected data

At the beginning of the study, sample sizes from all 10 horses were small, and gradually increased in quantity and quality towards the end of the study as I improved the attachment method of the GPS trackers. Another reason for increasing data quality and quantity was that during summer and early spring months of the study area were very hot and humid which favoured loss and damage of the trackers. In total I undertook five tracking sessions in November 2014, February, March, June and August 2015. The effective data recorded in each session was from 3, 4, 6, 4 and 7/10 horses respectively. Out of a theoretical maximum of 15840 fixes (number of minutes in 11 days) per session the number of effective fixes per horse is given in table 8.1.

Table 8.1: Number of fixes per session per horse. The number in parenthesis is the paddock number where tracking and vegetation sampling took place. The blank spaces are due to GPS malfunction/damage or falling off the horse. In some instances recovery was not possible.

Horse	Nov	Feb	Mar	Jun	Aug	Property
Bart	1455 (1)	8644 (1)	11787 (1)	3334 (1)		1
Milly		3141 (1)				1
Maverick			301 (4)	9572 (5)	5543 (3)	2
Mary	8298 (2)			1311 (5)	12522 (3)	2
Nickel	8048 (2)			4291 (5)	5504 (3)	2
Tellitha			6202 (4)			2
Locky		672 (6)	11919 (6)		9977 (6)	3
Sasha			13917		1480 (7)	4
Larry		1355 (7)			7137 (7)	4
Foal					7020 (7)	4

The explanatory variables that were recorded are grass and weed average, standard deviation, minimum and maximum height (centimetres); canopy openness (proportion of the ground receiving direct sunlight), tree cover (binary), distance to trees (metres), size of the paddock and number of horses in each paddock. Table 16 (Appendix 9.6.3.2) contains summary statistics of

Table 8.2: Tree cover characteristics of the properties and paddocks where horses were tracked.

Pty/Paddock	% Tree cover (N)	Canopy sizes (m)	Paddock size (m^2)	Tracked/Total
1/1	19.7 (14)	3-26	4847	2/2
2/2	10.9 (26)	2-57	23500	3/5
2/3	20.5 (21)	3-73	12700	3/5
2/4	0.52 (4)	4.5-8.5	17300	4/5
2/5	0.64 (4)	4-14	15800	4/5
3/6	10.9 (41)	3-18	16000	1
4/7	2.5 (22)	4-106	70000	3/5

each of these explanatory variables and the response.

The exploratory analysis revealed that all the explanatory variables were correlated to some degree with each other. As a result I only kept average grass and weed heights, tree cover, size and number of horses as explanatory variables because these variables had a correlation coefficient $\rho < 0.75$, and had a more straightforward interpretation than the rest. Table 8.2 contains a description on the paddocks where sampling took place.

In general terms, the proportion of time spent under trees was mostly affected by the proportion of the paddock covered by trees (example in Figure 8.1). All other paddock attributes included in the models had smaller statistical contributions, either towards explaining the proportion of time spent under trees, or to explain differences between time spent under trees during the day and night. In the following sections I describe how the different paddock attributes affect 1) proportion of time that horses spent under trees during the entire time they had the GPS tracker; 2) the daily proportion of time spent under trees; 3) effects of the paddock on the daily differences between day and night of the proportion of time spend under trees; 4) paddock determinants of daily proportion of time spent under trees during the day and night separately.

Statistical analyses

Total time spent under trees

The model matrix that had the lowest DIC was:

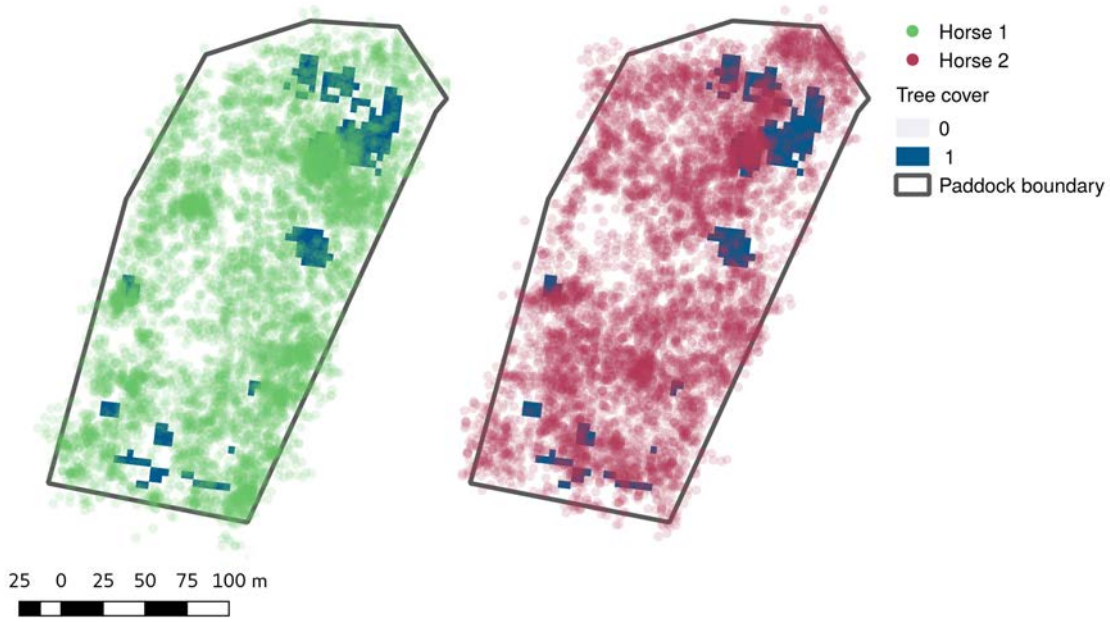

Figure 8.1: Tracks followed by two horses in property 2 during the tracking session in November 2014.

$$\mathbf{X} = \text{diag}\,(1, C, S, G, W, S \cdot G, S \cdot W, C \cdot G, C \cdot W, C \cdot S \cdot G, C \cdot S \cdot W) \tag{8.2}$$

Whose elements are: C = tree cover, S = paddock size, G = grass height, W = weed height and their products (e.g. $S \cdot G$). From here on all parameter values β_i are subscripted after the explanatory variable's effect they describe. Where indicated with the *sim* subscript, it refers to the parameter estimates for the model fitted to the simulated data set.

Most of the interactions were between cover, size and grass or weed, which can be interpreted as the effect that the amount of grass or weed in the area covered by trees have on horses spending time under trees.

Of all the statistically significant effects, the interaction $S \cdot W$, of paddock size (S) and weed height (W) explained the most deviance although its coefficient was small, $\beta_{SW} = -0.05$ (-0.058 – -0.047, 95% credibility interval, Cr. I.). The second most influential variable, according to the model was weed height, its coefficient was of a greater magnitude, $\beta_W = 26.455$ (12.583 – 41.372, 95% Cr.I.). These two effects indicate that weed height alone increases the time horses spend under trees more than the size of the paddock. However, when paddocks are larger, greater weed height tends to decrease the time spent under trees (because β_{SW} is negative). The third variable explaining the most deviance was the interaction $C \cdot W$, and the magnitude of its coefficient was

equally large, $\beta_{CW} = -143.04$ (-191.04 – -94.289, 95% Cr. I.). The DIC of this model was 263.3, with an average of 20.0 effective degrees of freedom. Table 8.3 shows the effects of the remaining variables and interactions. The model fitted to the simulated data, had similar effects, however the variable explaining the majority of deviance was W with a large and significant coefficient, $\beta_{W\ \text{sim}} = 26.68$ (23.41 – 29.96, 95% Cr.I.). Despite these similarities, a more parsimonious model for the simulated data was:

$$\mathbf{X} = \text{diag}\,(1, C) \tag{8.3}$$

The DIC of the model fitted to simulated data with matrix 8.3 was higher than the full model fitted with matrix 8.2 but its residuals were normally distributed, unlike the model with matrix 8.3. This indicates that the full model that was adequate for the collected data, was biased for the simulated data. In both models (model matrices 8.2 and 8.3) fitted to simulated data, time under trees increases significantly with tree cover (C) (Table 12, Appendix 9.6.3.2). The effect of tree cover in the full model fitted to collected data was not significant, $\beta_C = 8.220$ (-6.79 – 25.217, 95% Cr.I.). This indicates that the effects of the model fitted to collected data are real, and that horse movement is unlikely to be completely random despite the similarities of the models fitted to collected and simulated data.

Daily time under trees

Differences between day and night First I compared the time spent under trees during the day and night with ANCOVA models. The model with the lowest DIC (4702.9) was:

$$\mathbf{X} = \text{diag}\left(1_{day}, 1_{night}, C_{day}, C_{night}\right) \tag{8.4}$$

A random intercept model where 1_{day} and 1_{night} are the intercepts for each day time category. The model parameters explaining the most deviance are the night intercept and β_{night}, which were both significantly different from zero, although not significantly different from the *day* parameters (Table 13, Appendix 9.6.3.2). The overlap between *day* and *night* parameter estimates' credible intervals indicates that there were no statistically significant differences between time spent under trees during the day and night (Table 13, Figure 8.2), $\beta_{day} = 9.3$ (8.38 – 10.25, 95% Cr. I.), $\beta_{night} = 13.68$ (12.72– 14.66, 95% Cr. I.). However, the greater intercept of time under trees by day is close to statistical significance, indicating that horses tend to spend more time under trees at lower levels of tree cover during the day compared with night. These results suggest that horses

Table 8.3: Parameter estimates of the models with collected and simulated data for determinants of total time under trees.

β	Collected (DIC=263.3)			Simulated (DIC=190.9)		
	Mean	95% Cr. I.	Deviance	Mean	95% Cr. I.	Deviance
Cover	8.220	-6.794, 25.217	1.042	8.646	3.760, 17.591	0.971
Size	-0.009	-0.011, -0.007	9.303	-0.001	-0.003, 0.002	1.010
Grass	-0.183	-0.235, -0.132	1.752	-0.219	-0.242, -0.157	2.114
Weed	26.455	12.583, 41.273	38.393	25.823	21.905, 30.413	39.496
Size · grass	0.000	0.000, 0.001	8.662	0.000	0.000	2.860
Size · weed	-0.050	-0.058, -0.042	41.238	-0.007	-0.017, 0.004	6.411
Cover · Size	0.015	-0.044, 0.067	1.723	-0.054	-0.090, -0.024	3.726
Cover · Grass	-5.789	-9.907, -2.208	6.142	-4.304	-7.105, -3.164	4.843
Cover · Weed	-143.040	-191.656, -94.289	30.597	-88.363	-110.442, -68.343	19.835
Cover · Size · grass	0.009	0.000, 0.019	6.591	0.012	0.009, 0.019	9.118
Cover · Size · weed	0.305	0.169, 0.431	29.500	-0.155	-0.269, -0.043	15.921

do not necessarily seek shelter from the sun in tree shaded areas. When this model was fitted to simulated data, there was no difference between day and night as expected. The difference between collected and simulated data models was very small (Table 14, Appendix 9.6.3.2).

Determinants of time spent under trees during the day and night The model I fitted to find the determinants of differences on time spent under trees during the day and at night was:

$$\begin{aligned} \mathrm{X} = &\mathrm{diag}(0, C, C_{day}, C_{night}, C \cdot S_{day}, C \cdot S_{night}, C \cdot G_{day}, \\ &C \cdot G_{night}, C \cdot W_{day}, C \cdot W_{night}, C \cdot S \cdot G_{day}, C \cdot S \cdot G_{night}, \\ &C \cdot S \cdot W_{day}, C \cdot S \cdot W_{night}, C \cdot S \cdot H_{day}, C \cdot S \cdot H_{night}) \end{aligned} \tag{8.5}$$

where 0 indicates no intercept and H = number of horses (rest of the variables defined above). Its DIC = 3817.7 and with normal residuals indicated that it is an adequate model for the data. In this model the variable explaining most deviance was tree cover (C) which as expected had a positive effect, although it was not significantly different from zero, β_C = 37.12 (-1060.65 – 1157.43,

95% Cr.I.). Next in importance to tree cover alone, was tree cover during the day, and its effect was not significant, $\beta_{C-day} = -0.25$ (-1111.4 – 1105.43, 95% Cr.I.). The third variable explaining most deviance was tree cover during the night, $\beta_{C-night} = 79.416$ (-1036.59 – 1185.65, 95% Cr.I.). These parameter estimates indicate that there was little effect of tree cover on differences between daily time spent under trees during the day and night. As for other parameters representing the effect of other paddock attributes, the effect of paddock size has a significant effect during the night, and the deviance it explained was almost equally large (Table 8.4). This means that larger areas covered by trees increase the chances of horses interacting with them.

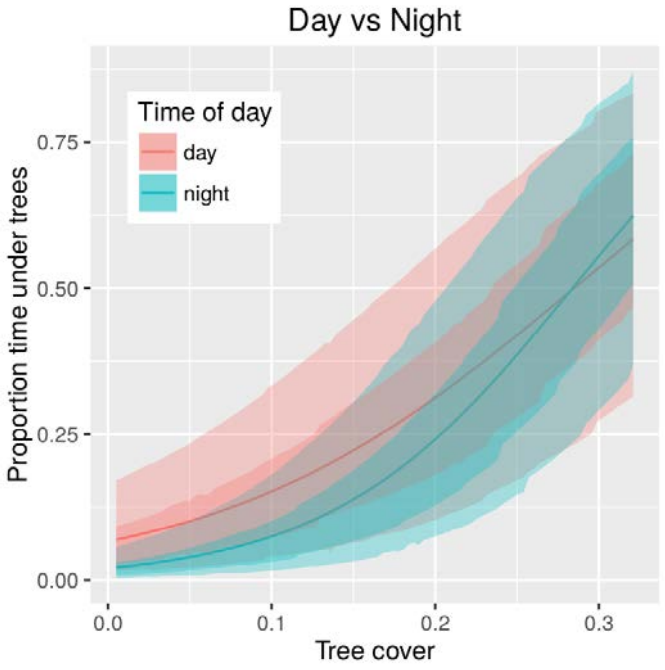

Figure 8.2: Differences between time spent under trees at day and night. None of the parameters (intercepts and slopes) were significantly different from each other, hence the overlap. Solid lines represent the average estimates and the ribbons are the 68 and 95% credibility intervals.

While the size of the paddock has a negative effect during the day it was not statistically significant. The comparison of this model with the simulated data was not possible because the simulated data model did not converge, even with an extremely large number of iterations. This indicates that although the model proved to be adequate for the collected data it was not so for the simulated data. The effects of the remaining variables and interactions are shown in Table 8.4.

Separate models for day and night Based on the findings of the above model I fitted two separate models to determine specifically how paddock structure affects time spent under trees during the day

Table 8.4: Parameter values of the model of determinants of time spent under trees at day and night fitted with the collected data.

β	Mean	95% Cr. I.	Deviance (mean)
Cover	37.121	-1060.652, 1157.436	49.296
Cover_{day}	-0.258	-1111.403, 1105.430	47.003
Cover_{night}	79.416	-1036.594, 1185.653	44.160
$\text{Cover} \cdot \text{Size}_{day}$	-0.157	-0.618, 0.265	13.967
$\text{Cover} \cdot \text{Size}_{night}$	-0.724	-1.179, -0.290	43.689
$\text{Cover} \cdot \text{Grass}_{day}$	-0.615	-3.763, 3.908	1.571
$\text{Cover} \cdot \text{Grass}_{night}$	2.736	-0.355, 7.236	2.338
$\text{Cover} \cdot \text{Weed}_{day}$	-5.701	-23.611, 10.667	1.583
$\text{Cover} \cdot \text{Weed}_{night}$	-23.667	-41.668, -6.691	4.090
$\text{Cover} \cdot \text{Size} \cdot \text{grass}_{day}$	0.002	-0.003, 0.007	1.956
$\text{Cover} \cdot \text{Size} \cdot \text{grass}_{night}$	0.002	-0.003, 0.006	1.677
$\text{Cover} \cdot \text{Size} \cdot \text{weed}_{day}$	0.022	-0.044, 0.091	2.881
$\text{Cover} \cdot \text{Size} \cdot \text{weed}_{night}$	0.100	0.032, 0.170	7.969
$\text{Cover} \cdot \text{Size} \cdot \text{horses}_{day}$	0.024	-0.050, 0.100	10.198
$\text{Cover} \cdot \text{Size} \cdot \text{horses}_{night}$	0.120	0.043, 0.197	31.754

and during the night separately. The model matrices that minimised the DIC, while retaining normality of residuals were:

$$\mathbf{X}_{day} = \text{diag}\left(C, C \cdot S \cdot G, C \cdot S \cdot H, C \cdot S \cdot W, C \cdot S \cdot G \cdot W\right) \tag{8.6a}$$

$$\mathbf{X}_{night} = \text{diag}\left(H, C \cdot S, G \cdot W, C \cdot S \cdot H, C \cdot S \cdot G \cdot W\right) \tag{8.6b}$$

Day During the day, the variable explaining most deviance was the four-way interaction between tree cover, paddock size, grass height and number of horses, although its effect was not statistically significant ($P > 0.05$). None of the parameters were significantly different from zero. Of all parameters, the one with the largest value was $\beta_{C-day} = 15.47$ (-8.935 – 28.08, 95% Cr. I., tree cover during the day). In the model fitted to simulated data, tree cover had a positive and significant effect, and while other parameters were also significant or explained more deviance than tree

cover, the parameter for tree cover was the largest (Table 15, Appendix 9.6.3.2). The best model for simulated data was the model of time under trees vs tree cover without intercept (DIC = 742.5, vs 772.4 of the full model, Figure 8.3).

When I compared the models fitted to collected and simulated day data the probability of spending more time under trees than moving randomly was < 0.05, across all levels of tree cover (Figure 8.3). However, in response to grass the probability of spending more time under trees than moving randomly decreased to nearly zero around 10-15 cm long, but increased to 0.1 at maximum grass height. This indicates that in response to 10-15 cm of grass length, horses spent significantly less time under trees than if they were moving randomly. Unlike grass, the abundance of weed apparently drove horses to increase the expected time spent under trees, until it resembled random movements ($P \approx 0.5$) at the greatest weed height.

During the day, the variable explaining most deviance was the interaction between tree cover, paddock size, grass height and number of horses, although its effect was not statistically significant ($P > 0.05$). None of the parameters were significantly different from zero. Of all parameters, the one with the largest value was $\beta_{C-day} = 15.47$ (-8.935 – 28.08, 95% Cr. I., tree cover during the day). In the model fitted to simulated data, tree cover had a positive and significant effect, and while other parameters were also significant or explained more deviance than tree cover, the parameter for tree cover was the largest (Table 15, Appendix 9.6.3.2). The best model for simulated data was the model of time under trees vs tree cover without intercept (DIC = 742.5, vs 772.4 of the full model).

Night The factor that explained most deviance during the night was the interaction between tree cover and paddock size, with a positive effect, $\beta_{CS-night} = 0.059$ (0.005 – 0.12, 95% Cr.I.). The only other parameter that had a significant effect was the number of horses, $\beta_{H-night} = -1.91$ (-3.0 – -1.026, 95% Cr.I.). The effect of $\beta_{H-night}$ relative to the magnitude of H ($\overline{|\beta_{H-night} \times \overline{H}|} = 7.48$) is more than twice the effect of the interaction of tree cover – paddock size ($C \cdot S$, $\overline{|\beta_{CS-night} \times \overline{C \cdot S}|} = 3.25$). Hence, despite the larger values of $C \cdot S$, the effect of the posterior estimates for $\beta_{H-night}$ are greater. The probability that time under trees is greater than in the simulated data decreases with the number of horses (Figure 8.4). The fitted effect in the collected data is, however, very similar in the model fitted to simulated data. In fact, the number of horses explained the majority of the deviance in the model fitted to simulated data (Tables 14-15). However, the best model for the simulated data was time under trees vs tree cover without intercept

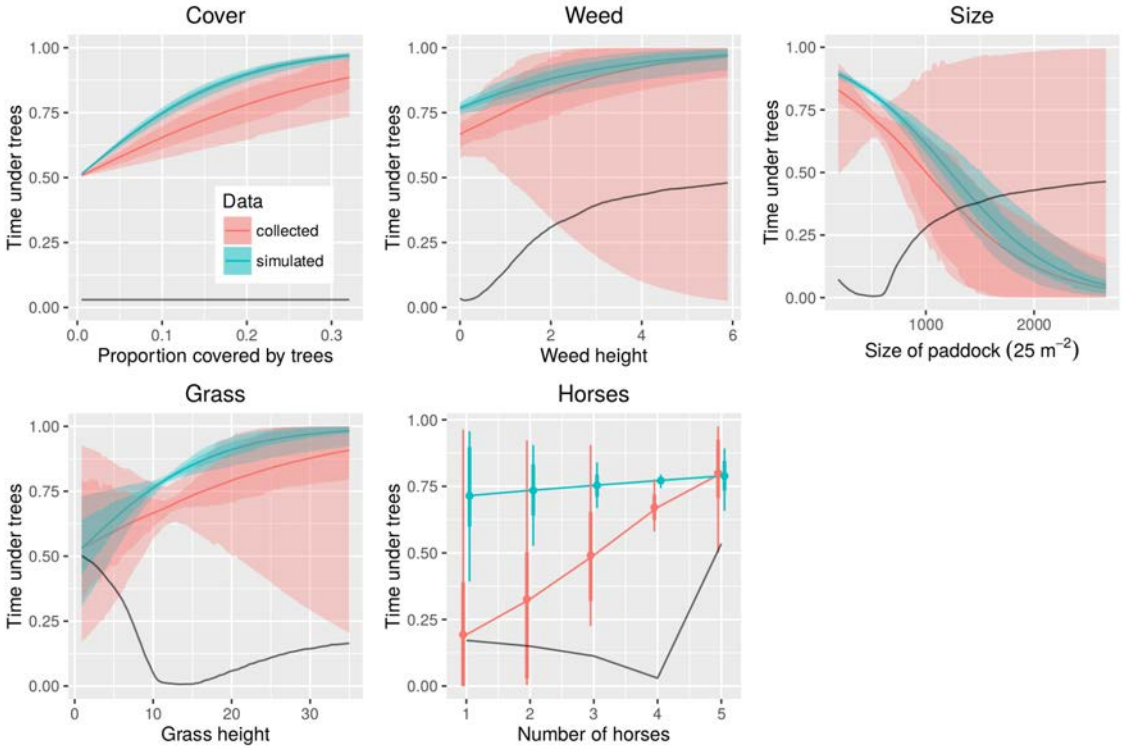

Figure 8.3: Partial responses fitted by the models (colour) explaining time under trees at day. Black lines show the probability that time spent under trees is greater than expected with the simulated data.

(DIC = 563.3, vs 596.1 of the full model).

Validating random expectations with random walks

I verified that the time spent under trees when horses move randomly approaches the proportion of paddocks covered by trees by simulating random walks by. To incorporate artefact sources in the collected data, I simulated random walks of different lengths representing the time that horses had a GPS tracker.

In these simulated walks, the effect of increasing the length of the sampling period was a decrease of the variance of time spent under trees at all levels of tree cover. In addition, variance increased with the proportion covered by trees. Therefore the highest variance or proportion of time spent under trees occurred in short walks with high tree cover (Figures 35-36, Appendix 9.6.3.2). The correlation between time spent under trees in the simulated walks and a binomial process generated from the tree coverage and the simulated walks was $\rho = 0.91$ ($P < 0.05$).

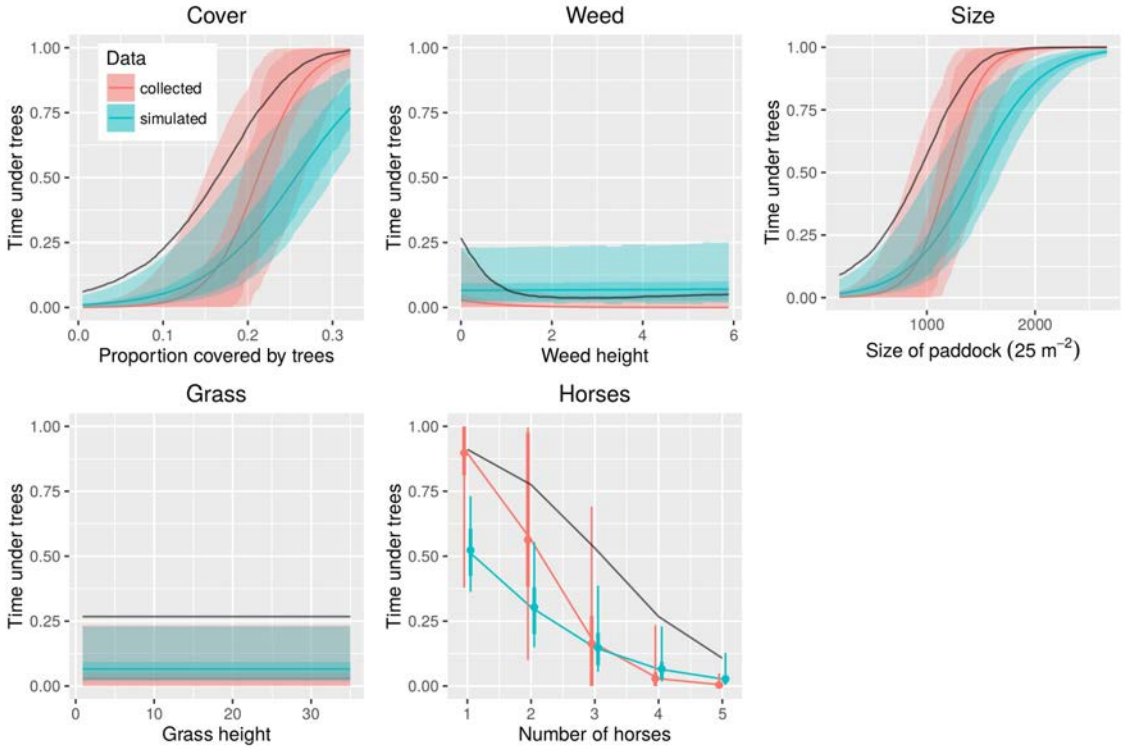

Figure 8.4: Partial responses fitted by the models (colour) explaining time under trees during the night. Black lines show the probability that time spent under trees is greater than expected with the simulated data.

Discussion

Our study shows that the effect of paddock environments on time horses spent under trees is relatively weak. However, contrary to scenarios of completely random movement, the time horses spend under trees is not completely determined by the tree coverage of a paddock. In some cases time spent under trees is lower than expected by random movements in response to tree cover (Figure 8.3). In addition, time under trees is higher during the day than during the night. While under some paddock structure scenarios, horses spend significantly less time under trees than if they moved randomly, the very large variability of outcomes would make HeV risk mitigation based on modification of paddock structure highly uncertain. Because responses to paddock structure differ between day and night, finding an optimal configuration such that horses are encouraged to spend as little time as possible under trees would be very complicated. Given that HeV is more likely to be transmitted during the night shortly after the virus is excreted (Martin et al., 2015), the most effective mitigation strategy is restriction of access during the night to areas covered with trees.

To the best of my knowledge, the determinants of the use of tree shaded areas by horses have infrequently been investigated. Some studies suggest that their use is mainly for shelter from the heat (Jørgensen and Bøe, 2007), although avoidance of insect harassment can override the need for lower temperatures in certain areas and seasons (Duncan and Cowtan, 1980; Keiper and Berger, 1982). These studies were performed in areas where horses have a wide range of habitat types available. In this case, paddock size restricts the availability of areas to seek refuge (Duncan, 1983). As a result, the horse movements I detected are closer to random than where habitats can be actively selected.

Paddock size consistently explained a high proportion of the deviance in my study. The higher variability of time spent under trees compared with random movements is likely to be a consequence of context specific horse preferences. These unexplored factors might involve interactions between paddock characteristics and weather. Therefore more detailed analyses might reveal which paddock attributes are more important under certain weather conditions, or if some areas are used more than expected by their availability. For instance the use of tree shaded areas could be for sheltering from the sun, rain or both.

Overall, I observed high similarity between the binomial process to represent expectations from random movements and the collected data models. The random walk simulations I used to validate this procedure had higher variance than the binomial process itself (Figures 35-36, Appendix 9.6.3.2). However I was unable to obtain a parameter to scale the variance of the binomial process in response to the sample size and tree cover. Consequently it is possible that the random walk expectations I simulated with the binomial process underrepresent the total expected variance of time spent under trees in a random walk. At least based on the correlation coefficient $\rho = 0.91$ between the binomial process and random walk, I failed to represent approximately 10% of the variance. Therefore, the differences that I registered between the apparent responses in the collected and simulated data are likely to be smaller, which could result in greater resemblance of the collected data to random movements, at the temporal scales investigated here (1-10 days).

Horses have been observed to use different areas of paddocks during the day or night (Field et al., 2015b). Field et al. (2015b), who tracked horses on a HeV infected property, did not provide a description of the paddock or whether behavioural differences between day and night could be explained by paddock characteristics. I also found behavioural differences between day and night, as evidenced by the different model structures for daily time under trees (equations 8.6a and 8.6b). However I did not find any paddock characteristics determining the differences. Moreover,

the models' structure for time under trees during day and night were very different and fitted opposing effects of paddock size and number of horses. Therefore, attempting to manipulate horse behaviour by modifying the paddock environment (such that it does not involve removing all trees) could have misleading outcomes.

According to the data, there appears to be a region of grass length 10-15 cm, where horses spend significantly less time under trees during the day than if their movements were random (Figure 8.3). It has been suggested that this range of grass height is the optimal height preferred by horses for grazing (Edouard et al., 2009; Naujeck et al., 2005). The presence of grass in areas distant from trees could deter horses from spending time under trees. However, the null response to grass at night suggests that greater abundance of grass would not result in any decrease in risk of exposure to HeV. These relationships might be a potential area of research of horse behaviour that might result in reduction of exposure to HeV during the day, if restriction of access to trees during the day is not possible or desired. Other potential areas of research in this respect, could involve the effect of supplement feeding. Given sample size limitations there were many factors that I could not assess. One of them is the effect of supplement feeding and shelter provision. Supplement feeding is very common throughout Australia, it tends to reduce the frequency of vicious behaviours (van den Berg et al., 2015) and might carry grazing behaviour changes.

Adequately interpreting the biological meaning of the parameter estimates at the moment is hampered by our poor understanding of the natural responses of horses to paddock structures. For instance two factors that explained large amounts of deviance were cover and size. While these interactions could be interpreted as responses to the size of the areas covered by trees and the potential amount of grass under trees, it is unclear how exactly these affect time spent under trees. One possibility is that spatial autocorrelation due to larger areas leads to higher variance of time spent under trees. Alternatively, these larger areas could provide better shelter during the day, and horses spend more time feeding away from these areas during the night where there is more grass (Fensham et al., 1999; Fulco et al., 2001), however this is purely speculative. More detailed analyses of feeding time allocation in relation to tree cover is needed to understand what drives opposing responses to paddock size between day and night.

To model daily time spent under trees there is an assumption that regardless of day to day variability there is a substantial proportion of the variance explained by tree cover and overall paddock structure. Given our current knowledge I cannot assess yet what proportion of that variance is explained by the paddock and what is explained by daily weather patterns. One reason

for this is that temperature and rainfall might influence time spent under trees (Jørgensen and Bøe, 2007). Consequently, I might have overfitted models and some of the paddock attributes could be acting as confounders in the models. In addition the sample size was small, and including more horses and paddocks with different analytical techniques can improve the estimates and understanding of the relationships between paddock characteristics and time spent under trees.

Habitat selection within paddocks is highly limited (Duncan, 1983), and horses will tend to use the available space not completely randomly. It is probable that modification of paddock environments will result in modification of horse behaviour, however, risk of exposure to HeV is unlikely to be reduced significantly because responses during the day and night are different. Overall, interaction with the tree covered areas (the drip zone) on a daily basis resembles the proportion of the paddock covered by trees but it is more variable, and I need to understand what causes the observed variability. Added variability is probably caused by interactions between the paddock environment and weather conditions . A potential approach to study variability is finding stages of behavioural stationarity and relating those stages to the joint state of the paddock and weather (Benhamou, 2014). Analyses of HeV survival indicate that survival within short grass is lower than in tall grass (Martin et al., 2017, Chapter 4), so keeping grass short under trees is desirable. However it is not clear if removing grass under trees will cause behavioural changes that increase interactions with the drip zone. Given that reducing time spent under trees in response to managing paddock characteristics is highly uncertain, especially at night, the most effective strategy is to restrict access to areas covered by trees.

Conclusions

More research is needed to understand specifically what causes variability of horse habitat use in paddocks. However modification of horse behaviour in response to alterations of the structure of the paddock is unlikely to be successful for decreasing risk of exposure to HeV. The most successful preventive strategy is restriction of access to areas covered by trees. Understanding specifically how horses use the paddock environment based on pasture abundance will determine if reduction of grass to decrease HeV survival once excreted is likely to successfully reduce risk of exposure to HeV. Because the horse–paddock habitat relationships are likely to be context specific, prior assessment is necessary to implement the most effective mitigation strategies.

Part V

Concluding remarks

Chapter 9

General discussion and conclusions

The main objective of my PhD project was to develop models that could be used to improve the understanding of the HeV spillover system and our predictive capacity. Along these lines (Chapter 2) I contributed to better understand of how HeV is transmitted from flying foxes to horses (Chapter 3) and in what circumstances HeV can spill over indirectly to horses (Chapter 4). I found that HeV is more likely transmitted to horses where *Pteropus alecto* and *P. conspicillatus* can have higher population densities (Chapter 5). In Chapter 6 I identified that the climatic correlates of the spatiotemporal pattern of spillover are probably minimum temperature and rainfall seasonal amplitudes. How these two variables influence the underlying biological mechanism is unclear. However, the bimodal responses to several climatic factors suggest that seasonality is related to specific traits of the two bat species along the latitudinal gradient. The result from Chapters 5 and 6 were then used to model risk of HeV spillover in response to the effects of climate change on the two bat species involved in spillover. The resulting risk maps indicate that spillover risk is more likely to increase southwards, and involve a reservoir host replacement in northern Queensland (Chapter 7). Finally, in Chapter 8, the analyses I did on horse movement data indicate that there is a very weak effect of paddock characteristics on how frequently horses interact with tree covered areas and hence HeV excreted by flying foxes. To summarise:

1. Hendra virus transmission to horses could follow a gradient, likely from direct to relatively direct, probably involving short periods of environmental survival

2. The reservoir hosts and therefore, bat species more likely involved in spillover are *Pteropus alecto* and *P. conspicillatus*, because spillover mostly occurs where climatic suitability favours higher population density of these two species

3. The seasonal spillover pattern could be driven by flying fox species specific traits in the

latitudinal regions below and above 22° south. The different seasonal patterns might occur in response to minimum temperature and rainfall seasonal amplitudes

4. Future risk as explained by the distribution of *Pteropus alecto* and *P. conspicillatus* is likely to expand southwards. In the north *P. alecto* could replace *P. conspicillatus* as the main HeV reservoir host

5. Of all vegetation attributes (amount of grass and weed and tree cover), size and number of horses, the proportion of the paddock covered by trees is likely to be the most important factor to influence contact with HeV

The methods I learned to use during these studies have proved useful for inferring large scale biological mechanisms that could be applied to other disease systems. For instance using spatiotemporal patterns of survival to infer transmission pathways, and climatic suitability to identify potential reservoir hosts.

I also realised as I made progress that I could have done things differently. For instance, a more detailed time series analysis of spillover events would have helped to identify with more certainty environmental drivers of spillover risk. The analyses in Chapter 6 resemble this approach, but focus only on the conditions of spillover months, and place greater emphasis on spatial climate variability. In addition the spatial environmental data used in these analysis could have been used from more reliable sources like remote sensing.

Regarding the field work, I now realise that while analyses are innovative and provide ground for future more detailed studies, could have been better planed with more specific objectives that allowed obtaining higher quality data with less effort.

Below I discuss in detail each of the chapters in the context of each other, and more generally the spillover ecology of HeV.

Conceptual model of the spillover system

By following the conceptual model of Plowright et al. (2015) (Chapter 2) I identified my areas of research: Hendra virus survival, reservoir host distribution and husbandry practices. The framework was useful at the time it was published, however as of 17 May 2017 some key aspects have changed as a result of my own research and the National Hendra virus Reseacth Program.

Regarding HeV survival, my own research has shown that HeV transmission to horses can occur directly (Chapter 3), therefore the layer "*pathogen survival outside hosts*" (figure 1 from Plowright

et al., 2015) could include direct connections between the layer "*pathogen shedding*"and the layer "*spillover host exposure*". Consequently, spillover host exposure does not depend exclusively on HeV environmental survival, but on potential contacts between fresh bat urine and horses, which result from heterogeneous shedding patterns. While these changes increase the potential sources of contact with HeV, risk mitigation strategies need not be entirely different; vaccination would still provide protection (regardless of the unfounded claims that HeV is developing vaccine resistance Zahoor and Mudie, 2015; Peel et al., 2016, Appendix 9.6.3.2[1]), and restricting access to trees and keeping grass short under trees would decrease risk of contact with HeV.

Similarly, my findings in Chapter 7, indicate that the likelihood of spillover host exposure is not heavily influenced by paddock and grass management, making contact with HeV more probabilistic. The final layer "*spillover host susceptibility*", is likely to remain unknown, and future modelling studies would have to assume uniform susceptibility among unvaccinated horses. This assumption is unlikely to result in poor biological relationships between models and data, because the main aim of a predictive framework is reducing exposure to HeV and probability of spillover.

Hendra virus survival

In part II I showed that the poor performance of HeV survival as a predictor of spillover could be biologically interpreted as potential for direct transmission. In addition, the high HeV survival in some spillover events suggested that transmission could also occur indirectly. The results led me to conclude that transmission to horses could be a gradient. These conclusions, based solely on the observed survival rates at spillover event locations, assume that the effects of temperature on HeV survival is the only process driving spillover risk. However, spillover is the result of many different temperature-influenced processes; flowering of *Eucalyptus* species (Hudson et al., 2010; Giles et al., 2016), distribution of flying foxes (Martin et al., 2016). The higher predictive ability of the models in Chapter 7 (climate change scenarios), indicate that the effects of climate on bats are more important than its effects on HeV after being excreted to determine HeV spillover risk. Consequently, by analysing bat climatic preferences and requirements, I found more support for the relatively direct transmission conclusion of Chapter 3.

One of the major limitations of survival estimates under microclimatic conditions obtained in Chapter 4 is that the survival experiments were performed under tightly controlled conditions

[1] I co-authored a rebuttal letter in Infection Ecology and Epidemiology on defence of the HeV vaccine for horses as an effective mitigation strategy.

(Scanlan et al., 2014). The BLS4 classification of HeV impedes the possibility of more complicated experiments with more replicates that account for the simultaneous effects of more variables and treatments. While UV radiation can in fact further reduce survival rates based on both evaporation and temperature (Murray and Jackson, 1993), we are more interested in determining decay rates during the night, which is when HeV is excreted in paddocks and there is no UV radiation. Given that we already know that HeV is highly sensitive to desiccation (Fogarty et al., 2008) I produced estimates of how likely it is that evaporation occurs in the mircoclimates where it is excreted. These analyses indicate that evaporation is highly likely to occur even in the more vegetation-sheltered microhabitats. To what extent the predicted potential evaporation would affect survival is still unknown. A potential approach to estimate the effects of evaporation is by using the evaporation rates or potential evaporation during Fogarty et al.'s experiments. Then by assuming an additive effect of evaporation on the observed temperature dependent decay rates in Chapter 4, a closer survival estimate can be obtained. An experimental alternative to estimate survival in the environment might involve the use of a surrogate virus, like Cedar virus, a non-pathogenic *Henipavirus* closely related to HeV (Marsh et al., 2012).

Reservoir host distribution

I investigated the effects of climate on the spatial patterns of HeV spillover by finding the climatic preferences and requirements of the four flying fox species. These models helped me find the minimum area where HeV spillover to horses can occur. In the context of Chapter 2 (Plowright et al., 2015), the distribution models correspond to the first component of the spillover system. The main conclusion of Chapter 5 was that spillover tends to occur where climate allows *P. alecto* and *P. conspicillatus* to occur in higher densities. Therefore the minimum area for HeV spillover to occur is the potential distribution of these two species.

Recent analyses (Giles et al., 2016) have shown that HeV spillover occurs at times when bat densities are lower in a single camp, not in the entire area around the spillover events. This characteristic of HeV spillover does not contradict my predictions of HeV spillover occurring where *P. alecto* and *P. conspicillatus* can occur in greater densities. This is because Giles et al. (2016)'s analyses and mine have different scales of spatial, temporal and ecological organisation. My analyses in Chapter 5 do not take into account temporal variability; what the distance to the niche centroid models represent is the capacity of a 4×4 km area to determine flying fox carrying capacities (VanDerWal et al., 2009).

In contrast with Chapter 5, in Chapter 6 I addressed HeV spillover risk variability between seasons. Based on the bimodal response shapes to many climatic factors, I found that The most parsimonious explanation for the observed spatio temporal pattern, was that seasonality could be the product of two bat species involved in spillover, resulting in two spillover systems (north and south). These processes occur at similar scales as those considered in Chapter 5, however the model represents risk variability between months. The fact that spillover occurs while bat densities are lower (Giles et al., 2016), show that the biological mechanism is not exactly related to reservoir host density, as it usually occurs in other disease systems (Pascual and Dobson, 2005; Dowell, 2001). Despite the presence of some methodological artefacts, there are coincidences with Giles et al.'s analyses; minimum temperatures affect *Eucalyptus sp.* flowering and the number of bats in a camp and risk of spillover.

In Chapter 6 I found that horses have a negative effect on spillover risk. To try and explain this relationship I argued that land clearing for paddocks could be affecting bat feeding habitat. Regardless of the actual cause of this effect I decided to use the same horse density model as a population-at-risk offset (Taylor et al., 2013) in Chapter 7. The main reason was that the effects of climate on HeV are indirect (climate has a more variable effect on bats than on HeV survival, Chapter 3), and because disease transmission is a probabilistic contact phenomenon (Anderson and May, 1992), I had to eliminate the effect of the places where contact between HeV and horses was more likely to occur. This step in addition to the Gaussian field to model spatial effects resulted in the prediction of additional areas at risk of HeV spillover, mainly across far northern Queensland (Figure 7.2). In the context of Chapters 3 and 4, transmission in northern areas is more likely to occur directly because high temperatures would impede indirect transmission. Hence, opportunities for spillover could be more limited. The temporal scale of these predictions is the same as those in Chapter 5. As for how risk will vary between months, we have to take into account that, despite being in northern Queensland, these areas only have *P. alecto* as a HeV reservoir host. Therefore, the timing of spillover risk would entirely depend on specific traits of this species across the predicted areas at risk.

Horse behaviour and husbandry practices

In part IV I saw how horses interact with paddock areas covered by trees (the *drip zone*, Field et al., 2011). The aim was finding paddock characteristics that decreased interactions between horses and the drip zone. My main finding that horses move nearly randomly inside paddocks

suggests that the best paddock modification is restricting access to the drip zone. However, I also found that some responses between the optimal models for day and night were opposite (see figures 8.3 and 8.4). The most parsimonious explanation for the difference between optimal models is that there are behavioural differences between day and night, which have actually been previously reported (Field et al., 2015b). Nevertheless, the relationship between paddock structure and horse behaviour, has been poorly studied. Consequently, there is a lack of theoretical tools to adequately interpret my results. In response to these limitations I suggested that the effectiveness of some of the mitigation strategies that I made in Chapters 3 and 4, should be assessed prior to implementation. For example, if reducing grass under trees to decrease HeV survival rates results in horses spending more time under trees during the night, because horses prefer grass between a specific range of heights (Edouard et al., 2009; Fleurance et al., 2010), then restricting access to trees will likely be more effective than reducing HeV survival to prevent spillover. I recommend that particular emphasis on enforcing these mitigation strategies should be practised along with vaccination within and in around the areas predicted to be at risk in figures 7.4 and 7.5 (Chapter 7). In addition to adequately assess the impact of these preventive measures there would have to be surveys to find if there is the willingness among horse owners to implement them.

title

Future directions

Research recommendations

Throughout my PhD research I identified areas for future research. With the studies of HeV survival, I have recommended possible avenues to construct a model that better accounts for the additional effects of the environment on HeV survival. First, while UV radiation is a very successful germicide (Chang et al., 1985), it is only present during the day; hence, the effect of evaporation is more important for HeV survival as it is excreted at night. Second, the effects of evaporation/desiccation have already been briefly studied (Fogarty et al., 2008). By studying in more detail the specific environmental conditions during those experiments in order to determine the evaporation rates, we could, given a set of assumptions, approximate HeV's desiccation dependent decay.

A key step towards validating our survival predictions from Chapter 4 would require survival experiments with temperatures that vary over time, with either HeV or Cedar virus. Finally,

microclimates samples from additional locations are also necessary to validate the survival predictions for high risk areas like Brisbane and Cairns in 9.6.3.2.

With the models generated in part III, I identified the following avenues for future research:

1. The physiological changes and susceptibility to infection in both horses and flying foxes between seasons along the latitudinal gradient, specifically in response to minimum temperature and rainfall
2. The distributional and population response of *P. alecto* and *P. conspicillatus* to climate change
3. The changes in HeV dynamics in areas where *P. conspicillatus* was predicted to decline and *P. alecto* was predicted to colonise
4. The role of inter-species interactions in shaping flying fox distributions and HeV spillover risk

Finally, to better understand how the paddock environment influences horse behaviour, more detailed analyses of horse behavioural states and of the transitions between them are needed. For instance state space models that relate moving speed, turning angles and body position to current behavioural states, and that predict transitions to other behavioural states based on current and previous states, would be useful to find general rules of horse behaviour (Benhamou, 2014; Patterson et al., 2008). Furthermore, relating behavioural states of multiple horses sharing the same paddock would help to find if dominance hierarchies are important for risk of contact with HeV. Similar methods can be used to study horse behavioural responses to weather.

Other potential research might involve detailed study of the vegetation in horse paddocks throughout the areas at risk of HeV spillover. More specifically, research might focus on determining the tree species that are favoured by flying foxes and allow growth of grass species that are preferred by horses.

Implementing and adapting mitigation strategies

To adequately mitigate HeV spillover risk a series of measures have to be undertaken at different levels of ecological organisation. The levels at which I have contributed are, from large to small, reservoir host distribution, seasonal variability, and the paddock environment. The spillover risk distribution, based on the reservoir hosts' climatic preferences and needs (Chapters 5 and 7), can be used to allocate resources towards prevention within these areas. An adaptive strategy towards

this approach might include allocating resources around the areas, by accounting for the flying fox foraging range of 40 km (Field et al., 2015b). In addition, there have been rare spillover events outside the areas contained within the mentioned 40 km buffer, like Chinchilla (Figure 3.1). These locations should also be included in resource allocation schemes for HeV spillover risk mitigation, but should be of less concern.

The seasonal risk variability (Figure 6.2), indicates that the high risk season is shorter farther south. However, what is currently recognised as the high risk season (Figure 2 from Plowright et al., 2015, Chapter 2), is influenced by the reporting date. I addressed this issue by assuming a delay of two weeks between transmission and reporting, based on experimental horse infections that found up to 8 days between inoculation and obvious signs of disease (Marsh et al., 2011; Williamson et al., 1998). With the one week discrepancy between experiments and the assumed delay I allowed some error due to potential differences of time to disease signs due to the still unknown infectious dose. While these assumptions could have an effect on the spatiotemporal pattern reproduced by the model, they are unlikely to cause strikingly different patterns because the model should mostly represent the conditions that precede spillover and influence the biological mechanism that facilitate its occurrence. Because we still do not know when the best conditions for spillover occur, how variable between years the risk season could be I recommended a further one month delay to allow uptake of mitigation strategies. The final result, is a high risk season from March to November below 22° south.

The mitigation strategies I suggest at the paddock level include keeping grass short under trees especially around trees with high canopy openness that allow more grass growth (Fensham et al., 1999; Fulco et al., 2001). This would decrease HeV potential survival and restricting access by horses could further prevent exposure to HeV. However, given the complexity of horse behavioural responses to paddock characteristics, I suggested that the effectiveness of keeping grass low under trees should be assessed for horse behavioural responses. Consequently, if short grass under trees encourages horses to feed under trees (by increasing fresh regrowth, for instance, Edouard et al., 2009), the best alternative is restriction of access during the night along with keeping grass short.

A component of the spillover system that I did not address are flying fox spatial population dynamics, and HeV dynamics within those flying fox populations. Better understanding of this component is necessary for optimising mitigation strategies at finer temporal scales based on spillover prediction, and to explain HeV emergence. Regardless of current data and technical limitations, the work presented in this thesis provides insights on certain components of the HeV

spillover system. In the section below I describe a mechanistic framework for HeV spillover risk prediction that incorporates some of the findings of my thesis.

Towards a predictive framework for Hendra virus spillover

The mechanism by which HeV is transmitted and maintained among bat populations is still matter of debate (Plowright et al., 2016). Because this particular aspect of HeV epidemiology and ecology was out of the scope of my PhD, I am presenting a framework that focuses mostly on spillover and could eventually be extended for risk prediction. What is presented here is a brief description of the full model, greater detail is given in Appendix 9.6.3.2.

To represent dynamics of HeV in bats assumed that there is a mechanism representable by a mathematical function that regulates the number of infected bats, such that:

$$\frac{dI}{dt} = F(B, I) + i(t) \tag{9.1}$$

Equation 9.1 means that the number of newly infected bats in time is a function of the number of infectious bats, I, and bats that can become infectious, B. Bats that get infected could occur in the form of susceptible or latent, (Plowright et al., 2016). The most basic form of disease transmission models assume homogeneous mixing, however horses are aggregated in paddocks, therefore we need a way of representing such aggregation. By combining pseudo-mass action transmission and the concept of mean crowding (Lloyd, 1967), I modelled transmission from bats to horses with a negative binomial distribution (Barlow, 1991, 2000). When infectious contacts are uniformly distributed, the rate at which susceptibles become infectious is a product of the density of susceptible and infectious individuals, βSI. However, if contacts are aggregated, there are subgroups at greater risk, and this can be modelled by including an aggregation factor, such that the function that regulates the rate at which susceptibles become infectious is $kS \ln [1 + \beta I/k]$, where k is the aggregation factor. As $k \longrightarrow \infty$ the expression reduces to βSI (Lloyd, 1967).

A common approach to model the transmission of a reservoir to a non-reservoir host is by assuming that the transmission rate β is the same, but there is a scaling factor ε that could represent different susceptibility to infection or lower probability of contact than established by β. Hence I suggest that transmission to horses could be modelled by including the scaling factor ε in the negative binomial function of transmission. This approach would allow to include the spatial aggregation of horses within bat foraging habitat. Consequently transmission to horses would follow:

$$\frac{dH_I}{dt} = kH_S \ln\left[1 + \frac{\varepsilon}{k}\left(\beta I + \frac{p_c}{D_{50}}V\right)\right] \tag{9.2}$$

Where H_s is the density of horses, I is the density of bats, and V is the amount of excreted virus by I, p_c is the probability of contact with the virus contaminated areas and D_{50} is the minimum infectious dose. Once this transmission function was formulated, to compute spillover probability between a specific time frame $[t_1, t_2]$, I followed Keeling and Rohani (2007); $P(t_1, t_2) = 1 - \exp\left(-\varepsilon\beta S \int_{t_1}^{t_2} I dt\right)$, such that when taking the aggregated distribution of contacts, probability of spillover with 100% detection rate is:

$$P(t_1, t_2) = 1 - \exp\left[-kH_S \ln\left(1 + \frac{\varepsilon}{k}\left(\beta \int_{t_1}^{t_2} I\, dt + \frac{p_c}{D_{50}} \int_{t_1}^{t_2} V\, dt\right)\right)\right] \tag{9.3}$$

The horse population at risk, H_S besides being aggregated, is highly spatially structured within a network of bat feeding patches that surrounds bat camps. To represent this structuring I suggest that it is possible to find a spatial structure of ϵ. By finding the spatial structure of ε, it is possible to represent multiple mechanisms and factors:

1. The effects of the geographical location of the horse population with respect to the bat colony
2. The effect of food abundance within and around horse paddocks
3. The probability that there are horses inside a bat foraging patch
4. The natural susceptibility of horses to HeV

To find how ε varies across space I used published and unpublished data; the horse census database of Biosecurity Queensland, the tree density model of Crowther et al. (2015) and the *P. poliocephalus* bi-monthly feeding habitat ranks of Eby and Law (2008). Data were arranged according to characteristics of flying fox foraging behaviour (Hazel Parry, *pers. comm*) and following Giles et al. (2016). To begin I created a horse density model at 100 × 100 m pixels, which is the average size of a bat foraging patch. To match this resolution, I downscaled the tree density model from 700 m to 100 m grid size. The Eby and Law (2008) data was combined with the downscaled tree density model to find the maximum flowering by season, assuming that the weighted score of feeding habitats can somehow represent the proportion of trees per grid cell that are flowering. *P. alecto* is more generalist in its foraging preferences than *P. poliocephalus*.

To represent this difference, Eby and Law (2008) data was adapted to a more generalist feeding behaviour increasing by 10% the weight of all foraging habitats lower than 0.3. The resulting timeline of foraging habitat was aggregated in 4×4 km grid cells around each flying fox camp. With this data I calculated the probability that flying foxes find a foraging patch, the probability that there are horses inside a bat foraging patch, and a series of parameters that control flowering rates in each 4×4 km grid cell.

To show how the parametrised framework might work, I modelled HeV dynamics in a bat camp with a *MSIR* model. To represent seasonal birth pulses I used Peel et al. (2014) birth function. In addition I kept a constant random influx of infected bats that create periodic epidemics once $R_0 > 1$. Specific details of the framework are in Appendix 9.6.3.2. I ran simulations with a τ-leap stochastic simulation algorithm (Mauch and Stalzer, 2011) implemented in iPython, and analysed the outputs in R.

An example of the potential outcomes of the framework

To show how the framework might help improve spillover predictability and understanding I ran simulations of HeV dynamics in bats. Each day bats leave their camp site and so equation 9.3 is re-evaluated in each foraging patch containing a specific number of horses that are at risk of spillover.

In the simulation example, nine spillover events occurred over the course of five years, during times where the number of HeV infected bats was high (Figure 9.1).

As it is evident the number of simultaneous spillover events is possible at times of higher HeV levels in bats, which coincides with field observations in other bat borne viruses that spillover to humans (Amman et al., 2012). The horse HeV cases recorded in the simulation were spatially referenced, and so it is possible to see their location with respect to the source camp site in figure 9.2.

The location of the spillover events responded to risk dynamics in space and time, which were calculated with equation 9.3. In figure 9.3 I show how risk varied across space at the moment each of the spillover events in figures 9.1 and 9.2 occurred.

In Chapter 6 I saw that there is a negative effect of horse density on spillover risk (Figure 22). With this model it is actually possible to show how such a relationship arises as a result of the mechanism represented by the scaling parameter ϵ. First, there is a weak non-linear correlation between horses and tree density, which is negative in regions along the potential range of horse

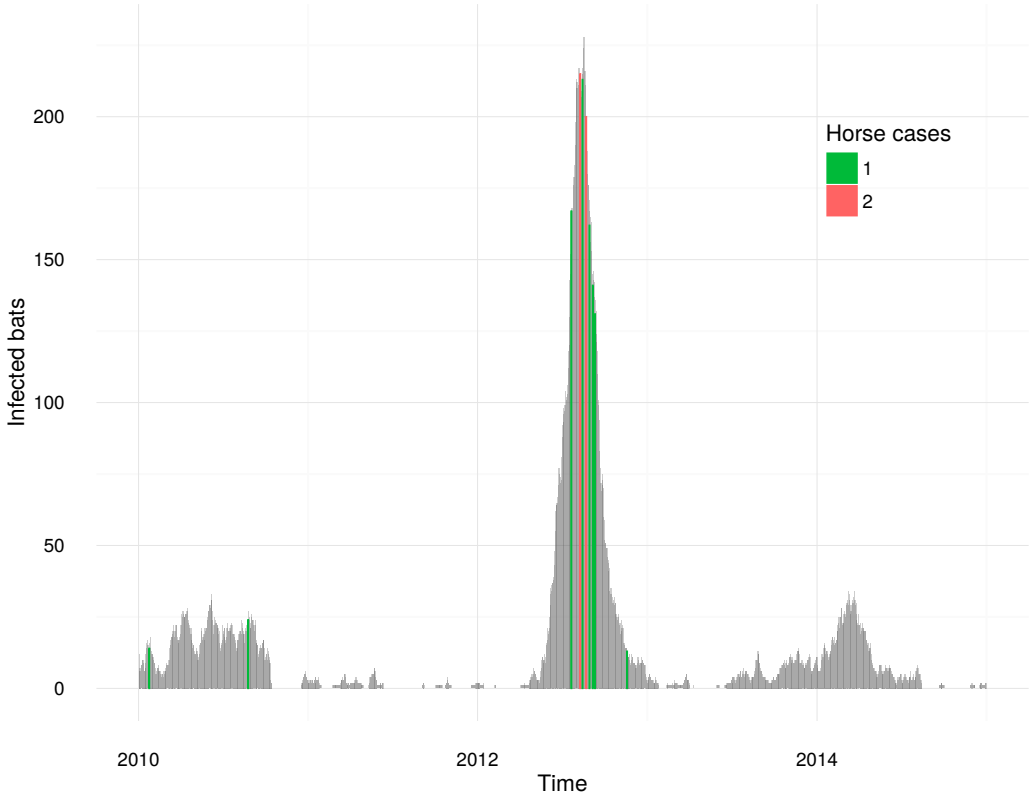

Figure 9.1: Hendra virus dynamics in a population of approximately 5000 bats. Coloured bars show the timing and the number of horse cases that occurred.

densities (Figure 9.4). Because tree density affects the foraging decisions of bats, there are fewer chances of contact between horses and bats in areas where the best foraging habitat is present. These areas have intermediate-low horse densities (Figure 9.4).

From the timing of registered spillover events, there is a tendency to occur both in late spring-summer and winter. The hypothetical bat population is located in southern Queensland, where foraging habitat data is available (Eby and Law, 2008). This suggests that the influx of susceptible bats during the birth pulses and waning maternal immunity in early summer and winter increase R_0, and potential for a HeV epidemic. In times when there are many recovered bats, epidemics occur in winter, when maternal immunity wanes and the pool of adult susceptible bats is replenished. Additionally, I observed that the spillover probability computed in the simulation was 0 in the known location of some spillover events (results not shown). This shows the limitations of both the data and the model. Therefore improved understanding of bat decisions based on spatial distribution of resources is critical, as well as more detailed accounts of bat foraging habitat and their spatio-temporal dynamics.

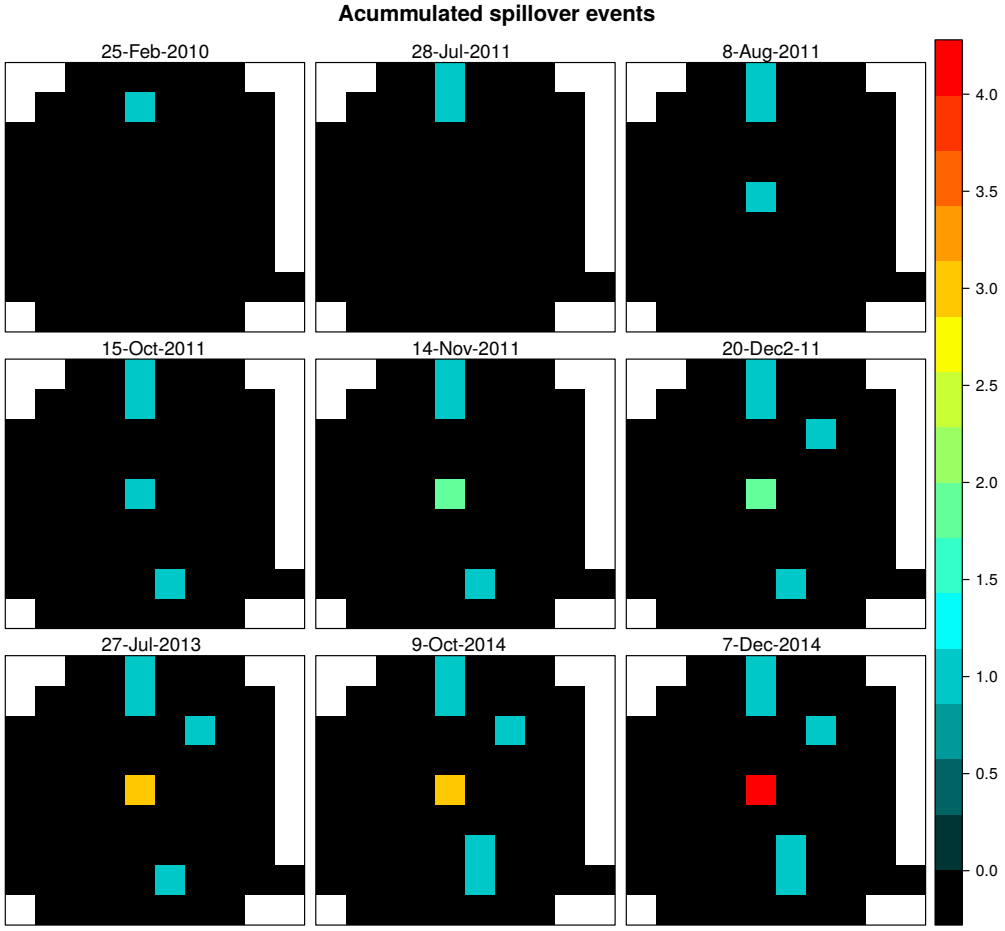

Figure 9.2: Acummulated number of spillover events that occurred in the simulation. The dates and spillover events represent only the course of the simulation and are not related to the spillover events registered to date.

A feasible improvement to the model would be including the immigration and emigration of bats in response to the pooled flowering dynamics around camp sites. For example the population flux predicted by Giles et al. (2016) could be used as the response to the number of flowering trees using a single differential equation. The immigration and emigration rates could then be estimated with MCMC sampling, just as the flowering rates were estimated for the present model. However, the poor understanding of HeV infection dynamics limits this approach as it would require many assumptions regarding the imports of infected, recovered and potentially latent individuals (Plowright et al., 2016) and the imports of bats in different developmental stages that are likely to be important drivers of seasonal patterns (Jaewoon Jeong *pers. comm.*).

Once HeV dynamics are better understood, a natural extension of this model would be its

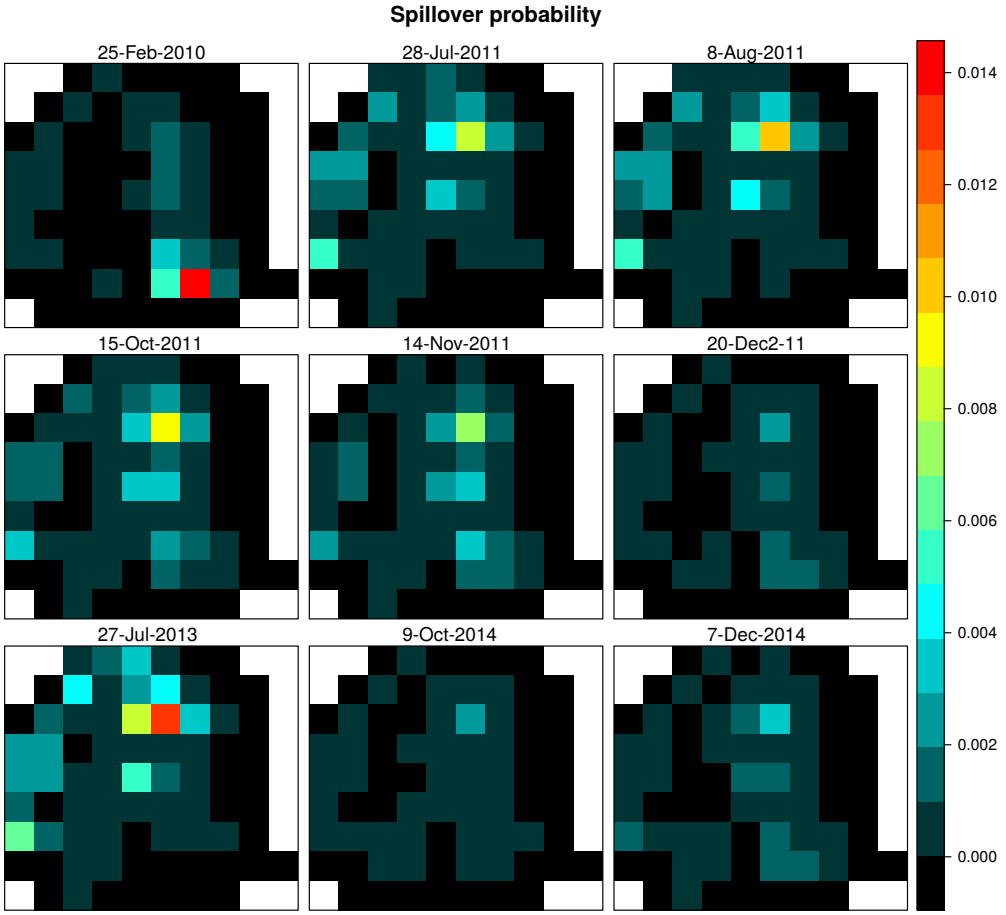

Figure 9.3: Spatial variability of spillover probability at the moment of spillover to horses.

incorporation into a network-patch model as in Plowright et al. (2011). And while its predictions would not be completely accurate, given data limitations, it would provide invaluable insights into the behaviour of the spillover system as a whole.

As for its extension in the context of this thesis, validating the microclimate model predictions for Brisbane and Cairns would be necessary. Similarly, remote sensing estimates of grass height variability would facilitate the use of the survival models in space and time. In addition, detailed analyses of spatial variability of HeV survival based on the remote sensing data would help summarise the effect of HeV survival on likelihood of transmission with a single parameter.

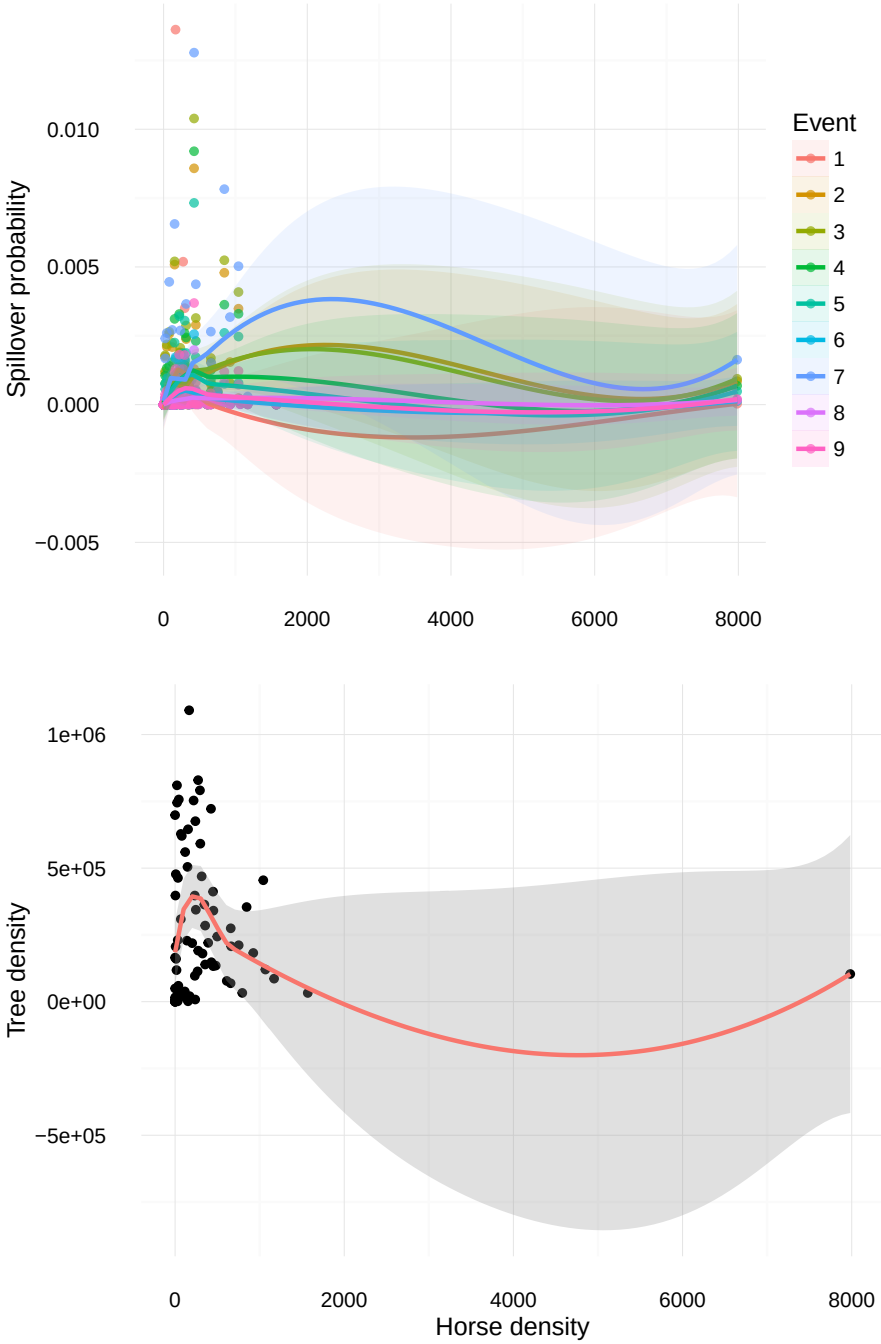

Figure 9.4: Top: Relationship between horse density and spillover probability at the moment of each spillover event. Bottom: Relationship between horse and tree density (approximate number of trees per 4 × 4 km pixel).

Conclusions

The currently available data hampers full implementation of a mechanistic framework to predict HeV spillover. However, I have shown that coupling HeV dynamics with flying foxes foraging

patterns and landscape attributes is possible with simple and transparent methods. On the mechanistic side, the model suggests that the correlation between bat foraging habitat and horse density have a strong effect at the 4 km scale in determining HeV spillover risk. This phenomenon could well be related to HeV emergence, thus opening opportunities for mitigation strategies that address the causes of HeV emergence, rather than on avoiding contact between susceptible spillover and infectious reservoir hosts. For example, one of the caveats of vaccination as a mitigation strategy is that spillover risk will always be > 0 unless the entire horse population is vaccinated.

Bibliography

Sonia Altizer, Andrew Dobson, Parviez Hosseini, Peter Hudson, Mercedes Pascual, and Pejman Rohani. Seasonality and the dynamics of infectious diseases. *Ecology letters*, 9(4):467–84, apr 2006. ISSN 1461-0248. doi: 10.1111/j.1461-0248.2005.00879.x. URL http://www.ncbi.nlm.nih.gov/pubmed/16623732.

Brian R Amman, Serena a Carroll, Zachary D Reed, Tara K Sealy, Stephen Balinandi, Robert Swanepoel, Alan Kemp, Bobbie Rae Erickson, James a Comer, Shelley Campbell, Deborah L Cannon, Marina L Khristova, Patrick Atimnedi, Christopher D Paddock, Rebekah J Kent Crockett, Timothy D Flietstra, Kelly L Warfield, Robert Unfer, Edward Katongole-Mbidde, Robert Downing, Jordan W Tappero, Sherif R Zaki, Pierre E Rollin, Thomas G Ksiazek, Stuart T Nichol, and Jonathan S Towner. Seasonal pulses of Marburg virus circulation in juvenile Rousettus aegyptiacus bats coincide with periods of increased risk of human infection. *PLoS pathogens*, 8(10): e1002877, jan 2012. ISSN 1553-7374. doi: 10.1371/journal.ppat.1002877. URL http://www.pubmedcentral.nih.gov/articlerender.fcgi?artid=3464226{&}tool=pmcentrez{&}rendertype=abstract.

Roy Anderson and Robert M. May. *Infectious diseases of humans:Dynamics and control*. Oxford University Press, Oxford, 1992.

David A. Ashford, Rana A. Hajjeh, Michael F. Kelley, Leo Kaufman, Lori Hutwagner, and Michael M. McNeil. Outbreak of histoplasmosis among cavers attending the National Speleological Society Annual Convention, Texas, 1994. *American Journal of Tropical Medicine and Hygiene*, 60(6):899–903, 1999. ISSN 00029637.

Nicolas Bacaër and Souad Guernaoui. The epidemic threshold of vector-borne diseases with seasonality: The case of cutaneous leishmaniasis in Chichaoua, Morocco. *Journal of Mathematical Biology*, 53(3):421–436, 2006. ISSN 03036812. doi: 10.1007/s00285-006-0015-0.

Morgane Barbet-Massin, Frederic Jiguet, Cecile H Albert, and Wilfried Thuiller. Selecting pseudo-absences for species distribution models: how, where and how many? *Methods in Ecology and Evolution*, (3):85–107, 2012. ISSN 02172445. doi: 10.1111/j.2041-210X.2011.00172.x.

Nigel D Barlow. A Spatially Aggregated Disease / Host Model for Bovine Tb in New Zealand Possum Populations. *Journal of Applied Ecology*, 28(3):777–793, 1991.

Nigel D Barlow. Non - linear transmission and simple models for bovine tuberculosis. *Journal of Applied Ecology*, 69(4):703–713, 2000.

Narayani Barve. Tool for Partial-ROC, 2008.

Narayani Barve, Vijay Barve, Alberto Jiménez-Valverde, Andres Lira-Noriega, Sean P Maher, a. T Peterson, Jorge Soberón, and Fabricio Villalobos. The crucial role of the accessible area in ecological niche modeling and species distribution modeling. *Ecological Modelling*, 222(11):1810–1819, jun 2011. ISSN 03043800. doi: 10.1016/j.ecolmodel.2011.02.011. URL http://linkinghub.elsevier.com/retrieve/pii/S0304380011000780.

Simon Benhamou. Of scales and stationarity in animal movements. *Ecology letters*, 17(3):261–72, mar 2014. ISSN 1461-0248. doi: 10.1111/ele.12225. URL http://www.ncbi.nlm.nih.gov/pubmed/24350897.

Leo Breiman. Random forests. *Machine learning*, 45(1):5–32, 2001.

Stephen P Brooks and Andrew Gelman. General methods for monitoring convergence of iterative simulations. *Journal of Computational and Graphical Statistics*, 7(4): 434–455, 1998.

J R Busby. BIOCLIM - a bioclimate analysis and prediction system. In C R Margules and M P Austin, editors, *Nature conservation: cost effective biological surveys and data analysis*, pages 64–68. CSIRO, 1991.

Charles H. Calisher, James E. Childs, Hume E. Field, Kathryn V. Holmes, and Tony Schountz. Bats: Important reservoir hosts of emerging viruses. *Clinical Microbiology Reviews*, 19(3):531–545, 2006. ISSN 08938512. doi: 10.1128/CMR.00017-06.

Hong J. Chang, Nicole Huang, Cheng H. Lee, Yea J. Hsu, Chi Jeng Hsieh, and Yiing Jenq Chou. The Impact of the SARS Epidemic on the Utilization of Medical Services: SARS and the Fear of SARS. *American Journal of Public Health*, 94(4):562–564, 2004. ISSN 00900036. doi: 10.2105/AJPH.94.4.562.

John C H Chang, Susan F Ossoff, David C Lobe, Mark H Dorfman, Constance M Dumais, Robert G Qualls, and J. Donald Johnson. UV inactivation of pathogenic and indicator microorganisms. *Applied and Environmental Microbiology*, 49(6):1361–1365, 1985. ISSN 00992240.

Jiquan Chen, Sari C Saunders, Thomas R Crow, Robert J Naiman, Kimberley D Brosofske, Glenn D Mroz, Brian L Brookshire, and Jerry F Franklin. Microclimate in Forest Ecosystem and Landscape Ecology: Variations in local climate can be used to monitor and compare the effects of different management regimes. *BioScience*, 49(4), 1996.

Heng Thay Chong, Sree Raman Kunjapan, Tarmizi Thayaparan, JennyMayGeok Tong, Vijayasingham Petharunam, Mohd Rani Jusoh, and Chong Tin Tan. Nipah encephalitis outbreak in Malaysia, clinical features in patients from Seremban. *The Canadian journal of neurological sciences. Le journal canadien des sciences neurologiques*, 29(1):83–7, 2002. ISSN 0317-1671. URL http://www.ncbi.nlm.nih.gov/pubmed/11858542.

Kau Bing Chua. Nipah virus outbreak in Malaysia. *Journal of Clinical Virology*, 26(3): 265–75., 2003.

Thomas W Crowther, Henry B Glick, K R Covey, C Bettigole, Daniel S Maynard, Stephen M Thomas, Jeffrey R Smith, G Hintler, Marlyse C Duguid, Giuseppe Amatulli, Mao-Ning Tuanmu, W Jetz, Christian Salas, C Stam, D Piotto, R Tavani, Stephen Green, Gareth Bruce, S J Williams, Susan K Wiser, Markus O Huber, Geerten M Hengeveld, Gert-Jan Nabuurs, Elena Tikhonova, Peter Borchardt, Ching-Feng Li, Leslie W Powrie, M Fischer, A Hemp, Juergen Homeier, Percival Cho, Alexander C Vibrans, P M Umunay, S L Piao, C W Rowe, Mark S Ashton, P R Crane, and M A Bradford. Mapping tree density at a global scale. *Nature*, 525 (7568):201–205, 2015. ISSN 1476-4687. doi: 10.1038/nature14967. URL http://www.ncbi.nlm.nih.gov/pubmed/26331545.

Hoang Quoc Cuong, Nguyen Thanh Vu, Bernard Cazelles, Maciej F. Boni, Khoa T D Thai, Maia A. Rabaa, Luong Chan Quang, Cameron P. Simmons, Tran Ngoc Huu, and Katherine L. Anders. Spatiotemporal dynamics of dengue epidemics, Southern Vietnam. *Emerging Infectious Diseases*, 19(6):945–953, 2013. ISSN 10806040. doi: 10.3201/eid1906.121323. URL http://wwwnc.cdc.gov/eid/article/19/6/12-1323{_}article.htm.

Peter Daszak. Emerging infectious diseases of wildlife - Threats to biodiversity and human health (vol 287, pg 443, 2000). *Science*, 287(5459):1756, 2000.

Peter Daszak, Ccarlos Zambrana-Torrelio, Tiffany L Bogich, Miguel Fernandez, Jonathan H Epstein, Kris A Murray, and Healy Hamilton. Interdisciplinary approaches to understanding disease emergence: the past, present, and future drivers of Nipah virus emergence. *Proceedings of the National Academy of Sciences of the United States of America*, 110 Suppl: 3681–8, feb 2013. ISSN 1091-6490. doi: 10.1073/pnas.1201243109. URL http://www.pubmedcentral.nih.gov/articlerender.fcgi?artid=3586606{&}tool=pmcentrez{&}rendertype=abstract.

Troy Day. Parasite transmission modes and the evolution of virulence. *Evolution*, 55 (12):2389–400, dec 2001. ISSN 0014-3820. URL http://www.ncbi.nlm.nih.gov/pubmed/11831655.

Peter J. Diggle, Paula Moraga, Barry Rowlingson, and Benjamin M. Taylor. Spatial and Spatio-Temporal Log-Gaussian Cox Processes: Extending the Geostatistical Paradigm. *Statistical Science*, 28(4):542–563, 2013. ISSN 0883-4237. doi: 10.1214/13-STS441. URL http://projecteuclid.org/euclid.ss/1386078878.

Katarzyna Domanska-Blicharz, Zenon Minta, Krzysztof Smietanka, and Sylvie Marché. H5N1 High Pathogenicity Avian Influenza Virus Survival in Different Types of Water. *Avian Diseases*, 54(s1):734–737, 2010.

S. F. Dowell. Seasonal variation in host susceptibility and cycles of certain infectious diseases. *Emerging infectious diseases*, 7(3):369–374, 2001. ISSN 10806040. doi: 10.3201/eid0703.010301.

Patrick Duncan. Determinants of the Use of Habitat By Horses. *Journal of Animal Ecology*, 52(1):93–109, 1983.

Patrick Duncan and Pamela Cowtan. An unusual choice of habitat helpps Camargue horses to avoid blood-sucking horse flies. *Biology of Behaviour*, 5:55–60, 1980.

Bryan T Eaton, Christopher C Broder, Deborah Middleton, and Lin-Fa Wang. Hendra and Nipah viruses: different and dangerous. *Nature reviews. Microbiology*, 4 (1):23–35, jan 2006. ISSN 1740-1526. doi: 10.1038/nrmicro1323. URL http://www.ncbi.nlm.nih.gov/pubmed/16357858.

Peggy Eby. Seasonal movements of grey-headed flying-foxes, Pteropus poliocephalus (Chiroptera : Pteropodidae), from two maternity camps in northern New South Wales. *Wildlife Research*, 18:547, 1991. ISSN 1035-3712. doi: 10.1071/WR9910547.

Peggy Eby and Bradley S Law. Ranking the feeding habitats of Grey-headed flying foxes for conservation management. Technical Report October, The Department of Environment and Climate Change (NSW), 2008.

Nadège Edouard, Géraldine Fleurance, Bertrand Dumont, René Baumont, and Patrick Duncan. Does sward height affect feeding patch choice and voluntary intake in horses? *Applied Animal Behaviour Science*, 119(3-4):219–228, 2009. ISSN 01681591. doi: 10.1016/j.applanim.2009.03.017.

Daniel Edson, Hume Field, Lee McMichael, Miranda Vidgen, Lauren Goldspink, Alice Broos, Deb Melville, Joanna Kristoffersen, Carol de Jong, Amanda McLaughlin, Rodney Davis, Nina Kung, David Jordan, Peter Kirkland, and Craig Smith. Routes of Hendra Virus Excretion in Naturally-Infected Flying-Foxes: Implications for Viral Transmission and Spillover Risk. *Plos One*, 10(10):e0140670, 2015. ISSN 1932-6203. doi: 10.1371/journal.pone.0140670. URL http://dx.plos.org/10.1371/journal.pone.0140670.

Jane Elith and John R Leathwick. Species Distribution Models: Ecological Explanation and Prediction Across Space and Time. *Annual Review of Ecology, Evolution, and Systematics*, 40(1):677–697, dec 2009. ISSN 1543-592X. doi: 10.1146/annurev.ecolsys.110308.120159. URL http://www.annualreviews.org/doi/abs/10.1146/annurev.ecolsys.110308.120159.

Jane Elith, John R Leathwick, and Trevor Hastie. A working guide to boosted regression trees. *The Journal of animal ecology*, 77(4):802–13, jul 2008. ISSN 1365-2656. doi: 10.1111/j.1365-2656.2008.01390.x. URL http://www.ncbi.nlm.nih.gov/pubmed/18397250.

Jane Elith, Steven J Phillips, Trevor Hastie, Miroslav Dudík, Yung E Chee, and Colin J Yates. A statistical explanation of MaxEnt for ecologists. *Diversity and Distributions*, 17(1):43–57, jan 2011. ISSN 13669516. doi: 10.1111/j.1472-4642.2010.00725.x. URL http://doi.wiley.com/10.1111/j.1472-4642.2010.00725.x.

Luis E Escobar, A Townsend Peterson, Myriam Favi, Verónica Yung, Daniel J Pons, and Gonzalo Medina-Vogel. Ecology and geography of transmission of two bat-borne rabies lineages in Chile. *PLoS neglected tropical diseases*, 7 (12):e2577, jan 2013. ISSN 1935-2735. doi: 10.1371/journal.pntd.0002577. URL http://www.pubmedcentral.nih.gov/articlerender.fcgi?artid=3861194{&}tool=pmcentrez{&}rendertype=abstract.

Agustín Estrada-Peña, Richard S. Ostfeld, a. Townsend Peterson, Robert Poulin, and José de la Fuente. Effects of environmental change on zoonotic disease risk: An ecological primer. *Trends in Parasitology*, 30(4):205–214, 2014. ISSN 14715007. doi: 10.1016/j.pt.2014.02.003.

Jeffrey S Evans, Melanie A Muphy, Zachary A Holden, and Samuel A Cushman. Modelling Species Distribution and Change Using Random Forest. In C. Ashton Drew, Yolanda F. Wiersma, and Falk Huettmann, editors, *Predictive Species and Habitat Modeling in Landscape Ecology: Concepts and Applications*, chapter 8, pages 139–159. Springer Verlag, 2011. ISBN 9781441973894. doi: 10.1007/978-1-4419-7390-0.

Paul W Ewald. Transmission modes and evolution of parasitism. *New York Academy of Sciences*, 503:295–306, 1987.

Oren Farber and Ronen Kadmon. Assessment of alternative approaches for bioclimatic modeling with special emphasis on the Mahalanobis distance. *Ecological Modelling*, 160, 2003.

R J Fensham, J E Holman, and M J Cox. Plant species responses along a grazing disturbance gradient in Australian grassland. *Journal of Vegetation Science*, 10(1):77–86, 1999. ISSN 11009233. doi: 10.2307/3237163. URL http://onlinelibrary.wiley.com/doi/10.2307/3237163/abstract.

Hume Field, Kylie Schaaf, Nina Kung, Craig Simon, David Waltisbuhl, Heather Hobert, Frederick Moore, Deborah Middleton, Allison Crook, Greg Smith, Peter Daniels, Rron Glanville, and David Lovell. Hendra virus outbreak with novel clinical features, Australia. *Emerging infectious diseases*, 16 (2):338–40, feb 2010. ISSN 1080-6059. doi: 10.3201/eid1602.090780. URL http://www.pubmedcentral.nih.gov/articlerender.fcgi?artid=2958006{&}tool=pmcentrez{&}rendertype=abstract.

Hume Field, David Jordan, Daniel Edson, Stephen Morris, Debra Melville, Kerryn Parry-Jones, Alice Broos, Anja Divljan, Lee McMichael, Rodney Davis, Nina Kung, Peter Kirkland, and Craig Smith. Spatiotemporal Aspects of Hendra Virus Infection in Pteropid Bats (Flying-Foxes) in Eastern Australia. *PloS one*, 10 (12):e0144055, 2015a. ISSN 1932-6203. doi: 10.1371/journal.pone.0144055. URL http://www.pubmedcentral.nih.gov/articlerender.fcgi?artid=4666458{&}tool=pmcentrez{&}rendertype=abstract.

Hume E Field, Carol de Jong, Debra Melville, Craig Smith, Ina Smith, Alice Broos, Nina Kung, Amanda McLaughlin, and Anne Zeddeman. Hendra virus infection dynamics in Australian fruit bats. *PloS one*, 6(12):e28678, jan 2011. ISSN 1932-6203. doi: 10.1371/journal.pone.0028678. URL http://www.pubmedcentral.nih.gov/articlerender.fcgi?artid=3235146{&}tool=pmcentrez{&}rendertype=abstract.

Hume E Field, Craig S Smith, Carol E de Jong, Deb Melville, Alice Broos, Nina Kung, Joshua Thompson, and Dina K N Dechmann. Landscape Utilisation, Animal Behaviour and Hendra Virus Risk. *EcoHealth*, 13(1):26–38, 2015b. ISSN 16129210. doi: 10.1007/s10393-015-1066-8.

David N Fisman. Seasonality of infectious diseases. *Annual review of public health*, 28:127–43, jan 2007. ISSN 0163-7525. doi: 10.1146/annurev.publhealth.28.021406.144128. URL http://www.ncbi.nlm.nih.gov/pubmed/17222079.

Geraldine Fleurance, Patrick Duncan, Herve Fritz, Jacques Cabaret, Jacques Cortet, and Iain J. Gordon. Selection of feeding sites by horses at pasture: Testing the anti-parasite theory. *Applied Animal Behaviour Science*, 108(3-4):288–301, 2007. ISSN 01681591. doi: 10.1016/j.applanim.2006.11.019.

Geraldine Fleurance, Patrick Duncan, Herve Fritz, Iain J Gordon, and Marie-Florence Grenier-Loustalot. Influence of sward structure on daily intake and foraging behaviour by horses. *Animal : an international journal of animal bioscience*, 4(3):480–5, 2010. ISSN 1751-7311. doi: 10.1017/S1751731109991133. URL http://www.ncbi.nlm.nih.gov/pubmed/22443953.

Rhys Fogarty, Kim Halpin, Alex D Hyatt, Peter Daszak, and Bruce A Mungall. Henipavirus susceptibility to environmental variables. *Virus research*, 132(1-2):140–4, mar 2008. ISSN 0168-1702. doi: 10.1016/j.virusres.2007.11.010. URL http://www.ncbi.nlm.nih.gov/pubmed/18166242.

Grodon W Frazer, Charles D Canham, Pamela Sallaway, and Dimitri Marinakis. Gap Light analyzer Version 2.0, 1999.

Ludwig Fulco, Hans de Kroon, Herbert H T Prins, and Frank Berendse. Effects of Nutrients and Shade on Tree-Grass Interactions in an East African Savanna Effects of nutrients and shade on tree-grass interactions in an East African savanna. *Journal of Vegetation Science*, 12(4):579–588, 2001.

Thomas W Geisbert, Heinz Feldmann, and Christopher C Broder. Animal Challenge Models of Henipavirus Infection and Pathogenesis. *Current Topics in Microbiology and Immunology*, 359, 2012. doi: 10.1007/82.

Andrew Gelman, John B Carlin, Hal S Stern, David B Dunson, Aki Vehtari, and Donald B Rubin. *Bayesian Data Analysis*. CRC Press, Boca Raton, 3rd edition, 2013.

John Geweke. Evluating the accuracy of sampling-based approaches to the calculation of posterior moments. In J M Bernardo, J O Berger, A P David, and A F M Smith, editors, *Bayesian Statistics 4*, pages 169–193. Oxford University Press, Oxford, 1992.

Maria M Gil, Fatima A Miller, Teresa R S Brandão, and Cristina L M Silva. On the Use of the Gompertz Model to Predict Microbial Thermal Inactivation Under Isothermal and Non-Isothermal Conditions. *Food Engineering Reviews*, 3(1):17–25, jan 2011. ISSN 1866-7910. doi: 10.1007/s12393-010-9032-2. URL http://www.springerlink.com/index/10.1007/s12393-010-9032-2.

John R Giles, Raina K Plowright, Peggy Eby, Alison J Peel, and Hamish McCallum. Models of Eucalypt phenology predict bat population flux. *Ecology and Evolution*, pages 1–16, 2016. ISSN 20457758. doi: 10.1002/ece3.2382. URL http://doi.wiley.com/10.1002/ece3.2382.

Lauren K Goldspink, Daniel W Edson, Miranda E Vidgen, John Bingham, Hume E Field, and Craig S Smith. Natural Hendra Virus Infection in Flying-Foxes - Tissue Tropism and Risk Factors. *Plos One*, 10(6):e0128835, 2015. ISSN 1932-6203. doi: 10.1371/journal.pone.0128835. URL http://dx.plos.org/10.1371/journal.pone.0128835.

Nicholas C Grassly and Christophe Fraser. Seasonal infectious disease epidemiology. *Proceedings. Biological sciences / The Royal Society*, 273(1600):2541–50, oct 2006. ISSN 0962-8452. doi: 10.1098/rspb.2006.3604. URL http://www.pubmedcentral.nih.gov/articlerender.fcgi?artid=1634916{&}tool=pmcentrez{&}rendertype=abstract.

Micah B Hahn, Jonathan H Epstein, Emily S Gurley, Mohammad S Islam, Stephen P Luby, Peter Daszak, and Jonathan A Patz. Roosting behaviour and habitat selection of Pteropus giganteus reveal potential links to Nipah virus epidemiology. *Journal of Applied Ecology*, 51:376–387, 2014. ISSN 13652664. doi: 10.1111/1365-2664.12212.

Robert Haining. *Spatial data Analysis: Theory and Practice*. Cambridge University Press, Edinburgh, 2003. ISBN 0521774373.

Kim Halpin and Hume E. Field. Identification of likely natural hosts for equine Morbillivirus. *Communicable Diseases Intelligence*, 20(22):1996, 1996.

Kim Halpin, Peter L Young, Hume E Field, and John S Mackenzie. Isolation of Hendra virus from pteropid bats: a natural reservoir of Hendra virus. *The Journal of general virology*, 81(Pt 8):1927–32, aug 2000. ISSN 0022-1317. URL http://www.ncbi.nlm.nih.gov/pubmed/10900029.

Kim Halpin, Alex D Hyatt, Rhys Fogarty, Debborah Middleton, John Bingham, Jonathan H Epstein, S A Rahman, T Hughes, Craig Smith, Hume E Field, and Peter Daszak. Pteropid bats are confirmed as the reservoir hosts of henipaviruses: a comprehensive experimental study of virus transmission. *The American journal of tropical medicine and hygiene*, 85(5):946–51, nov 2011. ISSN 1476-1645. doi: 10.4269/ajtmh.2011.10-0567. URL http://www.ajtmh.org/content/85/5/946.full.

Jian-Feng He, Jun Min, De-wen Yu, Wen-jia Liang, Rui-heng Xu, Zhan-hui Wang, Ling Fang, Xin Zhang, Hui Li, Xin-ge Yan, Zhi-hong Hu, Ji-cheng Huang, Jun Zhou, Bo-wei Gu, Xiang-lin Zhang, Mei He, Kui Zheng, Fei Wang, Gang Fu, Xiao-ning Wang, Zhu Chen, Qi Liu, Xiang-yin Kong, Wei-zhong He, Chung-i Wu, Stephen S C Chim, Yu-kwan Tong, John S Tam, Y M Dennis Lo, Zhongshan Road, Nanfang Hospital, First Med, Ruijin Hospital, Bo Road, Zhang Jiang, High Tech, and Shanghai Jiao. Molecular evolution of the SARS coronavirus during the course of the SARS epidemic in China. *Science (New York, N.Y.)*, 303(5664):1666–1669, 2004. ISSN 0036-8075. doi: 10.1126/science.1092002.

Robert J Hijmans. Cross-validation of species distribution models : removing spatial sorting bias and calibration with a null model. *Ecology*, 93(3):679–688, 2012.

Robert J Hijmans. raster: Geographic data analysis and modeling, 2013. URL http://cran.r-project.org/package=raster.

Robert J Hijmans, Susan E Cameron, Juan L Parra, Peter G Jones, and Andy Jarvis. Very high resolution interpolated climate surfaces for global land areas. *International Journal of Climatology*, 25(15):1965–1978, dec 2005. ISSN 0899-8418. doi: 10.1002/joc.1276. URL http://doi.wiley.com/10.1002/joc.1276.

Robert J Hijmans, John L Leathwick, and Jane Elith. dismo: Species distribution modelling, 2013. URL http://cran.r-project.org/web/packages/dismo/index.html.

Robert D Holt and John Pickering. Infectious Disease and Species Coexistence : A Model of Lotka-Volterra Form. *The American Naturalist*, 126(2):196–211, 1985. URL http://www.jstor.org/stable/2461507.

M Jahangir Hossain, Emily S Gurley, Joel M Montgomery, Michael Bell, Darin S Carroll, Vincent P Hsu, P Formenty, A Croisier, E Bertherat, M a Faiz, Abul Kalam Azad, Rafiqul Islam, M Abdur Rahim Molla, Thomas G Ksiazek, Paul a Rota, James a

Comer, Pierre E Rollin, Stephen P Luby, and Robert F Breiman. Clinical presentation of nipah virus infection in Bangladesh. *Clinical infectious diseases : an official publication of the Infectious Diseases Society of America*, 46(7):977–984, 2008. ISSN 1537-6591. doi: 10.1086/529147.

Katherine A Houpt, Michael F O'Connell, and Thomas F Houpt. Night-Time Behaviour of Stabled and Pastured Peri-Parturient Ponies.Pdf. *Applied Animal Behaviour Science*, (15):103–111, 1986.

Irene L Hudson, Susan W Kim, and Marie R Keatley. Climatic Influeces on the Flowering Phenology of Four Eucalypts: A GAMLSS Approach. In I L Hudson and M R Keatley, editors, *Phenological Research*, chapter 10, pages 209–228. Springer, London, 2010.

G Evelyn Hutchinson. Concluding remarks. In *Cold Spring Harbor Symposium on Quantitative Biology*, pages 415–457, 1957.

A Jiménez-Valverde, J M Lobo, and J Hortal. Not as good as they seem: the importance of concepts in species distribution modelling. *Diversity and Distributions*, 14(6): 885–890, nov 2008. ISSN 13669516. doi: 10.1111/j.1472-4642.2008.00496.x. URL http://doi.wiley.com/10.1111/j.1472-4642.2008.00496.x.

Kate Jones, Nikkita Patel, Marc Levy, Adam Storeygard, Deborah Balk, John Gittleman, and Peter Daszak. Global trends in emerging infectious diseases. *Nature*, 451(7181):990–993, 2008. ISSN 14764687. doi: 10.1038/nature06536.

Grete H M Jørgensen and Knut E Bøe. A note on the effect of daily exercise and paddock size on the behaviour of domestic horses (Equus caballus). *Applied Animal Behaviour Science*, 107(1-2):166–173, 2007. ISSN 01681591. doi: 10.1016/j.applanim.2006.09.025.

Michael Kearney and Warren Porter. Mechanistic niche modelling: combining physiological and spatial data to predict species' ranges. *Ecology letters*, 12(4): 334–50, apr 2009. ISSN 1461-0248. doi: 10.1111/j.1461-0248.2008.01277.x. URL http://www.ncbi.nlm.nih.gov/pubmed/19292794.

Michael R Kearney, Andrew P Isaac, and Warren P Porter. microclim: Global estimates of hourly microclimate based on long-term monthly climate averages. *Scientific Data*, 1:1–9, may 2014. ISSN 2052-4463. doi: 10.1038/sdata.2014.6. URL http://www.nature.com/articles/sdata20146.

Matt J Keeling and Pejman Rohani. *Modelling Infectious Diseases in Humans and Animals*. Princeton University Prees, New Jersey, 1 edition, 2007.

Ronald R Keiper and Joel Berger. Refuge-seeking and pest avoidance by feral horses in desert and island environments. *Applied Animal Ethology*, 9(2):111–120, 1982. ISSN 03043762. doi: 10.1016/0304-3762(82)90187-0.

Axel Kramer, Ingeborg Schwebke, and Günter Kampf. How long do nosocomial pathogens persist on inanimate surfaces? A systematic review. *BMC infectious diseases*, 6:130, jan 2006. ISSN 1471-2334. doi: 10.1186/1471-2334-6-130. URL http://www.pubmedcentral.nih.gov/articlerender.fcgi?artid=1564025{&}tool=pmcentrez{&}rendertype=abstract.

Kevin D Lafferty. The ecology of climate change and infectious diseases. *Ecology*, 90 (4):888–900, 2009.

Eric M Leroy, Brice Kumulungui, Xavier Pourrut, Pierre Rouquet, Alexandre Hassanin, Philippe Yaba, André Délicat, Janusz T Paweska, Jean-Paul Gonzalez, and Robert Swanepoel. Fruit bats as reservoirs of Ebola virus. *Nature*, 438(7068):575–576, 2005. ISSN 0028-0836. doi: 10.1038/438575a.

Wendong Li, Zhengli Shi, Mengu Yu, Wuze Ren, Craig Smith, Jonathan H Epstein, Hanzhong Wang, Gary Crameri, Hu Zhihong, Zhang Huajun, Zhang Jianhong, Jennifer McEachern, Hume E Field, Peter Daszak, Bryan T Eaton, Shuyi Zhang, and Lin-Fa Wang. Bats Are Natural Reservoirs of SARS-Like Coronaviruses. *Science*, 310(5748):676–679, 2005. ISSN 0036-8075. doi: 10.1126/science.1118391. URL http://www.sciencemag.org/cgi/doi/10.1126/science.1118391papers2://publication/doi/10.1126/science.1118391.

Monte Lloyd. Mean Crowding. *Journal of Animal Ecology*, 36(1):1–30, 1967.

Giovanni L Lo Iacono, Andrew A Cunningham, Lina M Moses, Giovanni Lo Iacono, Andrew A Cunningham, and Elisabeth Fichet-calvet. A Unified Framework for the Infection Dynamics of Zoonotic Spillover and Spread. *PloS one*, (September), 2016. doi: 10.1371/journal.pntd.0004957.

Deborah D Markwell and Kennedy F Shortridge. Possible waterborne transmission and maintenance of influenza viruses in domestic ducks. *Applied Environmental Microbiology*, 43(1), 1982.

Mathieu Marmion, Miia Parviainen, Miska Luoto, Risto K. Heikkinen, and Wilfried Thuiller. Evaluation of consensus methods in predictive species distribution modelling. *Diversity and Distributions*, 15(1):59–69, jan 2009. ISSN 13669516. doi: 10.1111/j.1472-4642.2008.00491.x. URL http://doi.wiley.com/10.1111/j.1472-4642.2008.00491.x.

Glenn A Marsh, Jessica Haining, Timothy J Hancock, Rachel Robinson, Adam J Foord, Jennifer A Barr, Shane Riddell, Hans G Heine, John R White, Gary Crameri, Hume E Field, Lin-Fa Wang, and Deborah Middleton. Experimental infection of horses with Hendra virus/Australia/horse/2008/Redlands. *Emerging infectious diseases*, 17(12):2232–8, dec 2011. ISSN 1080-6059. doi: 10.3201/eid1712.111162. URL http://www.pubmedcentral.nih.gov/articlerender.fcgi?artid=3311212{&}tool=pmcentrez{&}rendertype=abstract.

Glenn A Marsh, Carol E de Jong, Jennifer A Barr, Mary Tachedjian, Craig Smith, D Middleton, Meng Yu, Shawn Todd, Adam J Foord, Volker Haring, Jean Payne, R Robinson, Ivano Broz, Gary Crameri, Hume E Field, and Lin-Fa Wang. Cedar virus: a novel Henipavirus isolated from Australian bats. *PLoS pathogens*, 8(8): e1002836, aug 2012. ISSN 1553-7374. doi: 10.1371/journal.ppat.1002836. URL http://www.pubmedcentral.nih.gov/articlerender.fcgi?artid=3410871{&}tool=pmcentrez{&}rendertype=abstract.

Gerardo Martin, Rebecca J Webb, Carla Chen, Raina K Plowright, and Lee F Skerratt. Tree cover in paddocks is the main determinant of exposure to Hendra virus in horses. *Preventive Veterinary Medicine*, a.

Gerardo Martin, Carlos Yanez-Arenas, Carla Chen, Raina K Plowright, Billie J Roberts, and Lee F Skerratt. Seasonal spillover of Hendra virus: distribution and climatic dirvers. *EcoHealth*, b.

Gerardo Martin, Carlos Yanez-Arenas, Carla Chen, Raina K Plowright, Rebecca J Webb, and Lee F Skerratt. Climate change will increase the extent of areas at risk of Hendra virus spillover. *Emerging Infectious Diseases*, c.

Gerardo Martin, Raina Plowright, Carla Chen, David Kault, Paul Selleck, and Lee Skerratt. Hendra virus survival does not explain spillover patterns and implicates relatively direct transmission routes from flying foxes to horses. *The Journal of General Virology*, pages vir.0.000073–, feb 2015. ISSN 1465-2099. doi: 10.1099/vir.0.000073. URL http://vir.sgmjournals.org/content/early/2015/02/09/vir.0.000073.abstract.

Gerardo Martin, Carlos Yanez-Arenas, Billie J. Roberts, Carla Chen, Raina K. Plowright, Rebecca J. Webb, and Lee F. Skerratt. Climatic suitability influences species specific abundance patterns of Australian flying foxes and risk of Hendra virus spillover. *One Health*, 2:115–121, 2016. ISSN 23527714. doi: 10.1016/j.onehlt.2016.07.004. URL http://dx.doi.org/10.1016/j.onehlt.2016.07.004.

Gerardo Martin, Rebecca J. Webb, Carla Chen, Raina K. Plowright, and Lee F. Skerratt. Microclimates Might Limit Indirect Spillover of the Bat Borne Zoonotic Hendra Virus. *Microbial Ecology*, pages 1–10, 2017. ISSN 0095-3628. doi: 10.1007/s00248-017-0934-x. URL http://link.springer.com/10.1007/s00248-017-0934-x.

Enrique Martínez-Meyer, Daniel Díaz-Porras, a Townsend Peterson, and Carlos Yáñez-Arenas. Ecological niche structure and rangewide abundance patterns of species. *Biology letters*, 9(1):20120637, feb 2013. ISSN 1744-957X. doi: 10.1098/rsbl.2012.0637. URL http://www.ncbi.nlm.nih.gov/pubmed/23134784.

Sean Mauch and Mark Stalzer. Efficient formulations for exact stochastic simulation of chemical systems. *IEEE/ACM transactions on computational biology and bioinformatics / IEEE, ACM*, 8(1):27–35, 2011. ISSN 1557-9964. doi: 10.1109/TCBB.2009.47. URL http://www.ncbi.nlm.nih.gov/pubmed/21071794.

Hamish McCallum. *Population Parameters : Estimation for Ecological Models*. Blackwell Science, Brisbane, 2000. ISBN 0865427402.

Hamish McCallum, Nigel Barlow, and Jim Hone. How should pathogen transmission be modelled? *TRENDS in Ecology and Evolution*, 16(6):295–300, 2001.

Kim R McConkey and Donald R Drake. Flying Foxes Cease to Function as Seed Dispersers Long Before they Become Extinct. *Ecology*, 87(2):271–276, 2006.

James McDevitt, Stephen Rudnick, Melvin First, and John Spengler. Role of Absolute Humidity in the Inactivation of Influenza Viruses on Stainless Steel Surfaces at Elevated Temperatures. *Applied and Environmental Microbiology*, 76(12):3943–3947, 2010. ISSN 0099-2240. doi: 10.1128/AEM.02674-09. URL http://aem.asm.org/cgi/doi/10.1128/AEM.02674-09.

Rosemary McFarlane, Niels Becker, and Hume Field. Investigation of the climatic and environmental context of Hendra virus spillover events 1994-2010. *PloS one*, 6(12):e28374, jan 2011. ISSN 1932-6203. doi: 10.1371/journal.pone.0028374. URL http://www.pubmedcentral.nih.gov/articlerender.fcgi?artid=3228733{&}tool=pmcentrez{&}rendertype=abstract.

Mohsen B Mesgaran, Roger D Cousens, and Bruce L Webber. Here be dragons: a tool for quantifying novelty due to covariate range and correlation change when projecting species distribution models. *Diversity and Distributions*, pages n/a–n/a, apr 2014. ISSN 13669516. doi: 10.1111/ddi.12209. URL http://doi.wiley.com/10.1111/ddi.12209.

V Michel, N Ruvoen-Clouet, A Menard, C Sonrier, C Fillonneau, F Rakotovao, J P Ganiere, and G Andre-Fontaine. Role of the Coypu (Myocastor coypus) in the Epidemiology of Leptospirosis in Domestic Animals and Humans in France. *European Journal of Epidemiology*, 17(2):111–121, 2001.

Deborah Middleton, Jackie Pallister, Reuben Klein, Yan-Ru Feng, Jessica Haining, Rachel Arkinstall, Leah Frazer, Jin-An Huang, Nigel Edwards, Mark Wareing, Martin Elhay, Zia Hashmi, John Bingham, Manabu Yamada, Dayna Johnson, John White, Adam Foord, Hans G Heine, Glenn a Marsh, Christopher C Broder, and Lin-Fa Wang. Hendra virus vaccine, a one health approach to protecting horse, human, and environmental health. *Emerging infectious diseases*, 20(3):372–9, mar 2014. ISSN 1080-6059. doi: 10.3201/eid2003.131159. URL http://www.pubmedcentral.nih.gov/articlerender.fcgi?artid=3944873{&}tool=pmcentrez{&}rendertype=abstract.

Barbara J Moloney. Overview of the epidemiology of equine influenza in the Australian outbreak. *Australian veterinary journal*, 89 Suppl 1(July):50–6, jul 2011. ISSN 1751-0813. doi: 10.1111/j.1751-0813.2011.00748.x. URL http://www.ncbi.nlm.nih.gov/pubmed/21711290.

Michael D Morecroft, Michele E Taylor, and Howard R Oliver. Air and soil microclimates of deciduous woodland compared to an open site. *Agricultural and Forest Meteorology*, 90(1-2):141–156, 1998. ISSN 01681923. doi: 10.1016/S0168-1923(97)00070-1.

Vincent J Munster, Joseph B Prescott, Trenton Bushmaker, Dan Long, Rebecca Rosenke, Tina Thomas, Dana Scott, Elizabeth R Fischer, Heinz Feldmann, and Emmy de Wit. Rapid Nipah virus entry into the central nervous system of hamsters via the olfactory route. *Scientific reports*, 2:736, jan 2012. ISSN 2045-2322. doi: 10.1038/srep00736. URL http://www.pubmedcentral.nih.gov/articlerender.fcgi?artid=3471094{&}tool=pmcentrez{&}rendertype=abstract.

G Alexander Murray and George A Jackson. Viral dynamics II: a model of the interaction of ultraviolet light and mixing processes on virus survival in seawater. *Marine Ecology Progress Series*, 102:105–114, 1993.

K Murray, P Selleck, P Hooper, a Hyatt, a Gould, L Gleeson, H Westbury, L Hiley, L Selvey, and B Rodwell. A morbillivirus that caused fatal disease in horses and humans. *Science (New York, N.Y.)*, 268(5207):94–7, apr 1995a. ISSN 0036-8075. URL http://www.ncbi.nlm.nih.gov/pubmed/7701348.

Keith Murray, Russell Rogers, Linda A Selvey, Paul Selleck, Alex Hyatt, Allan Gould, Laurie Gleeson, Peter Hooper, and Harvey Westbury. A Novel Morbillivirus Pneumonia of Horses and its Transmission to Humans. *Emerging infectious diseases*, 1(1):31–3n oubr, 1995b.

Kris A Murray and Lee F Skerratt. Predicting Wild Hosts for Amphibian Chytridiomycosis: Integrating Host Life-History Traits with Pathogen Environmental Requirements. *Human and Ecological Risk Assessment*, 18(1, SI):200–224, 2012. ISSN 1080-7039. doi: 10.1080/10807039.2012.632310.

Theodore a Myatt, Matthew H Kaufman, Joseph G Allen, David L MacIntosh, M Patricia Fabian, and James J McDevitt. Modeling the airborne survival of influenza virus in a residential setting: the impacts of home humidification. *Environmental health : a global access science source*, 9:55, jan 2010. ISSN 1476-069X. doi: 10.1186/1476-069X-9-55. URL http://www.pubmedcentral.nih.gov/articlerender.fcgi?artid=2940868{&}tool=pmcentrez{&}rendertype=abstract.

A Naujeck, Julian Hill, and Malcolm J Gibb. Influence of sward height on diet selection by horses. *Applied Animal Behaviour Science*, 90(1):49–63, 2005. ISSN 01681591. doi: 10.1016/j.applanim.2004.08.001.

F O Odberg and K Francis-Smith. A Study on Eliminative and Grazing Behaviour - The Use of the Field by Captive Horses. *Equine Veterinary Journal*, 8(4):147–149, 1976.

Richard S Ostfeld, Gregory E Glass, and Felicia Keesing. Spatial epidemiology: an emerging (or re-emerging) discipline. *Trends in ecology & evolution*, 20(6):328–36, jun 2005. ISSN 0169-5347. doi: 10.1016/j.tree.2005.03.009. URL http://www.ncbi.nlm.nih.gov/pubmed/16701389.

Hannah L Owens, Lindsay P Campbell, L Lynnette Dornak, Erin E Saupe, Narayani Barve, Jorge Soberón, Kate Ingenloff, Andrés Lira-Noriega, Christopher M Hensz, Corinne E Myers, and A Townsend Peterson. Constraints on interpretation of ecological niche models by limited environmental ranges on calibration areas. *Ecological Modelling*, 263:10–18, aug 2013. ISSN 03043800. doi: 10.1016/j.ecolmodel.2013.04.011. URL http://linkinghub.elsevier.com/retrieve/pii/S0304380013002159.

Carol Palmer, Owen Price, and Christine Bach. Foraging ecology of the black flying fox (Pteropus alecto) in the seasonal tropics of the Northern Territory, Australia. *Wildlife Research*, 27:169–178, 2000.

J G Parsons, J VanDerWal, S K a Robson, and L a Shilton. The Implications of Sympatry in the Spectacled and Grey Headed Flying-Fox, Pteropus conspicillatus and P. poliocephalus (Chiroptera: Pteropodidae). *Acta Chiropterologica*, 12 (2):301–309, dec 2010. ISSN 1508-1109. doi: 10.3161/150811010X537882. URL http://www.bioone.org/doi/abs/10.3161/150811010X537882.

Mercedes Pascual and Andy Dobson. Seasonal patterns of infectious diseases. *PLoS medicine*, 2(1):e5, jan 2005. ISSN 1549-1676. doi: 10.1371/journal.pmed.0020005. URL http://www.pubmedcentral.nih.gov/articlerender.fcgi?artid=545198{&}tool=pmcentrez{&}rendertype=abstract.

David L Paterson, P Keith Murray, and Joseph G McCormack. Zoonotic disease in Australia caused by a novel member of the paramyxoviridae. *Clinical infectious diseases*, 27(1):112–8, jul 1998. ISSN 1058-4838. URL http://www.ncbi.nlm.nih.gov/pubmed/9675464.

T A Patterson, L Thomas, C Wilcox, O Ovaskainen, and J Matthiopoulos. State-space models of individual animal movement. *Trends in ecology & evolution*, 23(2):87–94, feb 2008. ISSN 0169-5347. doi: 10.1016/j.tree.2007.10.009. URL http://www.ncbi.nlm.nih.gov/pubmed/18191283.

Peter B Pearman, Antoine Guisan, Olivier Broennimann, and Christophe F Randin. Niche dynamics in space and time. *Trends in ecology & evolution*, 23(3):149–58, mar 2008. ISSN 0169-5347. doi: 10.1016/j.tree.2007.11.005. URL http://www.ncbi.nlm.nih.gov/pubmed/18289716.

Richard G. Pearson, Christopher J. Raxworthy, Miguel Nakamura, and A. Townsend Peterson. Predicting species distributions from small numbers of occurrence records: a test case using cryptic geckos in Madagascar. *Journal of Biogeography*, 34 (1):102–117, sep 2006. ISSN 03050270. doi: 10.1111/j.1365-2699.2006.01594.x.

Alison J Peel, Juliet R C Pulliam, Angie D Luis, Raina K Plowright, Thomas J O'Shea, David T S Hayman, James L N Wood, Colleen T Webb, and Olivier Restif. The effect of seasonal birth pulses on pathogen persistence in wild mammal populations The effect of seasonal birth pulses on pathogen persistence in wild mammal populations. *Proceedings of The Royal Society Biological Sciences*, 281:1–9, 2014. ISSN 1471-2954. doi: 10.1098/rspb.2013.2962.

Alison J Peel, Hume E Field, Peter A Reid, Bvsc Hons, K Plowright, C Broder, Lee F Skerratt, David T S Hayman, Dip Eczm, Olivier Restif, Melanie Taylor, Gerardo Martin, Gary Crameri, Ina Smith, Basc Hons, Michelle Baker, A Marsh, Basc Hons, Jennifer Barr, Andrew C Breed, James L N Wood, Jenny-ann Toribio, Med Higher Education, Population Health, Ian Fulton, Facvsc Specialist, and Cristy Secombe. The equine Hendra virus vaccine remains a highly effective preventative measure against infection in horses and humans: 'The imperative to develop a human vaccine for the Hendra virus in Australia'. *Infection Ecology and Epidemiology*, 1:4–6, 2016. ISSN 2000-8686.

M Peleg, M D Normand, and M G Corradini. Generating microbial survival curves during thermal processing in real time. *Journal of applied microbiology*, 98(2): 406–17, jan 2005. ISSN 1364-5072. doi: 10.1111/j.1365-2672.2004.02487.x. URL http://www.ncbi.nlm.nih.gov/pubmed/15659195.

Micha Peleg. Evaluation of the Fermi equation as a model of dose-response curves. *Applied Microbiology and Biotechnology*, 46(3):303–306, oct 1996. ISSN 0175-7598. doi: 10.1007/s002530050821. URL http://www.springerlink.com/openurl.asp?genre=article{&}id=doi:10.1007/s002530050821.

Micha Peleg and Martin B Cole. Reinterpretation of Microbial Survival Curves. *Critical Reviews in Food Science and Nutrition*, 38(5):37–41, 1998. doi: http://dx.doi.org/10.1080/10408699891274246.

A Townsend Peterson. Ecologic niche modeling and spatial patterns of disease transmission. *Emerging infectious diseases*, 12(12):1822–6, dec 2006. ISSN 1080-6040. doi: 10.3201/eid1212.060373. URL http://www.pubmedcentral.nih.gov/articlerender.fcgi?artid=3291346{&}tool=pmcentrez{&}rendertype=abstract.

A Townsend Peterson. Ecological niche modelling and understanding the geography of disease transmission. *Veterinaria italiana*, 43(3):393–400, 2007. ISSN 1828-1427. URL http://www.ncbi.nlm.nih.gov/pubmed/20422515.

A Townsend Peterson. Mapping Risk of Nipah Virus Transmission Across Asia and Across Bangladesh. *Asia-Pacific journal of public health*, jan 2013. ISSN 1941-2479. doi: 10.1177/1010539512471965. URL http://www.ncbi.nlm.nih.gov/pubmed/23343646.

A Townsend Peterson, John T Bauer, and James N Mills. Ecologic and geographic distribution of filovirus disease. *Emerging infectious diseases*, 10 (1):40–7, jan 2004. ISSN 1080-6040. doi: 10.3201/eid1001.030125. URL http://www.pubmedcentral.nih.gov/articlerender.fcgi?artid=3322747{&}tool=pmcentrez{&}rendertype=abstract.

A Townsend Peterson, Monica Papes, and Jorge Soberon. Rethinking receiver operating characteristic analysis applications in ecological niche modeling. *Ecological Modelling*, 213(1):63–72, apr 2008. ISSN 03043800. doi: 10.1016/j.ecolmodel.2007.11.008. URL http://linkinghub.elsevier.com/retrieve/pii/S0304380007006163.

Steven J Phillips, Robert P Anderson, and Robert E Schapire. Maximum entropy modeling of species geographic distributions. *Ecological Modelling*, 190(3-4):231–259, jan 2006. ISSN 03043800. doi: 10.1016/j.ecolmodel.2005.03.026. URL http://linkinghub.elsevier.com/retrieve/pii/S030438000500267X.

David M Pigott, Nick Golding, Adrian Mylne, Zhi Huang, Andrew J Henry, Daniel J Weiss, Oliver J Brady, Moritz U G Kraemer, David L Smith, Catherine L Moyes, Samir Bhatt, Peter W Gething, Peter W Horby, Isaac I Bogoch, John S Brownstein, Sumiko R Mekaru, Andrew J Tatem, Kamran Khan, and Simon I Hay. Mapping the zoonotic niche of Ebola virus disease in Africa. *eLife*, 2013(December 2013): 1–29, 2014. ISSN 2050-084X. doi: 10.7554/eLife.04395.

David M Pigott, Nick Golding, Aadrian Mylne, Zhi Huang, Daniel J Weiss, Oliver J Brady, Moritz U G Kraemer, and Simon I Hay. Mapping the zoonotic niche of Marburg virus disease in Africa. *Transactions of the Royal Society of Tropical Medicine and Hygiene*, pages 1–13, 2015. ISSN 0035-9203. doi: 10.1093/trstmh/trv024. URL http://trstmh.oxfordjournals.org/cgi/doi/10.1093/trstmh/trv024.

Raina K Plowright, Hume E Field, Craig Smith, Anja Divljan, Carol Palmer, Gary Tabor, Peter Daszak, and Janet E Foley. Reproduction and nutritional stress are risk factors for Hendra virus infection in little red flying foxes (Pteropus scapulatus). *Proceedings. Biological sciences / The Royal Society*, 275 (1636):861–9, apr 2008. ISSN 0962-8452. doi: 10.1098/rspb.2007.1260. URL http://www.pubmedcentral.nih.gov/articlerender.fcgi?artid=2596896{&}tool=pmcentrez{&}rendertype=abstract.

Raina K Plowright, Patrick Foley, Hume E Field, Andy P Dobson, Janet E Foley, Peggy Eby, and Peter Daszak. Urban habituation, ecological connectivity and epidemic dampening: the emergence of Hendra virus from flying foxes (Pteropus spp.). *Proceedings. Biological sciences / The Royal Society*, may 2011. ISSN 1471-2954. doi: 10.1098/rspb.2011.0522. URL http://www.ncbi.nlm.nih.gov/pubmed/21561971.

Raina K Plowright, Peggy Eby, Peter J Hudson, Ina Smith, David Westcott, Wayne Bryden, Deborah J Middleton, Peter Reid, Rosemary McFarlane, Gerardo Martin, Gary Tabor, Lee F Skerratt, Dale Anderson, Gary Cramery, David Quammen, David

Jordan, Paul Freeman, Wang Lin-Fa, Jonathan H Epstein, Glenn Marsh, Nina Kung, and Hamish McCallum. Ecological dynamics of emerging bat virus spillover. *Proceedings B.*, 282, 2015.

Raina K Plowright, Alison J Peel, Daniel G Streicker, Amy Gilbert, Hamish McCallum, James Wood, Michelle L. Baker, and Olivier Restif. Transmission or within-host dynamics driving pulses of zoonotic viruses in reservoir-host populations. *PLoS neglected tropical diseases*, pages 1–21, 2016. ISSN 1935-2735. doi: 10.1371/journal.pntd.0004796.

Mateusz M Plucisnki, Timothee Guilavogui, Sidibe Sidikiba, Nouman Diakite, Souleymane Diakite, Mohamed Dioubate, Ibrahima Bah, Ian Hennesse, Jessica K Butts, Eric Halsey, Peter McElrow, S Patrick Kachur, Jamila Aboulhad, Richard James, and Keita Moussa. Effect of the Ebola-virus-disease epidemic on malaria case management in Guinea, 2014: a cross-sectional survey of health facilities. *Lancet Infectious Diseases*, 15(9):1–18, 2015. ISSN 0036-8075. doi: 10.1016/B978-0-12-420118-7.00008-1.Dopamine.

Martyn Plummer. JAGS: A program for analysis of Bayesian graphical models using Gibbs sampling, 2003.

Alison G Power and Charles E Mitchell. Pathogen spillover in disease epidemics. *The American naturalist*, 164 Suppl(November 2004):S79–S89, 2004. ISSN 0003-0147. doi: 10.1086/424610.

R Core Team. R: A Language and Environment for Statistical Computing, 2016. URL https://www.r-project.org/.

R-Development-Team. R: A language and environment for statistical computing, 2014.

Niels Raes and Hans Ter Steege. A null-model for significance testing of presence-only species distribution models. *Ecography*, 30(5):727–736, 2007. ISSN 09067590. doi: 10.1111/j.2007.0906-7590.05041.x.

Ian W Renner and David I Warton. Equivalence of MAXENT and Poisson point process models for species distribution modeling in ecology. *Biometrics*, 69(1):274–81, mar 2013. ISSN 1541-0420. doi: 10.1111/j.1541-0420.2012.01824.x. URL http://www.ncbi.nlm.nih.gov/pubmed/23379623.

Ian W Renner, Jane Elith, Adrian Baddeley, William Fithian, Trevor Hastie, Steven J Phillips, Gordana Popovic, and David I Warton. Point process models for presence-only analysis. *Methods in Ecology and Evolution*, 6:366–379, 2015. ISSN 2041210X. doi: 10.1111/2041-210X.12352.

Olivier Restif, David T S Hayman, Juliet R C Pulliam, Raina K Plowright, Dylan B George, Angela D Luis, Andrew a Cunningham, Richard a Bowen, Anthony R Fooks, Thomas J O'Shea, James L N Wood, and Colleen T Webb. Model-guided fieldwork: practical guidelines for multidisciplinary research on wildlife ecological and epidemiological dynamics. *Ecology letters*, 15(10):1083–94, oct 2012. ISSN 1461-0248. doi: 10.1111/j.1461-0248.2012.01836.x. URL http://www.pubmedcentral.nih.gov/articlerender.fcgi?artid=3466409{&}tool=pmcentrez{&}rendertype=abstract.

G C Richards. The spectacled flying-fox, Pteropus conspicillatus (Chiroptera: Pteropodidae), in north Queensland. 2. Diet, seed dispersal and feeding ecology. *Journal of Australian Mammalogy*, 13:25–31, 1990.

Greg Ridgeway. Generalized boosted regression models, 2013. URL http://www.ipensieri.com/gregr/gbm.shtml.

Billie J Roberts, Carla P Catterall, Peggy Eby, and John Kanowski. Latitudinal range shifts in Australian flying-foxes: A re-evaluation. *Austral Ecology*, 37(1):12–22, feb 2012. ISSN 14429985. doi: 10.1111/j.1442-9993.2011.02243.x. URL http://doi.wiley.com/10.1111/j.1442-9993.2011.02243.x.

Jodie J L Rowley and Ross A Alford. Behaviour of Australian rainforest stream frogs may affect the transmission of chytridiomycosis. *Diseases of Aquatic Organisms*, 77(1):1–9, 2007. ISSN 01775103. doi: 10.3354/dao01830.

Osvaldo E Sala, F Stuart Chapin III, Juan J Armesto, Eric Berlow, Janine Bloomfield, Rodolfo Dirzo, Elisabeth Huber-Sanwald, Laura F Huenneke, Robert B Jackson, Ann Kinzig, Rik Leemans, David M Lodge, Harold A Mooney, Martın Oesterheld, N LeRoy Poff, Martin T Sykes, Brian H Walker, Marilyn Walker, and Diana H Wall. Global Biodiversity Scenarios for the Year 2100. *Science*, 287(5459):1770–1774, 2009. ISSN 00368075. doi: 10.1126/science.287.5459.1770.

Joe C Scanlan, Nina Kung, Paul Selleck, and Hume Field. Survival of Hendra Virus in the Environment: Modelling the Effect of Temperature. *EcoHealth*, mar 2014. ISSN 1612-9210. doi: 10.1007/s10393-014-0920-4. URL http://www.ncbi.nlm.nih.gov/pubmed/24643861.

Joe C Scanlan, Nina Kung, Paul Selleck, and Hume Field. The Effect of Environmental Temperature on Hendra Virus Survival. *EcoHealth*, 12(2014):10393, 2015. ISSN 1612-9202. doi: 10.1007/s10393-015-1044-1. URL http://link.springer.com/10.1007/s10393-015-1044-1.

Linda Selvey, Roscoe Taylor, Antony Arklay, and John Gerrard. Screening of Bat Carers for Antibodies To Equine Morbillivirus. *Communicable Disease Intelligence*, 20(22):477–478, 1996.

Jeffrey Shaman and Melvin Kohn. Absolute humidity modulates influenza survival, transmission, and seasonality. *Proceedings of the National Academy of Sciences of the United States of America*, 106(9):3243–3248, 2009. ISSN 0027-8424. doi: 10.1073/pnas.0806852106.

Jeffrey Shaman, Virginia E. Pitzer, Cécile Viboud, Bryan T. Grenfell, and Marc Lipsitch. Absolute Humidity and the Seasonal Onset of Influenza in the Continental United States. *PLoS Biology*, 8(2):e1000316, 2010. ISSN 1545-7885. doi: 10.1371/journal.pbio.1000316. URL http://dx.plos.org/10.1371/journal.pbio.1000316.

Craig Smith, Chris Skelly, Nina Kung, Billie Roberts, and Hume Field. Flying-fox species density - a spatial risk factor for hendra virus infection in horses in eastern australia. *PloS one*, 9(6):e99965, jan 2014. ISSN 1932-6203. doi: 10.1371/journal.pone.0099965. URL http://www.pubmedcentral.nih.gov/articlerender.fcgi?artid=4061024{&}tool=pmcentrez{&}rendertype=abstract.

Craig S. Smith, A. McLaughlin, Hume E. Field, Daniel Edson, D. Mayer, S. Ossedryver, Janine Barrett, and D. Waltisbuhl. Twenty years of Hendra virus: laboratory submission trends and risk factors for infection in horses. *Epidemiology and Infection*, (2016):1–8, 2016. ISSN 0950-2688. doi: 10.1017/S0950268816001400. URL http://www.journals.cambridge.org/abstract{_}S0950268816001400.

Jorge Soberon and Miguel Nakamura. Niches and distributional areas : Concepts , methods , and assumptions. *PNAS*, 106(2):19644–19650, 2009. URL http://www.pnas.org/content/106/suppl.2/19644.full.

Jorge Soberón and a Townsend Peterson. Interpretation of Models of Fundamental Ecological Niches and Species Distributional Areas. *Biodiversity Informatics*, 2:1–10, 2005. ISSN 15469735. doi: 10.1093/wber/lhm022.

Karline Soetaert, Thomas Petzoldt, and R Woodrow. Solving Differential Equations in R. *The R Journal*, 2(December):5–15, 2010.

David J Spiegelhalter, Nicola G Best, Bradley P Carlin, and Angelika van der Linde. Bayesian Measures of Model Complexity and Fit. *Journal of the Royal Society of Statistics*, 64(4):583–639, 2002.

David A Stainforth, Tolu Aina, Carl Christensen, Matthew Collins, N Faull, David J Frame, J A Kettleborough, Susie Knight, Andrew Martin, J M Murphy, Claudio Piani, D Sexton, Leonard A Smith, Robert A Spicer, A J Thorpe, and M R Allen. Uncertainty in predictions of the climate response to rising levels of greenhouse gases. *Nature*, 433(7024):403–6, 2005. ISSN 1476-4687. doi: 10.1038/nature03301. URL http://dx.doi.org/10.1038/nature03301.

D Stockwell and D Peters. The GARP modelling system : problems and solutions to automated spatial prediction. *International Journal of Geographical Information Science*, 13(2):143–158, 1999.

Benjamin Sultan, Karima Labadi, Jean-François Guégan, and Serge Janicot. Climate drives the meningitis epidemics onset in west Africa. *PLoS medicine*, 2 (1):e6, jan 2005. ISSN 1549-1676. doi: 10.1371/journal.pmed.0020006. URL http://www.pubmedcentral.nih.gov/articlerender.fcgi?artid=545199{&}tool=pmcentrez{&}rendertype=abstract.

Robert Swanepoel, Sheilagh B. Smit, Pierre E. Rollin, Pierre Formenty, Patricia a. Leman, Alan Kemp, Felicity J. Burt, Antoinette a. Grobbelaar, Janice Croft, Daniel G. Bausch, Hervé Zeller, Herwig Leirs, L. E O Braack, Modeste L. Libande, Sherif Zaki, Stuart T. Nichol, Thomas G. Ksiazek, and Janusz T. Paweska. Studies of reservoir hosts for Marburg virus. *Emerging Infectious Diseases*, 13(12):1847–1851, 2007. ISSN 10806040. doi: 10.3201/eid1312.071115.

Benjamin M Taylor, Barry S Rowlingson, Tilman M Davies, and Peter J Diggle. lgcp: an R Package for Inference with Spatial and Spatio-temporal Log-Gaussian Cox Processes. *Journal of Statistical Software*, 52(4), 2013. URL www.jstatsoft.org/.

Benjamin M Taylor, Barry S Rowlingson, Tilman M Davies, and Peter J Diggle. Bayesian Inference and Data Augmentation Schemes for Spatial, Spatiotemporal and Multivariate Log-Gaussian Cox Processes in R. *Journal of Statistical Software*, 35(11), 2015. ISSN 19390068. doi: 10.1359/JBMR.0301229.

Louise H Taylor, Sophia M Latham, Mark E J Woolhouse, Sophia M Lathamt, and Easter Bush. Risk factors for human disease emergence. *Philosophical Transactions: Biological Sciences*, 356(1411):983–989, 2001. ISSN 0962-8436. doi: 10.1098/rstb.2001.0888.

Maria L Taylor, Catalina B Chávez-Tapia, R Vargas-Yañez, Gabriela Rodríguez-Arellanes, Gabriela R Peña-Sandoval, Conchita Toriello, Amelia Pérez, and Maria del R Reyes-Montes. Environmental conditions favoring bat infection with Histoplasma capsulatum in Mexican shelters. *American Journal of Tropical Medicine and Hygiene*, 61(6):914–919, 1999. ISSN 00029637.

Wilfried Thuiller, B Araújo, Miguel, and Sandra Lavorel. Generalized models vs. classification tree analysis: predicting spatial distributions of plant species at different scales. *Journal of Vegetation Science*, 14(5):669–680, 2003. ISSN 11009233. doi: DOI10.1111/j.1654-1103.2003.tb02199.x.

Christopher R Tidemann, Michael J Vardon, Ronald a Loughland, and Peter J Brocklehurst. Dry season camps of flying-foxes (Pteropus spp.) in Kakadu World Heritage Area , north Australia. *Journal of Zoology*, 247(September 2000):155–163, 1999.

A. Townsend Peterson, B Araújo, Miguel, Miguel Nakamura, Robert P Anderson, Enrique Martinez-Meyer, and Jorge Soberon. *Ecological Niches and Geographic Distributions*. Princeton University Press, 2011. ISBN 9780691136882.

Martinus J S van Boekel. On the use of the Weibull model to describe thermal inactivation of microbial vegetative cells. *International journal of food microbiology*, 74 (1-2):139–59, mar 2002. ISSN 0168-1605. URL http://www.ncbi.nlm.nih.gov/pubmed/11930951.

Mariette van den Berg, Wendy Y. Brown, Caroline Lee, and Geoffrey N. Hinch. Browse-related behaviors of pastured horses in Australia: A survey. *Journal of Veterinary Behavior: Clinical Applications and Research*, 10(1):48–53, 2015. ISSN 15587878. doi: 10.1016/j.jveb.2014.11.001. URL http://dx.doi.org/10.1016/j.jveb.2014.11.001.

Detlef P. van Vuuren, Jae Edmonds, Mikiko Kainuma, Keywan Riahi, Allison Thomson, Kathy Hibbard, George C. Hurtt, Tom Kram, Volker Krey, Jean Francois Lamarque, Toshihiko Masui, Malte Meinshausen, Nebojsa Nakicenovic, Steven J. Smith, and Steven K. Rose. The representative concentration pathways: An overview. *Climatic Change*, 109(1):5–31, 2011. ISSN 01650009. doi: 10.1007/s10584-011-0148-z.

Jeremy VanDerWal, Luke P Shoo, Christopher N Johnson, and Stephen E Williams. Abundance and the environmental niche: environmental suitability estimated from niche models predicts the upper limit of local abundance. *The American naturalist*, 174(2):282–291, 2009. ISSN 0003-0147. doi: 10.1086/600087.

Michael J Vardon, Peter S Brocklehurst, John C Z Woinarski, Ross B Cunningham, Christine F Donnelly, and Christopher R Tidemann. Seasonal habitat use by flying-foxes , Pteropus alecto and P . scapulatus (Megachiroptera), in monsoonal Australia. *Journal of Zoology*, 253:523–535, 2001. ISSN 09528369. doi: 10.1017/S0952836901000486. URL http://doi.wiley.com/10.1017/S0952836901000486.

Samuel D. Veloz. Spatially autocorrelated sampling falsely inflates measures of accuracy for presence-only niche models. *Journal of Biogeography*, 36(12):2290–2299, 2009. ISSN 03050270. doi: 10.1111/j.1365-2699.2009.02174.x.

J H Wagenvoort and R J Penders. Long-term in-vitro survival of an epidemic MRSA phage-group III-29 strain. *The Journal of hospital infection*, 35(4):322–325, 1997.

Bruno A Walther and Paul W Ewald. Pathogen survival in the external environment and the evolution of virulence. *Biological Reviews*, 79(4):849–869, nov 2004. ISSN 1464-7931. doi: 10.1017/S1464793104006475. URL http://doi.wiley.com/10.1017/S1464793104006475.

Lin-fa Wang and Peter Daniels. Diagnosis of Henipavirus Infection: Current Capabilities and Future Directions. *Current Topics in Microbiology and Immunology*, 359, 2012. doi: 10.1007/82.

Lin-Fa Wang and Bryan T Eaton. Bats, civets and the emergence of SARS. In J E Childs, J S Mackenzie, and J A Richt, editors, *Wildlife and Emerging Zoonotic Diseases: The Biology, Circumstances and Consequences of Cross-Species Transmission*, volume 315, chapter 13, pages 325–344. Springer Verlag, 2007. ISBN 9783540709619. doi: 10.1007/978-3-540-70962-6_13.

M P Ward, PF Black, AJ Childs, FC Baldock, WR Webster, BJ Rodwell, and SL Brouwer. Negative findings from serological studies of equine morbillivuris in the Queensland horse population. *Australian Veterinary Journal*, pages 241 – 243, 1996. ISSN 0005-0423. doi: 10.1111/j.1751-0813.1996.tb15412.x.

Richard L Ward, Elmer W Akin, and Donn J D Alessio. Minimum infective dose of animal viruses. *Critical Reviews in Environmental Control*, 14(4):37–41, 1984. doi: http://dx.doi.org/10.1080/10643388409381721.

Helen J Wearing, Pejman Rohani, and Matt J Keeling. Appropriate models for the management of infectious diseases. *PLoS Medicine*, 2(7):0621–0627, 2005. ISSN 15491277. doi: 10.1371/journal.pmed.0020174.

Thomas P Weber and Nikolaos I Stilianakis. Inactivation of influenza A viruses in the environment and modes of transmission: a critical review. *The Journal of infection*, 57(5):361–73, nov 2008. ISSN 1532-2742. doi: 10.1016/j.jinf.2008.08.013. URL http://www.ncbi.nlm.nih.gov/pubmed/18848358.

Hana Weingartl, Stefanie Czub, John Copps, Yohannes Berhane, Deborah Middleton, Peter Marszal, Jason Gren, Greg Smith, Shelley Ganske, Lisa Manning, and Markus Czub. Invasion of the central nervous system in a porcine host by nipah virus. *Journal of virology*, 79(12):7528–34, jun 2005. ISSN 0022-538X. doi: 10.1128/JVI.79.12.7528-7534.2005. URL http://www.pubmedcentral.nih.gov/articlerender.fcgi?artid=1143674{&}tool=pmcentrez{&}rendertype=abstract.

Justin A Welbergen. Variation in twilight predicts the duration of the evening emergence of fruit bats from a mixed-species roost. *Animal Behaviour*, 75(4):1543–1550, apr 2008. ISSN 00033472. doi: 10.1016/j.anbehav.2007.10.007. URL http://linkinghub.elsevier.com/retrieve/pii/S0003347207005349.

Kathie Wickwire. Mathematical Models for the Control of Pests and Infectious Disease: A Survey. *Theoretical Population Biology*, 11:182–238, 1977.

Stephen E Williams, Elizabeth E Bolitho, and Samantha Fox. Climate change in Australian tropical rainforests: an impending environmental catastrophe. *Proceedings. Biological sciences / The Royal Society*, 270(1527): 1887–92, 2003. ISSN 0962-8452. doi: 10.1098/rspb.2003.2464. URL http://www.pubmedcentral.nih.gov/articlerender.fcgi?artid=1691452{&}tool=pmcentrez{&}rendertype=abstract.

Matthew M Williamson, Peter T Hooper, Paul W Selleck, Laurie J Gleeson, Peter W Daniels, Harvey A Westbury, and P Keith Murray. Transmission studies of Hendra virus (equine morbilli-virus) in fruit bats, horses and cats. *Australian Veterinary Journal*, 76(12):813–818, dec 1998. ISSN 0005-0423. doi: 10.1111/j.1751-0813.1998.tb12335.x. URL http://doi.wiley.com/10.1111/j.1751-0813.1998.tb12335.x.

Matthew M Williamson, Peter T Hooper, Paul W Selleck, Harvey A Westbury, and Ron F Slocombe. Experimental hendra virus infectionin pregnant guinea-pigs and fruit Bats (Pteropus poliocephalus). *Journal of comparative pathology*, 122 (2-3):201–7, 2000. ISSN 0021-9975. doi: 10.1053/jcpa.1999.0364. URL http://www.ncbi.nlm.nih.gov/pubmed/10684689.

Scott D Wilson and David Tilman. Component of Plant Competition Along an Experimental Gradient of Nitrogen Availability. *Ecology*, 72(3):1050–1065, 1991.

Mark E J Woolhouse and Sonya Gowtage-Sequeria. Host range and emerging and reemerging pathogens. *Emerging infectious diseases*, 11(12):1842–7, dec 2005. ISSN 1080-6040. doi: 10.3201/eid1112.050997. URL /pmc/articles/PMC3367654/?report=abstract.

P L Young, K Halpin, P W Selleck, H Field, J L Gravel, M a Kelly, and J S Mackenzie. Serologic evidence for the presence in Pteropus bats of a paramyxovirus related to equine morbillivirus. *Emerging infectious diseases*, 2(3):239–40, 1996. ISSN 1080-6040. doi: 10.3201/eid0203.960315. URL http://www.pubmedcentral.nih.gov/articlerender.fcgi?artid=2626799{&}tool=pmcentrez{&}rendertype=abstract.

Bilal A Zahoor and Lucy I Mudie. The imperative to develop a human vaccine for the Hendra virus in Australia. *Infection ecology & epidemiology*, 5: 29619, 2015. ISSN 2000-8686. URL http://www.ncbi.nlm.nih.gov/pubmed/26519254{%}5Cnhttp://www.pubmedcentral.nih.gov/articlerender.fcgi?artid=PMC4627939.

Yang Zhao, Andre J a Aarnink, Remco Dijkman, Teun Fabri, Mart C M de Jong, and Peter W G Groot Koerkamp. Effects of temperature, relative humidity, absolute humidity, and evaporation potential on survival of airborne Gumboro vaccine virus. *Applied and environmental microbiology*, 78(4): 1048–54, feb 2012. ISSN 1098-5336. doi: 10.1128/AEM.06477-11. URL http://www.pubmedcentral.nih.gov/articlerender.fcgi?artid=3273001{&}tool=pmcentrez{&}rendertype=abstract.

Appendix

HeV survival implicates transmission routes

Methods

The data used to fit the models is a series of two averaged virus titrations. Each titration was divided by the initial titer and the remaining model fitting was performed over the natural logarithm of the surviving proportion. Originally data contained 15, 14 and 8 measurements at 4, 22 and 56°C respectively. Due to heavy tailing with very few remaining particles in the final titrations we only used the first five measurements. The fitting procedure began with data for each temperature. We estimated parameters for the Weibull and exponential CDFs for each of the temperatures and then modelled parameter values as a response variable dependent on temperature. The resulting parameter models were substituted in both the Weibull and exponential models. Finally, we ran an additional optimization with a time-temperature coupled model (equations are below). We used normality, autocorrelation of residuals and the Akaike information criterion (AIC) to compare models. AIC's were compared with the Akaike weights test. The selected model was transformed to a differential equation. Then we generated the temperature profiles with the average minimum and maximum temperatures for each month. These profiles assume that minimum temperatures occur at 3 am and maximum at 3 pm (equations below). Simulations were run with the conditions of four locations comprising the latitudinal extremes of the spillover distribution, Cairns in far north Queensland, Kempsey in central New South Wales (southernmost part of the distribution), and Rockhampton and Redlands for the center and the hotspot of the distribution, respectively.

For spatial simulations we used a series of layers of ground temperature at zero cm depth and two shade levels, 0 and 50%, obtained from the microclim dataset (11). For each shade cover we accounted for the effect of the soil types available in microclim. The areas with the soil types of Australia were obtained from a categorical layer generated by the Australian Bureau of Agricultural and Resource Economics and Sciences (ABARES), from which we only distinguished the three types; soil, sand and rock. We extracted the areas with each soil type from their corresponding ground temperature layer and then merged them with its complementary layers. For simulations

we assumed that shade cover did not affect minimum temperatures as these occur in the night. Each pixel of the minimum and maximum temperature layers were used as the parameters of the oscillating temperature profiles. Then we ran a simulation for every pixel in the layer and the last value of each simulation was stored in another layer. We also performed these simulations with interpolated air temperature layers (provided by BOM) to measure survival 24 h after excretion. From the resulting simulated maps we extracted the value of the pixels corresponding to the location of every event by season. Then the values of all the pixels in summer, autumn, winter and spring maps were cross tabulated to run the partial ROC test with the Partial ROC tool allowing a 20% omission rate.

Equations

Weibull model and half-life:

$$S(t) = \exp(-(\rho t)^{\kappa}) \tag{4a}$$

$$t = \frac{(-\ln S)^{\frac{1}{\kappa}}}{\rho} \tag{4b}$$

Dependence of parameters on temperature:

$$\rho(T) = \exp(\alpha_{\rho} + \beta_{\rho} T) \tag{5a}$$

$$\kappa(T) = \alpha_{\kappa} + \exp(\beta_{\kappa} T) \tag{5b}$$

Oscillating temperature profiles:

$$T(t) = a + b \times \left(\frac{1 - \cos(\pi t)}{2}\right) \tag{6}$$

In equation 6, a is the minimum temperature at 3 am and b is the difference between the minimum and maximum temperature (assumed to occur periodically at the exact same time of the day 12 h later than the minimum).

Implicit form of the Weibull probability density function:

$$\frac{dS}{dt} = -\left[\rho\kappa(-\ln S)^{1-\frac{1}{\kappa}}\right] \times S \tag{7}$$

The main disadvantage of this form of the Weibull model is that is has no solution when $S = 1$ and $\kappa < 1$. When $\kappa > 1$ and $S = 1$ simulations result in no mortality. the problem can be fixed with $S = 0.9999$ (a value very close but $S \neq 1$).

Parameters and temperature were substituted in equation 7 for simulations.

Similarly, the exponential model was coupled with the same time dependent temperature and temperature dependent parameter.

$$\frac{dS}{dt} = -\rho S \tag{8}$$

For the exponential model the equation decribing the change of parameter ρ was:

$$\rho = \exp(\alpha_\rho + \beta_\rho T^2) \tag{9}$$

Figures

Difference between separate models and coupled for both the Weibull and exponential.

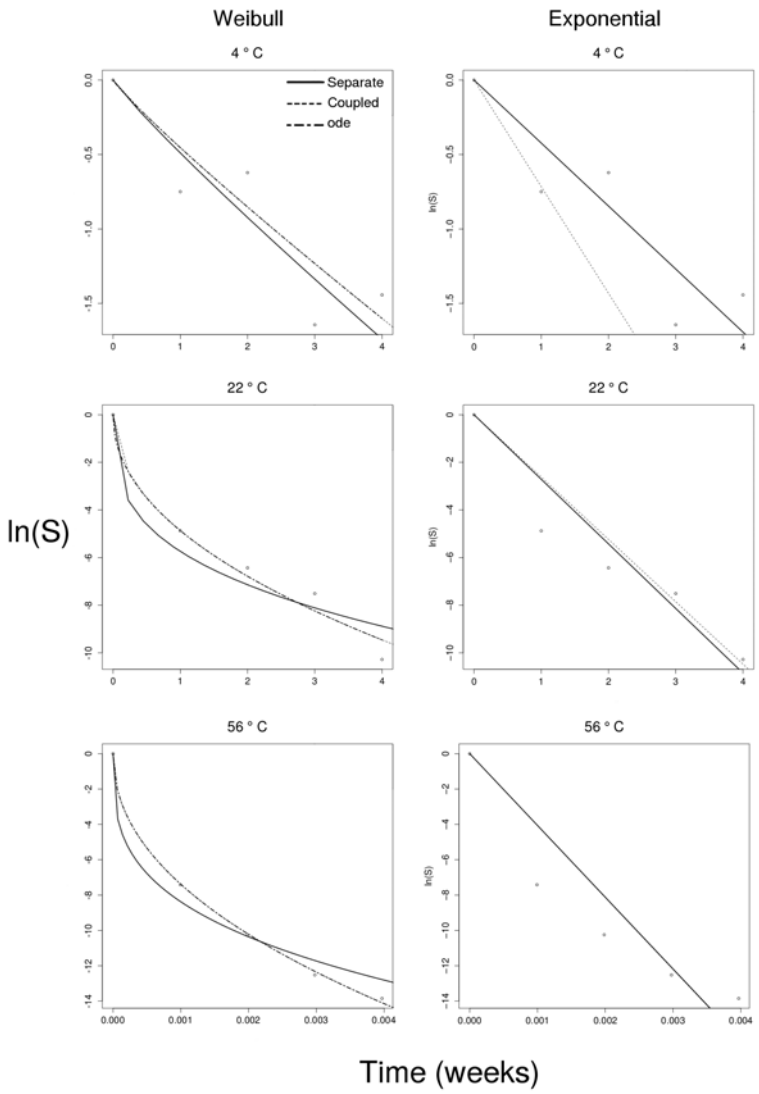

Figure 5: Difference between fitted models. The left hand side graphs correspond to the Weibull models: the separate Weibull model fitted to individual temperatures, the coupled version of the model and the simulated version of the numerically integrated ordinary differential equation form of the coupled model.

Maps of the simulated survival with the microclim data set:

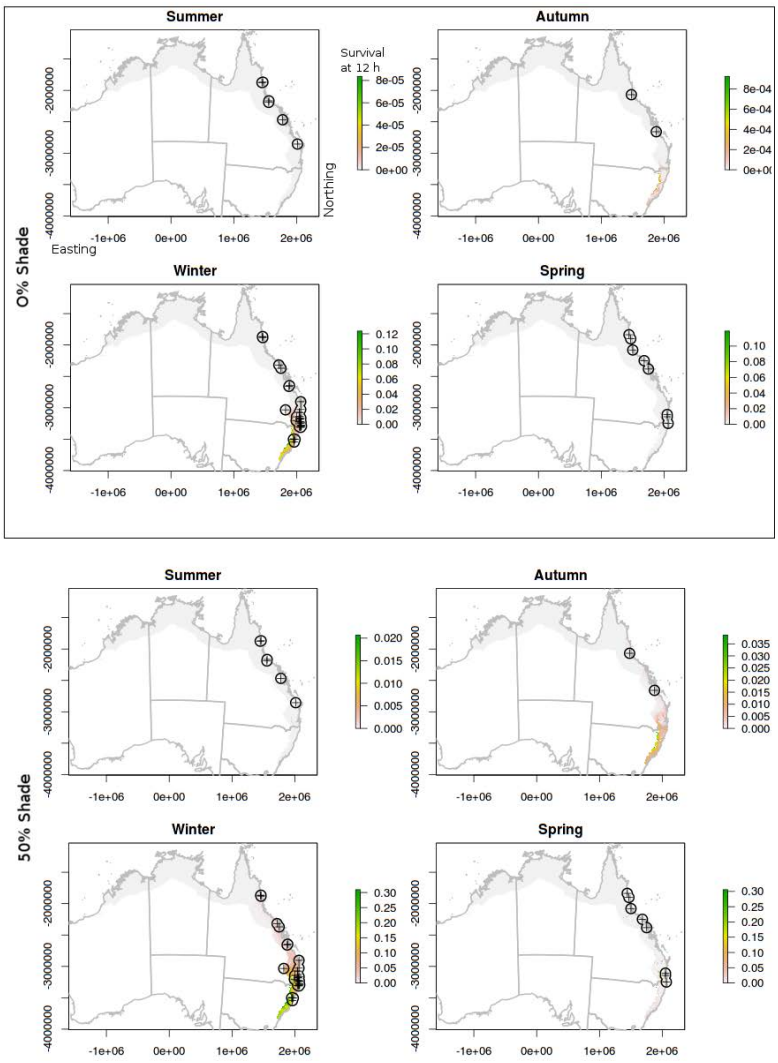

Figure 6: The top four maps correspond to survival at ground temperature with 0% shade. The bottom four maps are under 50% shade. The temperature layers for these simulations were projected to GDA 94 datum to suit the projection of the categorical layers of the soil types of Australia, hence the different geographical coordinates, degrees and decimals in the main manuscript versus meters in this figure. Survival is estimated 12h after excretion at the minimum temperature.

Density of survival and time to 2-log reduction in ground temperature of spillover events

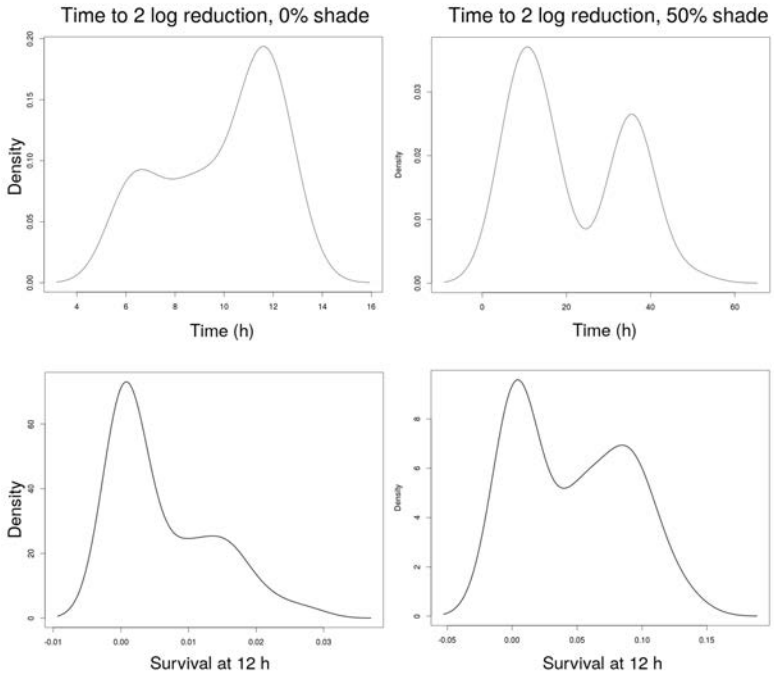

Figure 7: Kernel density estimation of time to a 2 log reduction in live virus in ground temperatures in 0% shade (left) and 50% shade (right). The bottom densities correspond to the proportion of virus surviving 12 h after excretion.

Microclimates might limit indirect spillover

Methods

Transforming the relative humidity data

Desiccation rates can be estimated with potential evaporation. Evaporation in turn can be calculated with relative humidity and temperature data. Absolute humidity is the mass of water per cubic metre of air (kg/m^3), and the difference between absolute humidity and absolute humidity at saturation is the potential for evaporation (McDevitt et al., 2010; Zhao et al., 2012). We used relative humidity and microhabitat temperatures to estimate the absolute humidity and evaporation potential based on the definition of relative (R_h) and absolute humidity (H_A):

$$R_h = \frac{p_w}{P^o} \tag{10}$$

where p_w is the pressure of water vapour, P^o is the water vapour pressure at saturation. And absolute humidity:

$$H_A = \frac{m_w}{V} = \frac{M_w \times p_w}{R \times T} = 0.00217 \times \frac{p_w}{T} \tag{11}$$

Where m_w is the mass of water vapour, V is volume, M_w molecular weight of water, R is the universal gas constant and T is temperature in °K. We solved equation 10 for p_w to substitute it for $R_h \times P^o$ in equation 11, which gives equation 12:

$$H_A = 0.00217 \times \frac{p_w}{T} = 0.00217 \times \frac{R_h \times P^o}{T} \tag{12}$$

Finally we only had to calculate P^o (McDevitt et al., 2010):

$$P^o = \exp\left(-\frac{5800}{T} - 0.04864 \times T + 4.17 \times 10^{-5} \times T^2 - 1.445 \times 10^{-8} T^3 + 5.546 \times \ln T\right) \tag{13}$$

Which is true only for a temperature range 0-200 ℃ (273-473 °K). Using the same relationship the maximum amount of water held per m^3 of air is (at 100% relative humidity):

$$H_{A_{max}} = 0.00217 \times \frac{100 \times P^0}{T} \tag{14}$$

Therefore, potential evaporation is $E_{pot} = H_{a_{max}} - H_A$.

These transformations change the statistical distribution of data, for which we decided to model potential evaporation for minimum humidity data, and absolute humidity for maximum humidity. Outputs of the absolute humidity model where then transformed to potential evaporation.

Results

Survival model

Table 1: Parameters of the survival model

Parameter	Meaning	Mean	2.5%	97.5%
α_ρ	Intercept of effect of Temperature on rate parameter	-3.911	-5.206	-2.518
β_ρ	Rate of effect of Temperature on rate parameter	0.120	0.095	0.144
α_κ	Intercept of effect of Temperature on shape parameter	-0.521	-0.983	-0.2
β_κ	Rate of effect of Temperature on shape parameter	-0.005	-0.01	0.004

Microclimate models

Table 2: Parameter posteriors for the minimum temperature model

Parameter	Variable	Mean	2.5%	97.5%
α	Intercept	3.802	3.193	4.416
β_1	Air minimum temperature	0.845	0.837	0.847
β_2	Grass	-0.012	-0.016	-0.009
β_3	Openness	-0.011	-0.013	-0.009
$\gamma_{property}$	Random effects for property			

Table 3: Parameter posteriors for the maximum temperature model

Parameter	Variable	Mean	2.5%	97.5%
α	Intercept	-3.112	-7.140	0.889
β_1	Air maximum temperature	0.869	0.829	0.909
β_2	Grass	0.1	0.083	0.118
β_3	Openness	0.196	0.171	0.219
β_4	Hours of sunshine	0.323	0.224	0.421
β_5	Interaction between sunshine and openness	0.01	0.008	0.012
β_6	Interaction between grass and openness	-0.005	-0.006	-0.005
$\gamma_{property}$	Random effects for property			

Table 4: Parameter posteriors for the Absolute maximum humidity model (calculated from relative humidity at minimum temperature).

Parameter	Variable	Mean	2.5%	97.5%
α	Intercept	0.127	0.1	0.156
β_1	Air absolute maximum humidity	0.937	0.959	0.987
β_2	Grass	0.001	0.001	0.001
β_3	Openness	0.0	0.0	0.0
β_4	interaction between grass and air maximum asbolute humidity	-0.002	-0.003	-0.001
$\gamma_{property}$	Random effects for property			

Table 5: Parameter posteriors for the Evaporation potential model (calculated from relative humidity at maximum temperature).

Parameter	Variable	Mean	2.5%	97.5%
α	Intercept	0.760	0.652	0.870
β_1	Soil maximum temperature	0.0	0.0	0.0
β_2	Air potential evaporation at minimum humidity	-0.027	-0.03	-0.024
β_3	Air maximum temperature	-0.032	-0.034	-0.031
β_4	Interaction between hours of sunshine and openness	0.001	0.001	0.001
β_5	Interaction between grass and air potential evaporation at minimum humidity	0.0	0.0	0.0
$\gamma_{property}$	Random effects for property			

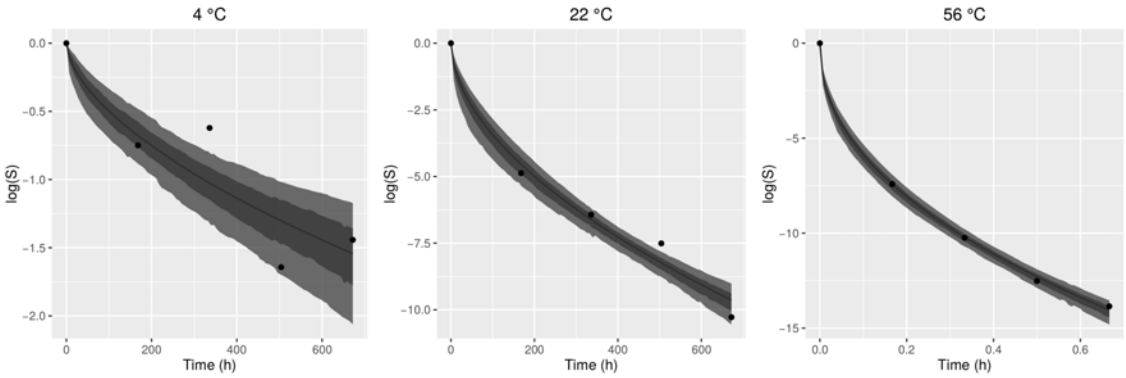

Figure 8: Hendra virus decay at the experimental temperatures

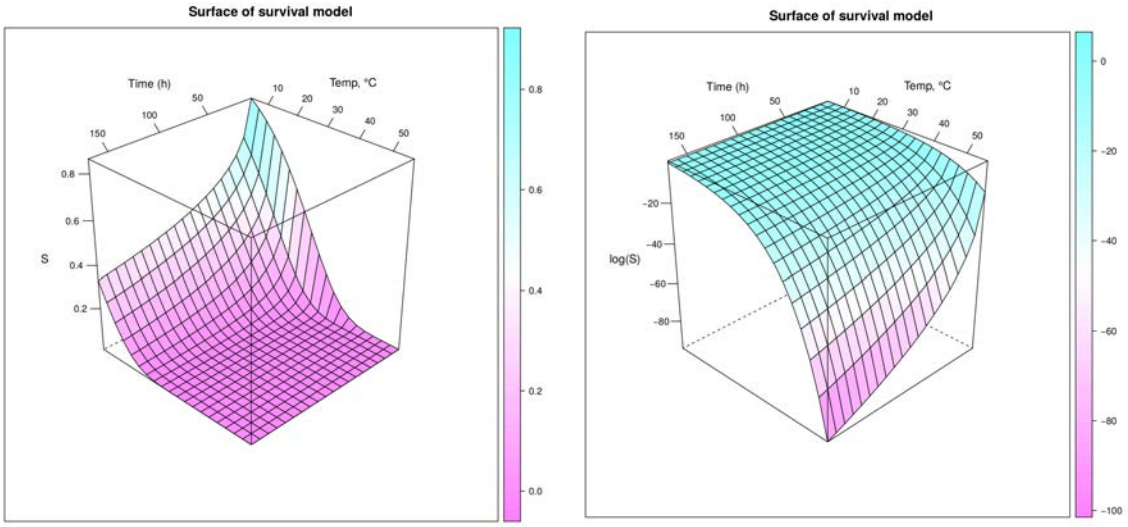

Figure 9: Model surface on linear (left) and logarithmic scales (right).

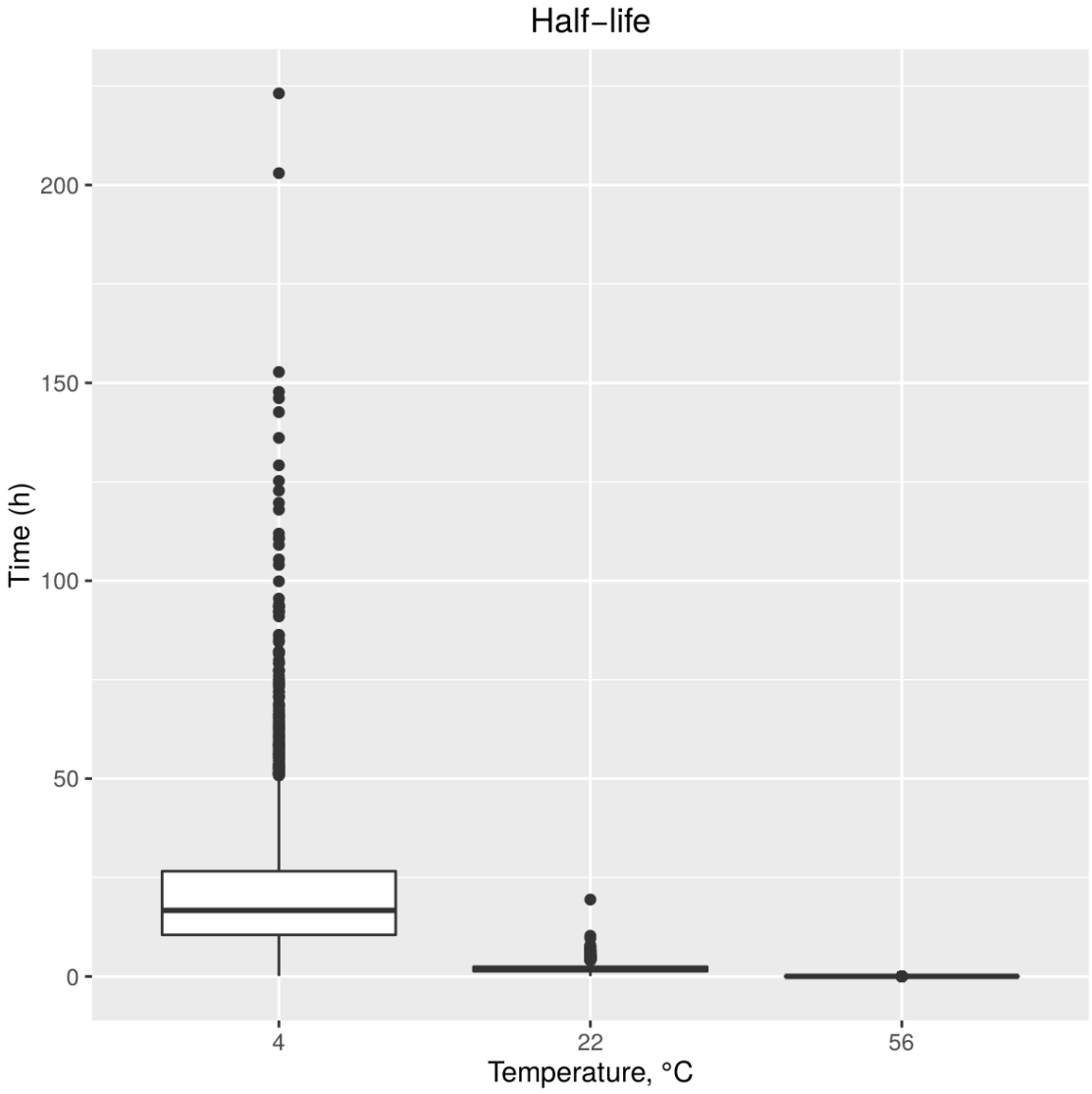

Figure 10: Fitted half-lives.

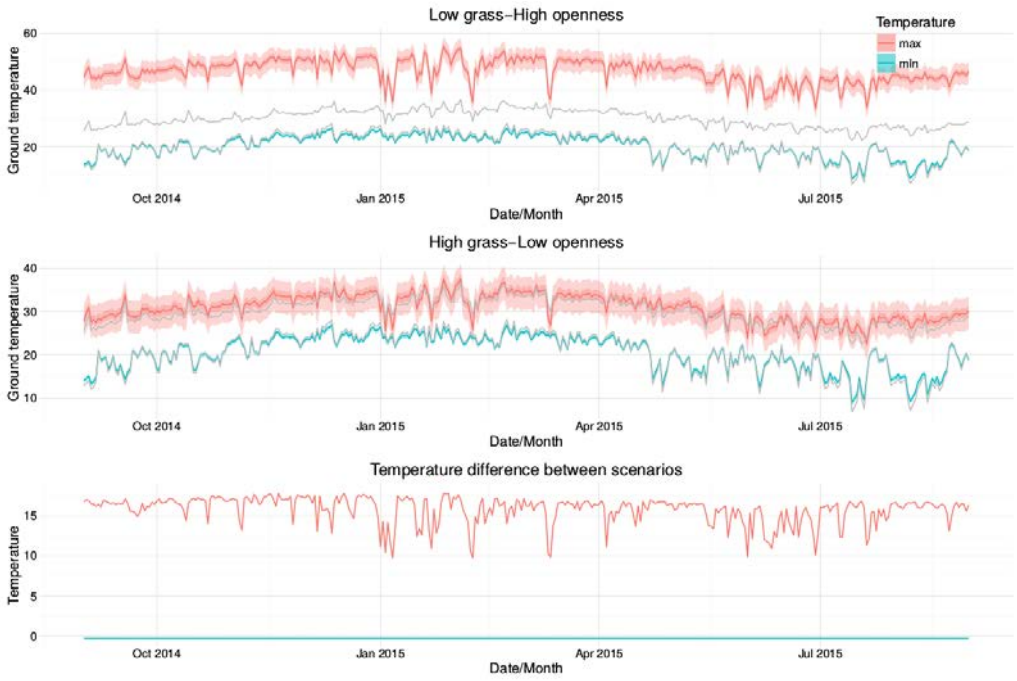

Figure 11: Predicted temperatures for Townsville.

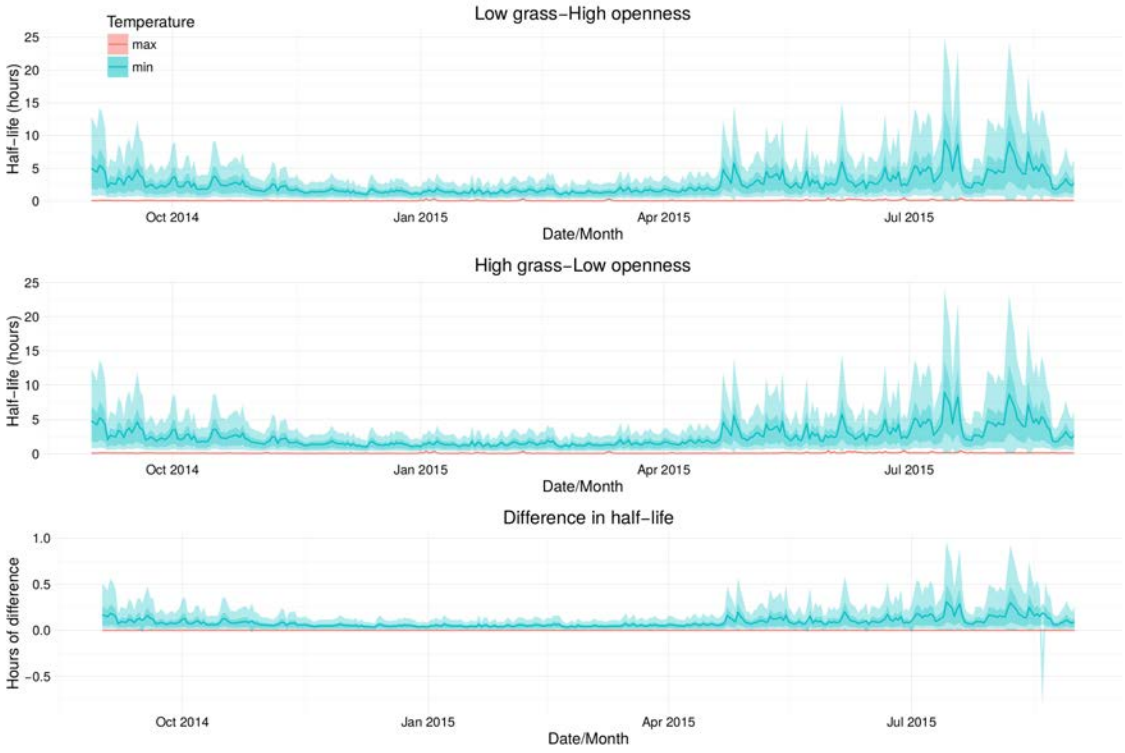

Figure 12: Hendra virus half life at the predicted minimum and maximum temperatures for Townsville.

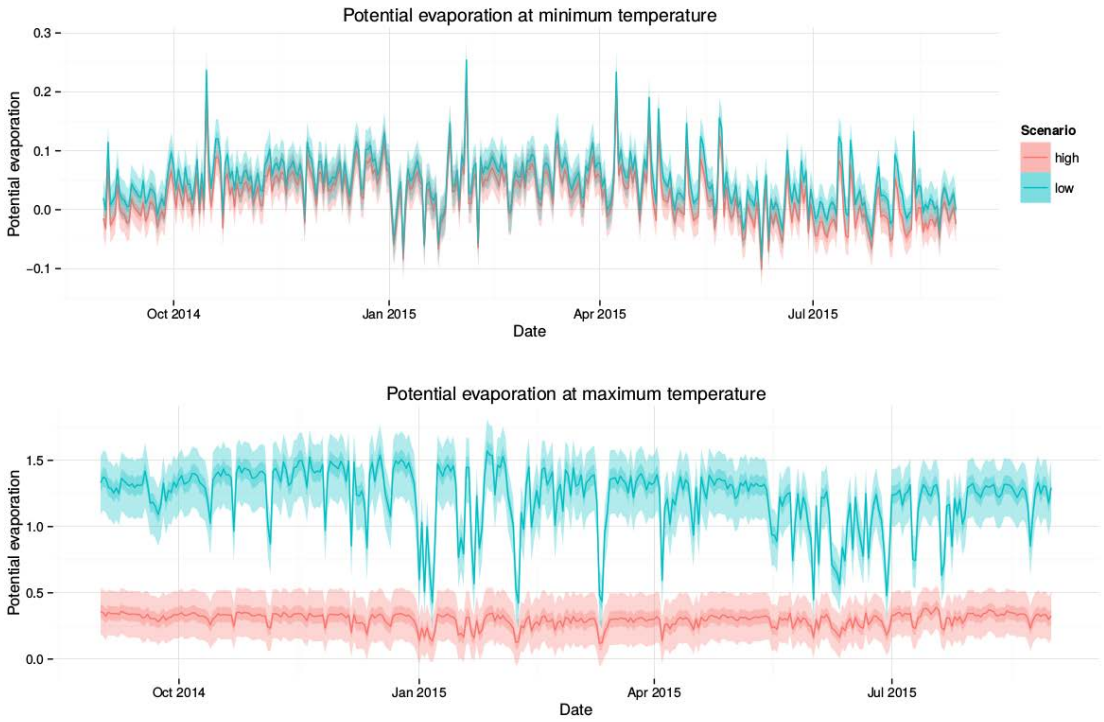

Figure 13: Predicted potential evaporation for Townsville

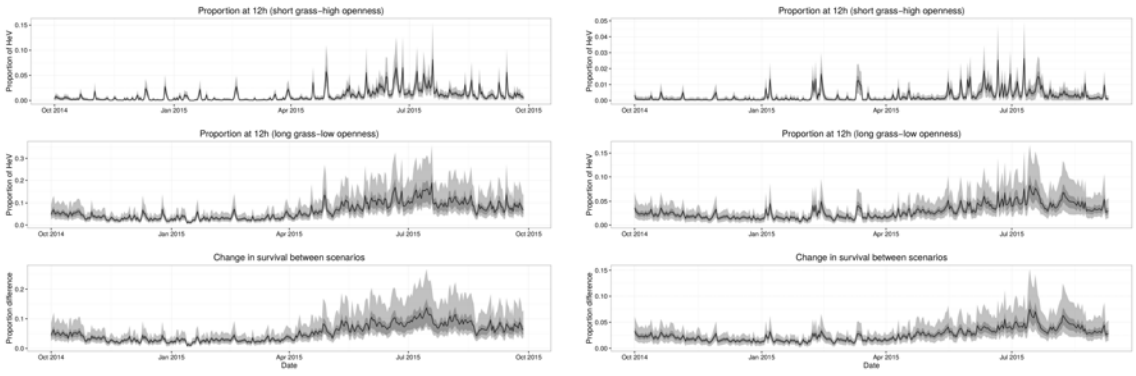

Figure 14: Timeline of HeV survival 12h after excretion in Brisbane (left) and Cairns (right).

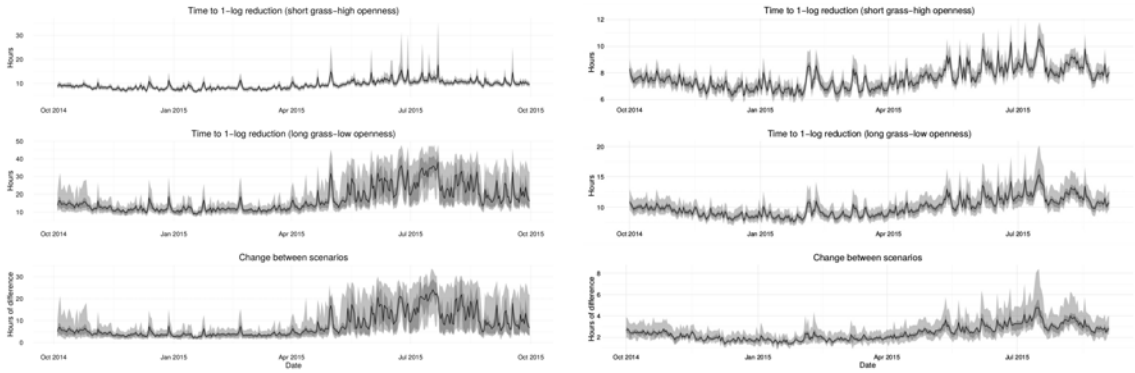

Figure 15: Timeline of time elapsed until death of 90% of excreted HeV in Brisbane (left) and Cairns (right).

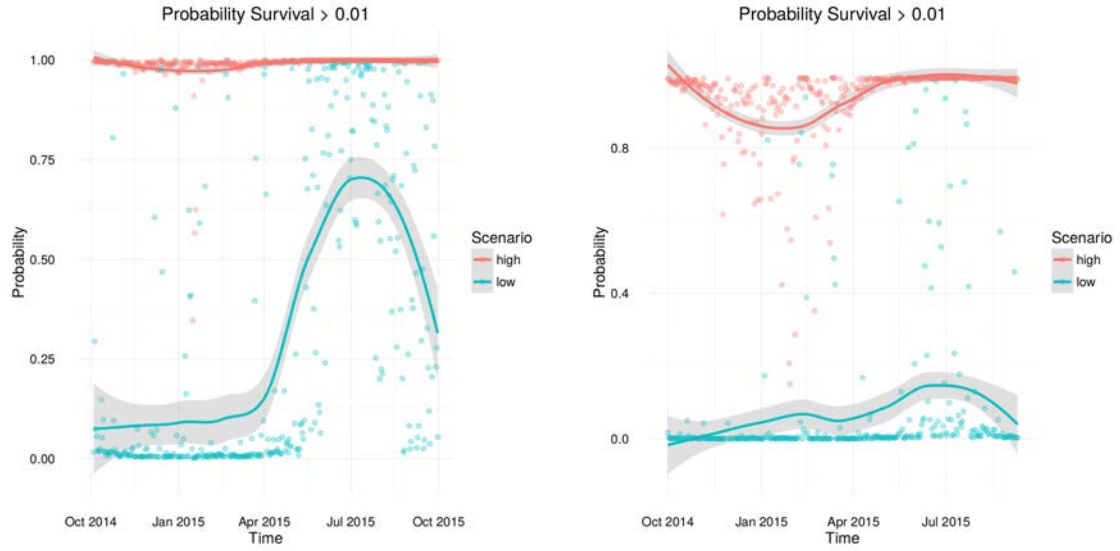

Figure 16: Timeline of probability that HeV survives more than 24 h after excretion Brisbane (left) and Cairns (right).

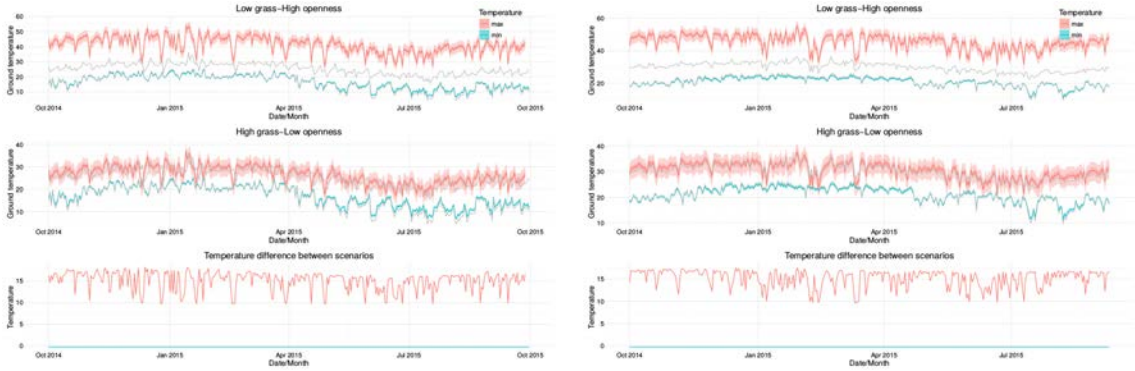

Figure 17: Predicted microclimate temperatures in Brisbane (left) and Cairns (right).

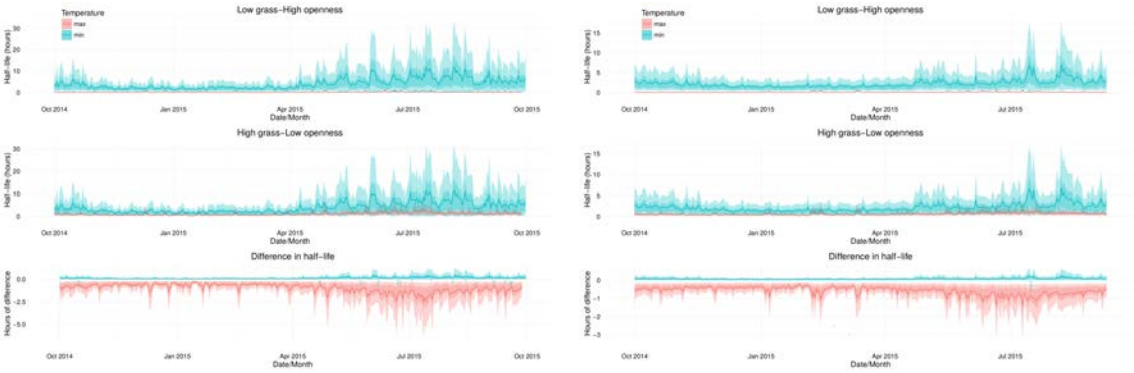

Figure 18: Timeline HeV half-life in microclimate temperatures in Brisbane (left) and Cairns (right).

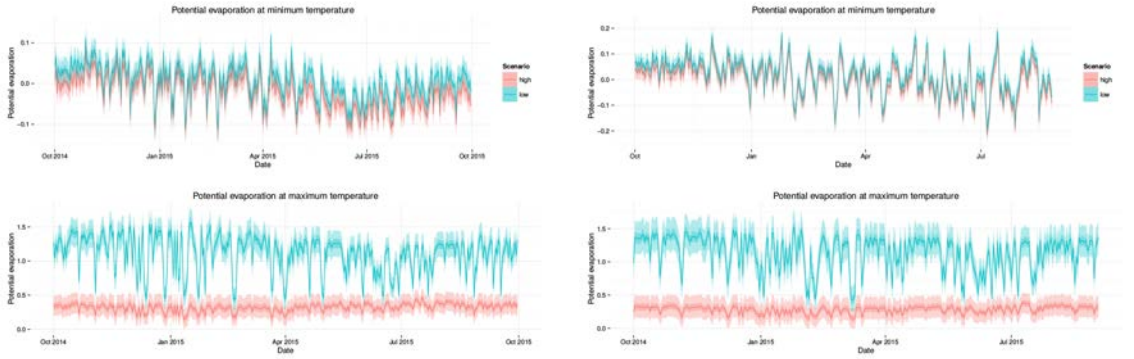

Figure 19: Timeline of predicted potential microclimate evaporation in Brisbane (left) and Cairns (right).

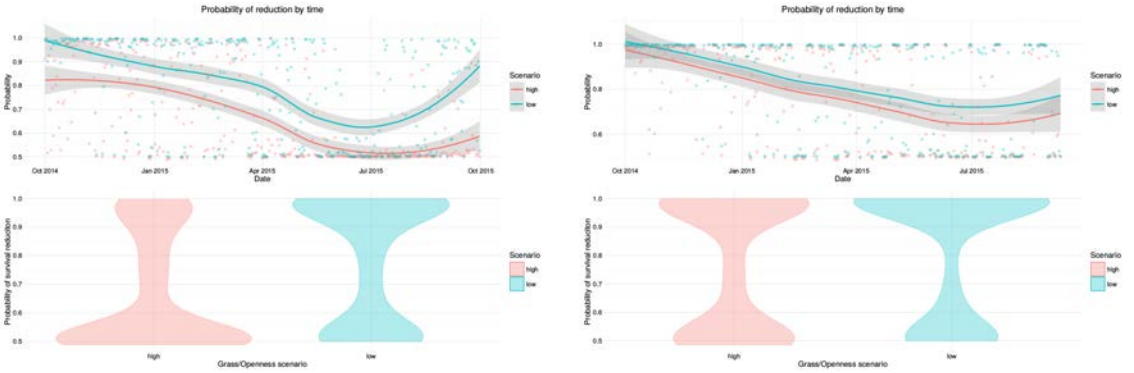

Figure 20: Probability of evaporation occurence in microclimates in Brisbane (left) and Cairns (right).

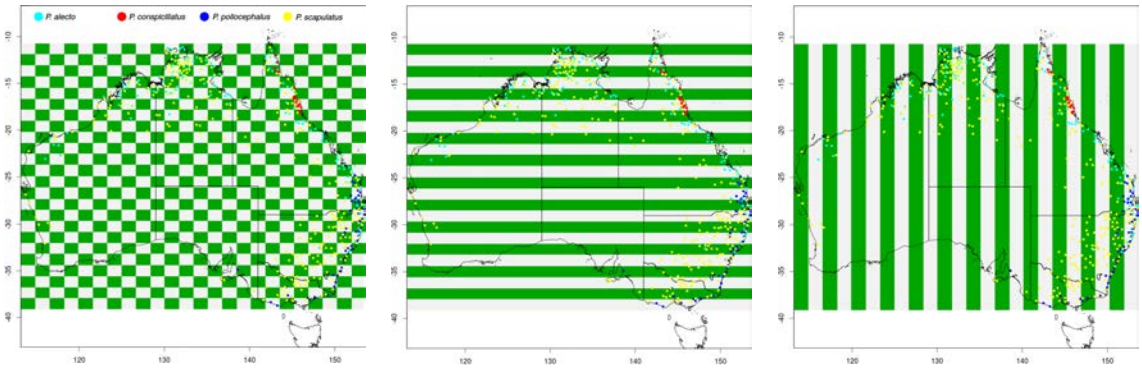

Figure 21: Spatial patterns used to select training and testing data. Colour points represent the four FF species presence points used to train models after filtering to reduce spatial autocorrelation.

Table 6: Variables selected to model each bat species

Variable	Meaning	*P. alecto*	*P. conspicillatus*	*P. poliocephalus*	*P. scapulatus*
bio1	Annual Mean Temperature	✓		✓	
bio2	Mean Diurnal Temperature Range	✓	✓	✓	✓
bio3	Isothermality (BIO2/BIO7) (* 100)			✓	
bio4	Temperature Seasonality (standard deviation *100)		✓		
bio5	Max Temperature of Warmest Month			✓	✓
bio6	Min Temperature of Coldest Month			✓	
bio7	Temperature Annual Range (BIO5-BIO6)	✓	✓		
bio8	Mean Temperature of Wettest Quarter			✓	✓
bio9	Mean Temperature of Driest Quarter				✓
bio10	Mean Temperature of Warmest Quarter				
bio11	Mean Temperature of Coldest Quarter				
bio12	Annual Precipitation	✓			✓
bio13	Precipitation of Wettest Month		✓		
bio14	Precipitation of Driest Month	✓			
bio15	Precipitation Seasonality (Coefficient of Variation)				✓
bio16	Precipitation of Wettest Quarter		✓		
bio17	Precipitation of Driest Quarter				
bio18	Precipitation of Warmest Quarter	✓			✓
bio19	Precipitation of Coldest Quarter		✓	✓	

Table 7: Performance of models selected. P values indicate the probability that the measured AUC ratio is less than 1 (the random prediction threshold) out of a maximum possible value of 2. In 1000 bootstraps the proportion of models with an AUC ratio < 1 is another measure of statistical significance of the test. *P. conspicillatus* was tested with a jacknife procedure.

Species	AUC ratio	S.D.	P	Proportion iterations <1
P. alecto	1.45	0.08	0	0
P. scapulatus	1.35	0.05	0	0
P. poliocephalus	1.58	0.11	0	0

Table 8: Jacknife data used to validate *P. conspicillatus* model. Prediction rate of 0.92 (average omission rate of 0.8), $P = 0$

Test point	Proportion area predicted	Test point	Proportion area predicted
1	0.2352693898	1	0.235899951
1	0.2379317593	1	0.2527149163
1	0.2211167939	1	0.2810201079
1	0.2246899741	0	0.2495621103
1	0.2614026484	1	0.2459188678
1	0.2374413228	1	0.2220276046
1	0.2179639879	1	0.2737336229
1	0.2445176207	1	0.2303650249
1	0.2773068031	1	0.2525747916
1	0.3039304981	1	0.2292440272
1	0.2951026414	1	0.2520843551
1	0.2272822812	1	0.245568556
0	0.2024802074	1	0.2251103482
1	0.2341483921		

Table 9: Species-wise distances to the niche centroid at spillover sites.

Spillover event	*P. alecto*	*P. conspicillatus*	*P. poliocephalus*	*P. scapulatus*	Minimum distance
1	5.3378609373	2.0608370502	11.7284151214	6.3683779325	*P. conspicillatus*
2	1.7242371724	16.7547937523	3.0736370577	2.1999593564	*P. alecto*
3	1.9786841497	4.6784806044	12.4348779627	2.4110835646	*P. alecto*
4	1.862397829	9.5371496092	17.34425031	3.2799188377	*P. alecto*
5	3.5268589296	22.590081733	4.0645363201	2.4194593175	*P. scapulatus*
6	2.3612793677	23.5458505055	2.4577651498	1.0724874264	*P. scapulatus*
7	2.7019279402	28.7587918178	5.6553650656	3.4192612445	*P. alecto*
8	1.3628660926	24.9629570367	2.6513789046	1.967012115	*P. alecto*
9	4.6406867346	32.0148873395	5.7301276137	1.649617618	*P. scapulatus*
10	1.9963440475	23.0686633191	3.0661586038	2.4810369866	*P. alecto*
11	2.3358903246	29.6367344474	3.8693518006	3.1539513424	*P. alecto*
12	1.5150527128	25.0224868495	2.6600498686	2.1504162905	*P. alecto*
13	1.978225318	4.9354574887	19.1765322354	3.2916636042	*P. alecto*
14	3.1305652337	3.413093958	11.1965212264	3.656908625	*P. alecto*
15	2.8799202334	3.3244337457	12.9351282905	2.2982371657	*P. scapulatus*
16	1.6425273756	21.0182273399	7.8396541016	2.0265268391	*P. alecto*
17	3.2282839327	1.9868616657	12.3936342845	3.807534739	*P. conspicillatus*
18	3.4908804042	2.4810350429	11.0169336043	3.9579914047	*P. conspicillatus*
19	1.399550698	9.8364951405	11.4480224992	1.8665053486	*P. alecto*
20	3.550425979	1.5409291413	9.3790484644	3.4596168151	*P. conspicillatus*
21	1.3308690772	20.6190381131	1.5666768181	1.4110347145	*P. alecto*
22	2.7334669983	26.8232258622	2.6322680235	0.6215221819	*P. scapulatus*
23	1.1891054827	22.3968525276	2.1087483904	1.7058767457	*P. alecto*
24	1.6041437369	20.7127499489	1.2055787599	1.0276671388	*P. scapulatus*
25	1.8689899487	25.0144936757	1.6563401201	1.6425312935	*P. scapulatus*
26	1.4124156699	24.1628136	4.8941808435	2.0007800599	*P. alecto*
27	1.208672631	26.3904097129	1.428703113	1.3808124008	*P. alecto*

Spatiotemporal distribution of spillover

Methods

Our models of the seasonal distribution of HeV spillover were built in three phases. First we modelled the distance to black and spectacled FF camps across the area where spillover occurs. For these models we used the Mahalanobis distance algorithm (MD) (Farber and Kadmon, 2003). This method calculates a similarity index based on environmental distance accounting for correlation between variables. Then we built a horse density model using the horse census data from the 2007 equine influenza outbreak (Moloney, 2011). Each of these models is explained in more detail below. Finally we combined the model-generated and environmental data to model the seasonal distribution of HeV spillover with three different methods and then used the weighted average of their predictions to produce a consensus model. The three methods used were boosted regression trees (BRT) (Elith et al., 2008), Random Forests (RF) (Ridgeway, 2013; Breiman, 2001) and logistic regression (LR).

Boosted regression trees and random forests are non parametric techniques based on classification and regression trees (CART). They are similar methods that combine several fitted CARTs on random samples of the data to a subset of the explanatory variables. Each of the fitted trees are then combined which creates a continuous smooth function. The main difference between BRT and RF methods is the boosting step undertook by BRT (Breiman, 2001; Elith et al., 2008). The algorithm "learns" from the poorly classified training data in each of the fitted trees by fitting additional trees to the residuals. Then residuals are used to adjust the splits and variables selected in the final series of trees. In comparison RF averages a series of trees fitted to random samples of the data, also known as bagging (Elith et al., 2008). BRT is also capable of using bagging but is subject to control by the user, so the randomness of the analysis can be adjusted to the characteristics of the data (Elith et al., 2008). These two analytical methods are capable of finding more complex relationships and interactions among variables and data, and can even account for the effect of uncontrolled spatial patterns and effects compared with GLM (Evans et al., 2011).

However, GLM is a more transparent and better understood tool. Therefore, we generated a statistical model by averaging the outputs of these three regression methods. These consensual methods are capable of generating robust and readily interpretable models with high predictive accuracy (Marmion et al., 2009).

Distribution and niche of flying foxes

Presence records of FF are an incomplete account of the total number of camps present in Australia, even more so if we account for temporal scales. To fill these gaps we developed a model that aims to reasonably predict the location of camps during the time frame between HeV's emergence and today. To do so we used the most comprehensive data set to date for training andvalidation. Training data was Roberts et al. (2012) black flying fox (BFF) records which includes dates for many records and allows the use of more fine-grained data from shorter time frames than the usual long term averages used in species distribution modelling. From this data set we only used the records dated between 1992 and 2007. The source of the presence records for spectacled flying foxes (SFF) and BFF testing data was the national flying fox monitoring program of Australia [2].

To fit the MD models we obtained climatic data for every presence location and date from BOM. Analyses and data processing were done with the 'dismo' package in R 3.1.1 (Hijmans et al., 2013; R-Development-Team, 2014). The fitted model was projected to the conditions of every month where spillover events have been recorded. Because the outputs of MD is 1-minimum MD to any other record, projections were then thresholded to a MD > 95 th quantile of the model projection values for that month. The resulting binary maps were reprojected to the geocentric datum of Australia (GDA94) to accurately calculate the linear distance to the pixels with the most similar conditions to any of the FF records. The distance to FF colonies maps were then re-projected back to WGS84 datum, the source reference system of the environmental data. As a result, for every spillover event we obtained a map with the linear distance to the pixels with the conditions where a bat colony was registered between 1993 and 2014. The two thresholded set of models were combined to generate a model of distance to BFF and SFF camps.

The distance to camps models were validated with a partial ROC analysis (Peterson et al. 2008). This validation method differs from the traditional area under the ROC curve in that it compares the fraction of the predicted area versus the fraction of predicted records (Peterson et al. 2008). Therefore, randomness of predictions is assessed by means of comparing the area under the curve

[2] http://www.environment.gov.au/webgis-framework/apps/ffc-wide/ffc-wide.jsf

with a random binomial predictor based on the proportion of area predicted. For the analysis of the performance of these bat models we only allowed an omission rate of 0.05. Validation data was obtained from the online maps of the national flying fox monitoring program.

Additionally, the pixels derived from the thresholded models were used to calculate the niche centroid for each FF species and project the Mahalanobis distance to the niche centroid (Yañez-Arenas et al. 2012; Martínez-Meyer et al. 2013). The niche centroid is defined as the multidimensional centre of the environmental space where the mean of all dimensions is 0, and is defined only across the geographic limits of a species' distribution (Martínez-Meyer et al. 2013). The reason for doing this is that there is a relationship between the abundance patterns of FF across their geographic distribution and the distance to the niche centroid, and that abundance is an important driver of disease dynamics (Martin et al. unpublished).

Horse density

The chances of interaction between horses and flying foxes might scale with density, hence, to account for this phenomena we created a horse density model with the 2007 horse census (Moloney 2011). To represent the density of horses per grid cell we iteratively counted the number of horses that lie within each cell. In each of the 100 iterations we introduced non parametric noise proportional to 50% of the cell width and counted the number of points that represent each of the horses. At the end we averaged the layers in GDA 94 projection to obtain the model of horse density. With this method we avoided the problem of having very smallnumbers per grid cell as results from a kernel density estimation. The main purpose was to somehow account for the size of properties that span more than one pixel but whose centroids restricted its influence to only that pixel.

Model tuning and testing

Consensus models (Marmion et al., 2009) were developed by averaging the predictions of the three regression methods, boosted regression trees and random forest in R 3.1.1, implemented in R packages, "gbm" and "randomForest" respectively, and logistic regression. More details of algorithm tuning are given in the supplementary information. The environmental variables used to construct these models are listed in Table 6.1.

We trained 10 models with each algorithm in a k-fold partition framework to make sure that all filtered presence points were used in the training and testing stage. From the 750 absences we

randomly selected 150 for model testing. The same 150 absences were used consistently to test all models to make sure that model performance was an effect of the presences used for training and not of the spatio – temporal sorting of the absences ((Hijmans, 2012)). Model selection in this initial stage was based on the traditional area under the receiver operator characteristic curve (AUC ROC) to measure the discriminative ability of each model and algorithm. We assessed the significance of the model's AUC values with the AUC values of 1000 null models trained with randomly generated presences and absences (Raes and Ter Steege, 2007). The AUC values of the null models were used to create a statistical distribution of AUC values with which we compared the AUC values of the real data models. The BRT models were generated without assessing the optimal number of trees because the sparsity of the data did not allow convergence given the learning rate used in the real data BRT models.

After model training and prior to projection we performed an extrapolation analysis with the extrapolation detection tool (ExDet, Mesgaran et al., 2014) [3]. The projection data for the analyses were the average conditions of the months where spillover has occurred between August 1994 and December 2014. Then we projected the models to these conditions. With these geographical projections we then assessed if models predicted the seasonal distribution of HeV risk of spillover.

[3] http://www.climond.org

Tables

Table 10: Variables used to calibrate flying fox models

Variable	Source
NDVI average	BOM
NDVI anomaly	BOM
Minimum temperature	Calculated from BOM
Temperature range	BOM
Vapour pressure at 9:00 h	BOM
Vapour pressure at 15:00 h	BOM
Rainfall	BOM
Distance to cities	Bureau of Statistics
Distance to rivers	Calculated from Bureau of statistics
Human population density	Bureau of Statistics

Table 11: Individual variable's contribution by method and consensus model. Variable influence has been descaled so that values represent proportions of the contribution metric for each method (explained deviance in logistic regression and incremental node purity in random forest, for instance).

Variable	Logistic regression	Random forest	Boosted regression trees	Weighted mean
NDVI average	0.0265218138	0.0822897993	0.0581631333	0.055242626
Minimum temperature average	0.1842491899	0.0824090844	0.0646522574	0.1109858062
Temperature difference from hottest month	0.1308561101	0.0535145893	0.026019653	0.0704994228
Temperature difference from coldest month	0.3464459305	0.0763090204	0.0436831223	0.1569846931
Temperature range	0.0332760371	0.0881916668	0.0954456208	0.0720005364
Solar exposure	0.050221069	0.0652289297	0.043720652	0.052894018
Rainfall	0.0018350817	0.0774999831	0.0304539593	0.0359838083
Distance to bat camps	0.0232535535	0.0843974006	0.0887695118	0.0651225297
Distance to bats' niche centroid	0.0141872594	0.0704642356	0.0721045288	0.0519208851
Horse density	0.1828075893	0.090664857	0.1947156795	0.156967504
Rainfall difference from wettest month	0.0022513437	0.1655746951	0.2545987897	0.1401336059
Rainfall difference from driest month	0.004095022	0.0634557387	0.0276730919	0.0312645646

Figures

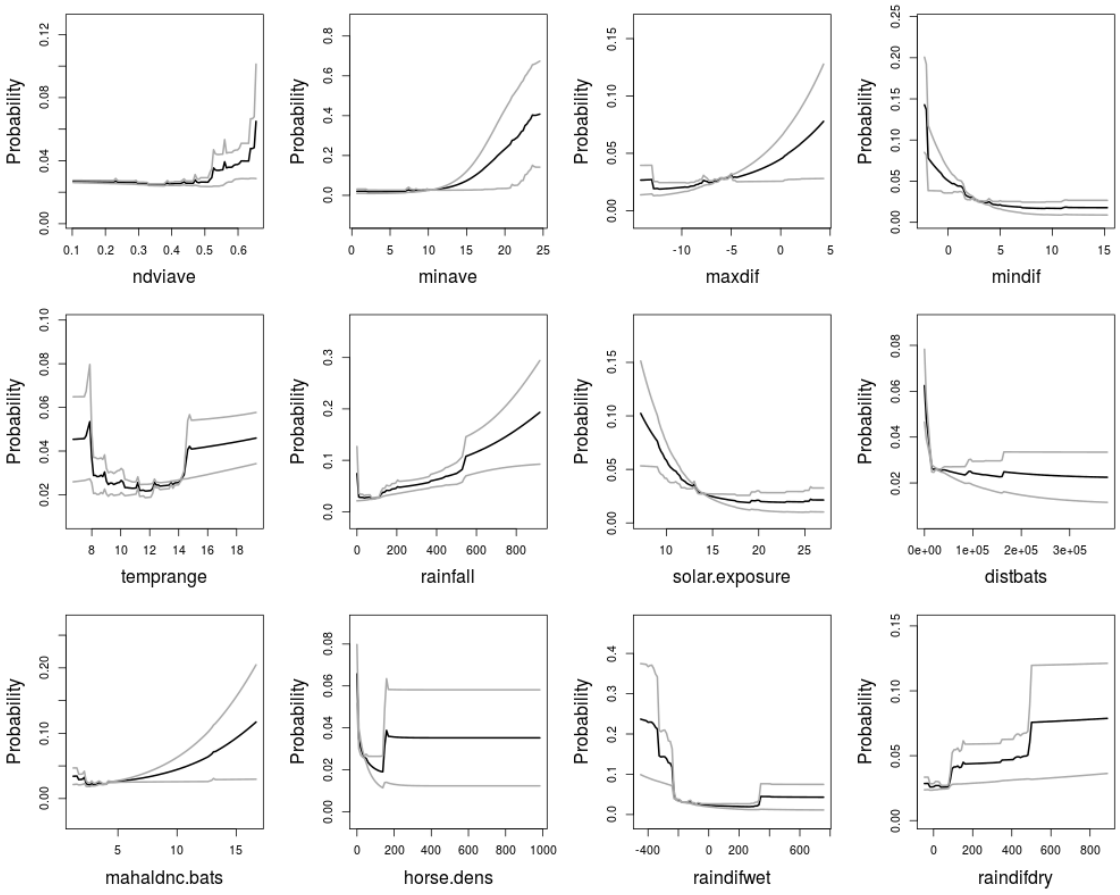

Figure 22: Response curves of additive probabilities to each of the variables used in model training. Grey lines indicate weighted standard errors.

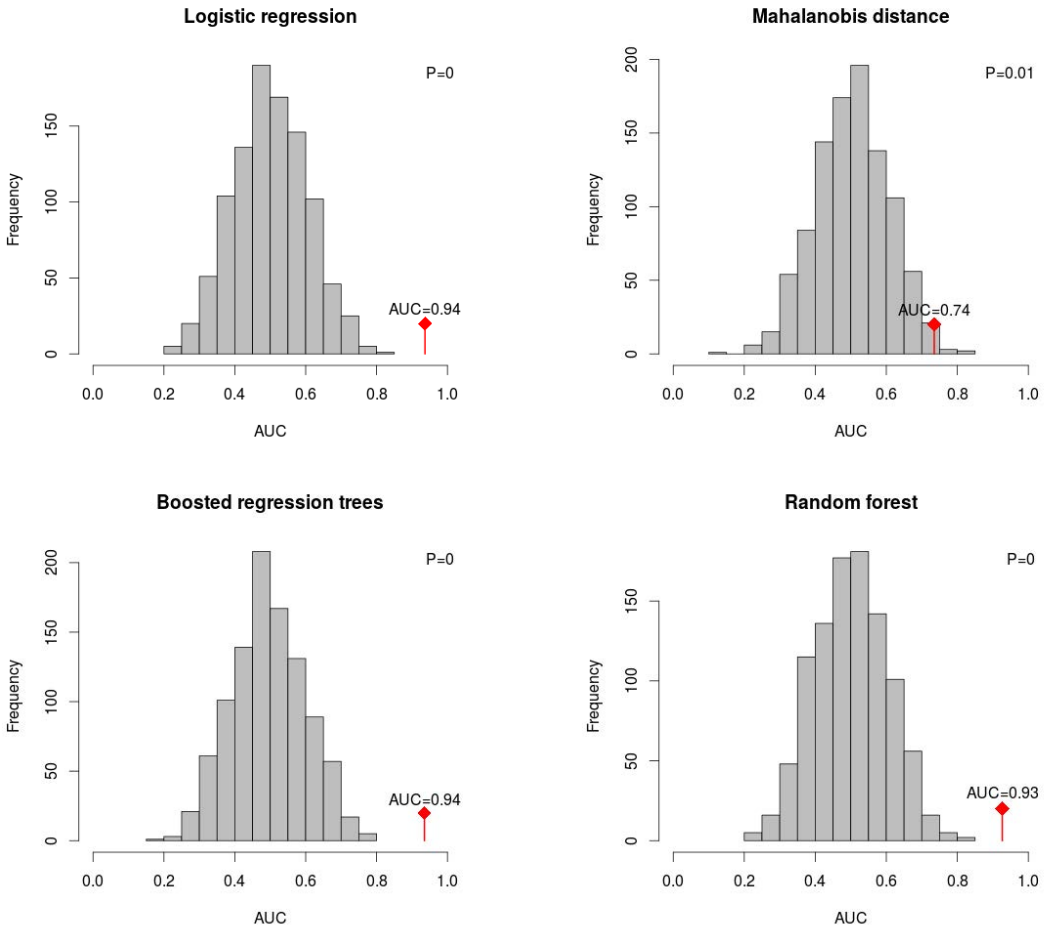

Figure 23: Histograms show the distribution of AUC values of 1000 null models with which the AUC values of the best performing model were compared. All models performed significantly better than random.

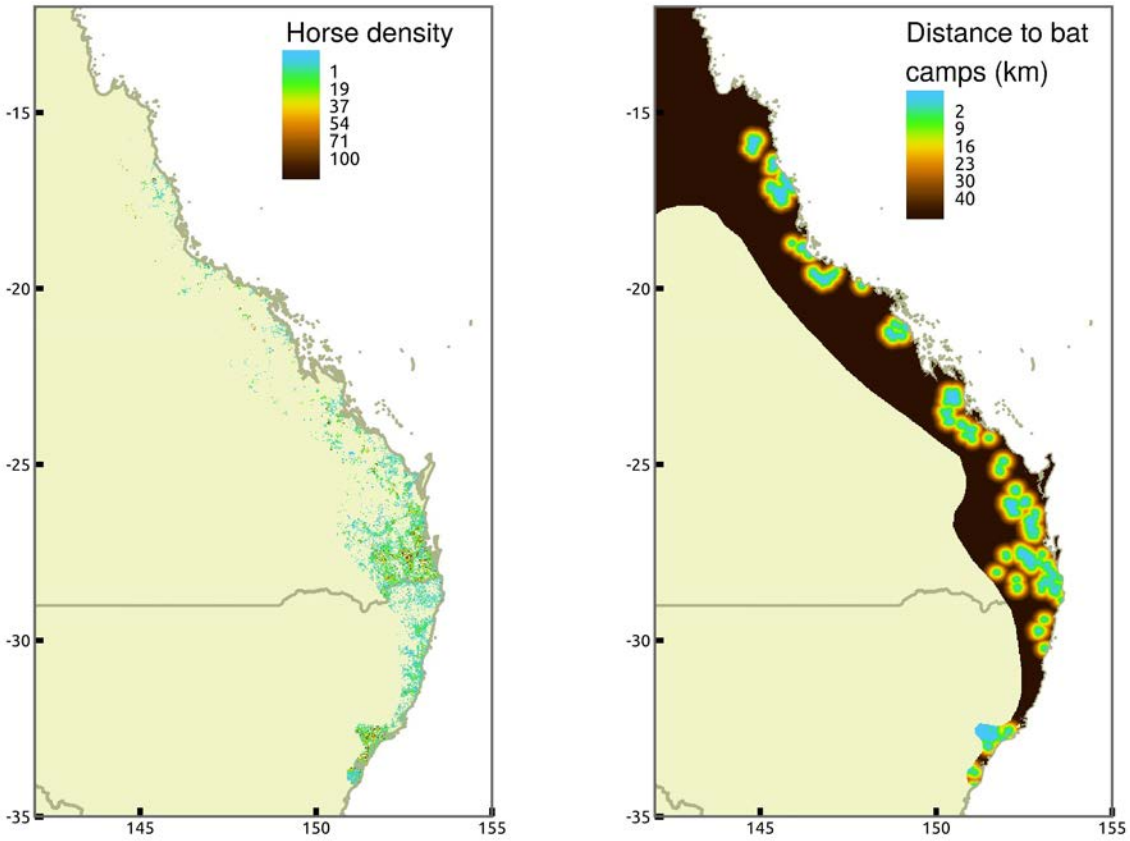

Figure 24: On the left hand side, horse density model used to obtain horse density. Right side, model of predicted distances to bat camps for August 2014.

Climate change effects on HeV spillover

Partial dependence plots

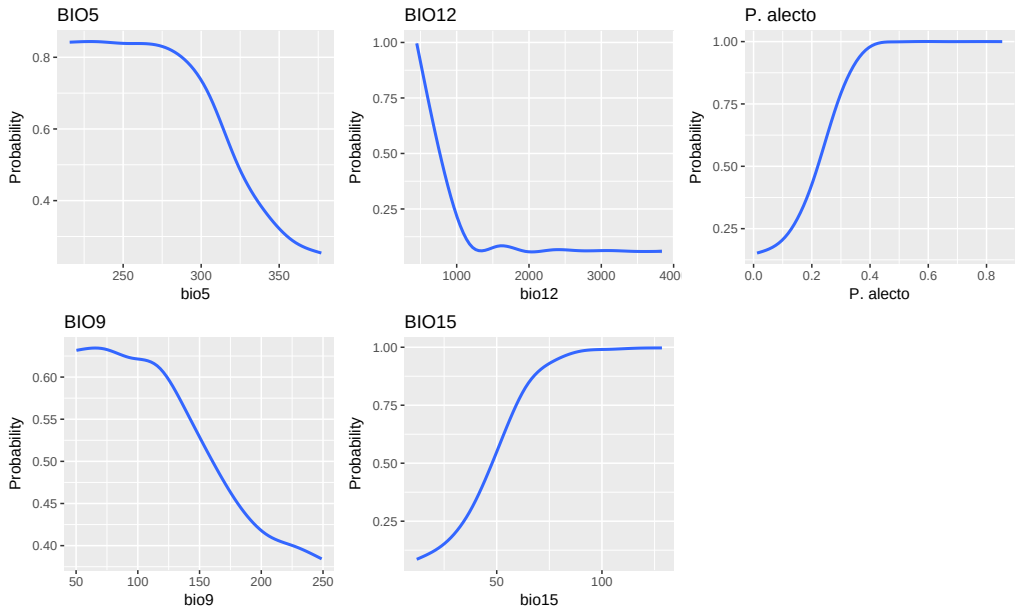

Figure 25: Partial dependence response plots of the *P. alecto* system

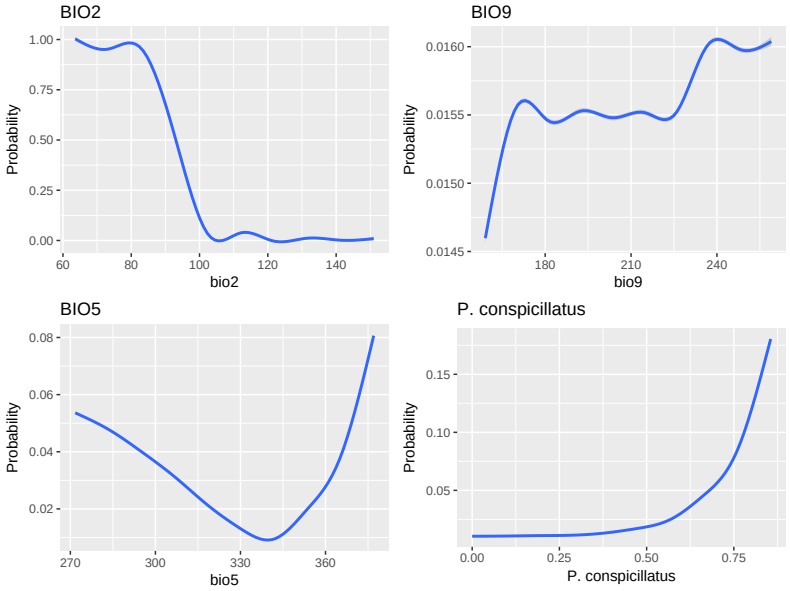

Figure 26: Partial dependence response plots of the *P. conspicillatus* system

Spatial effects

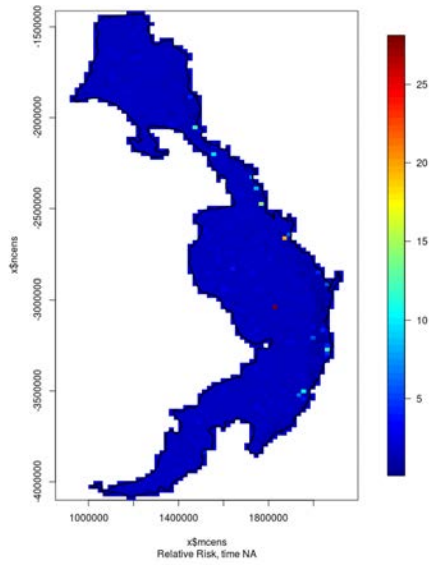

Figure 27: Spatial effects in the *P. alecto* system.

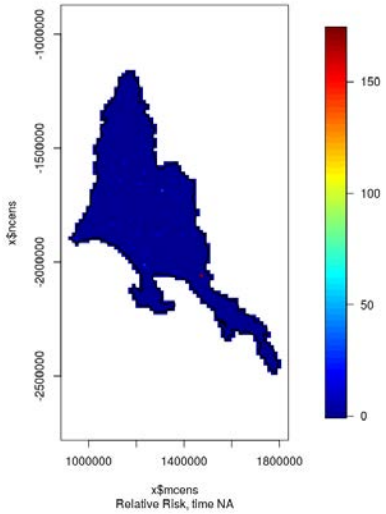

Figure 28: Spatial effects in the *P. conspicillatus* system.

Model diagnostics

P. alecto model

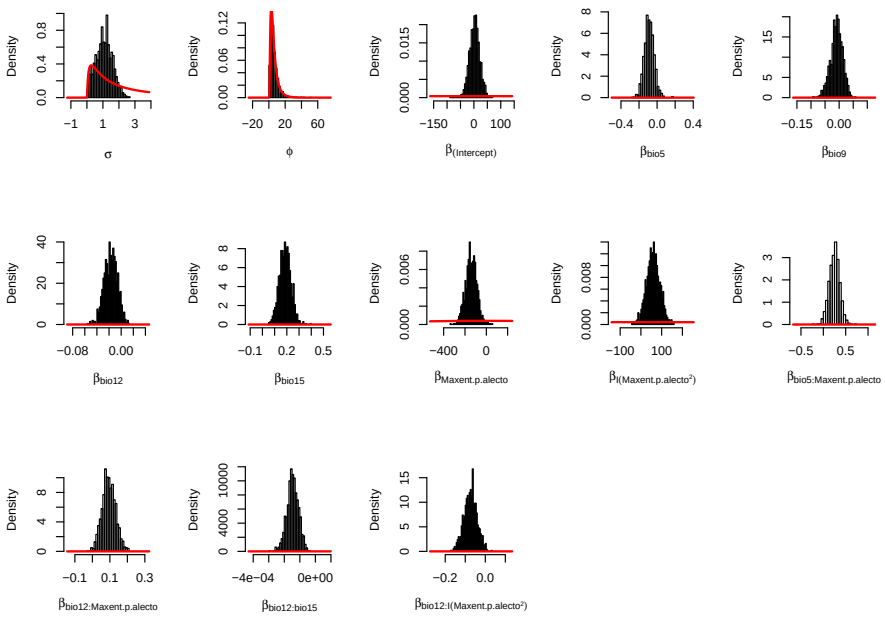

Figure 29: Distribution of prior and posterior samples. Red lines are the prior distributions.

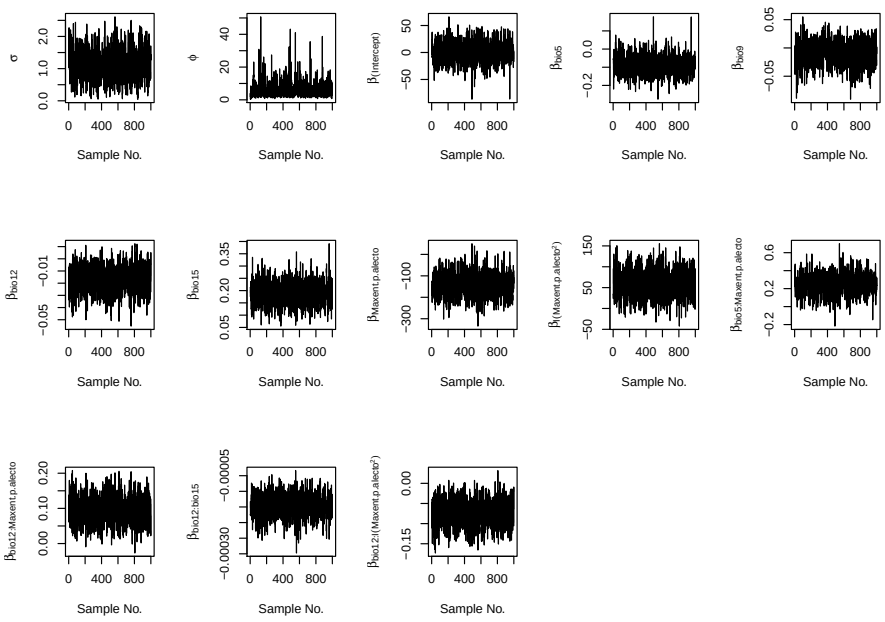

Figure 30: Trace of parameter samples.

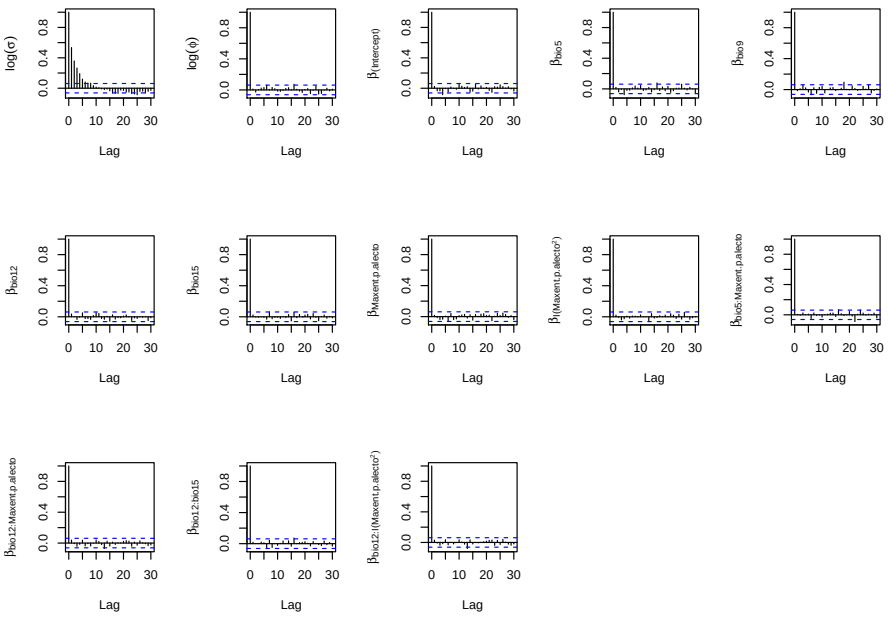

Figure 31: Autocorrelation of posterior samples of parameters.

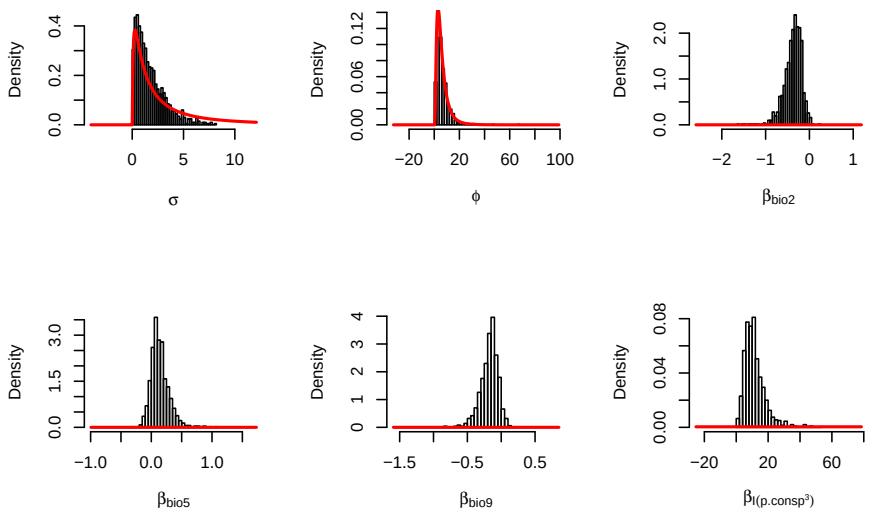

Figure 32: Distribution of prior and posterior samples. Red lines are the prior distributions.

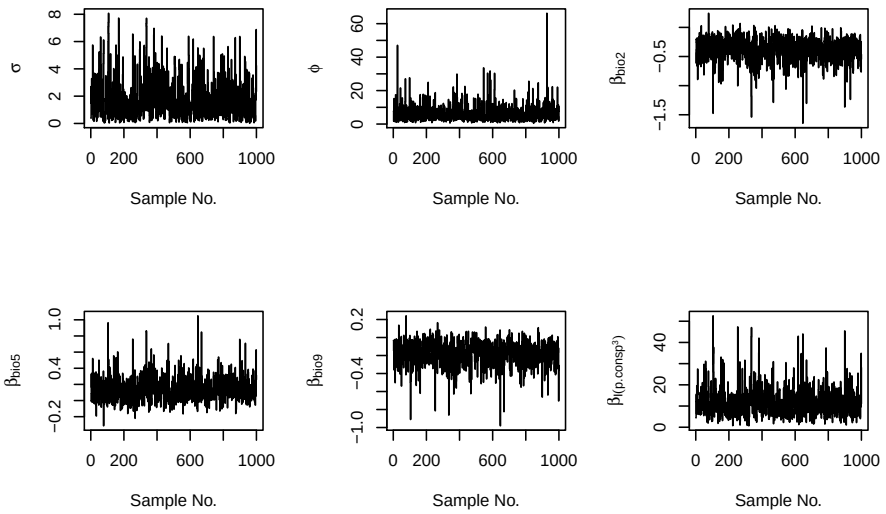

Figure 33: Trace of parameter samples.

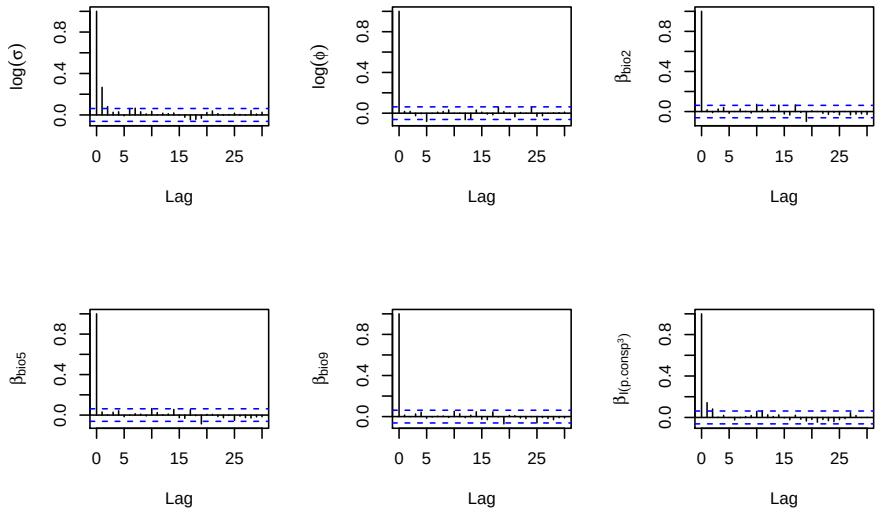

Figure 34: Autocorrelation of posterior samples of parameters.

Influence of tree cover on HeV exposure

Results

Model tables

Table 12: Parameter estimates of the model fitted to simulated data. DIC = 753.4.

β	Mean	2.5 - 97.5% Cr. I.	Deviance
Intercept	-3.729	-4.293 – -3.185	0.00
Cover	9.130	8.822 – 9.451	1.025

Table 13: Parameter estimates of the ANCOVA models. All effects are statistically significant because none of the credibility intervals include zero. However none of the estimates are significantly different from each other.

β	Collected (DIC = 4702.9)		Simulated (DIC = 1338.6)	
	Mean	2.5–97.5% Cr. I.	Mean	2.5 – 97.5% Cr. I.
Day intercept	-2.642	-3.793 – -1.421	-4.073	-4.794 – -3.334
Night intercept	-3.873	-5.023 – -2.656	-4.097	-4.848 – -3.336
Cover Day	9.309	8.380 – 10.252	13.298	12.350 – 14.227
Cover Night	13.681	12.722 – 14.662	13.407	12.432 – 14.338

Figures

Table 14: Parameter estimates of the ANCOVA models. All effects are statistically significant because none of the credibility intervals include zero. However none of the estimates are significantly different from each other.

β	Collected (DIC = 2238.8)			Simulated (DIC = 772.4)		
	Mean	2.5 - 97.5% Cr. I.	Deviance	Mean	2.5 - 97.5% Cr. I.	Deviance
Cover	15.475	-8.935 – 28.082	1.802	22.428	19.748 – 25.129	2.441
Cover · size · grass	-0.005	-0.014 – 0.008	4.598	-0.002	-0.005 – 0.000	1.713
Cover · size · horses	-0.006	-0.017 – 0.006	2.214	-0.009	-0.013 – -0.005	2.847
Cover · size · weed	0.005	-0.014 – 0.017	0.898	0.006	0.002 – 0.009	0.629
Cover · size · grass · horses	0.001	-0.002 – 0.003	5.723	0.001	0.001 – 0.001	3.233

Table 15: Coefficients of the model of time under trees at night.

β	Collected (DIC = 1143.4)			Simulated (DIC = 596.1)		
	Mean	2.5 - 97.5% Cr. I.	Deviance	Mean	2.5 - 97.5% Cr. I.	Deviance
Horses	-1.913	-3.002 – -1.026	2.934	-1.146	-1.480 – -0.651	1.758
Cover·size	0.059	0.005 – 0.120	3.929	0.015	0.007 – 0.026	0.989
Grass·weed	0.085	-0.640 – 0.913	3.661	-0.027	-0.219 – 0.154	0.930
Cover·size·horses	-0.001	-0.017 – 0.015	1.914	0.003	0.000 – 0.006	1.135
Cover·size·grass·weed	-0.003	-0.014 – 0.007	3.927	0.000	-0.002 – 0.003	0 .934

!htb

Table 16: Summary statistics of the recorded data.

Variable	Type	Median	1st - 3rd Quantiles
Proportion of time under trees	Response	0.119	0.016 – 0.27
Total time under trees (min)	Response	46	4 – 116.25
Total time with GPS (min)	Response	599	300 – 836
Number of horses	Explanatory	4	2 – 5
Size of the paddock ($\times 25m^2$)	Explanatory	1108	219 – 2664
Openness (proportion of paddock receiving direct sunlight)	Explanatory	79.2	0.021 – 0.19
Tree cover (proportion of the paddock covered by trees)	Explanatory	0.112	0.021 – 0.198
Distance to trees (metres)	Explanatory	18.50	10.20 – 34.10
Grass max (cm)	Explanatory	19.40	7.0 – 30.0
Grass mean (cm)	Explanatory	10.40	1.77 – 17.80
Grass SD	Explanatory	6.161	0.79 – 9.92
Weed max (cm)	Explanatory	0.285	0.00 – 4.84
Weed mean (cm)	Explanatory	0.00	0.00 – 2.31
Weed SD	Explanatory	0.00	0.00 – 1.99

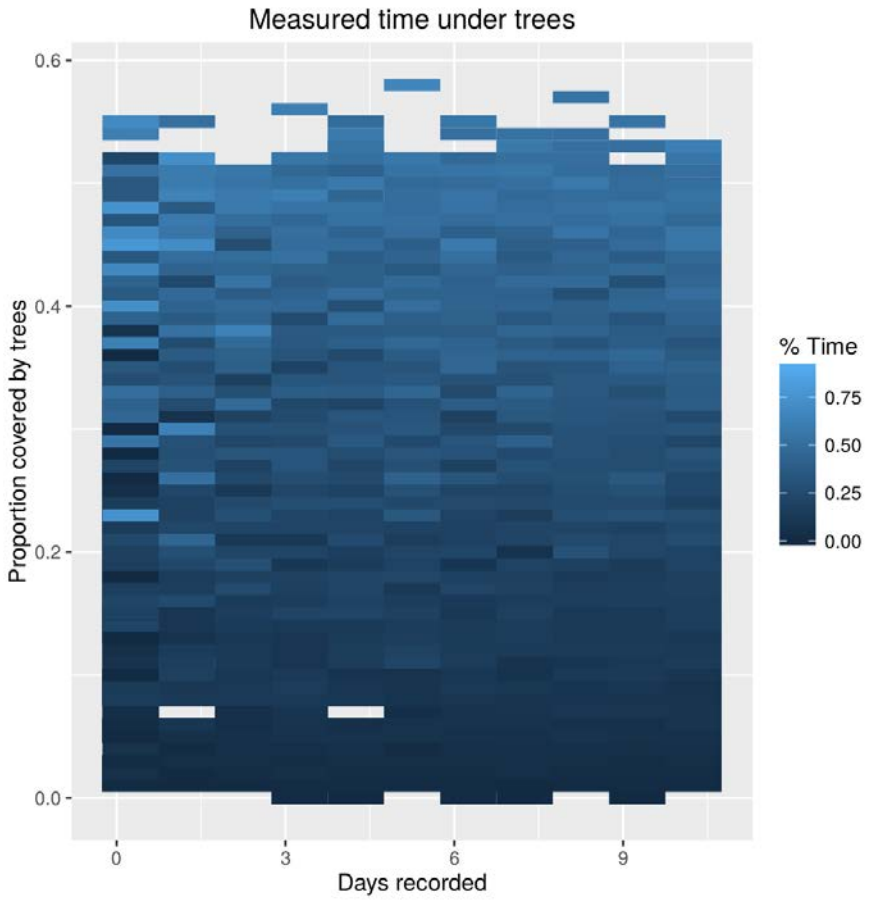

Figure 35: Response of expected time under trees in response to tree cover (X) and length of the sampling period (Y). Colorscale represents the recorded time under trees.

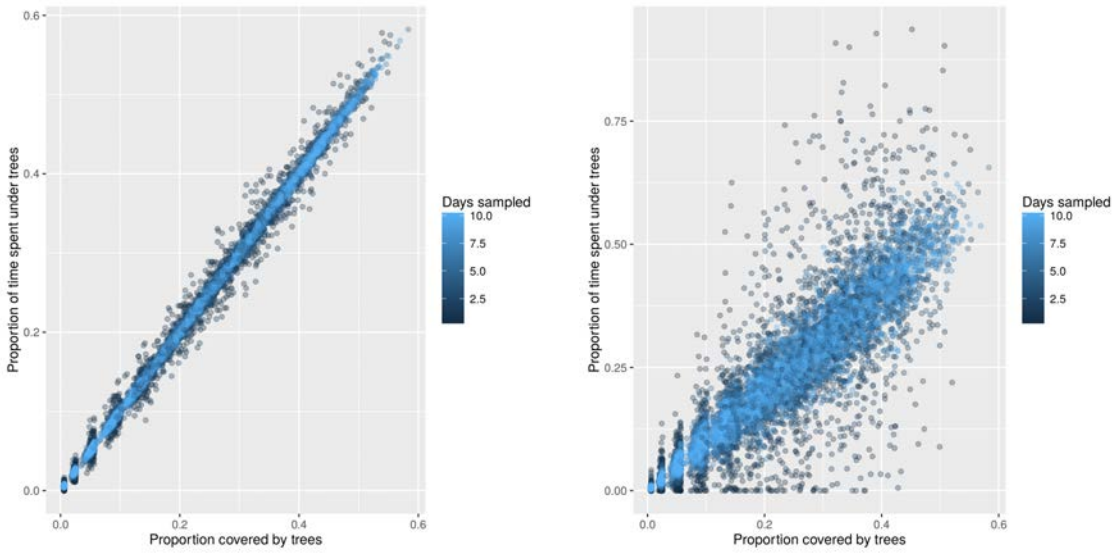

Figure 36: Expected time under trees in response to proportion of paddock covered by trees. Left side figure is the simulated random walk, and the right hand figure if the simulation of time spent under trees as a Bernoulli process. Same as above but the aim is to have a better idea of the increasing variance that results from spatio-temporal autocorrelation. Despite this we could not find a variance structure that significantly departed from a Bernoulli process (assessed with a Bayesian model, results not shown).

In defense of horse vaccination

This paper is a collective response to a commentary published in Infection Ecology & Epidemiology:

- Bilal A Zahoor and Lucy I Mudie. The imperative to develop a human vaccine for the Hendra virus in Australia. *Infection ecology & epidemiology*, 5:29619, 2015. ISSN 2000-8686. URL http://www.ncbi.nlm.nih.gov/pubmed/26519254{%}5Cnhttp://www.pubmedcentral.nih.gov/articlerender.fcgi?artid=PMC4627939

The main reason for its publication was that it contained several inaccuracies regarding HeV genetic diversity, evolution and the effectiveness of the HeV horse vaccine efficacy.

INFECTION ECOLOGY & EPIDEMIOLOGY
THE ONE HEALTH JOURNAL

co action PUBLISHING

LETTER TO THE EDITOR

The equine Hendra virus vaccine remains a highly effective preventative measure against infection in horses and humans: 'The imperative to develop a human vaccine for the Hendra virus in Australia'

Alison J. Peel, BSc (Vet), BVSc, MSc, PhD[1], Hume E. Field, BVSc, MSc, PhD, MACVS[2], Peter A. Reid, BVSc (Hons), BAgrSc[3], Raina K. Plowright, BVSc, MSc (Epidemiology), PhD (Ecology)[4], Christopher C. Broder, BSc, MSc, PhD[5], Lee F. Skerratt, BAnSc, BVSc, PhD, MANZCVSc[6], David T. S. Hayman, BVM&S, MSc, Dip. ECZM, PhD[7], Olivier Restif, MEng, MSc, PhD[8], Melanie Taylor, BSc (Hons) Psychology, PhD[9], Gerardo Martin, BVSc, MSc[6], Gary Crameri, BSc[10], Ina Smith, BASc (Hons), PhD[10], Michelle Baker, PhD[10], Glenn A. Marsh, BASc (Hons), PhD[10], Jennifer Barr, BSc (Hons)[10], Andrew C. Breed, BSc, BVMS, MSc, PhD[11], James L. N. Wood, BSc, BVetMed, MSc, PhD, Dip. ECVPH[8], Navneet Dhand, BVSc&AH, MVSc, MANZCVS (Vet epidemiology), PhD, GradCert (Higher Education)[12], Jenny-Ann Toribio, BVSc, MANZCVSc, MEd (Higher Education), PhD[12], Andrew A. Cunningham, BVMS, PhD, MRCVS, Dip. ECZM (Wildlife Population Health)[13], Ian Fulton, BVSc, MSc, FACVSc (Specialist in Equine Surgery)[14], Wayne L. Bryden, BRurSc, MRurSc, Dip Ed, PhD, FAIAST, FNSA, FASAP[15], Cristy Secombe, BSc, BVMS, MACVS, MVSc (Hons), Dip. ACVIM[16] and Lin-Fa Wang, BSc, PhD, FTSE[17]

[1]Environmental Futures Research Institute, Griffith University, Nathan, QLD, Australia; [2]EcoHealth Alliance, New York, NY, USA; [3]Australian Veterinary Association Representative, Queensland Government Hendra virus Interagency Technical Working Group, Brisbane, Australia; [4]Department of Microbiology & Immunology, Montana State University, Bozeman, MT, USA; [5]Department of Microbiology & Immunology, Uniformed Services University, Bethesda, MD, USA; [6]One Health Research Group, College of Public Health, Medical and Veterinary Sciences, James Cook University, Townsville, QLD, Australia; [7,m]EpiLab, Infectious Disease Research Centre, Hopkirk Research Institute, Massey University, Palmerston North, New Zealand; [8]Department of Veterinary Medicine, University of Cambridge, Cambridge, United Kingdom; [9]Department of Psychology, Macquarie University, Sydney, NSW, Australia; [10]CSIRO Australian Animal Health Laboratory, Geelong, VIC, Australia; [11]Department of Epidemiological Sciences, Animal and Plant Health Agency (APHA), Surrey, United Kingdom; [12]Faculty of Veterinary Science, The University of Sydney, Sydney, NSW, Australia; [13]Institute of Zoology, Zoological Society of London, NW1 4RY London, United Kingdom; [14]President Equine Veterinarians Australia, St Leonards, NSW, Australia; [15]Equine Research Unit, School of Agriculture and Food Sciences, University of Queensland, Gatton, QLD, Australia; [16]School of Veterinary and Life Sciences, Murdoch University, Murdoch, WA, Australia; [17]Programme in Emerging Infectious Diseases, Duke-NUS Medical School, Singapore

The Commentary to which this Letter to the Editor responds can be found at: http://dx.doi.org/10.3402/iee.v5.29619. A rebuttal to this Letter to the Editor can be found at: http://dx.doi.org/10.3402/iee.v6.31659

To the Editor

In their commentary article, 'The imperative to develop a human vaccine for the Hendra virus in Australia', Zahoor and Mudie (1) argue the case for a human Hendra virus (HeV) vaccine. The statements supporting their arguments are incorrect and have the potential to cause

Citation: Infection Ecology and Epidemiology 2016, **6**: 31658 - http://dx.doi.org/10.3402/iee.v6.31658
(page number not for citation purpose)

confusion and ultimately undermine confidence in current evidence-based risk management strategies, thereby placing equine and human lives at risk.

The central argument in Zahoor and Mudie (1) is that HeV is 'rapidly mutating', with consequent loss of efficacy of the equine HeV vaccine, changing clinical syndromes in humans, and infection in new animal species. There is no scientific basis to their central argument. Zahoor and Mudie (1) offer no citations to support their statements regarding the mutation rate of HeV. Indeed, primary research indicates the HeV genome has minimal variability (less than 1% at both the nucleotide and amino acid levels) in both flying-foxes and horses and is highly stable (the same variant has been detected at disparate locations at the same time, and over periods of at least 12 years) (2, 3).

There is no evidence that the equine HeV vaccine is becoming less effective. Continuing equine HeV cases do not reflect loss of vaccine efficacy as stated by Zahoor and Mudie (1), but rather a failure of some horse owners to vaccinate their horses. There have been no HeV cases in vaccinated horses. The efficacy and safety of the recombinant equine vaccine has been clearly demonstrated (4–6), and both government and industry animal health authorities strongly recommend its use as 'the single most effective way of reducing the risk of Hendra virus infection in horses' (7).

There is no evidence that the nature of human HeV infection is changing. The seven recognised human cases have shared clinical features but are insufficient in number to determine changes over time (8–13).

There is no evidence that recently reported canine cases indicate that HeV is 'seeking new co-hosts'. The wide host range of HeV in experimental studies is well established (14, 15). The two observed cases of natural HeV infection in dogs most likely resulted from exposure to infected horses, or contaminated material from these horses, and their detection may reflect increased surveillance of canines on infected equine premises (16).

There is no evidence that HeV infections 'are emerging in locations far beyond bats' typical migratory boundaries'. Several recent publications demonstrate that the spatial occurrence of equine HeV cases reflects the distribution of black and spectacled flying-foxes (17–19).

In conclusion, we express no objection to the development of a human vaccine against HeV; however, we are emphatic that Zahoor and Mudie (1) are unjustified in using viral evolution, vaccine inefficiency, and changing clinical syndromes as motivations. There are no data to support their case.

Conflict of interest and funding

Dr. Broder reports a grant (CRADA) from Zoetis, Inc., outside the submitted work. In addition, Dr. Broder is a coinventor on U.S. Patent No. 8,865,171 and 9,045,532, with royalties paid by Zoetis, Inc., and Australian Patent No. 2005327194 Patent assignees are the United States of America as represented by the Department of Health and Human Services (Washington DC) and the Henry M. Jackson Foundation (Bethesda, MD).

Dr. Restif reports grants from The Royal Society, during the conduct of the study; he further discloses that he is the sponsor of a Junior Research Fellowship supported by the Axa Research Fund.

Dr. Dhand has communicated with Zoetis for submitting a joint ARC linkage project but this submission did not materialize.

Dr. Secombe is a core executive member of Equine Veterinarians Australia.

References

1. Zahoor BA, Mudie LI. The imperative to develop a human vaccine for the Hendra virus in Australia. Infect Ecol Epidemiol 2015; 5: 29619. doi: http://dx.doi.org/10.3402/iee.v5.29619
2. Smith I, Broos A, De Jong C, Zeddeman A, Smith C, Smith G, et al. Identifying Hendra virus diversity in pteropid bats. PLoS One 2011; 6: e25275.
3. Marsh GA, Todd S, Foord A, Hansson E, Davies K, Wright L, et al. Genome sequence conservation of Hendra virus isolates during spillover to horses, Australia. Emerg Infect Dis 2010; 16: 1767–9.
4. Broder CC, Xu K, Nikolov DB, Zhu Z, Dimitrov DS, Middleton D, et al. A treatment for and vaccine against the deadly Hendra and Nipah viruses. Antiviral Res 2013; 100: 8–13.
5. Middleton D, Pallister J, Klein R, Feng Y-R, Haining J, Arkinstall R, et al. Hendra virus vaccine, a one health approach to protecting horse, human, and environmental health. Emerg Infect Dis 2014; 20: 372–9.
6. Australian Pesticides and Veterinary Medicines Authority (2015). Summary of adverse experience reports made to the APVMA about Hendra virus vaccine. [Online]. APVMA. Available from: http://apvma.gov.au/node/15786 [cited 18 December 2015].
7. Hendra Virus Interagency Working Group (Biosecurity Queensland, Australian Veterinary Association, Queensland Health, Workplace Health & Safety Queensland) (2014). Hendra virus infection prevention advice. Available from: https://www.health.qld.gov.au/ph/documents/cdb/hev-inf-prev-adv.pdf [cited 18 December 2015].
8. Selvey LA, Wells RM, McCormack JG, Ansford AJ, Murray K, Rogers RJ, et al. Infection of humans and horses by a newly described morbillivirus. Med J Aust 1995; 162: 642–5.
9. O'Sullivan JD, Allworth AM, Paterson DL, Snow TM, Boots R, Gleeson LJ, et al. Fatal encephalitis due to novel paramyxovirus transmitted from horses. Lancet 1997; 349: 93–5.
10. Paterson DL, Murray PK, McCormack JG. Zoonotic disease in Australia caused by a novel member of the Paramyxoviridae. Clin Infect Dis 1998; 27: 112–18. doi: http://doi.org/10.1086/514614
11. Hanna JN, McBride WJ, Brookes DL, Shield J, Taylor CT, Smith IL, et al. Hendra virus infection in a veterinarian. Med J Aust 2006; 185: 562–4.
12. Wong KT, Robertson T, Ong BB, Chong JW, Yaiw KC, Wang LF, et al. Human Hendra virus infection causes acute and relapsing encephalitis. Neuropathol Appl Neurobiol 2009; 35: 296–305.
13. Playford EG, McCall B, Smith G, Slinko V, Allen G, Smith I, et al. Human Hendra virus encephalitis associated with

equine outbreak, Australia, 2008. Emerg Infect Dis 2010; 16: 219–23.
14. Westbury HA, Hooper PT, Selleck PW, Murray PK. Equine morbillivirus pneumonia – Susceptibility of laboratory animals to the virus. Aust Vet J 1995; 72: 278–9.
15. Geisbert TW, Feldmann H, Broder CC. Animal challenge models of henipavirus infection and pathogenesis. Curr Top Microbiol Immunol. 2012; 359: 153–77.
16. Kirkland PD, Gabor M, Poe I, Neale K, Chaffey K, Finlaison DS, et al. Hendra virus infection in dog, Australia, 2013. Emerg Infect Dis 2015; 21: 2182–5.
17. Smith CS, Skelly C, Kung N, Roberts BJ, Field HE. Flying-fox species diversity – A spatial risk factor for Hendra virus infection in horses in Eastern Australia. PLoS One 2014; 9: 1–7.
18. Edson D, Field H, McMichael L, Vidgen M, Goldspink L, Broos A, et al. Routes of Hendra virus excretion in naturally-infected flying-foxes: implications for viral transmission and spillover risk. PLoS One 2015; 10: e0140670. doi: http://dx.doi.org/10.1371/journal.pone.0140670
19. Field H, Jordan D, Edson D, Morris S, Melville D, Parry-Jones K, et al. Spatio-temporal aspects of Hendra virus infection in pteropid bats (flying-foxes) in eastern Australia. PLoS One 2015; 10: e0144055. doi: http://dx.doi.org/10.1371/journal.pone.0144055

Spillover simulations

HeV in bats

To implement the framework I modelled HeV dynamics among bats with a *MSIR* structure, with gamma distributted matternal immunity, because this type of distribution can synchronise peak prevalence with the high spillover risk season (Jaewoon Jeong *pers. comm.*; Plowright et al., 2015; Wearing et al., 2005). To adequately represent the maternally immune stage the bat population is structured by age into pups (0–6 mo. old) and adults (6> mo old, equations 15).

$$\frac{dM_1}{dt} = b(t) \cdot R - (\sigma \cdot l + \mu)M_1 \tag{15a}$$

$$\frac{dM_i}{dt} = \sigma \cdot l \cdot M_{i-1} - (\sigma \cdot l + \mu)\, M_i \tag{15b}$$

$$\frac{dS_p}{dt} = b(t) \cdot (S + I) - \Big(\beta(I + I_p) + \sigma + \mu\Big)\, S_p \tag{15c}$$

$$\frac{dI_p}{dt} = \beta(I + I_p)S_p - (\sigma + \mu + \gamma)\, I_p \tag{15d}$$

$$\frac{dR_p}{dt} = \gamma I_p - (\sigma + \mu)R_p \tag{15e}$$

$$\frac{dS}{dt} = \sigma(l \cdot M_n + S_p) - (\beta(I + I_p) - \mu)S \tag{15f}$$

$$\frac{dI}{dt} = \beta(I + I_p)S + \sigma I_p - (\mu + \gamma)I \tag{15g}$$

$$\frac{dR}{dt} = \gamma I + \sigma R_p - \mu R \tag{15h}$$

Where the birth rate $b(t)$ is a function of time that regulates seasonal birth pulses (Peel et al., 2014):

$$b(t) = \sqrt{\frac{s}{\pi}} \exp\left[-s\left(1 - \cos(\pi t - \phi)^2\right)\right]$$

Because HeV is a directly transmitted disease, with a slight environmental transmission component, we have to model these two transmission pathways in spillover. In addition, the transmission rate from reservoir to spillover host usually depends on scaling the transmission rate among reservoir hosts (Keeling and Rohani, 2007). In this case, transmission to horses might be scaled by the probability of finding a foraging patch inside horse properties:

$$\frac{dH_{I_j}}{dt} = k_j H_{s_j} \ln\left[1 + \frac{\varepsilon_j(t)}{k_j}\left(\beta I_j + \frac{p_c}{D_{50}} V_j\right)\right] \tag{16a}$$

$$\frac{dV_j}{dt} = \epsilon I_j - \mu_v V_j \tag{16b}$$

Where ε and p_h are auxiliary variables that are:

$$\varepsilon_j(t) = p_{h_j} \cdot p_{f_j} \cdot \frac{T_{b_j}(t)}{T_{b_{jmax}}}$$

$$p_c = p_a \cdot p_{eating} \tag{17a}$$

Where p_{h_j} is the probability that there are horses inside a bat foraging patch per area unit (4×4 km grid cells) and p_{f_j} is the probability that bats find a foraging patch in area j. Foraging patches are defined as any 1 ha patch within area j that contains at least 14 flowering trees at peak flowering. And p_a is the proportion of a 1 ha foraging patch that is contaminated with infected bat urine.

Lastly the way we determine the number of flying foxes that feed in area j where we evaluate spillover to horses is:

$$T'_{b_j}(t) = T_{b_j} \exp(-1/10^4 d_j)$$

$$T'_{b_{jmax}} = T_{b_{jmax}} \exp(-1/10^4 d_j)$$

$$I_j(t) = I\frac{\frac{T'_{b_j}(t)}{T'_{b_{jmax}}}p_{f_j}T'_{b_j}(t)}{\sum_{j=1}^{n}\frac{T'_{b_j}(t)}{T'_{b_{jmax}}}p_{f_j}T'_{b_j}(t)}$$

This means that the number of bats that feed in area j depends on the proportion of trees that are flowering at time t weighted by their distance from the source bat camp and the probability of finding a foraging patch. d_j is the distance from the bat colony to the area j that contains n foraging patches.

Dynamics of flowering and fruiting

This part of the system comprises a series of equations that assume that the tree population dynamics are negligible. Phenologic status is represented compartmentally and the time to state transision are exponentially distributted.

$$\frac{dT_{n_j}}{dt} = m_j T_{b_j} - p_j(t)T_{n_j} \tag{18a}$$

$$\frac{dT_{b_j}}{dt} = p_j(t)T_{n_j} - m_j T_{b_j} \tag{18b}$$

Where the flowering (blossoming) rate is controlled by $p_j(t)$:

$$p_j(t) = a_j + b_j \cos\left(c_j \pi t - \phi_j\right)^2$$

Where a_j and b_j are the minimum and maximum flowering rates respectively of patch j. c_j controls the periodicity of flowering (how often flowering occurs in patch j) and ϕ_j is the offset, that controls the time of the year at which peak flowering occurs in patch j. The first stage is composed by trees that are awaiting to flower, the second are flowering trees.

Parametrisation

All parameters pertaining HeV dynamics in bats were obtained from Plowright et al. (2011) and by personal communication with Jaewoon Jeong. The rest of parameters to scale the contact rates with horses were estimated using MCMC sampling and with data from Crowther et al. (2015) and Eby and Law (2008). These data wree used to find tree density (Crowther et al., 2015),flowering frequency and peaks respectively (Eby and Law, 2008). Horse density data was obtained from Biosecurity Queensland.

Tree density and flowering

Crowther et al. (2015) modelled tree density globally at 1 km^2 using remote sensing data. While the data is not completely accurate it represents the best account of tree density yet available. Eby and Law modelled the relevance of vegetation communities in Southeastern Queensland as foraging habitat for *P. poliocephalus*. This spatialised data set assigns different score values to polygons that represent the type of plant communities based on how productive they are and how relevant they are for *P. poliocephalus* at bimonthly intervals. Given that *P. poliocephalus* and *P. alecto* have different dietary preferences, Eby and Law data might underestimate the relevance of the periurban vegetation for *P. alecto*. Therefore, we assumed that the relevance of all areas for *P. alecto* was at least 10% higher in absolute terms than they are for *P. poliocephalus*. With these assumptions then the density of flowering trees per spatial and time unit was assumed to be $Flowering_j(t) = Trees_j \times Relevance_j(t)$.

To perform these calculations we rasterised the flowering scores of Eby and Law (2008) with the grid size of the tree density data from Crowther et al (2015). The resulting flowering density maps for each bimonthly period were used to find parameters a, b, c, ϕ from equation 18b for all j areas using MCMC sampling with JAGS 4.1 (Plummer, 2003),integrating the system of equations with the Euler method using a time step of 1 day. Priors for these parameters were normally distributed and truncated between 0 and 1 with mean 0 and precision of 1, expcept for ϕ which was drawn from a normal distriution with mean π and precision of $\pi/2$ and truncated at $\pi/2, \pi$.

Calculating probability of finding foraging patches per area j

The 40 km radius buffer around camps was divided into quadrants of 4×4 km, at which I evaluated the probability of finding foraging patches and the probability that a foraging patch is inside a horse paddock. We did this by downscaling the tree density model from 700 m wide grids (after converting from WGS84 to GDA94) to 100 m. The probability of finding a foraging patch per area unit is therefore the proportion of 100×100 m patches with more than 14 trees. And the probability that a foraging patch has horses is the proportion of foraging patches with a horse density > 0.

To calculate the latter probability we had to create a horse density ha^{-1} model. To create this model we iteratively rasterised the coordinates of the paddocks' centroids after adding noise generated from a uniform distribution with mean 0 and minimum and maximum values equivalent

to $\pm\frac{1}{2}\sqrt{area}$ (m^2).